Springer Series in Solid-State Sciences 184

Dmitry A. Ryndyk

Theory of Quantum Transport at Nanoscale

An Introduction

Springer

Springer Series in Solid-State Sciences

Volume 184

The Springer Series in Solid-State Sciences consists of fundamental scientific books prepared by leading researchers in the field. They strive to communicate, in a systematic and comprehensive way, the basic principles as well as new developments in theoretical and experimental solid-state physics.

More information about this series at http://www.springer.com/series/682

Dmitry A. Ryndyk

Theory of Quantum Transport at Nanoscale

An Introduction

Springer

Dmitry A. Ryndyk
TU Dresden
Dresden
Germany

ISSN 0171-1873 ISSN 2197-4179 (electronic)
Springer Series in Solid-State Sciences
ISBN 978-3-319-24086-2 ISBN 978-3-319-24088-6 (eBook)
DOI 10.1007/978-3-319-24088-6

Library of Congress Control Number: 2015950445

Springer Cham Heidelberg New York Dordrecht London

Printed on acid-free paper

Springer International Publishing AG Switzerland is part of Springer Science+Business Media (www.springer.com)

Preface

This book is an introduction to a rapidly developing field of modern theoretical physics—the theory of quantum transport at nanoscale. The theoretical methods considered in the book are in the basis of our understanding of charge, spin, and heat transport in nanostructures and nanostructured materials and are widely used in nanoelectronics, molecular electronics, spin-dependent electronics (spintronics), and bioelectronics. Although some of these methods are already 20–25 years old, it is not so easy to find their systematic and consecutive description in one place. The main theoretical models and methods are distributed among many original publications, often written in different style and with different notations. During my research and teaching activities I had to overcome many obstacles to find required information. The results of my search I now present to your attention in more or less ordered form together with some original investigations.

The book is based on the lecture notes I used in the courses for graduate and postgraduate students at the University of Regensburg and Technische Universität Dresden (TU Dresden). Some base knowledge of theoretical physics, especially quantum mechanics, is assumed. But otherwise I have tried to make the text self-consistent and to derive all formulas. In some cases I have given the references for additional reading.

As this book grew up from the lecture notes, I hope it will serve as an advanced-level textbook for Master and Ph.D. students, and it can also be interesting to the experts working in the fields of quantum transport theory and nanoscience. To this end I have tried to combine modern theoretical results with the pedagogical level of explanations. This book will help to cover, to some extent, the gap between undergraduate-level textbooks and present day theoretical papers and reviews.

The book includes the Introduction and two parts. The first part is devoted to the basic concepts of quantum transport: Landauer–Büttiker method and matrix Green function formalism for coherent transport, Tunneling (Transfer) Hamiltonian and master equation methods for tunneling, Coulomb blockade, vibrons and polarons. The results in this part are obtained as possible without sophisticated techniques,

such as nonequilibrium Green functions, which are considered, in detail, in the second part. We give a general introduction to the nonequilibrium Green function theory. We describe in detail the approach based on the equation-of-motion technique, as well as a more sophisticated one based on the Dyson–Keldysh diagrammatic technique. The attention is mainly paid to the theoretical methods able to describe the nonequilibrium (at finite voltage) electron transport through interacting nanosystems, specifically the correlation effects due to electron-electron and electron-vibron interactions. We consider different levels of theoretical treatment, starting from a few-level model approach, such as the single-level electron-vibron (polaron) model and the Hubbard–Anderson model for Coulomb interaction. The general formalism for multilevel systems is considered, and some important approximations are derived.

The book is focused on the ideas and techniques of quantum transport theory in discrete-level systems, as it is discussed in detail in the Introduction. But we do not consider here explicitly particular applications of the theory to semiconductor devices or the molecular transport theory based on atomistic methods, in particular density functional theory (DFT).

The Introduction includes a comprehensive literature review, but for sure not complete. In the main text I did not try to cite all relevant publications, because it is more a textbook than a review. Nevertheless, I want to apologize for possibly missing important references.

Despite large efforts and time spent to improve the manuscript and to check it for misprints, the book definitely contains some mistakes, misprints, something is missed and should be added, as well as something would be better removed. I will greatly appreciate any comments and suggestions for improvement.

Dresden, Germany Dmitry A. Ryndyk

Acknowledgments

First of all, I am grateful to Joachim Keller, Gianaurelio Cuniberti, and Klaus Richter for their interest in my work and support during the years of my stay at the University of Regensburg and the Technische Universität Dresden (TU Dresden).

I want to thank the members of the Nanoscale Modeling Group and the Chair for Materials Science and Nanotechnology at TU Dresden, especially Artem Fediai, Thomas Lehmann, and Seddigheh Nikipar for many useful discussions and help with proofreading.

Some of the results presented in this book were obtained in collaboration with Joachim Keller, Gianaurelio Cuniberti, Klaus Richter, Milena Grifoni, Andrea Donarini, Rafael Gutierrez, Bo Song, Michael Hartung, Pino D'Amico, Artem Fediai, and Thomas Lehmann. I thank them and all colleagues at the universities of Regensburg and Dresden.

Finally, I am thankful to the patience of my family.

Contents

1 Introduction 1
1.1 Quantum Transport in Mesoscopic and Nanoscale Systems 1
1.2 Nanojunctions 4
1.3 From Basic Concepts to Advanced Methods 5
1.4 Notations 9
References 10

Part I Basic Concepts

2 Landauer-Büttiker Method 17
2.1 Quantum Junctions 18
2.1.1 Electrodes, Leads, Scatterer 18
2.1.2 Transport Channels 19
2.1.3 Reflection and Transmission 23
2.1.4 Scattering Matrix S and Transfer Matrix M 26
2.1.5 A Series of Scatterers: Transfer Matrix Method 30
2.2 Landauer Formula 31
2.2.1 Single-Channel Formulas 31
2.2.2 Heuristic Derivation 33
2.2.3 Conductance Quantization 37
2.2.4 Contact Resistance 39
2.3 Multi-channel Scattering and Transport 41
2.3.1 S-Matrix and the Scattering States 41
2.3.2 Multi-channel Landauer Formula 44
2.3.3 Derivation from the Linear Response Theory 47
2.4 Multi-terminal Systems 49
2.4.1 Multi-terminal Landauer-Büttiker Formula 49
2.4.2 Büttiker Conductance Formalism 51
References 54

3 Green Functions 55
3.1 Green Functions and the Scattering Problem 56
3.1.1 Retarded and Advanced Green Functions 56
3.1.2 Green Functions in the Coordinate Representation 59
3.1.3 Lippmann-Schwinger Equation 62
3.1.4 Fisher-Lee Relation Between S and G^R 65
3.2 Matrix Green Functions 67
3.2.1 Matrix (Tight-Binding, Lattice) Hamiltonian 67
3.2.2 Retarded Single-Particle Matrix Green Function 71
3.2.3 Electrode Self-Energies 72
3.2.4 Transmission Function and Current 74
3.3 Recursive Method 77
3.3.1 Dyson Equation 77
3.3.2 Recursive Method for 1D Systems 78
3.3.3 Multi-connected Systems 82
3.4 Semi-infinite Electrodes 83
3.4.1 Surface Green Function 83
3.4.2 Analytical Solution 85
3.4.3 The Iterative Method for 1D Electrodes 87
3.4.4 The Iterative Method for 2D and 3D Electrodes 88
3.5 Resonant Transport 89
3.5.1 Single-Level Model 90
3.5.2 Two-Level Model, Interference 93
References 97

4 Tunneling 99
4.1 Tunneling (Transfer) Hamiltonian Method 100
4.1.1 Planar Barrier 100
4.1.2 Tunneling Hamiltonian 102
4.1.3 Bardeen's Matrix Elements 108
4.1.4 Current Through a Planar Junction 110
4.1.5 Tersoff-Hamann Theory of STM 115
4.2 Sequential Tunneling 116
4.2.1 Sequential Tunneling Through a Single Level 117
4.2.2 Rate Equations for Noninteracting Systems 117
4.2.3 The Basis of Many-Body Eigenstates 118
4.2.4 Master Equation in the Basis of Many-Body Eigenstates 119
References 121

5 Electron-Electron Interaction and Coulomb Blockade 123
5.1 Electron-Electron Interaction in Nanosystems 123
5.1.1 Single-Electron Tunneling: Charging Energy 123
5.1.2 Discrete Energy Levels 125
5.1.3 Hubbard-Anderson and Constant-Interaction Models 126

5.2 Single-Electron Box . . . 128
5.3 Single-Electron Transistor . . . 132
5.3.1 Tunneling Transition Rates . . . 132
5.3.2 Master Equation . . . 134
5.3.3 Conductance: CB Oscillations . . . 135
5.3.4 Current-Voltage Curve: Coulomb Staircase . . . 136
5.3.5 Contour Plots. Stability Diagrams . . . 137
5.4 Coulomb Blockade in Quantum Dots . . . 139
5.4.1 Linear Conductance . . . 141
5.4.2 Transport at Finite Bias Voltage . . . 142
5.5 Cotunneling . . . 144
5.5.1 Inelastic Cotunneling . . . 145
5.5.2 Elastic Cotunneling . . . 147
References . . . 147

6 Vibrons and Polarons . . . 149
6.1 Electron-Vibron Interaction in Nanosystems . . . 150
6.1.1 Linear Vibrons . . . 150
6.1.2 Electron-Vibron Hamiltonian . . . 152
6.2 Inelastic Electron Tunneling Spectroscopy (IETS) . . . 154
6.3 Local Polaron . . . 159
6.3.1 Canonical (Lang-Firsov) Transformation . . . 159
6.3.2 Spectral Function . . . 161
6.3.3 Weak Coupling to the Metallic Lead . . . 162
6.3.4 Strong Coupling to the Metallic Lead . . . 163
6.4 Inelastic Tunneling in the Single-Particle Approximation . . . 164
6.4.1 The Inelastic Transmission Matrix . . . 165
6.4.2 Exact Solution in the Wide-Band Limit . . . 166
6.5 Sequential Inelastic Tunneling . . . 167
6.5.1 Master Equation . . . 167
6.5.2 Franck-Condon Blockade . . . 168
References . . . 170

Part II Advanced Methods

7 Nonequilibrium Green Functions . . . 173
7.1 Definition and Properties . . . 174
7.1.1 Retarded (G^R) and Advanced (G^A) Functions . . . 174
7.1.2 Lesser ($G^<$) and Greater ($G^>$) Functions . . . 177
7.1.3 Some Useful Relations . . . 178
7.1.4 Equilibrium Case. Fluctuation-Dissipation Theorem . . . 179
7.1.5 Free Fermions . . . 180
7.1.6 Free Bosons . . . 183
7.1.7 Green Functions for Vibrons . . . 183
7.2 Interaction Representation . . . 186

7.3 Schwinger-Keldysh Time Contour 189
7.3.1 Closed Time-Path Integration 189
7.3.2 Contour (Contour-Ordered) Green Function. 191
7.3.3 Contour Green Function in the Interaction Representation 192
7.4 Nonequilibrium Equation of Motion Method 193
7.4.1 Spectral (Retarded and Advanced) Functions 194
7.4.2 EOM at the Schwinger-Keldysh Contour 195
7.4.3 Kinetic (Lesser) Function 195
7.5 Kadanoff-Baym-Keldysh Method 196
7.5.1 Perturbation Expansion and Diagrammatic Rules for Contour Functions 196
7.5.2 Langreth Rules 198
7.5.3 First-Order Self-Energy and Polarization Operator 200
7.5.4 Self-consistent Equations 202
References 205

8 NGF Method for Transport Through Nanosystems 207
8.1 Standard Transport Model: A Nanosystem Between Ideal Electrodes 207
8.2 Nonequilibrium Current and Charge 210
8.3 Dyson-Keldysh Equations 212
8.3.1 General Time-Dependent Equations 212
8.3.2 Time-Independent Equations 215
8.4 Meir-Wingreen-Jauho Formula for Current 216
8.4.1 General Expression 216
8.4.2 Stationary Time-Independent Current 218
References 220

9 Some Nonequilibrium Problems 221
9.1 Vibronic Effects (Self-consistent Dyson-Keldysh Method). 221
9.1.1 The Electron-Vibron Hamiltonian. 222
9.1.2 Dyson-Keldysh Equations and Self-energies 223
9.1.3 Single-Level Model: Spectroscopy of Vibrons 226
9.1.4 Multi-level Model: Nonequilibrium Vibrons 229
9.2 Coulomb Blockade (EOM Method) 233
9.2.1 The Hubbard-Anderson Hamiltonian 234
9.2.2 Nonequilibrium EOM Formalism 235
9.2.3 Anderson Impurity Model 240
References 242

Index 245

Chapter 1
Introduction

1.1 Quantum Transport in Mesoscopic and Nanoscale Systems

What systems, models and methods are considered in this book? What is the meaning of the term "nanoscale" and what is its difference from the other known term "mesoscopic"?

One can note that *nanoscale* simply assumes *nanometer scale spatial dimensions*, very often any structure with at least one spatial dimension smaller than 100 nm ($1\,\text{nm} = 10^{-9}\,\text{m}$) is considered as a subject of nanoscience. This definition, however, includes all types of nanostructures independently of their behavior and physical properties, which can be more or less quantum or quite the contrary (semi)classical in the sense of required physical models. Many nanostructures actually can be described by well established classical or semiclassical models.

We will focus on *quantum transport* of charge, spin and heat. *Nanoscale* in this respect characterizes not the size, but rather a specific type of systems and effects, which can be distinguished from both classical systems and mesoscopic quantum systems.

If you insert the word "nanoscale" into the search line of your internet browser, you will probably find about 10 times more links than for the word "mesoscopic". Nevertheless, about 20 years ago, when the first books about quantum transport in mesoscopic systems and nanostructures had been published [1–5], almost any quantum transport was considered as mesoscopic. Actually the term "mesoscopic" characterized the intermediate size between atomic (microscopic) and bulk (macroscopic). On the other hand, the main methods required to describe experiments in the eighties of the 20th century, first of all the experiments with semiconductor heterostructures with μm sizes in transport directions, were based on the quasiclassical methods for quantum systems with dense (or even continuous) energy spectra. Besides, the theoretical description was not based on discrete-level models and could be considered in the language of real-space propagation paths and phase shifts. As a result, nowa-

D.A. Ryndyk, *Theory of Quantum Transport at Nanoscale*,
Springer Series in Solid-State Sciences 184,
DOI 10.1007/978-3-319-24088-6_1

days, mesoscopic is associated with quasiclassical systems with continuous or dense energy spectra.

But in last years, due to development of molecular electronics and computational methods for direct modeling at the atomic level, the methods specific for discrete-level systems become more and more important. At present, quantum nanoscale transport constitutes its own field of research separated not by hard walls, but by some visible boundaries from the remaining field of quantum mesoscopic transport. Let's try to estimate the parameters responsible for this boundary.

To some extent, the classification can be given based on the characteristic lengths and times. The most important scales are:

L—the size of the system or characteristic internal length *in transport direction*;
l_p, τ_p—the elastic scattering length (mean free path) and time;
l_ε, τ_ε—the inelastic scattering (energy relaxation) length and time;
l_φ, τ_φ—the phase-decoherence length and time;
λ_B—the de Broglie wave length (depends on the kinetic energy, for electrons in metals it is taken at the Fermi surface).

Typically the characteristic lengths go in the following order

$$\lambda_B < l_p < l_\phi < l_\varepsilon.$$

For example, in semiconductor (GaAs, Si) 2D electron gas at low temperatures the values can be $\lambda_F \approx 0.05\ \mu\text{m} = 50\,\text{nm}$, $l_p \approx 0.5\ \mu\text{m}$, $l_\varphi \approx 1\ \mu\text{m}$, $l_\varepsilon \approx 3\ \mu\text{m}$. In metals the numbers are similar: $l_\varphi \approx 1\ \mu\text{m}$ in gold at $T = 1$ K. At room temperatures all these lengths in metals and semiconductors are very small and transport is described by semiclassical models. Note that this is not the case for carbon nanostructures like nanotubes, where even at room temperature both electron and phonon transport can be quantum.

Two scales: the de Broglie wave length λ_B and the phase-decoherence length l_φ are specific for quantum transport (other exist also in the classical limit) and are most important for classification of transport regimes. In the case

$$\lambda_B \ll L \leqslant l_\varphi$$

the motion of electrons is phase-coherent and can not be described by classical equations, but in most cases it is still quasiclassical, which means that classical trajectories can be used as a starting point and quantum effects are included mainly into the phases of quasiclassical wave functions. This is just a case of *mesoscopic* system.

Based on the definition of mesoscopic systems as the systems with continuous energy spectrum, we define *nanoscale* systems as the systems with essentially discrete energy spectrum in some parts. Usually it means that a discrete-level system is coupled to infinitely large electrodes (or substrate) with continuous spectrum.For example, assume that the characteristic size of the central region in *transport*

direction starts to be comparable with the electron wave length:

$$L \sim \lambda_B.$$

In this case quantization of the single-particle energy levels starts to be important.

Of course, we are interested also in other cases when some system is naturally represented by discrete-level models. In particular, molecular junctions are described using the basis of atomic or molecular orbitals. One more origin of discrete *many-body* energy spectra is Coulomb interaction (the charging energy) in quantum dots and small grains. Finally, nanostructured low-dimensional materials (e.g. short nanotubes, graphene flakes, etc.) are described by discrete tight-binding (lattice) models.

Thus, we suggest a point of view that the boundary between mesoscopic and nanoscale systems is mainly the boundary between: (i) a continuous energy spectrum and continuity in real space of the equations for wave functions in the mesoscopic case; and (ii) discrete energy spectrum and discrete basis wave functions in nanosystems. Of course, there is no strict separation between meso- and nano- transport and very often people actually mix these two terms. However, to have practical limits in the extremely wide field of nanoscience, I consider in this book only transport through *quantum nanosystems with discrete energy spectrum*, such as metal grains, semiconductor quantum dots and single molecules, coupled to one, two, or larger number of electrodes.

We *do not consider* in this book the methods and approaches, which are typical only for mesoscopic transport and focus instead specifically on nanoscale transport questions. In particular, the following topics are not included:

- quantum interference of Aharonov-Bohm type;
- weak localization;
- universal conductance fluctuations;
- random matrix theory;
- quantum Hall effect;
- quasiclassical and semiclassical transport.

I refer the readers to numerous special reviews on mesoscopic transport.

Still, there are some topics important for both quasiclassical (mesoscopic) and pure quantum (nanoscale) systems, for example the Landauer scattering approach. That is the reason why we start from the "mesoscopic" Landauer-Büttiker method in Chap. 2. However, in the next Chap. 3 we formulate the Landauer approach for discrete basis using the technique of matrix Green functions, in such a way we get a nanoscale version of this approach.

There is one other significant peculiarity of nanoscale systems: the enhanced role of interactions. The theory of mesoscopic transport is based usually on free particles or weakly interacting particles, the perturbation theory is widely used. At nanoscale, as we already mentioned, both electron-electron and electron-vibron interactions may be strong and the Landauer approach can not be used anymore. Fortunately, we can use the powerful methods of Nonequilibrium Green Functions and Quantum Master Equation, able to treat the many-body problems.

1.2 Nanojunctions

We focus on the models describing some *central system*, placed between two or many *ideal electrodes*, which are assumed to be noninteracting and being in thermal equilibrium. On the contrary, the central system can be interacting and can be nonequilibrium if finite voltage is applied. One can call such systems *nanojunctions*. Depending on the ratio between the energy scales associated with electron-electron or electron-vibron *interactions* in the central system (examples of these energy scales are the effective charging energy and the polaron energy) and coupling to the leads, nanojunctions can be classified in several groups.

In the case of strong coupling to the electrodes and weak interactions, the electronic states of the central system are hybridized with states in the electrodes, charge quantization is suppressed, transport is mainly coherent and the conductance is of the order of the conductance quantum $G_0 = 2e^2/h$. In some cases one can ignore completely the atomistic structure and formulate the model in the continuum medium approximation (a typical example is the nanojunction shown in Fig. 1.1), or use the lattice (tight-binding) model with given parameters. The basic way to understand quantum coherent transport in noninteracting systems is Landauer-Büttiker method (usually formulated for atomistic or lattice systems with Green function formalism). We consider coherent transport in Chaps. 2 and 3.

In the case of very weak coupling to the electrodes (Fig. 1.2), the electronic states of the central system are only weakly disturbed, strong charge quantization and Coulomb blockade take place and transport is mainly determined by sequential tunneling. The central region in this case is often called *quantum dot*. In this case the master equation for probabilities of the many-body states is a good starting point. We consider different examples of sequential tunneling through the systems with Coulomb blockade and polaron effects in Chaps. 5 and 6.

Besides, the important limiting case is a strongly asymmetric nanojunction (Fig. 1.3), when the central region is strongly coupled to one electrode and weakly coupled to other one. This is a typical situation for STM experiments. The peculiarity of this case is that the central region (quantum dot, molecule) is in equilibrium or weakly nonequilibrium state even at large voltage, because it keeps the state in

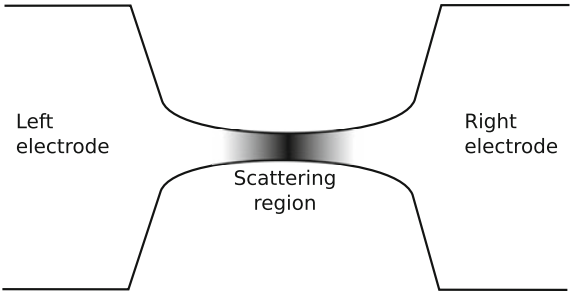

Fig. 1.1 Schematic picture of a nanojunction with strong coupling to the electrodes

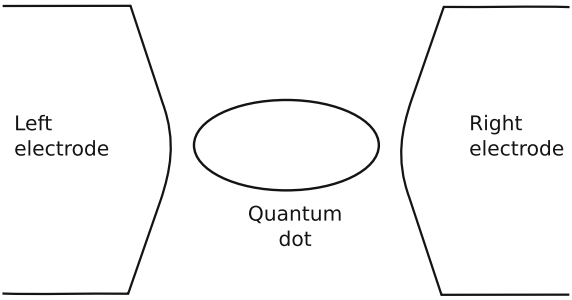

Fig. 1.2 Schematic picture of a nanojunction (quantum dot) with weak coupling to the electrodes

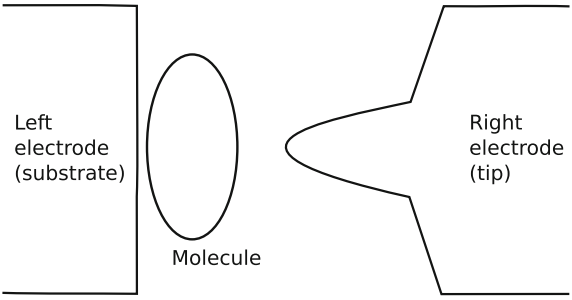

Fig. 1.3 Schematic picture of a strongly asymmetric nanojunction (STM set-up)

equilibrium with stronger coupled electrode. This type of junctions (as well as any direct contacts between two electrodes without any central region) can be describe by the so-called Tunneling (or Transfer) Hamiltonian method without use of more sophisticated methods. We consider tunneling in Chap. 4.

1.3 From Basic Concepts to Advanced Methods

The theoretical treatment of transport at nanoscale (see introduction in [1–12]) requires the combined use of different techniques and approximations. We will consider discrete-level models starting from few-level and tight-binding noninteracting models and going in the direction towards the many-body models with strong electron-electron and electron-vibron interactions. Let us now outline the main concepts.

Landauer-Büttiker method [13–22] establishes the fundamental relation between the wave functions (scattering amplitudes) of a junction and its conducting properties. The method can be applied to find the current through a noninteracting system or through an *effectively noninteracting* system, for example if the mean-field description is valid and the inelastic scattering is not essential. Such type of an electron transport is called coherent, because there is no phase-breaking and quantum interference is preserved during the electron motion across the system. In fact, coherence is assumed in many *ab initio* based transport methods using the density-

functional theory and Landauer approach (DFT/Landauer), so that the Landauer-Büttiker method is now routinely applied to any basic transport calculation through nanosystems and single molecules. Besides, it is directly applicable in many semiconductor quantum dot systems with weak electron-electron interactions. Due to simplicity and generality of this method, it is now widely accepted and is in the base of our understanding of coherent transport.

However, the peculiarity of single-molecule transport is the essential role of electron-electron and electron-vibron interactions, so that Landauer-Büttiker method is usually not enough to describe essential physics even qualitatively.

The methods required to describe transport in weakly coupled junctions are usually different from the strong coupling case, because the effects of interactions are controlled by the parameters U/Γ for Coulomb interaction and λ/Γ for electron-vibron interaction and become larger for tunneling junctions. Here U is the characteristic Coulomb energy of electron-electron interaction ("Hubbard U"), λ is the electron-vibron interaction constant, and Γ is the coupling to electrodes.

During last years many new methods were developed to describe transport at finite voltage, with focus on correlation and inelastic effects, in particular in the cases when Coulomb blockade, Kondo effect and vibronic effects take place. There are two main theoretical frameworks that can be used to study quantum transport with interactions and at finite voltage: quantum master equation and nonequilibrium Green function techniques .

Quantum Master Equation (QME) [23, 24] is usually formulated in the basis of the many-body eigenstates of the molecule. It gives a fairly complete description of sequential tunneling, the main features of Coulomb blockade and even can capture Kondo physics for temperatures of the order of or larger than the Kondo temperature [25]. The QME technique leads to more simple "classical" master equations in the case where (i) the electrode-system coupling can be considered as a weak perturbation, and (ii) off-diagonal elements of the reduced density matrix in the eigenstate representation (coherences) can be neglected due to very short decoherence times.

Nonequilibrium Green function (NGF) [2, 26–29] formalism is able to deal with a very broad variety of physical problems related to quantum transport.

The method, which was proposed about 50 years ago [26, 27], then was used successfully in the theory of nonequilibrium superconductivity [30–34], and later was proposed as a standard approach in mesoscopic physics and molecular electronics [35–37]. We consider the general NGF formalism in Chap. 7 and the NGF method for transport through nanosystems in Chap. 8. The advantage of the NGF formalism is that it can be successfully applied to a variety of systems and problems, that it is in principle exact, and many powerful approximations can be derived from it.

It can deal with strong non-equilibrium situations via an extension of the conventional Green Function formalism to the Schwinger-Keldysh contour [27] and it can also include interaction effects (electron-electron, electron-vibron, etc.) in a systematic way (diagrammatic perturbation theory, equation of motion techniques). Proposed the first time for the mesoscopic structures in the early seventies by Caroli et al. [38–41], this approach was formulated in an elegant way by Meir, Wingreen and Jauho [2, 35, 37, 42, 43], who derived an exact expression for nonequilibrium

current through an interacting nanosystem placed between large noninteracting leads in terms of the nonequilibrium Green functions of the nanosystem. Still, the problem of calculation of these Green functions is not trivial. We consider some possible approaches in the case of electron-electron and electron-vibron interactions. Moreover, as we will show later on, it can reproduce results obtained within the master equation approach in the weak coupling limit to the electrodes (Coulomb blockade), but it can also go *beyond* this limit and cover intermediate coupling (Kondo effect) and strong coupling (Fabry-Pérot) domains. It thus offers the possibility of dealing with different physical regimes in a unified way.

Both approaches, the QME and NGF techniques, can yield formally exact expressions for many observables. For noninteracting systems, one can even solve many models analytically. However, once interactions are introduced—and these are the most interesting cases containing a very rich physics—different approximation schemes have to be introduced to make the problems tractable. We consider some examples of nonequilibrium problems in Chap. 9.

Coulomb interaction is in the origin of such fundamental effects as Coulomb blockade and Kondo effect. The most convenient and simple enough is the Hubbard-Anderson model, combining the formulations of Anderson impurity model [44] and Hubbard many-body model [45–47]. To analyze strongly correlated systems several complementary methods can be used: master equation and perturbation in tunneling, equation-of-motion method, self-consistent Green functions, renormalization group and different numerical methods.

When the coupling to the leads is weak, the electron-electron interaction results in Coulomb blockade, the sequential tunneling is described by the master equation method [48–55] and small cotunneling current in the blockaded regime can be calculated by the next-order perturbation theory [56–59]. This theory was used successfully to describe electron tunneling via discrete quantum states in quantum dots [60–63]. Recently there were several attempts to apply the master equation to multi-level models of molecules, in particular describing benzene rings [64–67].

To describe consistently cotunneling, level broadening and higher-order (in tunneling) processes, more sophisticated methods to calculate the reduced density matrix were developed, based on the Liouville–von Neumann equation [66, 68–74] or real-time diagrammatic technique [25, 75–81]. Different approaches were reviewed recently in [82].

The equation-of-motion (EOM) method is one of the basic and powerful ways to find the Green functions of interacting quantum systems. In spite of its simplicity it gives the appropriate results for strongly correlated nanosystems, describing qualitatively and in some cases quantitatively such important transport phenomena as Coulomb blockade and Kondo effect in quantum dots. The results of the EOM method could be calibrated with other available calculations, such as the master equation approach in the case of weak coupling to the leads, and the perturbation theory in the case of strong coupling to the leads and weak electron-electron interaction.

In the case of a single site junction with two (spin-up and spin-down) states and Coulomb interaction between these states (Anderson impurity model), the *linear con-*

ductance properties have been successfully studied by means of the EOM approach in the cases related to Coulomb blockade [83, 84] and the Kondo effect [85]. Later the same method was applied to some two-site models [86–89]. Multi-level systems started to be considered only recently [90, 91]. Besides, there are some difficulties in building the lesser Green function in the nonequilibrium case (at finite bias voltages) by means of the EOM method [92–94].

The diagrammatic method was also used to analyze the Anderson impurity model. First of all, the perturbation theory can be used to describe weak electron-electron interaction and even some features of the Kondo effect [95]. The family of non-perturbative current-conserving self-consistent approximations for Green functions has a long history and goes back to the Schwinger functional derivative technique, Kadanoff-Baym approximations and Hedin equations in the equilibrium many-body theory [96–103]. Recently GW approximation was investigated together with other methods [104–107]. It was shown that dynamical correlation effects and self-consistency can be very important at finite bias.

Vibrons (the localized phonons) is the other important ingredient of the models, describing single molecules because molecules are flexible. The theory of electron-vibron interaction has a long history, but many questions it implies are not answered up to now. While the isolated electron-vibron model can be solved exactly by the so-called polaron or Lang-Firsov transformation [108–110], the coupling to the leads produces a true many-body problem. The inelastic resonant tunneling of *single* electrons through the localized state coupled to phonons was considered in [111–116]. There the exact solution in the single-particle approximation was derived, ignoring completely the Fermi sea in the leads. At strong electron-vibron interaction and weak couplings to the leads the sidebands of the main resonant peak are formed in the spectral function.

The essential progress in calculation of transport properties in the strong electron-vibron interaction limit has been made with the help of the master equation approach [117–126]. This method, however, is valid only in the limit of very weak molecule-to-lead coupling and neglects all spectral effects, which are the most important at finite coupling to the leads.

At strong coupling to the leads and finite level width the master equation approach can no longer be used, and we apply alternatively the nonequilibrium Green function technique which has been recently developed to treat vibronic effects in a perturbative or self-consistent way in the cases of weak and intermediate electron-vibron interaction [127–144].

The case of intermediate and strong electron-vibron interaction *at intermediate coupling to the leads* is the most interesting, but also the most difficult. The existing approaches are mean-field [145–147], or start from the exact solution for the isolated system and then treat tunneling as a perturbation [148–154]. The fluctuations beyond mean-field approximations were considered in [155, 156]

In parallel, the related activity was in the field of single-electron shuttles and quantum shuttles [157–167]. Finally, based on the Bardeen's tunneling Hamiltonian method [168–172] and Tersoff-Hamann approach [173, 174], the theory of inelastic electron tunneling spectroscopy (IETS) was developed [127–130, 175–177].

For a recent review of the electron-vibron problem and its relation to the molecular transport see [178].

Finally, we want to mention briefly three important fields of research, that we do not consider in this book: the theory of Kondo effect [85, 179–185], spin-dependent transport [186–190], and time-dependent transport [37, 191–194].

1.4 Notations

Here we collect some notations that we use throughout the book.

$e = -|e|$ for electrons, $e = |e|$ for holes, in other words e is *with sign*,
$\eta \equiv 0^+$—infinitesimally small positive number,

$|...\rangle$—Dirac symbol for quantum state,
$\hat{...}$—general operator notations: $\hat{H}$, $\hat{V}$, $\hat{I}$, etc.,
$\breve{...}$—notation for matrices in Keldysh space: $\breve{G}$, $\breve{\Sigma}$, etc.,

Greek letters α, β, γ, δ—single-particle states of the central system, including spin,
Greek letters σ, σ'—spin indices,
Latin letters p, s, etc.—indices of electrodes,
Bold italic capital Latin letters $\boldsymbol{H}$, $\boldsymbol{V}$, $\boldsymbol{I}$, $\boldsymbol{E}$, etc.— are used for *matrices*,
μ_s—chemical potential of the s-th electrode,
φ_s—electrical potential of the s-th electrode,
$\boldsymbol{S}$—scattering matrix,
$\boldsymbol{G}^R$, $\boldsymbol{\Sigma}^R$—retarded functions,
$\boldsymbol{G}^A$, $\boldsymbol{\Sigma}^A$—advanced functions,
$\boldsymbol{G}^<$, $\boldsymbol{\Sigma}^<$—lesser functions,
$\boldsymbol{\Sigma}_L$, $\boldsymbol{\Sigma}_R$, $\boldsymbol{\Sigma}_s$.—self-energies (matrix) of the right, left, s-th electrode,
$\boldsymbol{\Gamma}_L$, $\boldsymbol{\Gamma}_R$, $\boldsymbol{\Gamma}_s$.—level-width functions (matrix) of the right, left, s-th electrode,

$T(E)$—transmission function,

$G_0 = \dfrac{2e^2}{h}$—conductance quantum.

The functions $f_F(x)$ and $f'_F(x)$ are always assumed to be

$$f_F(x) = \frac{1}{e^x + 1},$$

$$f'_F(x) = -\frac{e^x}{(e^x + 1)^2}.$$

References

1. S. Datta, *Electronic Transport in Mesoscopic Systems*. (Cambridge University Press, Cambridge, 1995)
2. H. Haug, A.P. Jauho, *Quantum Kinetics in Transport and Optics of Semiconductors*, vol. 123, Springer Series in Solid-State Physics (Springer, Berlin, 1996)
3. Y. Imry, *Introduction to Mesoscopic Physics* (Oxford University Press, New York, 1997)
4. D.K. Ferry, S.M. Goodnick, *Transport in Nanostructures* (Cambridge University Press, Cambridge, 1997)
5. T. Dittrich, P. Hänggi, G. Ingold, G. Schön, W. Zwerger, *Quantum Dissipation and Transport* (Wiley-VCH, Weinheim, 1998)
6. H. Bruus, K. Flensberg, *Many-Body Quantum Theory in Condensed Matter Physics* (Oxford University Press, Oxford, 2004)
7. G. Cuniberti, G. Fagas, K. Richter (eds.), *Introducing Molecular Electronics*, vol. 680, Lecture Notes in Physics (Springer, Berlin, 2005)
8. S. Datta, *Quantum Transport: Atom to Transistor* (Cambridge University Press, Cambridge, 2005)
9. M. Di Ventra, *Electrical Transport in Nanoscale Systems* (Cambridge University Press, Cambridge, 2008)
10. Y.V. Nazarov, Y.M. Blanter, *Quantum Transport: Introduction to Nanoscience* (Cambridge University Press, Cambridge, 2009)
11. D.K. Ferry, S.M. Goodnick, J.P. Bird, *Transport in Nanostructures*, 2nd edn. (Cambridge University Press, Cambridge, 2009)
12. J.C. Cuevas, E. Scheer, *Molecular Electronics: An Introduction to Theory and Experiment* (World Scientific, Singapore, 2010)
13. R. Landauer, IBM, J. Res. Develop. **1**, 223 (1957)
14. R. Landauer, Phil. Mag. **21**, 863 (1970)
15. E.N. Economou, C.M. Soukoulis, Phys. Rev. Lett. **46**, 618 (1981)
16. D.S. Fisher, P.A. Lee, Phys. Rev. B **23**, 6851 (1981)
17. M. Büttiker, Y. Imry, R. Landauer, S. Pinhas, Phys. Rev. B **31**, 6207 (1985)
18. M. Büttiker, Phys. Rev. Lett. **57**, 1761 (1986)
19. R. Landauer, IBM, J. Res. Develop. **32**, 306 (1988)
20. M. Büttiker, IBM, J. Res. Develop. **32**, 317 (1988)
21. A.D. Stone, A. Szafer, IBM, J. Res. Develop. **32**, 384 (1988)
22. H.U. Baranger, A.D. Stone, Phys. Rev. B **40**, 8169 (1989)
23. U. Weiss, *Quantum Dissipative Systems*, *Series in Modern Condensed Matter Physics*, vol. 10 (World Scientific, Singapore, 1999)
24. H.P. Breuer, F. Petruccione, *The Theory of Open Quantum Systems* (Oxford University Press, Oxford, 2002)
25. J. König, J. Schmid, H. Schoeller, G. Schön, Phys. Rev. B **54**, 16820 (1996)
26. L. Kadanoff, G. Baym, *Quantum Statistical Mechanics* (Benjamin, New York, 1962)
27. L.V. Keldysh, Zh. Eksp. Teor. Fiz. **47**, 1515 (1964). [Sov. Phys. JETP **20**, 1018 (1965)]
28. D. Langreth, in *Linear and Nonlinear Electron Transport in Solid*, ed. by J. Devreese, E. van Doren (Plenum, New York, 1976)
29. J. Rammer, H. Smith, Rev. Mod. Phys. **58**, 323 (1986)
30. G. Eliashberg, Zh. Eksp. Teor. Fiz. **61**, 1254 (1971). [Sov. Phys. JETP **34**, 668 (1972)]
31. A. Larkin, Y. Ovchinnikov, Zh. Eksp. Teor. Fiz. **68**, 1915 (1975). [Sov. Phys. JETP **41**, 960 (1975)]
32. K. Gray (ed.), *Nonequilibrium Superconductivity, Phonons, and Kapitza Boundaries (Proc. NATO ASI)* (Plenum, New York, 1981)
33. D. Langenberg, A. Larkin (eds.), *Nonequilibrium Superconductivity, Modern Problems in Condensed Matter Sciences*, vol. 12 (North-Holland, Amsterdam, 1986)
34. N.B. Kopnin, *Theory of Nonequilibrium Superconductivity* (Clarendon Press, Oxford, 2001)

35. Y. Meir, N.S. Wingreen, Phys. Rev. Lett. **68**, 2512 (1992)
36. E. Runge, H. Ehrenreich, Phys. Rev. B **45**, 9145 (1992)
37. A.P. Jauho, N.S. Wingreen, Y. Meir, Phys. Rev. B **50**, 5528 (1994)
38. C. Caroli, R. Combescot, P. Nozieres, D. Saint-James, J. Phys. C: Solid St. Phys. **4**, 916 (1971)
39. C. Caroli, R. Combescot, D. Lederer, P. Nozieres, D. Saint-James, J. Phys. C: Solid St. Phys. **4**, 2598 (1971)
40. R. Combescot, J. Phys. C: Solid St. Phys. **4**, 2611 (1971)
41. C. Caroli, R. Combescot, P. Nozieres, D. Saint-James, J. Phys. C: Solid St. Phys. **5**, 21 (1972)
42. N.S. Wingreen, A.P. Jauho, Y. Meir, Phys. Rev. B **48**, 8487 (1993)
43. A.P. Jauho, J. Phys.: Conf. Ser. **35**, 313 (2006)
44. P.W. Anderson, Phys. Rev. **124**, 41 (1961)
45. J. Hubbard, Proc. R. Soc. Lond. Ser. A **276**, 238 (1963)
46. J. Hubbard, Proc. R. Soc. Lond. Ser. A **277**, 237 (1964)
47. J. Hubbard, Proc. R. Soc. Lond. Ser. A **281**, 401 (1964)
48. D.V. Averin, K.K. Likharev, J. Low Temp. Phys. **62**(3/4), 345 (1986)
49. D.V. Averin, K.K. Likharev, in *Mesoscopic phenomena in solids*, ed. by B.L. Altshuler, P.A. Lee, R.A. Webb (Elsevier, Amsterdam, 1991), p. 173
50. H. Grabert, M.H. Devoret (eds.), *Single Charge Tunneling*, *NATO ASI Series B*, vol. 294 (Plenum, New York, 1992)
51. H. van Houten, C.W.J. Beenakker, A.A.M. Staring, in *Single Charge Tunneling. NATO ASI Series B. Vol. 294*, ed. by H. Grabert, M.H. Devoret (Plenum, New York, 1992), p. 167
52. L.P. Kouwenhoven, C.M. Markus, P.L. McEuen, S. Tarucha, R.M. Westervelt, N.S. Wingreen, in *Mesoscopic Electron Transport*, ed. by L.L. Sohn, L.P. Kouwenhoven, G. Schön (Kluwer, 1997), NATO ASI Series E: Applied Sciences, p. 105
53. H. Schoeller, in *Mesoscopic Electron Transport*, ed. by L.L. Sohn, L.P. Kouwenhoven, G. Schön (Kluwer, 1997), NATO ASI Series E: Applied Sciences, p. 291
54. G. Schön, in *Quantum Dissipation and Transport* (Wiley-VCH, Weinheim, 1998)
55. W.G. van der Wiel, S. De Franceschi, J.M. Elzerman, T. Fujisawa, S. Tarucha, L.P. Kouwenhoven, Rev. Mod. Phys. **75**, 1 (2002)
56. D.V. Averin, A.A. Odintsov, Phys. Lett. A **140**(5), 251 (1989)
57. D.V. Averin, Y.V. Nazarov, Phys. Rev. Lett. **65**, 2446 (1990)
58. D.V. Averin, Y.V. Nazarov, *Macroscopic Quantum Tunneling of Charge and Co-tunneling* (Plenum, 1992), *NATO ASI Series B*, vol. 294, Chap. 6, p. 217
59. I. Aleiner, P. Brouwer, L. Glazman, Phys. Rep. **358**(56), 309 (2002)
60. D.V. Averin, A.N. Korotkov, K.K. Likharev, Phys. Rev. B **44**, 6199 (1991)
61. C.W.J. Beenakker, Phys. Rev. B **44**, 1646 (1991)
62. J. von Delft, D.C. Ralph, Phys. Rep. **345**, 61 (2001)
63. E. Bonet, M.M. Deshmukh, D.C. Ralph, Phys. Rev. B **65**, 045317 (2002)
64. M.H. Hettler, W. Wenzel, M.R. Wegewijs, H. Schoeller, Phys. Rev. Lett. **90**, 076805 (2003)
65. B. Muralidharan, A.W. Ghosh, S. Datta, Phys. Rev. B **73**, 155410 (2006)
66. G. Begemann, D. Darau, A. Donarini, M. Grifoni, Phys. Rev. B **77**, 201406 (2008)
67. D.A. Ryndyk, A. Donarini, M. Grifoni, K. Richter, Phys. Rev. B **88**, 085404 (2013)
68. E.G. Petrov, V. May, P. Hanggi, Chem. Phys. **296**, 251 (2004)
69. E.G. Petrov, V. May, P. Hanggi, Chem. Phys. **319**, 380 (2005)
70. E.G. Petrov, V. May, P. Hanggi, Phys. Rev. B **73**, 045408 (2006)
71. F. Elste, C. Timm, Phys. Rev. B **71**, 155403 (2005)
72. U. Harbola, M. Esposito, S. Mukamel, Phys. Rev. B **74**, 235309 (2006)
73. J.N. Pedersen, B. Lassen, A. Wacker, M.H. Hettler, Phys. Rev. B **75**, 235314 (2007)
74. L. Mayrhofer, M. Grifoni, Eur. Phys. J. B **56**, 107 (2007)
75. H. Schoeller, G. Schön, Phys. Rev. B **50**, 18436 (1994)
76. J. König, H. Schoeller, G. Schön, Phys. Rev. Lett. **76**, 1715 (1996)
77. J. König, H. Schoeller, G. Schön, Phys. Rev. Lett. **78**, 4482 (1997)
78. J. König, H. Schoeller, G. Schön, Phys. Rev. B **58**, 7882 (1998)
79. A. Thielmann, M.H. Hettler, J. König, G. Schön, Phys. Rev. B **68**, 115105 (2003)

80. A. Thielmann, M.H. Hettler, J. Konig, G. Schon, Phys. Rev. Lett. **95**, 146806 (2005)
81. J. Aghassi, A. Thielmann, M.H. Hettler, G. Schon, Phys. Rev. B **73**, 195323 (2006)
82. C. Timm, Phys. Rev. B **77**, 195416 (2008)
83. C. Lacroix, J. Phys. F: Met. Phys. **11**, 2389 (1981)
84. Y. Meir, N.S. Wingreen, P.A. Lee, Phys. Rev. Lett. **66**, 3048 (1991)
85. Y. Meir, N.S. Wingreen, P.A. Lee, Phys. Rev. Lett. **70**, 2601 (1993)
86. C. Niu, L.J. Liu, T.H. Lin, Phys. Rev. B **51**, 5130 (1995)
87. P. Pals, A. MacKinnon, J. Phys.: Condens. Matter **8**, 5401 (1996)
88. S. Lamba, S.K. Joshi, Phys. Rev. B **62**, 1580 (2000)
89. B. Song, D.A. Ryndyk, G. Cuniberti, Phys. Rev. B **76**, 045408 (2007)
90. J.J. Palacios, L. Liu, D. Yoshioka, Phys. Rev. B **55**, 15735 (1997)
91. L. Yi, J.S. Wang, Phys. Rev. B **66**, 085105 (2002)
92. C. Niu, D.L. Lin, T.H. Lin, J. Phys.: Condens. Matter **11**, 1511 (1999)
93. R. Swirkowicz, J. Barnas, M. Wilczynski, Phys. Rev. B **68**, 195318 (2003)
94. B.R. Bulka, T. Kostyrko, Phys. Rev. B **70**, 205333 (2004)
95. T. Fujii, K. Ueda, Phys. Rev. B **68**, 155310 (2003)
96. J. Schwinger, PNAS **37**, 452
97. P.C. Martin, J. Schwinger, Phys. Rev. **115**, 1342 (1959)
98. G. Baym, L.P. Kadanoff, Phys. Rev. **124**, 287 (1961)
99. G. Baym, Phys. Rev. **127**, 1391 (1962)
100. L. Hedin, Phys. Rev. **139**, A796 (1965)
101. F. Aryasetiawany, O. Gunnarsson, Rep. Prog. Phys. **61**, 237 (1988)
102. J.A. White, Phys. Rev. B **45**, 1100
103. G. Onida, L. Reining, A. Rubio, Rev. Mod. Phys. **74**, 601 (2002)
104. K.S. Thygesen, A. Rubio, J. Chem. Phys. **126**, 091101 (2007)
105. K.S. Thygesen, Phys. Rev. Lett. **100**, 166804 (2008)
106. K.S. Thygesen, A. Rubio, Phys. Rev. B **77**, 115333 (2008)
107. X. Wang, C.D. Spataru, M.S. Hybertsen, A.J. Millis, Phys. Rev. B **77**, 045119 (2008)
108. I.G. Lang, Y.A. Firsov, Sov. Phys. JETP **16**, 1301 (1963)
109. A.C. Hewson, D.M. Newns, Jpn. J. Appl. Phys. Suppl. **2**(Pt. 2), 121 (1974)
110. G. Mahan, *Many-Particle Physics*, 2nd edn. (Plenum, New York, 1990)
111. L.I. Glazman, R.I. Shekhter, Zh. Eksp. Teor. Fiz. **94**, 292 (1988). [Sov. Phys. JETP **67**, 163 (1988)]
112. N.S. Wingreen, K.W. Jacobsen, J.W. Wilkins, Phys. Rev. Lett. **61**, 1396 (1988)
113. N.S. Wingreen, K.W. Jacobsen, J.W. Wilkins, Phys. Rev. B **40**, 11834 (1989)
114. M. Jonson, Phys. Rev. B **39**, 5924 (1989)
115. M. Cízek, M. Thoss, W. Domcke, Phys. Rev. B **70**, 125406 (2004)
116. M. Cízek, Czech. J. of Phys. **55**, 189 (2005)
117. S. Braig, K. Flensberg, Phys. Rev. B **68**, 205324 (2003)
118. V. Aji, J.E. Moore, C.M. Varma, cond-mat/0302222 (2003)
119. A. Mitra, I. Aleiner, A.J. Millis, Phys. Rev. B **69**, 245302 (2004)
120. J. Koch, F. von Oppen, Phys. Rev. Lett. **94**, 206804 (2005)
121. J. Koch, M. Semmelhack, F. von Oppen, A. Nitzan, Phys. Rev. B **73**, 155306 (2006)
122. J. Koch, F. von Oppen, A.V. Andreev, Phys. Rev. B **74**, 205438 (2006)
123. K.C. Nowack, M.R. Wegewijs, cond-mat/0506552 (2005)
124. A. Zazunov, D. Feinberg, T. Martin, Phys. Rev. B **73**, 115405 (2006)
125. D.A. Ryndyk, P. D'Amico, G. Cuniberti, K. Richter, Phys. Rev. B **78**, 085409 (2008)
126. D.A. Ryndyk, P. D'Amico, K. Richter, Phys. Rev. B **81**, 115333 (2010)
127. S. Tikhodeev, M. Natario, K. Makoshi, T. Mii, H. Ueba, Surf. Sci. **493**, 63 (2001)
128. T. Mii, S. Tikhodeev, H. Ueba, Surf. Sci. **502**, 26 (2002)
129. T. Mii, S. Tikhodeev, H. Ueba, Phys. Rev. B **68**, 205406 (2003)
130. S. Tikhodeev, H. Ueba, Phys. Rev. B **70**, 125414 (2004)
131. M. Galperin, M.A. Ratner, A. Nitzan, Nano Lett. **4**, 1605 (2004)
132. M. Galperin, M.A. Ratner, A. Nitzan, J. Chem. Phys. **121**(23), 11965 (2004)

133. M. Galperin, A. Nitzan, M.A. Ratner, D.R. Stewart, J. Phys. Chem. B **109**, 8519 (2005)
134. T. Frederiksen, Inelastic electron transport in nanosystems. Master's thesis, Technical University of Denmark (2004)
135. T. Frederiksen, M. Brandbyge, N. Lorente, A.P. Jauho, Phys. Rev. Lett. **93**, 256601 (2004)
136. M. Hartung, Vibrational effects in transport through molecular junctions. Master's thesis, University of Regensburg (2004)
137. D.A. Ryndyk, J. Keller, Phys. Rev. B **71**, 073305 (2005)
138. D.A. Ryndyk, M. Hartung, G. Cuniberti, Phys. Rev. B **73**, 045420 (2006)
139. D.A. Ryndyk, G. Cuniberti, Phys. Rev. B **76**, 155430 (2007)
140. M. Paulsson, T. Frederiksen, M. Brandbyge, Phys. Rev. B **72**, 201101 (2005). [Erratum: **75**, 129901(E) (2007)]
141. M. Paulsson, T. Frederiksen, M. Brandbyge, J. Phys.: Conf. Series **35**, 247 (2006)
142. P.I. Arseyev, N.S. Maslova, JETP Lett. **82**, 297 (2005)
143. P.I. Arseyev, N.S. Maslova, JETP Lett. **84**, 93 (2006)
144. A. Zazunov, R. Egger, C. Mora, T. Martin, Phys. Rev. B **73**, 214501 (2006)
145. A.C. Hewson, D.M. Newns, J. Phys. C: Solid State Phys. **12**, 1665 (1979)
146. M. Galperin, M.A. Ratner, A. Nitzan, Nano Lett. **5**, 125 (2005)
147. P. D'Amico, D.A. Ryndyk, G. Cuniberti, K. Richter, New J. Phys. **10**, 085002 (2008)
148. P. Král, Phys. Rev. B **56**, 7293 (1997)
149. U. Lundin, R.H. McKenzie, Phys. Rev. B **66**, 075303 (2002)
150. J.X. Zhu, A.V. Balatsky, Phys. Rev. B **67**, 165326 (2003)
151. A.S. Alexandrov, A.M. Bratkovsky, Phys. Rev. B **67**(23), 235312 (2003)
152. K. Flensberg, Phys. Rev. B **68**, 205323 (2003)
153. M. Galperin, M.A. Ratner, A. Nitzan, Phys. Rev. B **73**, 045314 (2006)
154. A. Zazunov, T. Martin, Phys. Rev. B **76**, 033417 (2007)
155. A. Mitra, I. Aleiner, A.J. Millis, Phys. Rev. Lett. **94**, 076404 (2005)
156. D. Mozyrsky, M.B. Hastings, I. Martin, Phys. Rev. B **73**, 035104 (2006)
157. L.Y. Gorelik, A. Isacsson, M.V. Voinova, B. Kasemo, R.I. Shekhter, M. Jonson, Phys. Rev. Lett. **80**, 4526 (1998)
158. D. Boese, H. Schoeller, Europhys. Lett. **54**, 668 (2001)
159. D. Fedorets, L.Y. Gorelik, R.I. Shekhter, M. Jonson, Europhys. Lett. **58**, 99 (2002)
160. D. Fedorets, Phys. Rev. B **68**, 033106 (2003)
161. D. Fedorets, L.Y. Gorelik, R.I. Shekhter, M. Jonson, Phys. Rev. Lett. **92**, 166801 (2004)
162. K.D. McCarthy, N. Prokof'ev, M.T. Tuominen, Phys. Rev. B **67**, 245415 (2003)
163. T. Novotný, A. Donarini, A.P. Jauho, Phys. Rev. Lett. **90**, 256801 (2003)
164. T. Novotný, A. Donarini, C. Flindt, A.P. Jauho, Phys. Rev. Lett. **92**, 248302 (2004)
165. Ya.M. Blanter, O. Usmani, Yu.V. Nazarov, Phys. Rev. Lett. **93**, 136802 (2004)
166. A.Y. Smirnov, L.G. Mourokh, N.J.M. Horing, Phys. Rev. B **69**, 155310 (2004)
167. N.M. Chtchelkatchev, W. Belzig, C. Bruder, Phys. Rev. B **70**, 193305 (2004)
168. J. Bardeen, Phys. Rev. Lett. **6**, 57 (1961)
169. W.A. Harrison, Phys. Rev. **123**, 85 (1961)
170. M.H. Cohen, L.M. Falicov, J.C. Phillips, Phys. Rev. Lett. **8**, 316 (1962)
171. R.E. Prange, Phys. Rev. **131**, 1083 (1963)
172. C.B. Duke, *Tunneling in Solids* (Academic Press, New York, 1969). Chapter VII
173. J. Tersoff, D.R. Hamann, Phys. Rev. Lett. **50**, 1998 (1983)
174. J. Tersoff, D.R. Hamann, Phys. Rev. B **31**, 805 (1985)
175. B.N.J. Persson, A. Baratoff, Phys. Rev. Lett. **59**, 339 (1987)
176. M.A. Gata, P.R. Antoniewicz, Phys. Rev. B **47**, 13797 (1993)
177. H. Raza, K.H. Bevan, D. Kienle, Phys. Rev. B **77**, 035432 (2008)
178. M. Galperin, M.A. Ratner, A. Nitzan, J. Phys.: Condens. Matter **19**, 103201 (2007)
179. L.I. Glazman, M.E. Raikh, Pis'ma Zh. Eksp. Teor. Fiz. **47**, 378 (1988). [JETP Lett. **47**, 452 (1988)]
180. T.K. Ng, P.A. Lee, Phys. Rev. Lett. **61**, 1768 (1988)
181. S. Hershfield, J.H. Davies, J.W. Wilkins, Phys. Rev. B **46**, 7046 (1992)

182. N.S. Wingreen, Y. Meir, Phys. Rev. B **49**, 11040 (1994)
183. R. Aguado, D.C. Langreth, Phys. Rev. Lett. **85**, 1946 (2000)
184. T.S. Kim, S. Hershfield, Phys. Rev. B **63**, 245326 (2001)
185. M. Plihal, J.W. Gadzuk, Phys. Rev. B **63**, 085404 (2001)
186. S. Sanvito, A.R. Rocha, J. Comp. Theor. Nanosci. **3**, 624 (2006)
187. A.R. Rocha, V.M. García-Suárez, S. Bailey, C. Lambert, J. Ferrer, S. Sanvito, Phys. Rev. B **73**, 085414 (2006)
188. W.J.M. Naber, S. Faez, W.G. van der Wiel, J. Phys. D: Appl. Phys. **40**, R205 (2007)
189. Y. Ke, K. Xia, H. Guo, Phys. Rev. Lett. **100**, 166805 (2008)
190. Z. Ning, Y. Zhu, J. Wang, H. Guo, Phys. Rev. Lett. **100**, 056803 (2008)
191. M. Grifoni, P. Hänggi, Phys. Rep. **304**, 229 (1998)
192. S. Kohler, J. Lehmann, P. Hänggi, Phys. Rep. **406**, 379 (2005)
193. R. Sanchez, E. Cota, R. Aguado, G. Platero, Phys. Rev. B **74**, 035326 (2006)
194. J. Maciejko, J. Wang, H. Guo, Phys. Rev. B **74** (2006)

Part I
Basic Concepts

Chapter 2
Landauer-Büttiker Method

The *Landauer-Büttiker* (LB) method (also known as the *scattering method*) establishes the relation between the wave functions (scattering amplitudes) of electrons in a quantum junction and the conducting properties of this junction. The LB method can be applied to find the current through a *noninteracting* junction or through a junction with effectively noninteracting quasiparticles, for example if the mean-field description is valid and the *inelastic scattering* is not essential. The other condition is absence of a *phase-breaking environment*. Such type of an electron transport is called *coherent*, because quantum coherence is preserved during the electron motion across the system and interference effects play an important role. Actually, the LB method is now routinely applied to basic transport calculations through nanostructures and single molecules. Besides, it is directly applicable in many semiconductor quantum dot systems with weak electron-electron interaction. Due to simplicity and generality of the LB method, it is now widely accepted and is in the base of our understanding of the coherent transport.

In this chapter we consider the foundations and some applications of the LB method, related directly to the problems of quantum transport at nanoscale. At the beginning (Sect. 2.1) we discuss a basic quantum junction model and introduce necessary results from the quantum scattering theory. Then we obtain the Landauer formula in the single-channel (and independent-channel) case and discuss its physical sense (Sect. 2.2). In Sect. 2.3 the general multi-channel formalism is discussed, and in Sect. 2.4 the multi-terminal case is considered.

Some topics are beyond our consideration, such as noise, thermal transport, hybrid systems with superconducting and magnetic electrodes, the LB method in combination with random matrix theory, localization theory, the attempts to introduce the analogous scattering description for interacting and dissipative systems. However, in spite of such popularity of the LB method, one should remember, that in its canonical form it is applicable only for noninteracting systems.

D.A. Ryndyk, *Theory of Quantum Transport at Nanoscale*,
Springer Series in Solid-State Sciences 184,
DOI 10.1007/978-3-319-24088-6_2

2.1 Quantum Junctions

2.1.1 Electrodes, Leads, Scatterer

As we already discussed in the Introduction, a nanojunction consists of three parts: left and right large equilibrium electrodes and central nanoscale region. In this chapter we neglect possible discrete nature of the central region and consider the nanojunction as a continuous medium. Moreover, we assume, that transport is completely coherent between the electrodes. It means that we neglect all inelastic effects inside the central region. The electrodes, however, are equilibrium and incoherent by definition, because the equilibrium state is established as a result of energy relaxation due to inelastic scattering. If an electron comes from the central region into the electrode, it is thermalized and any phase information is lost. On the other hand, electrons, which enter to the central region from the electrodes with random phases, keep the phase information until they return back to the electrodes, but their distribution function in the central part is determined by the boundary conditions and is nonequilibrium at finite voltage. For further consideration it is convenient to divide the central region into quantum leads and scattering region, or scatterer (Fig. 2.1).

Transport through a coherent region can be described by a wave function. The leads serve as quantum waveguides for electrons. They connect the electrodes with the scattering region and are assumed to have a well defined mode structure: incoming (from the left or right, $s = L, R$, electrode to the scatterer) modes $\psi_{s+}(\boldsymbol{r})$ and outgoing modes $\psi_{s-}(\boldsymbol{r})$ can be defined. In the simplest case the leads are noninteracting, but the electrochemical potentials of the electrodes can be shifted by finite bias voltage and in this case the distribution of electrons in the leads is nonequilibrium. The scattering region can be as simple as one tunneling barrier or impurity, or as complex as an interacting nonequilibrium molecule. In the continuous case the scatterer is described by some potential $U(\boldsymbol{r})$, it results from impurity scattering or external potential.

The case of ideally transparent central region (no scattering), when all electrons coming from one electrode to the lead go without reflection into the second electrode,

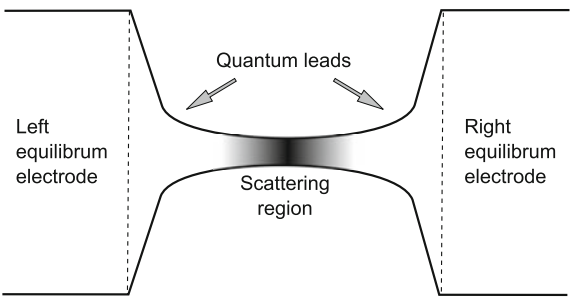

Fig. 2.1 Schematic picture of a quantum junction: the scattering region is connected to the electrodes through the quantum leads

is an important example of the system with nonclassical transport properties, showing famous *conductance quantization*.

Note, that the boundaries between electrodes, leads and scatterer are to a certain extent arbitrary. It is important only to take all conduction modes (transport channels) into account. The other important condition is that the boundaries for the electrodes should be taken far enough from the central region to be sure that the nonequilibrium region with electric fields and nonthermal distribution functions of electrons is localized completely in the central region. In the simplest case of bulk electrodes the distance between the boundary of "ideal, equilibrium electrode" and the physical surface of the electrode should be larger than electric field screening length and inelastic relaxation length. That is especially important at finite voltages, because in current calculation the electrodes are assumed to be equilibrium. For low-dimensional 1D and 2D electrodes the conditions of equilibrium electrodes is more difficult to fulfill because the electric fields are still 3-dimensional and the screening length is much larger. Besides, in 1D case it is quite difficult to have simultaneously finite current and equilibrium distribution in the electrodes. In contrast to 3D and 2D cases the current flowing through the junction can not spread into larger cross-section. Below we always assume that the lead can be low-dimensional, but it is always connected to larger equilibrium electrode.

2.1.2 Transport Channels

Let us introduce the important concept of *transport channels*. To start, we simplify the problem, assuming that the motion of electrons in the leads is effectively one-dimensional. For this purpose we factorize the wave function of the state with some energy E in the following form:

$$\Psi_E(\boldsymbol{r}) = \sum_n \phi_n(x, y, z)\psi_{nE}(z), \tag{2.1}$$

where the z axis denotes the direction of electron motion, $\phi_n(x, y, z)$ describes the transverse structure, n is called *mode* or *channel* index. At the first glance, we only complicated the problem, because instead of one unknown function we got many. But the trick is that the solution for $\phi_n(x, y, z)$ is fixed by the local geometry of the waveguide at point z, it can be easily obtained in many cases and we should solve only the equation for $\psi_{nE}(z)$. For example, in 3D layered systems a corresponding solution is

$$\Psi_E(\boldsymbol{r}) = \sum_{\boldsymbol{k}} e^{i(k_x x + k_y y)}\psi_{\boldsymbol{k}E}(z), \tag{2.2}$$

where $\boldsymbol{k}$ is the wave vector parallel to the layers. Initial 3D problem is reduced in this case to a 1D problem for the function $\psi_{\boldsymbol{k}E}(z)$. Similar situation takes place in

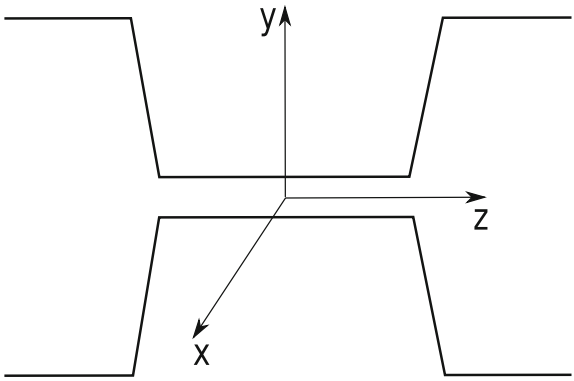

Fig. 2.2 A waveguide with constant cross-section between large electrodes

the effectively 1D or 2D spatially quantized systems (electronic waveguides), where $\phi_n(x, y, z)$ describes different transverse modes at different n.

To understand better, how transport channels are formed, let us consider two examples (Figs. 2.2 and 2.3): an electron waveguide with constant cross-section and an adiabatic junction (an example of so-called quantum point contact). Such quantum waveguides for electrons can be three-dimensional or formed from 2D electron gas, in the last case we assume that the motion in y direction is strongly quantized and y coordinate should be omitted in the equations below.

The wave functions are calculated from the Schrödinger equation

$$\left\{-\frac{\hbar^2}{2m}\left(\frac{\partial^2}{\partial x^2}+\frac{\partial^2}{\partial y^2}+\frac{\partial^2}{\partial z^2}\right)+U(x, y, z)\right\}\Psi_E(x, y, z)=E\Psi_E(x, y, z), \quad (2.3)$$

where $U(x, y, z)$ is the external potential, defining the geometry of the junction. This potential can be hard-wall or smooth, but should give confined in the channel transverse eigenstates. We will calculate the wave functions in the central part of a

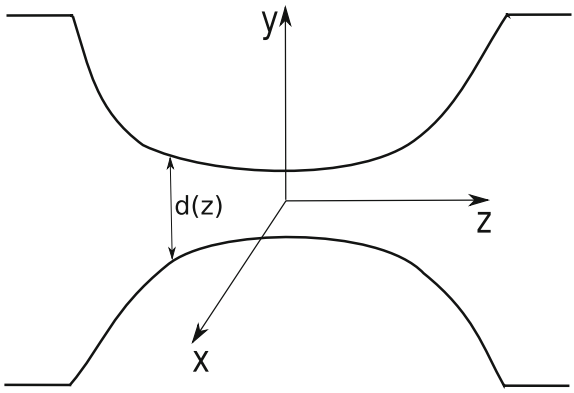

Fig. 2.3 An adiabatic junction

junction, assuming ideal reflectionless contacts between the waveguide and the large electrodes.

A Waveguide with Constant Cross-Section

For waveguides with constant cross-section (Fig. 2.2), when $U(x, y)$ is z-independent, the solution can be presented in the form (2.1) exactly as

$$\Psi_E(\boldsymbol{r}) = \sum_n \phi_n(x, y) e^{ik_n z}, \tag{2.4}$$

with the eigenfunctions $\phi_n(x, y)$ being the solution of the "transverse" Schrödinger equation

$$\left\{ -\frac{\hbar^2}{2m} \left(\frac{\partial^2}{\partial x^2} + \frac{\partial^2}{\partial y^2} \right) + U(x, y) \right\} \phi_n(x, y) = E_n \phi_n(x, y), \tag{2.5}$$

with the transverse energy eigenvalues E_n. The wave vectors $\hbar k_n = \pm\sqrt{2m(E - E_n)}$ are obtained from the expression for the full energy E, which is the sum of the transverse energy and the kinetic energy for longitudinal motion:

$$E = E_n + \frac{\hbar^2 k_n^2}{2m}. \tag{2.6}$$

For rectangular hard-wall potential with sizes L_x and L_y the eigenenergies are

$$E_{nm} = \frac{\hbar^2}{2m} \left[\left(\frac{\pi n}{L_x} \right)^2 + \left(\frac{\pi m}{L_y} \right)^2 \right], \quad n, m = 1, 2, 3.... \tag{2.7}$$

From these expressions it is clear, that the number of propagating modes (called *open* channels) at given energy E equals to the number of transverse modes with $E_n < E$:

$$N_{ch}(E) = \sum_n \theta(E - E_n). \tag{2.8}$$

At $E_n > E$ the wave number is imaginary and this mode can exist only at the end of the waveguide, these channels are called *closed*. It is important that N_{ch} is a function of energy and can be changed if the Fermi energy or the gate voltage are changed.

Adiabatic Junction

Now we consider a waveguide with the variable cross-section (Fig. 2.3). In the adiabatic approximation the spatial variation in the z-direction is much slower than in transverse directions. Thus, the second derivative with respect to z is small and it is reasonable to consider the Schrödinger equation for the transverse eigenfunctions $\phi_n(x, y)$ with z as a parameter

$$\left\{-\frac{\hbar^2}{2m}\left(\frac{\partial^2}{\partial x^2}+\frac{\partial^2}{\partial y^2}\right)+U(x,y,z)\right\}\phi_n(x,y,z)=E_n(z)\phi_n(x,y,z), \tag{2.9}$$

$E_n(z)$ is the (position-dependent) energy eigenvalue. If we substitute the Ansatz (2.1) with these eigenfunctions into (2.3) and neglect again the derivatives of $\phi_n(x,y,z)$ in the z-direction, we get the 1D equation for the function $\psi_{nE}(z)$:

$$\left\{-\frac{\hbar^2}{2m}\frac{\partial^2}{\partial z^2}+E_n(z)\right\}\psi_{nE}(z)=E\psi_{nE}(z), \tag{2.10}$$

where the energy $E_n(z)$ plays the role of an effective potential.

Consider a simple example, namely a 2D junction with the hard-wall potential. Assume, that the size of the waveguide in x-direction is $d(z)$. The transverse solution (at fixed z) is

$$\phi_n(x,z)=\sqrt{\frac{2}{d(z)}}\sin\left(\frac{2\pi n(x+d(z)/2)}{d(z)}\right), \tag{2.11}$$

and corresponding energy eigenvalue, e.g. the effective potential for z motion is

$$E_n(z)=\frac{\hbar^2\pi^2n^2}{2md^2(z)}. \tag{2.12}$$

If we plot now this energy as a function of z (Fig. 2.4), we can determine, which channels are open at given energy E. It will be all channels with the maximum $E_n(z)$ (which is in the place with minimum $d(z)$):

$$E_n^{max}=\frac{\hbar^2\pi^2n^2}{2md_{min}^2}, \tag{2.13}$$

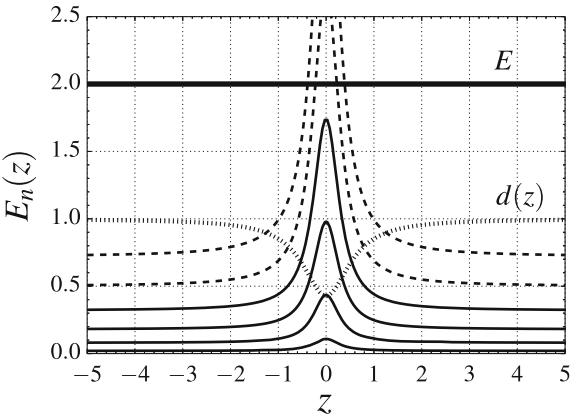

Fig. 2.4 Effective potential energy $E_n(z)$. The open transport channels are shown by the *solid lines*, the closed channels—by the *dashed lines*. The *dotted line* shows $d(z)$. The energy E is shown by the thick *horizontal line*

being smaller than E:

$$N_{ch}(E) = \sum_n \theta(E - E_n^{max}). \tag{2.14}$$

Note, that if the maximum of $E_n(z)$ is close to the energy E, the channel is only partially open, because both scattering and transmission are possible with some probabilities. For adiabatic junctions, however, this energy interval is very small, and all channels can be considered to be open or closed.

The condition of adiabaticity in two dimensional junctions can be written as $\partial d(z)/\partial z \ll \lambda_F/d(z)$. On the other hand, the position-dependent number of open channels is $N(z) = k_F d(z)/\pi$ and one gets

$$\frac{\partial d(z)}{\partial z} \ll \frac{1}{N(z)}. \tag{2.15}$$

This condition shows, that it is much easier to obtain the adiabatic transport for narrow junctions with small number of channels.

In the above considered examples the channels are independent, there are no transitions between different modes. This type of transport can be named *mode-conserving*. Below in this and next sections we consider only single channel and independent channels. More general situation with inter-mode scattering will be consider in the Sect. 2.3.

Actually some small inter-mode scattering always presents in an adiabatic junction. It is determined by the nonadiabatic corrections Δ_n to (2.10)

$$\left\{-\frac{\hbar^2}{2m}\frac{\partial^2}{\partial z^2} + E_n(z)\right\}\psi_{nE}(z) = E\psi_{nE}(z) + \Delta_n. \tag{2.16}$$

Considering Δ_n for particular junction shape, we can establish the limits of the adiabatic approximation. Calculation of Δ_n is straightforward from (2.3), we leave it as an exercise.

Other sources of scattering are also absent in ideal quantum junctions, they are perfect conductors in this case and demonstrate the conductance quantization phenomena. We will come back to it later. Before we consider how the scattering inside quantum junctions can be included.

2.1.3 Reflection and Transmission

As we will see below, the main formal problem to be solved in the Landauer theory is the single-particle scattering problem. The conductance is determined then from the elements of the transmission matrix. For this reason, the LB method is called also the scattering method. In the following sections we introduce the basic notions of

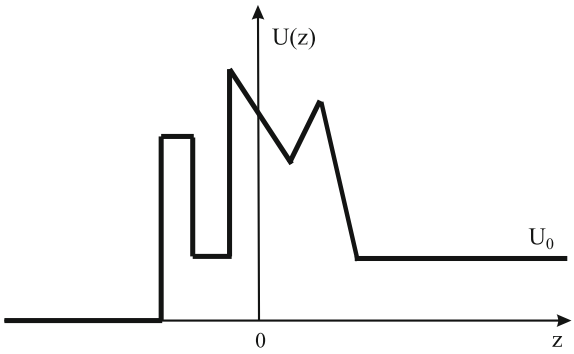

Fig. 2.5 Schematic one-dimensional potential for asymmetric junction

the quantum scattering theory, and formulate them in the form convenient for further calculations.

Now consider some one-dimensional potential (schematically shown in Fig. 2.5) which is constant far from the scattering region: $U(z \to -\infty) = 0$, $U(z \to \infty) = U_0$. Such energy shift U_0 appears when the left and right parts of a junction are not symmetric and have different E_n, it can be because of different transverse sizes of the confining potentials or because of different effective masses, as we can easily see from (2.12).

Thus, the wave function in the state with the energy E_z (the full energy E is assumed to be the sum of E_z and the part of the transverse energy E_n not included into U_0), and incident from the left, is

$$\psi(z \to -\infty) = A_+ e^{ikz} + A_- e^{-ikz}, \tag{2.17}$$

$$\psi(z \to +\infty) = B_- e^{ik'z}, \tag{2.18}$$

where A_+ is the incoming and A_-, B_- are the outgoing waves (Fig. 2.6). Wave vectors k and k' are defined as

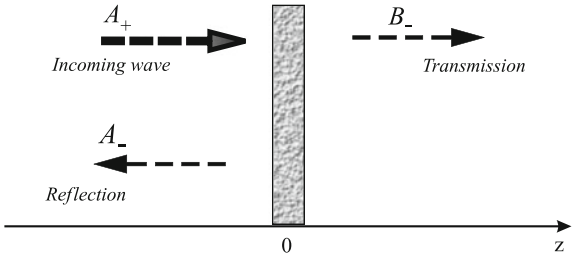

Fig. 2.6 Reflection (A_-) and transmission (B_-) amplitudes

$$k = \frac{\sqrt{2mE_z}}{\hbar}, \tag{2.19}$$

$$k' = \frac{\sqrt{2m(E_z - U_0)}}{\hbar}. \tag{2.20}$$

To determine the transmission and reflection probabilities, one should use the conservation of probability flux density ("current")

$$\mathbf{f} = \frac{i\hbar}{2m}\left[\psi(\mathbf{r})\nabla\psi^*(\mathbf{r}) - \psi^*(\mathbf{r})\nabla\psi(\mathbf{r})\right]. \tag{2.21}$$

From the time-dependent Schrödinger equation the conservation law follows:

$$\frac{\partial|\psi(\mathbf{r},t)|^2}{\partial t} + \mathrm{div}\mathbf{f} = 0, \tag{2.22}$$

which in the stationary case is simply

$$\mathrm{div}\mathbf{f} = 0. \tag{2.23}$$

For the plane wave Ae^{ikz} the probability flux density ("current") is reduced to

$$f = \frac{\hbar k}{m}|A|^2 = \upsilon|A|^2, \tag{2.24}$$

where we introduced the velocity $\upsilon = \hbar k/m$.

Now we are ready to define the *transmission coefficient* as the ratio of the transmitted to the incident probability flux

$$T(E_z) = \frac{f_{tran}}{f_{inc}} = \frac{\upsilon_\infty|B_-|^2}{\upsilon_{-\infty}|A_+|^2} = \frac{k'}{k}\frac{|B_-|^2}{|A_+|^2}, \tag{2.25}$$

and the *reflection coefficient* as the ratio of the reflected to the incident probability flux

$$R(E_z) = \frac{f_{ref}}{f_{inc}} = \frac{|A_-|^2}{|A_+|^2}. \tag{2.26}$$

From the probability flux conservation it follows that

$$T(E_z) + R(E_z) = 1. \tag{2.27}$$

Note, that if we consider the incident wave *from the right side* of the barrier, the transmission coefficient is the same at the same energy

$$T_{R\to L}(E_z) = T_{L\to R}(E_z). \tag{2.28}$$

This property guaranties absence of the current in equilibrium.

2.1.4 Scattering Matrix S and Transfer Matrix M

Now we consider the general scattering (or transmission) problem, assuming that there are incoming modes from the left and from the right sides of the barrier (Fig. 2.7).

Symmetric Junction with δ-Potential

We start from the symmetric junction with δ-potential at $z = 0$:

$$U(z) = \alpha\delta(z). \tag{2.29}$$

The solution is given by

$$\psi(z) = \begin{cases} A_+e^{ikz} + A_-e^{-ikz}, & z < 0, \\ B_-e^{ikz} + B_+e^{-ikz}, & z > 0, \end{cases} \tag{2.30}$$

where A_+, B_+ are incoming and A_-, B_- are outgoing waves, $k = \dfrac{\sqrt{2mE_z}}{\hbar}$. The boundary conditions at the δ-potential are

$$\psi(0-) = \psi(0+), \tag{2.31}$$

$$\psi'(0+) - \psi'(0-) = \frac{2m\alpha}{\hbar^2}\psi(0). \tag{2.32}$$

We can represent this boundary condition using *the transfer matrix* $\boldsymbol{M}$: $\left(K = \dfrac{\hbar^2 k}{m\alpha}\right)$

$$\begin{pmatrix} A_+ \\ A_- \end{pmatrix} = \boldsymbol{M}\begin{pmatrix} B_- \\ B_+ \end{pmatrix} = \begin{pmatrix} 1 + \frac{i}{K} & \frac{i}{K} \\ -\frac{i}{K} & 1 - \frac{i}{K} \end{pmatrix}\begin{pmatrix} B_- \\ B_+ \end{pmatrix}, \tag{2.33}$$

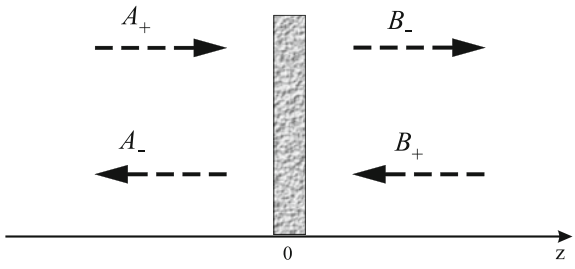

Fig. 2.7 Single barrier. General scattering problem

or, alternatively, *the scattering matrix* $\boldsymbol{S}$:

$$\begin{pmatrix} A_- \\ B_- \end{pmatrix} = \boldsymbol{S} \begin{pmatrix} A_+ \\ B_+ \end{pmatrix} = \begin{pmatrix} \frac{1}{iK-1} & \frac{iK}{iK-1} \\ \frac{iK}{iK-1} & \frac{1}{iK-1} \end{pmatrix} \begin{pmatrix} A_+ \\ B_+ \end{pmatrix}. \tag{2.34}$$

The transfer matrix relates the states from two sides of the barrier, while the scattering matrix relates the amplitudes of outgoing waves to the amplitudes of incoming waves.

To find the transmission and reflection coefficients we set now $B_+ = 0$, then

$$T(E_z) = \frac{|B_-|^2}{|A_+|^2} = \frac{1}{|M_{11}|^2} = |S_{21}|^2 = \frac{K^2}{1+K^2}, \tag{2.35}$$

$$R(E_z) = \frac{|A_-|^2}{|A_+|^2} = \frac{|M_{21}|^2}{|M_{11}|^2} = |S_{11}|^2 = \frac{1}{1+K^2}, \tag{2.36}$$

$$T + R = 1.$$

The descriptions in terms of scattering or transfer matrices are completely equivalent and the choice is only dependent on the convenience and the problem to be solved. Typically, in the end of a calculation the $\boldsymbol{S}$-matrix should be obtained, because it determines the conductivity by the Landauer formula. But to calculate scattering by complex structures, the $\boldsymbol{M}$-matrix can be convenient, as we shall see below.

Normalization of Wave Functions and S-Matrix

For symmetric junctions the $\boldsymbol{S}$-matrix (2.34) is unitary: $\boldsymbol{S}^\dagger \boldsymbol{S} = \boldsymbol{I}$. However, for asymmetric junctions with different (at the same energy) left and right velocities $\upsilon(E_z) = \hbar k(E_z)/m$, if we find the solution in the same form, but take into account different wave vectors (2.19), (2.20):

$$\psi(z) = \begin{cases} A_+ e^{ikz} + A_- e^{-ikz}, & z < 0, \\ B_- e^{ik'z} + B_+ e^{-ik'z}, & z > 0, \end{cases} \tag{2.37}$$

we find that the expression for the transmission function is changed ($R(E_z)$ is not changed):

$$T(E_z) = \left[\frac{\upsilon_L}{\upsilon_R}\right] \frac{|B_-|^2}{|A_+|^2} = \left[\frac{\upsilon_L}{\upsilon_R}\right] \frac{1}{|M_{11}|^2} = \left[\frac{\upsilon_L}{\upsilon_R}\right] |S_{21}|^2 = \frac{K^2}{1+K^2}, \tag{2.38}$$

and $\boldsymbol{S}$-matrix is obviously not unitary anymore, because of additional velocity factors in the expression for the transmission coefficient. Now $T(E_z) + R(E_z) = 1$, but $|S_{21}|^2 + |S_{11}|^2 \neq 1$.

If one needs to have the unitary matrix, it is possible to redefine it as

$$S'_{nm} = \sqrt{\frac{\upsilon_n}{\upsilon_m}} S_{nm}. \tag{2.39}$$

Or, equivalently, redefine the amplitudes of plane waves as $Ae^{ikz} = (A'/\sqrt{\upsilon})e^{ikz}$, and the flux density

$$f = \frac{\hbar k}{m}|A|^2 = \upsilon|A|^2 = |A'|^2. \tag{2.40}$$

Below we always assume that the $\boldsymbol{S}$-matrix is unitary, and the reflection and transmission coefficients acquire the simple form (2.35).

Usually we will write the wave functions in the form

$$\psi(z) = \begin{cases} \dfrac{A_+}{\sqrt{2\pi\hbar\upsilon_L}}e^{ikz} + \dfrac{A_-}{\sqrt{2\pi\hbar\upsilon_L}}e^{-ikz}, & z \to -\infty, \\ \dfrac{B_-}{\sqrt{2\pi\hbar\upsilon_R}}e^{ik'z} + \dfrac{B_+}{\sqrt{2\pi\hbar\upsilon_R}}e^{-ik'z}, & z \to \infty, \end{cases} \tag{2.41}$$

the factor $\sqrt{2\pi\hbar}$ is introduce here to simplify the normalization condition. Instead of the usual normalization for plane waves $\psi_k(z) = \exp(ikz)$:

$$\int \frac{dk'}{2\pi}\int_{-\infty}^{\infty}\psi_k(z)\psi_{k'}^*(z)dz = \int \frac{dk'}{2\pi}\left(2\pi\delta(k-k')\right) = 1, \tag{2.42}$$

we have for the functions $\psi_k(z) = (1/\sqrt{2\pi\hbar\upsilon})\exp(ikz)$:

$$\int dE'\int_{-\infty}^{\infty}\psi_k(z)\psi_{k'}^*(z)dz = \int dE'\left(\frac{2\pi}{2\pi\hbar\upsilon}\delta(k-k')\right) = 1, \tag{2.43}$$

because $dE' = \hbar\upsilon dk'$ for $E(k) = \dfrac{\hbar^2k^2}{2m}$.

Some General Properties of S and M Matrices

In general case (asymmetric junction, magnetic field, etc.) the scattering matrix is usually represented as

$$\boldsymbol{S} = \begin{pmatrix} r & t' \\ t & r' \end{pmatrix}. \tag{2.44}$$

The reflection and transmission coefficients *from left to right* are

$$T_{L\to R}(E) = |t|^2; \quad R_{L\to R}(E) = |r|^2, \tag{2.45}$$

and *from right to left*

$$T_{R\to L}(E) = |t'|^2; \quad R_{R\to L}(E) = |r'|^2. \tag{2.46}$$

The transfer matrix can be written explicitly in terms of transmission and reflection amplitudes r, r', t, t' as

$$\boldsymbol{M} = \begin{pmatrix} \dfrac{1}{t} & -\dfrac{r'}{t} \\ \dfrac{r}{t} & \dfrac{tt' - rr'}{t} \end{pmatrix}, \tag{2.47}$$

as well the scattering matrix in terms of the elements of $\boldsymbol{M}$ as

$$\boldsymbol{S} = \begin{pmatrix} \dfrac{M_{21}}{M_{11}} & \dfrac{M_{11}M_{22} - M_{12}M_{21}}{M_{11}} \\ \dfrac{1}{M_{11}} & -\dfrac{M_{12}}{M_{11}} \end{pmatrix}. \tag{2.48}$$

The unitarity means

$$\boldsymbol{S}^{\dagger}\boldsymbol{S} = \boldsymbol{S}\boldsymbol{S}^{\dagger} = \boldsymbol{I}, \tag{2.49}$$

so that

$$|r|^2 + |t|^2 = |r'|^2 + |t'|^2 = 1, \tag{2.50}$$
$$|r|^2 + |t'|^2 = |r'|^2 + |t|^2 = 1, \tag{2.51}$$
$$r^*t' + t^*r' = t'^*r + r'^*t = 0, \tag{2.52}$$
$$rt^* + t'r'^* = tr^* + r't'^* = 0. \tag{2.53}$$

In the time-reversal case (no magnetic field) the product of the S-matrix with its complex conjugate is the unity matrix

$$\boldsymbol{S}\boldsymbol{S}^* = \hat{I}, \tag{2.54}$$

from which follows

$$|r'|^2 = |r|^2, \quad |r|^2 + t^*t' = 1, \quad |t'|^2 = |t|^2, \tag{2.55}$$

and

$$R_{L\to R}(E) = R_{R\to L}(E); \quad T_{L\to R}(E) = T_{R\to L}(E). \tag{2.56}$$

Note, finally, that an unitary matrix in the time reversal case is symmetric, and $|r| = |r'|$, so that the S-matrix can be represented in the form

$$\boldsymbol{S} = \begin{pmatrix} r & t \\ t & re^{i\theta} \end{pmatrix}. \tag{2.57}$$

2.1.5 A Series of Scatterers: Transfer Matrix Method

If one has a series of scatterers, the calculation of the resulting transfer matrix can be simplified by the use of the transfer matrices of single scatterers. Consider two sequential barriers with transfer matrices $\boldsymbol{M}$ and $\boldsymbol{M}'$ (Fig. 2.8), so that

$$\begin{pmatrix} A_+ \\ A_- \end{pmatrix} = \boldsymbol{M} \begin{pmatrix} B_- \\ B_+ \end{pmatrix}, \quad \begin{pmatrix} A'_+ \\ A'_- \end{pmatrix} = \boldsymbol{M}' \begin{pmatrix} B'_- \\ B'_+ \end{pmatrix}. \tag{2.58}$$

In the case when both $\boldsymbol{M}$ and $\boldsymbol{M}'$ are calculated independently, assuming that the barrier is placed at $z = 0$, the outgoing coefficients B and incoming coefficients A' are related by the propagation transfer matrix $\boldsymbol{M}_L$

$$\begin{pmatrix} B_- \\ B_+ \end{pmatrix} = \boldsymbol{M}_L \begin{pmatrix} A'_+ \\ A'_- \end{pmatrix} = \begin{pmatrix} e^{-ikL} & 0 \\ 0 & e^{ikL} \end{pmatrix} \begin{pmatrix} A'_+ \\ A'_- \end{pmatrix}. \tag{2.59}$$

To show that in the most simple way, note that $B_- e^{ikz}$ and $A'_+ e^{ikz}$ describe the same plane wave in two different points $z = 0$ and $z = L$, the phase difference is obviously kL.

Finally we can write

$$\begin{pmatrix} A_+ \\ A_- \end{pmatrix} = \boldsymbol{M}_T \begin{pmatrix} B'_- \\ B'_+ \end{pmatrix} = \boldsymbol{M}\boldsymbol{M}_L\boldsymbol{M}' \begin{pmatrix} B'_- \\ B'_+ \end{pmatrix}. \tag{2.60}$$

Thus, the transfer matrix for a sequence of barriers can be defined as the product of the particular transfer matrices of the barriers and the propagating transfer matrices

$$\boldsymbol{M}_T = \boldsymbol{M}_1\boldsymbol{M}^L_{1,2}\boldsymbol{M}_2 ... \boldsymbol{M}_n\boldsymbol{M}^L_{n,n+1}\boldsymbol{M}_{n+1} ... \boldsymbol{M}_{N-1}\boldsymbol{M}^L_{N-1,N}\boldsymbol{M}_N. \tag{2.61}$$

Breit-Wigner Formula

As an example, we can calculate the transmission coefficient for the double-barrier system. We need only M_{T11} because it determines T and $R = 1 - T$. The transfer matrix $\boldsymbol{M}_T$ for a two-barrier structure is

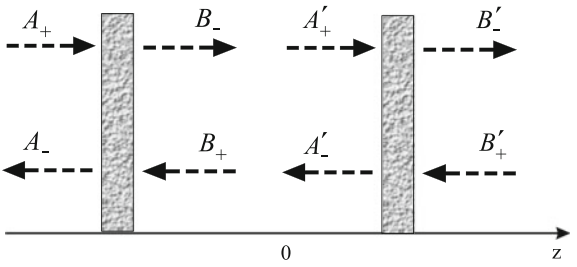

Fig. 2.8 Double barrier

$$\boldsymbol{M}_T = \boldsymbol{M}\boldsymbol{M}_L\boldsymbol{M}' = \begin{pmatrix} M_{11} & M_{12} \\ M_{21} & M_{22} \end{pmatrix} \begin{pmatrix} e^{-ikL} & 0 \\ 0 & e^{ikL} \end{pmatrix} \begin{pmatrix} M'_{11} & M'_{12} \\ M'_{21} & M'_{22} \end{pmatrix}. \tag{2.62}$$

$$M_{T11} = M_{11}M'_{11}e^{-ikL} + M_{12}M'_{21}e^{ikL} \tag{2.63}$$

In the case of two identical barriers, for transmission coefficient we find

$$T(E) = \frac{T_1^2}{T_1^2 + 4R_1\cos^2(kL - \theta)}, \tag{2.64}$$

where θ is the phase of the complex M_{11}. T_1 and R_1 are transmission and reflection coefficients of the single barrier.

From this general expression one can see the important property of two-barrier structures: there are transmission resonances, at some specific energies E_n the transmission coefficient is large ($T(E_n) = 1$ in symmetric structures), while between resonances it can be small.

When the barriers are δ-functions $M_{11} = 1 + \dfrac{i}{K}$, $\theta = \arctan\dfrac{1}{K} = \arctan\dfrac{m\alpha}{\hbar^2 k}$ and the equation for resonances ($T = 1$) is

$$\tan kL = -\frac{\hbar^2 k}{m\alpha}. \tag{2.65}$$

Close to the resonance, around one of the resonance energies E_n, the transmission coefficient has a *Lorentzian* form

$$T(E) \approx \frac{\Gamma_n^2}{(E - E_n)^2 + \Gamma_n^2}, \tag{2.66}$$

where the width Γ_n is given for two δ-barriers as

$$\Gamma_n = \left(\frac{2\hbar^2 E_n T_1^2}{mL^2 R_1}\right)^{1/2}. \tag{2.67}$$

2.2 Landauer Formula

2.2.1 Single-Channel Formulas

The main idea of the scattering approach to the conductance was first formulated by Rolf Landauer [1, 2]. He proposed, that the conductance of some segment of a 1D channel with elastic scatterers is determined by the quantum mechanical probabilities of transmission (T) and reflection ($R = 1 - T$) through this segment. It

should be noted, that Landauer considered the local resistance of a system (the zero-temperature residual resistance), but not the resistance of a quantum system between two equilibrium electrodes. As a result, he got for the zero temperature one-channel (effectively one-dimensional) conductance the so-called "first Landauer formula"

$$G' = \frac{e^2}{h}\frac{T}{1-T} = \frac{e^2}{h}\frac{T}{R}. \tag{2.68}$$

The result, which seems to be reasonable at least in two limiting cases. At small transmission $T \to 0$, the conductance is also small and proportional to T, the result, which is well known from the perturbation theory. In the opposite case, when $T \to 1$, $R \to 0$, there is no scattering at all, so that the conductance should go to infinity, in agreement with (2.68). To take into account the spin degeneracy in this formula, one has to multiply the conductance (2.68) by 2.

However, the further investigations [3, 4] show that the conductance of a 1D system, calculated by the exact linear response method, can have also quite different form (depending on the boundary conditions)

$$G = \frac{e^2}{h}T. \tag{2.69}$$

This conductance is finite even in the case of the perfectly transparent junction ($T = 1$). Actually, there is no contradiction between these two formulas. It was shown that both are reasonable and give the same current, but correspond to the voltages, defined between different points. As we shall see below, the key difference between the formulas (2.68) and (2.69) is that the first one is for the conductance *inside* the junction (between points A and B, see Fig. 2.13 below), while the second gives the conductance related to the equilibrium electrodes (between points L and R in Fig. 2.13). In Sect. 2.2.4 we obtain both formulas and discuss the relation between them. The puzzle with finite resistance at $T \to 1$ is also understood, it is clear now that the current through a junction is always accompanied by the voltage drop at the boundaries between electrodes and leads. The physical reason is that the number of open electron transport channels is limited, while many other electrons reflect from the junction and create some charge distribution. Not so obvious is, however, that this contact resistance has the universal value $R_c = h/e$ for one spinless channel.

For the transport problems, considered in this book, the second type of the Landauer formula is more important usually. Besides, the first type formulas are not exact for finite-size nanostructures, because they are dependent on the particular electrical potential distribution inside the junction.

The important question, discussed in connection with the Landauer resistance, is the origin of dissipation in this approach. Indeed, finite dc current at finite dc voltage means that the energy is permanently dissipated. On the other hand, we consider only elastic scattering, so that the energy can not be dissipated in the scattering process. This problem is closely related to the phenomena of the residual resistance at low temperature, caused by impurities. In both cases we should introduce some thermal-

ization. In the case of transport between the *equilibrium* electrodes, this problem is resolved quite easy, the energy is dissipated in the electrodes, the details of the dissipation are not relevant. More precisely, the *incoming* from the electrodes particles are equilibrium distributed, while *outgoing* particles propagate into the electrodes and are thermalized here.

At finite temperature and finite voltage the Landauer formula (2.69) is transformed into the more general formula for the current:

$$I(V) = \frac{e}{h} \int_{-\infty}^{\infty} T(E, V) \, [f_L(E) - f_R(E)] \, dE, \tag{2.70}$$

where $T(E, V)$ is the *transmission function* describing the probability of transmission as a function of energy and voltage $V = \varphi_L - \varphi_R$, $f_s(E)$ are the distribution functions in the left ($s = L$) or right ($s = R$) electrodes. In equilibrium the Fermi-Dirac distribution functions with the chemical potential (Fermi energy) μ_s, the electrical potential φ_s and the temperature T_s are

$$f_s(E) = \frac{1}{\exp\left(\frac{E - \mu_s - e\varphi_s}{T_s}\right) + 1}. \tag{2.71}$$

2.2.2 Heuristic Derivation

Now we are ready to see in detail, how the transmission coefficient can be used to calculate the current through a quantum junction, in particular we will derive the Landauer formulas (2.69) and (2.70). We start from the mode-conserving scattering and use here the heuristic arguments. More rigorous methods are summarized in Sect. 2.3.

From the scattering picture it follows that all particles, coming from the left electrode, are transmitted through the junction with the probability $T(n, k_z)$ and, after that, their excess energy, phase coherence, and the memory of their previous state

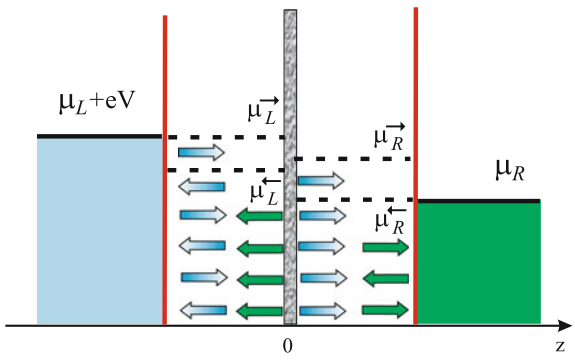

Fig. 2.9 Left-moving and right-moving particles in a wire with scatterer (energy diagram)

are lost in the right electrode. We assume in all cases, that an electron can go without scattering from the lead into the electrode, thus for incoming from the left electron there are only two possibilities: to go into right electrode with the probability T or to return back to the left electrode with the probability R. The same property takes place for all particles coming from the right and transmitted to the left. Transport through the junction is coherent in this model, energy E and transverse quantum number n are conserved (the case of the multi-channel scattering, when n is not conserved, will be considered later). Irreversibility is introduced through the relaxation in the electrodes. The main assumption is that *the right-moving particles in the left lead are populated with the equilibrium distribution function of the left electrode* $f_L^{eq}(E)$ and *the left-moving particles in the right lead are populated with the equilibrium distribution function of the right electrode* $f_R^{eq}(E)$ (see Fig. 2.9).

According to this model, the current of electrons, which enter from the left electrode is determined by the following expression

$$J_{L\to R} = e\sum_n \int_0^\infty T_{L\to R}(n,k_z)\upsilon_L(n,k_z) f_L(n,k_z)\frac{dk_z}{2\pi}, \tag{2.72}$$

where $\upsilon_L(n,k_z)$ is the group velocity of the particle with momentum k_z, $f_L(n,k_z)$ is the distribution function, the form of this function is considered below. The integration is only for right-moving particles with $k_z > 0$. Note, that it is not necessary to multiply this expression additionally by the factor like $(1 - f_R(n,k_z))$ as in the tunneling "golden rule" theory, because this factor describes the number of empty states in the right equilibrium electrode and should be included when the transition between left and right states is considered. Instead, in our approach we consider *scattering states in the leads*, which formally can be extended in the electrodes. The transmission coefficient from the left to the right is simply the probability to find a particle in the right part of this state.

Taking into account that

$$\upsilon(k_z) = \frac{\partial E_z(k_z)}{\hbar\partial k_z} = \frac{\partial E(k_z)}{\hbar\partial k_z}, \tag{2.73}$$

where $E(k_z) = E_n + E_z(k_z)$ is the full energy, we obtain

$$I_{L\to R} = \frac{e}{h}\sum_n \int_{E_{nL}}^\infty T_{L\to R}(n,E) f_L(E) dE, \tag{2.74}$$

and a similar expression for the current of right-incoming electrons

$$I_{R\to L} = \frac{e}{h}\sum_n \int_{E_{nR}}^\infty T_{R\to L}(n,E) f_R(E) dE. \tag{2.75}$$

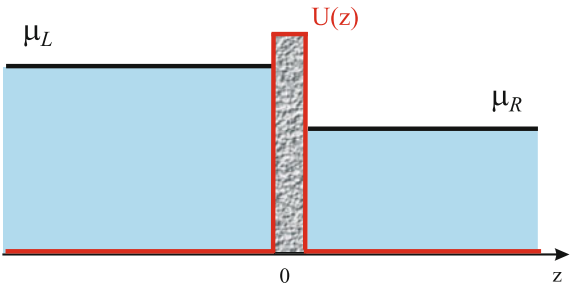

Fig. 2.10 Energy diagrams for chemical potential difference (the number of electrons in the band is changed, but not the potential)

Note that the integration in this expressions is done from the bottom of conduction band $E_{nL(R)}$. Taking into account the symmetry of transmission coefficients (2.28) we get the expression for the current

$$I = \frac{e}{h} \sum_n \int_{-\infty}^{\infty} T_n(E) \left[f_L^{eq}(E) - f_R^{eq}(E) \right] dE. \tag{2.76}$$

The limits of integration over E can be taken infinite, because the closed channels have $T_n(E) = 0$ and do not contribute to the current.

Finally, the distribution functions in this expression should be discussed. There are different possibilities to create a nonequilibrium state of the junction. In equilibrium the *electro-chemical potential* $\tilde{\mu} = \mu + e\varphi$ should be the same in both electrodes. Here μ is the *(internal) chemical potential*, which determines the filling of electron bands in the electrodes, and φ is the electrostatic potential. One can create a difference of only (internal) chemical potentials (Fig. 2.10) if one of the electrodes will be populated by extra particles. This case, however, is quite difficult to realize in nanostructures, because any change of the particle density causes the change in the electric field. Moreover, typically the external voltage is applied to the electrodes, while the (internal) chemical potentials of the electrodes far from the junction are not changed, $\mu_L = \mu_R = \mu$ (Fig. 2.11). More generally, one can say that the difference in the electro-chemical potentials between two points taken inside the equilibrium electrodes, is always produced by the external voltage ($\tilde{\mu}_L - \tilde{\mu}_R = eV$). To determine the exact distribution of the charge density and electrostatic potential near and inside the junction, the self-consistent solution of the coupled Schrödinger and Poisson equations is necessary. In this case the expression (2.76) should be used with care when the voltage is not small. Indeed, the potential $U(z)$ is now a function of the applied voltage, and consequently the transmission coefficient is a function of the voltage too.

The distribution functions in the general case are

$$f_L^0(E) = \frac{1}{\exp\left(\frac{E-\mu_L-e\varphi_L}{T_L}\right)+1}, \qquad f_R^0(E) = \frac{1}{\exp\left(\frac{E-\mu_R-e\varphi_R}{T_R}\right)+1}. \tag{2.77}$$

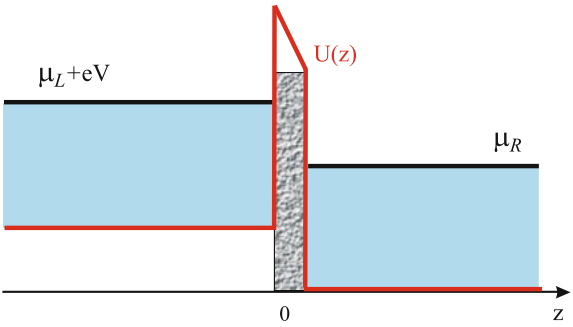

Fig. 2.11 Energy diagrams for voltage difference (the electron band is shifted up, the potential is modified)

The temperatures in the electrodes can be also different, but we consider it later. Usually the simplified form can be used, with explicitly written external voltage

$$I(V) = \frac{e}{h} \sum_n \int_{-\infty}^{\infty} T_n(E, V) \left[f_0(E - eV) - f_0(E) \right] dE. \tag{2.78}$$

where $f^0(E)$ is the Fermi-Dirac distribution function with the equilibrium chemical potentials $\mu_L = \mu_R = E_F$:

$$f_0(E) = \frac{1}{\exp\left(\frac{E - E_F}{T}\right) + 1}. \tag{2.79}$$

The distribution functions in the electrodes are the functions of energy E only, thus one can introduce *the transmission function*

$$T(E) = \sum_n T_n(E), \tag{2.80}$$

and obtain finally

$$I(V) = \frac{e}{h} \int_{-\infty}^{\infty} T(E, V) \left[f_0(E - eV) - f_0(E) \right] dE. \tag{2.81}$$

This formula can be wrong, however, if an external magnetic field is applied, because the magnetic field violates the time-reversal symmetry and the relation (2.28) may be violated too.

The conductance at zero temperature is given by

$$G = \frac{e^2}{h} \sum_n T_n(E_F). \tag{2.82}$$

2.2.3 Conductance Quantization

Perfect Wire

Consider now the conductance of a perfect wire adiabatically coupled to two electrodes. "Perfect wire" means that there are several open reflectionless channels with transmission coefficient $T_n(E) = 1$. Thus all right-going electrons inside the junction are populated only by the left electrode and left-going electrons are populated only by the right electrode (Fig. 2.12). We can say that right moving electrons have the (pseudo-) electro-chemical potential of the left electrode $\tilde{\mu}_L$, while left moving electrons of the right electrode $\tilde{\mu}_R$. Of course, the state of electrons inside the wire is not equilibrium, and these "left" and "right" chemical potentials give the number and energy of corresponding particles in the channel, but they are not usual thermodynamic potentials.

Now we simply use the expression for the current (2.81). The distribution functions in the electrodes at zero-temperature are the step-functions

$$f_L(E, V) = \theta(\mu + eV - E), \tag{2.83}$$

$$f_R(E) = \theta(\mu - E), \tag{2.84}$$

and for the current we obtain

$$\begin{aligned} I(V) &= \frac{e}{h} \sum_n \int_{-\infty}^{\infty} T_n(E, V) \left[\theta(\mu + eV - E) - \theta(\mu - E)\right] dE \\ &= \frac{e}{h} \sum_n \int_{\mu - E_n}^{\mu - E_n + eV} T_n(E, V) dE = \frac{e^2}{h} NV, \end{aligned} \tag{2.85}$$

where we used $T_n(E, V) = 1$, and N is the number of open channels between $\tilde{\mu}_L = \mu + eV$ and $\tilde{\mu}_R = \mu$. For the conductance one has

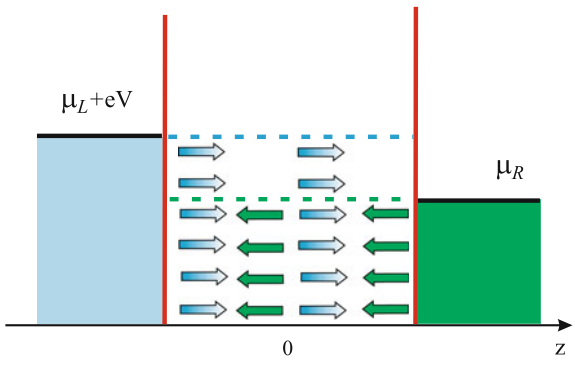

Fig. 2.12 Left-moving and right-moving particles in a perfect wire (energy diagram)

$$G = \frac{e^2}{h} N. \tag{2.86}$$

It is accepted to call the conductance of a single-channel perfect wire with spin *the conductance quantum*

$$G_0 = \frac{2e^2}{h} \approx 77.48\ \mu S = 7.748 \cdot 10^{-5}\ \Omega^{-1} \approx \frac{1}{12900}\ \Omega^{-1}. \tag{2.87}$$

The corresponding resistance is

$$R_0 = \frac{h}{2e^2} \approx 12.9\ k\Omega. \tag{2.88}$$

Where does the resistance of a *perfect* wire come from? The origin of this resistance is in the mismatch between the large number of modes in the electrodes and a few channels in the wire. So this is not the resistance of a perfect wire, but rather the contact resistance of the interface between electrodes and wire.

Quantum Point Contact

In quantum point contacts (QPC), which have usually the adiabatic form, the conductance at low temperatures is quantized in accordance with (2.86). In the spin-degenerate case it can be written as,

$$G = \frac{2e^2}{h} \sum_n \theta(E_F - E_n), \tag{2.89}$$

where E_F is the Fermi energy, and E_n is the maximum of the transverse energy $E_n(z)$. The Fermi energy in 2D electron gas can be changed by the gate voltage V_g, in this way the conductance quantization was observed experimentally in the form of steps at the function $G(V_g)$.

At finite temperature the conductance steps are smeared. Besides, the steps are not perfect, if the junction is not adiabatic. This can be seen from the exactly solvable model with the potential

$$V(x, z) = \frac{1}{2} m\omega_x^2 x^2 + V_0 - \frac{1}{2} m\omega_z^2 z^2. \tag{2.90}$$

The transmission coefficients have a simple form [5]:

$$T_n(E) = \frac{1}{\exp\left[-2\pi\ (E - V_0 - (n + 1/2)\hbar\omega_x)\ /(\hbar\omega_z)\right] + 1}. \tag{2.91}$$

At $\omega_z \ll \omega_x$ we return to the adiabatic approximation and well defined steps.

Classical Point Contact

It is interesting to compare the quantum conductance (2.86) with the conductance of a *classical* point contact with large width $d_0 \gg \lambda_F$, known as Sharvin conductance [6]. Following [7], this conductance for 2D ballistic channel with the width d_0 between two Fermi gases can be written as

$$I = \frac{e\upsilon_F}{\pi} d_0 \frac{\partial n}{\partial \mu} eV, \tag{2.92}$$

In 2D electron gas $\partial n/\partial \mu = m/\pi\hbar^2$, and we obtain (with spin degeneracy)

$$G_S = \frac{2e^2}{h} \frac{k_F d_0}{\pi}. \tag{2.93}$$

From quantum mechanical point of view $k_F d_0/\pi$ is the number of transverse channels N.

2.2.4 Contact Resistance

Consider now the single-channel case with the imperfect transmission $T \neq 1$, repeating the same calculation as in (2.85) we obtain

$$I = \frac{e}{h} T\,(\tilde{\mu}_L - \tilde{\mu}_R) = \frac{e^2}{h} TV, \tag{2.94}$$

$$G = \frac{e^2}{h} T. \tag{2.95}$$

This is the conductance between the reservoirs, e.g. between some two points "L" and "R" inside the electrodes (see Fig. 2.13). Now consider two other points "A" and "B" *inside the leads*. The distribution functions and corresponding "electro-chemical potentials" (these potentials are not true potentials, but give the correct number and energy of electrons, as we discussed before) are different for left and right moving electrons. Now, however, these potentials are different also at different sides of the scatterer (Fig. 2.12, right). The potential $\tilde{\mu}_L^{\rightarrow}$ of the right moving electrons is equal to $\tilde{\mu}_L$ only in the left part of the wire, as well as $\tilde{\mu}_R^{\leftarrow} = \tilde{\mu}_R$ in the right part. All other electro-chemical potentials are modified by the reflection from the barrier. Assume, that one can approximate the charge redistribution in the leads due to scattering by some quasi-equilibrium distributions with corresponding pseudo-potentials $\tilde{\mu}$. For example, only the part of right moving electrons is transmitted through the barrier and corresponding potential should be $T\tilde{\mu}_L$, but additionally $(1-T)\tilde{\mu}_R$ are reflected and move back. Finally, we obtain

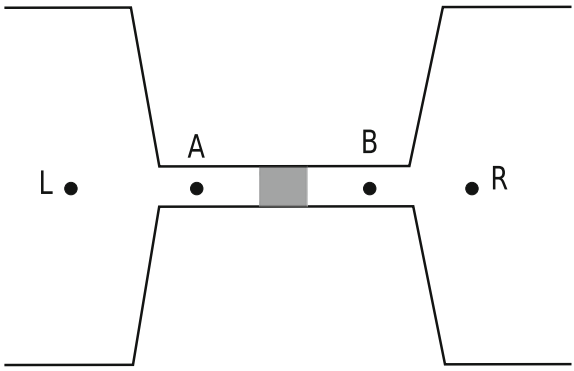

Fig. 2.13 The points of voltage measurement: L, R in the equilibrium electrodes; A, B inside the leads

$$\tilde{\mu}_L^{\rightarrow} = \tilde{\mu}_L, \quad \tilde{\mu}_R^{\rightarrow} = T\tilde{\mu}_L + (1-T)\tilde{\mu}_R, \tag{2.96}$$

$$\tilde{\mu}_R^{\leftarrow} = \tilde{\mu}_R, \quad \tilde{\mu}_L^{\leftarrow} = T\tilde{\mu}_R + (1-T)\tilde{\mu}_L. \tag{2.97}$$

The *difference* of both "left moving" and "right moving" chemical potentials across the barrier is the same

$$\tilde{\mu}_L^{\rightarrow} - \tilde{\mu}_R^{\rightarrow} = \tilde{\mu}_L^{\leftarrow} - \tilde{\mu}_R^{\leftarrow} = (1-T)(\tilde{\mu}_L - \tilde{\mu}_R). \tag{2.98}$$

We can identify this potential difference with the potential drop between points A and B

$$eV_{AB} = (1-T)(\tilde{\mu}_L - \tilde{\mu}_R). \tag{2.99}$$

Thus we can define the conductance (with the current (2.94))

$$G' = \frac{I}{V_{AB}} = \frac{e^2}{h}\frac{T}{1-T} = \frac{e^2}{h}\frac{T}{R}, \tag{2.100}$$

which is exactly "the first Landauer formula" (2.68). The voltage V_{AB} appears as a result of charge redistribution around the scatterer. Not surprising that for perfect wire with $T = 1$ and $R = 0$ this conductance is infinite.

The conductances (2.95) and (2.100) obey the following relation:

$$\frac{1}{G} = \frac{h}{e^2} + \frac{1}{G'}. \tag{2.101}$$

This result can be understood in the following way. G^{-1} can be considered as the full resistance of the junction, consisted from two sequential resistances of the scatterer (G'^{-1}) and of the contact resistance of the perfect wire (h/e^2).

Consider additionally the conductance of the *incoherent* series of N scatterers, each having the transmission coefficient T_1. If the phase coherence is broken, one

should summarize the probabilities of transmission instead of the quantum amplitudes. Thus, the transfer matrix method does not work in this case. Instead we use the probability theory. Let us consider first only two scatterers with the transmission coefficients T_1 and T_2. The probability of transmission trough both scatterers T is calculated as the sum of all possible (re)scattering processes

$$\begin{aligned} T &= T_1T_2 + T_1R_2R_1T_2 + T_1R_2R_1R_2R_1T_2 + \cdots \\ &= T_1(1 + R_1R_2 + (R_1R_2)^2 + \cdots)T_2 = \frac{T_1T_2}{1 - R_1R_2}, \end{aligned} \tag{2.102}$$

or

$$\frac{1-T}{T} = \frac{1-T_1}{T_1} + \frac{1-T_2}{T_2}, \tag{2.103}$$

which demonstrates the additivity of $(1 - T)/T$. Thus, for N scatterers we obtain

$$\frac{1-T}{T} = N\frac{1-T_1}{T_1}. \tag{2.104}$$

The resistance of the system is

$$R = \frac{h}{e^2}\frac{1}{T} = \frac{h}{e^2} + N\frac{h}{e^2}\frac{R_1}{T_1}. \tag{2.105}$$

We again obtain the series resistance of N Landauer scatterers and contact resistance.

2.3 Multi-channel Scattering and Transport

2.3.1 S-Matrix and the Scattering States

Consider now the general multi-channel case, when the scattering is possible between different modes. It is convenient to define separately left (L) and right (R), incoming (+) and outgoing (−) modes (Fig. 2.14). We assume that at $z < z_L$ and $z > z_R$ the leads have a constant cross-sections. To make the $\boldsymbol{S}$-matrix unitary, we introduce the normalization of incoming and outgoing modes, as was discussed in Sect. 2.1.4. Thus, outside the scattering region we define

$$\psi^{+}_{LnE}(\boldsymbol{r}) = \frac{1}{\sqrt{2\pi\hbar\upsilon_{Ln}}}\phi_{Ln}(x, y)A_{n+}e^{ik_nz}, \quad z < z_L \tag{2.106}$$

$$\psi^{-}_{LnE}(\boldsymbol{r}) = \frac{1}{\sqrt{2\pi\hbar\upsilon_{Ln}}}\phi_{Ln}(x, y)A_{n-}e^{-k_nz}, \quad z < z_L \tag{2.107}$$

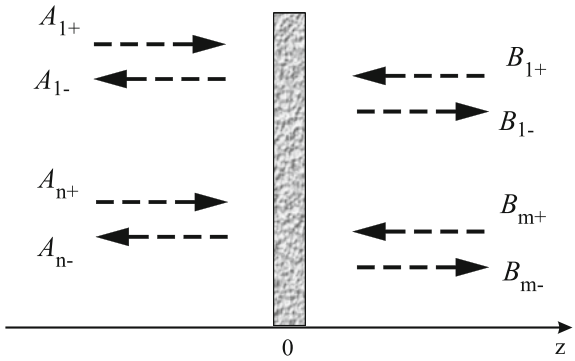

Fig. 2.14 Multi-channel scattering

$$\psi^{+}_{RmE}(\boldsymbol{r}) = \frac{1}{\sqrt{2\pi\hbar\upsilon_{Rm}}}\phi_{Rm}(x,y)B_{m+}e^{-ik'_m z}, \quad z > z_R \tag{2.108}$$

$$\psi^{-}_{RmE}(\boldsymbol{r}) = \frac{1}{\sqrt{2\pi\hbar\upsilon_{Rm}}}\phi_{Rm}(x,y)B_{m-}e^{ik'_m z}, \quad z > z_R. \tag{2.109}$$

Here n and m label the left and right transport channels respectively, $\phi_{Ln}(x,y)$ and $\phi_{Rm}(x,y)$ are the left and right transverse eigenfunctions, $\upsilon_{Ln} = \hbar k_n/m_L$ and $\upsilon_{Rm} = \hbar k'_m/m_R$ are the velocities, $\hbar k_n = \sqrt{2m_L(E-E_n)}$, $\hbar k'_m = \sqrt{2m_R(E-E_m)}$, E_n, E_m being transverse eigenenergies. As in the single-channel case, we mark the left wave amplitudes with $A_\pm$ and right with $B_\pm$.

The initial incoming states become now

$$\psi^{in}_{L(R)nE}(\boldsymbol{r}) = \frac{1}{\sqrt{2\pi\hbar\upsilon_{L(R)n}}}\phi_{L(R)n}(x,y)e^{+(-)ik_n z}. \tag{2.110}$$

It is important to remember, that we change the normalization, but we must keep the density of states. Indeed, the matrix element $\langle\psi^{in}_{nE}|\psi^{in}_{nE}\rangle$ acquires the additional multiplier $1/(h\upsilon)$. Thus, we should change

$$\int\frac{dk}{2\pi} = \int\frac{dE}{h\upsilon} \quad \Rightarrow \int\frac{dk}{2\pi}h\upsilon = \int dE. \tag{2.111}$$

This integration rule follows also from the normalization condition

$$\langle\psi^{in}_{L(R)nE}|\psi^{in}_{L(R)n'E'}\rangle = \int\left(\psi^{in}_{L(R)nE}(\boldsymbol{r})\right)^{*}\psi^{in}_{L(R)n'E'}(\boldsymbol{r})dxdydz = \delta_{nn'}\delta(E-E'). \tag{2.112}$$

Scattering matrix relates *all incoming* with *all outgoing* modes. In the single-channel case, considered previously, $\boldsymbol{S}$ is 2×2 matrix (2.44). In the general multi-channel case the $\boldsymbol{S}$-matrix is defined as $N\times N$ matrix

$$\begin{pmatrix} A_{1-} \\ \dots \\ A_{N_L-} \\ B_{1-} \\ \dots \\ B_{N_R-} \end{pmatrix} = \boldsymbol{S} \begin{pmatrix} A_{1+} \\ \dots \\ A_{N_L+} \\ B_{1+} \\ \dots \\ B_{N_R+} \end{pmatrix} = \begin{pmatrix} S_{11} & S_{12} & \dots & S_{1N} \\ S_{21} & S_{22} & \dots & S_{2N} \\ \dots & \dots & \dots & \dots \\ \dots & \dots & \dots & \dots \\ \dots & \dots & \dots & \dots \\ S_{N1} & S_{N2} & \dots & S_{NN} \end{pmatrix} \begin{pmatrix} A_{1+} \\ \dots \\ A_{N_L+} \\ B_{1+} \\ \dots \\ B_{N_R+} \end{pmatrix}, \tag{2.113}$$

where N_L and N_R are the numbers of left and right channels, $N = N_L + N_R$.

We represent it in the block form, analogous to (2.44):

$$\boldsymbol{S} = \begin{pmatrix} \hat{r} & \hat{t}' \\ \hat{t} & \hat{r}' \end{pmatrix} \tag{2.114}$$

where the matrices $\hat{r}$ ($N_L \times N_L$) and $\hat{t}$ ($N_L \times N_R$) describe transmission and reflection of the states incoming from the left, the matrices $\hat{r}'$ ($N_R \times N_R$) and $\hat{t}'$ ($N_R \times N_L$) describe transmission and reflection of the states incoming from the right, N_L (N_R) is the number of the left (right) channels.

The matrix $\hat{t}$ is called *transmission matrix*, $T_{mn} = |t_{mn}|^2$ are the probabilities of transmission from the left mode n into the right mode m, $R_{n'n} = |r_{n'n}|^2$ are the probabilities of reflection from the left mode n into the left mode n', etc.

The scattering matrix is unitary

$$\boldsymbol{S}^\dagger \boldsymbol{S} = \boldsymbol{S}\boldsymbol{S}^\dagger = \hat{I}, \tag{2.115}$$

from which the conservation of total probability is clear

$$\left(\boldsymbol{S}^\dagger \boldsymbol{S}\right)_{nn} = \sum_{n'} |r_{nn'}|^2 + \sum_{m} |t_{nm}|^2 = 1. \tag{2.116}$$

The other useful relations are

$$\hat{r}^\dagger \hat{r} + \hat{t}^\dagger \hat{t} = \hat{r}'^\dagger \hat{r}' + \hat{t}'^\dagger \hat{t}' = \hat{I}, \tag{2.117}$$
$$\hat{r}\hat{r}^\dagger + \hat{t}'\hat{t}'^\dagger = \hat{r}'\hat{r}'^\dagger + \hat{t}\hat{t}^\dagger = \hat{I}, \tag{2.118}$$
$$\hat{r}^\dagger \hat{t}' + \hat{t}^\dagger \hat{r}' = \hat{t}'^\dagger \hat{r} + \hat{r}'^\dagger \hat{t} = 0, \tag{2.119}$$
$$\hat{r}\hat{t}^\dagger + \hat{t}'\hat{r}'^\dagger = \hat{t}\hat{r}^\dagger + \hat{r}'\hat{t}'^\dagger = 0. \tag{2.120}$$

From which follows

$$\mathrm{Tr}\left(\hat{t}^\dagger \hat{t}\right) = \mathrm{Tr}\left(\hat{t}\hat{t}^\dagger\right) = \mathrm{Tr}\left(\hat{t}'^\dagger \hat{t}'\right) = \mathrm{Tr}\left(\hat{t}'\hat{t}'^\dagger\right), \tag{2.121}$$
$$\mathrm{Tr}\left(\hat{r}^\dagger \hat{r}\right) = \mathrm{Tr}\left(\hat{r}\hat{r}^\dagger\right) = \mathrm{Tr}\left(\hat{r}'^\dagger \hat{r}'\right) = \mathrm{Tr}\left(\hat{r}'\hat{r}'^\dagger\right). \tag{2.122}$$

In the time-reversal case the $\boldsymbol{S}$-matrix is symmetric

$$\boldsymbol{S} = \boldsymbol{S}^T, \tag{2.123}$$

thus the reflection matrix is also symmetric $r_{nn'} = r_{n'n}$, and $\hat{t}' = \hat{t}^T$.

In the external magnetic field more general conditions take place:

$$r_{nn'}(B) = r_{n'n}(-B), \tag{2.124}$$

$$t_{nm}(B) = t'_{mn}(-B). \tag{2.125}$$

The simplest way to proceed is to use the so-called scattering states. Using incoming and outgoing modes in the right and left leads (2.106)–(2.109), we can define the scattering states as

$$\Psi_{LnE}(\boldsymbol{r}) = \begin{cases} \dfrac{1}{\sqrt{2\pi\hbar\upsilon_{Ln}}}\phi_{Ln}(x,y)e^{ik_n z} + \displaystyle\sum_{n'} \frac{r_{n'n}(E)}{\sqrt{2\pi\hbar\upsilon_{Ln'}}}\phi_{Ln'}(x,y)e^{-ik_n z}, \ z < z_L, \\ \displaystyle\sum_{m} \frac{t_{mn}(E)}{\sqrt{2\pi\hbar\upsilon_{Rm}}}\phi_{Rm}(x,y)e^{ik'_m z}, \ z > z_R. \end{cases} \tag{2.126}$$

The physical sense of this state is quite transparent. It describes a particle moving from the left and splitting into reflected and transmitted parts. We established that it is important for Landauer transport, that only these states are populated from the left reservoir, so that one can accept the distribution of "left" scattering states to be equilibrium with the left electro-chemical potential. The "right" states, populated by the right reservoir, are defined as

$$\Psi_{RmE}(\boldsymbol{r}) = \begin{cases} \dfrac{1}{\sqrt{2\pi\hbar\upsilon_{Rm}}}\phi_{Rm}(x,y)e^{-ik'_m z} + \displaystyle\sum_{m'} \frac{r'_{m'm}(E)}{\sqrt{2\pi\hbar\upsilon_{Rm'}}}\phi_{Rm'}(x,y)e^{ik'_m z}, \ z > z_R, \\ \displaystyle\sum_{n} \frac{t'_{nm}(E)}{\sqrt{2\pi\hbar\upsilon_{Ln}}}\phi_{Ln}(x,y)e^{-ik_n z}, \ z < z_L. \end{cases} \tag{2.127}$$

Now, using the left and right states (2.106)–(2.109) or the scattering states (2.126), (2.127), it is straightforward to obtain the Landauer formula.

2.3.2 Multi-channel Landauer Formula

Below in the Sect. 2.3 we consider only time-reversal case, so that

$$R_{n'n} = |r_{n'n}|^2 = |r_{nn'}|^2 = R_{nn'}, \tag{2.128}$$

$$T_{mn} = |t_{mn}|^2 = |t'_{nm}|^2 = T'_{nm}. \tag{2.129}$$

Zero Temperature Conductance

The heuristic calculation of the conductance is straightforward. The current from the left mode $\psi^+_{Ln}(\boldsymbol{r})$ into the right mode $\psi^-_{Rm}(\boldsymbol{r})$ is determined by the transmission probability T_{mn}. The inverse current from $\psi^-_{Ln}(\boldsymbol{r})$ into $\psi^+_{Rm}(\boldsymbol{r})$ is determined by

$T'_{nm} = T_{mn}$. Assuming that all left states $\psi^{+}_{Ln}(\boldsymbol{r})$ are populated with the electrochemical potential of the left electrode, and right states $\psi^{-}_{Rm}(\boldsymbol{r})$ are populated with the electrochemical potential of the right electrode, we obtain the current of incoming left n and right m electrons as

$$I_{mn} = \frac{e}{h} T_{mn} \left(\tilde{\mu}_L - \tilde{\mu}_R\right), \tag{2.130}$$

summing contributions from all incoming left modes and all incoming right modes we obtain the full current

$$I = \frac{e}{h} \sum_{n=1}^{N_L} \sum_{m=1}^{N_R} T_{mn} \left(\tilde{\mu}_L - \tilde{\mu}_R\right). \tag{2.131}$$

After the obvious mathematical transformation

$$\begin{aligned} \sum_{n=1}^{N_L} \sum_{m=1}^{N_R} T_{mn} = \sum_{n=1}^{N_L} \sum_{m=1}^{N_R} |t_{mn}|^2 = \sum_{n=1}^{N_L} \sum_{m=1}^{N_R} t_{mn} t^*_{mn} = \sum_{n=1}^{N_L} \sum_{m=1}^{N_R} \left(\hat{t}^{\dagger}\right)_{nm} t_{mn} \\ = \sum_{n=1}^{N_L} \left(\hat{t}^{\dagger} \hat{t}\right)_{nn} = \mathrm{Tr}\left(\hat{t}^{\dagger} \hat{t}\right), \end{aligned} \tag{2.132}$$

we obtain the Landauer multi-channel current and conductance

$$I = \frac{e}{h} \mathrm{Tr}\left(\hat{t}^{\dagger} \hat{t}\right) \left(\tilde{\mu}_L - \tilde{\mu}_R\right) = \frac{e^2}{h} \mathrm{Tr}\left(\hat{t}^{\dagger} \hat{t}\right) V, \tag{2.133}$$

$$G = \frac{e^2}{h} \mathrm{Tr}\left(\hat{t}^{\dagger} \hat{t}\right). \tag{2.134}$$

General Expression

If we repeat the above summation procedure at finite temperature and voltage, we obtain a generalized form of (2.76)

$$I(V) = \frac{e}{h} \sum_{nm} \int_{-\infty}^{\infty} T_{nm}(E, V) \left[f_L(E) - f_R(E)\right] dE. \tag{2.135}$$

It is instructive, however, to consider an approach utilizing the scattering states. Let us calculate the current carrying by one scattering state $\Psi_{LnE}(\boldsymbol{r})$ (2.126). Direct application of the current density expression

$$\mathbf{j} = \frac{ie\hbar}{2m} \left[\psi(\boldsymbol{r}) \nabla \psi^*(\boldsymbol{r}) - \psi^*(\boldsymbol{r}) \nabla \psi(\boldsymbol{r})\right] \tag{2.136}$$

gives the following answer for the z-component of the current density:

$$j^z_{LnE} = \frac{ie\hbar}{2m} \sum_{mm'} \frac{t_{mn} t^*_{m'n}}{2\pi\hbar\sqrt{\upsilon_{Rm}\upsilon_{Rm'}}} \phi_{Rm}(x, y)\phi^*_{Rm'}(x, y)(-ik'_{m'} - ik'_m)e^{ik'_m z - ik'_{m'} z} \tag{2.137}$$

And integrating over (x, y) and using the orthogonality property

$$\int\int \phi_{Rm}(x, y)\phi_{Rm'}(x, y)dxdy = \delta_{mm'}, \tag{2.138}$$

we get

$$I_{LnE} = e \sum_m |t_{mn}|^2 = \frac{e}{h} \left(\hat{t}^\dagger \hat{t}\right)_{nn}. \tag{2.139}$$

We can summarize over transport channels, and obtain the following general two-terminal Landauer formula for the current

$$I(V) = \frac{e}{h} \int_{-\infty}^{\infty} T(E, V) \left[f_0(E - eV) - f_0(E)\right] dE, \tag{2.140}$$

with

$$T(E, V) = \sum_n \left(\hat{t}^\dagger \hat{t}\right)_{nn} = \mathrm{Tr}\left(\hat{t}^\dagger \hat{t}\right) = \sum_{nm} T_{mn} = \sum_{nm} |t_{mn}|^2. \tag{2.141}$$

$T(E, V)$ is the effective *transmission function* for the particles with the energy E. The most important advantage of this formula is, that the transmission function can be calculated from the quantum scattering theory. Thus, the kinetic problem is reduced to the pure quantum mechanical problem of a single particle in a static potential. The formula (2.140) is the most general *two-terminal* formula. All other Landauer formulas can be obtained in the limiting cases from (2.140). For the finite-temperature conductance we have

$$G = \frac{e^2}{h} \int_{-\infty}^{\infty} T(E) \left(-\frac{\partial f_0}{\partial E}\right) dE. \tag{2.142}$$

At zero temperature $(-\partial f_0/\partial E) = \delta(E - E_F)$, thus

$$G = \frac{e^2}{h} T(E_F). \tag{2.143}$$

In agreement with the previous results.

Transmission Probabilities and Transmission Eigenvalues

The physical sense of the transmission function (2.141) can be interpreted in two different ways.

First, $T_n = \left(\hat{t}^\dagger \hat{t}\right)_{nn}$ is the transmission probability for the incoming state in the n-th channel.

On the other hand, the $N \times N$ matrix $\hat{t}^\dagger \hat{t}$ can be diagonalized. One can consider the eigenvalues $\mathscr{T}_n$ as the transmission coefficients in the basis of independent transport channels.

The conductance has the same form in both cases because of the invariance of the trace

$$G = \frac{e^2}{h} \sum_n T_n = \frac{e^2}{h} \sum_n \mathscr{T}_n. \tag{2.144}$$

2.3.3 *Derivation from the Linear Response Theory*

In the previous sections we obtained the Landauer formula, valid at finite voltage, using some additional arguments about the populations of the states inside the junction. Here we restrict ourselves by the linear response approach, which is valid only in the limit of small voltage, but is exact.

We start from the Kubo formula for conductance (we follow here the book of H. Bruus and K. Flensberg [8])[1]:

$$G = \lim_{\omega \to 0} \frac{\hbar}{\omega} \mathrm{Re} \int_0^\infty dt e^{i(\omega + i\eta)t} \left\langle \left[\hat{I}(t), \hat{I}(0) \right]_- \right\rangle_{eq}, \tag{2.145}$$

where $[...]_-$ is the commutator, the matrix elements of the current operator $\hat{I}$ in the Hilbert space of single particle eigenfunctions $\Psi_\lambda(\boldsymbol{r})$ are

$$I_{\lambda\lambda'}(z) = \frac{ie\hbar}{2m} \int dxdy \left(\Psi_\lambda \frac{\partial \Psi^*_{\lambda'}}{\partial z} - \Psi^*_{\lambda'} \frac{\partial \Psi_\lambda}{\partial z} \right), \tag{2.146}$$

which should be independent of z in the stationary case because of current conservation, and can be evaluated at any cross-section.

To proceed, we use the current operators and the second quantization:

$$\hat{I} = \sum_{\lambda\lambda'} I_{\lambda\lambda'} c^\dagger_\lambda c_{\lambda'}, \tag{2.147}$$

and choose the scattering states (2.126), (2.127) as eigenfunctions Ψ_λ with λ being equivalent to the set s, n, E, where $s = L, R$ is the lead index, n is the number of channel in the lead s, and E is the energy. Straightforward calculation of the statistical average in equilibrium, using $\left\langle c^\dagger_\lambda c_{\lambda'} \right\rangle_{eq} = f_0(E_\lambda)\delta_{\lambda\lambda'}$ and $I_{\lambda\lambda'} = I^*_{\lambda'\lambda}$, gives

[1] We use here the second quantization, so it is a little bit beyond the "basic concepts".

$$\left\langle \left[\hat{I}(t), \hat{I}(0) \right]_- \right\rangle_{eq} = \sum_{\lambda\lambda'\mu\mu'} I_{\mu\mu'} I_{\lambda\lambda'} e^{i(E_\lambda - E_{\lambda'})} \left\langle \left[c_\lambda^\dagger c_{\lambda'}, c_\mu^\dagger c_{\mu'} \right]_- \right\rangle_{eq}$$
$$= \sum_{\lambda\lambda'} |I_{\lambda\lambda'}|^2 e^{i(E_\lambda - E_{\lambda'})} \Big[f_0(E_\lambda) - f_0(E_{\lambda'}) \Big]. \tag{2.148}$$

Inserting this into (2.145) and integrating, we get

$$G = \lim_{\omega\to 0} \frac{\hbar}{\omega} \mathrm{Im} \sum_{\lambda\lambda'} \frac{|I_{\lambda\lambda'}|^2}{\omega + i\eta + E_\lambda - E_{\lambda'}} \Big[f_0(E_\lambda) - f_0(E_{\lambda'}) \Big]$$
$$= \pi\hbar \sum_{\lambda\lambda'} |I_{\lambda\lambda'}|^2 \left(-\frac{\partial f_0}{\partial E} \right)_{E_\lambda} \delta(E_\lambda - E_{\lambda'}). \tag{2.149}$$

Now we use explicitly, that $\lambda \equiv s, n, E$, and integrating over the energy E' obtain

$$G = \pi\hbar \int_{-\infty}^{\infty} \sum_{ss'} \sum_{nn'} |I_{sn,s'n'}|^2 \left(-\frac{\partial f_0}{\partial E} \right) dE$$
$$= \pi\hbar \int_{-\infty}^{\infty} \sum_{nn'} \left[|I_{Ln,Ln'}|^2 + |I_{Ln,Rn'}|^2 + |I_{Rn,Ln'}|^2 + |I_{Rn,Rn'}|^2 \right] \left(-\frac{\partial f_0}{\partial E} \right) dE. \tag{2.150}$$

The calculation of $|I_{sn,s'n'}|^2$ for the scattering states (2.126), (2.127) is straightforward, left or right parts of these expressions can be equivalently used. It is essentially the same, as we made to get (2.139). Thus, we have (here $n, n' \in L$, $m, m' \in R$)

$$I_{n,n'} = \frac{e}{h} \left(\hat{t}^\dagger \hat{t} \right)_{n'n}, \quad I_{n,m} = \frac{e}{h} \left(\hat{r}'^\dagger \hat{t} \right)_{n'n}, \quad I_{m,n} = -\frac{e}{h} \left(\hat{r}^\dagger \hat{t}' \right)_{nn'}, \quad I_{m,m'} = -\frac{e}{h} \left(\hat{t}'^\dagger \hat{t}' \right)_{mm'}. \tag{2.151}$$

Using these expressions and the properties (2.118), it is easy to show that in the time-reversal case

$$\sum_{ss'} \sum_{nn'} |I_{sn,s'n'}|^2 = \left(\frac{e}{h} \right)^2 \mathrm{Tr} \left[\left(\hat{t}^\dagger \hat{t} \right)^2 + \left(\hat{t}'^\dagger \hat{t}' \right)^2 + \hat{t}^\dagger \hat{r}' \hat{r}'^\dagger \hat{t} + \hat{t}'^\dagger \hat{r} \hat{r}^\dagger \hat{t}' \right] = 2 \left(\frac{e}{h} \right)^2 \mathrm{Tr} \left(\hat{t}^\dagger \hat{t} \right), \tag{2.152}$$

and finally

$$G = \frac{e^2}{h} \int_{-\infty}^{\infty} \mathrm{Tr} \left(\hat{t}^\dagger \hat{t} \right) \left(-\frac{\partial f_0}{\partial E} \right) dE. \tag{2.153}$$

We derived again the Landauer formula.

2.4 Multi-terminal Systems

2.4.1 Multi-terminal Landauer-Büttiker Formula

The scattering theory, developed in the previous section, can be applied also in the multi-terminal case (Fig. 2.15) exactly in the same way, as in the multi-channel case. The only difference from the considered before two-terminal system is that now there are several electrodes with independent electrochemical potentials and the same number of leads with independent transport channels.

We use in this section the following notations: M is the number of terminals, N_s ($s = 1, ..., M$) is the number of transport channels in s lead, $N = \sum_s N_s$ is the full number of channels.

The left and right scattering states introduced by (2.126), (2.127) for 2-terminal geometry are straightforwardly generalized to a set of scattering states corresponding to incoming waves from any s lead:

$$\Psi_{snE}(\boldsymbol{r}) = \begin{cases} \dfrac{1}{\sqrt{2\pi\hbar\upsilon_{sn}}}\phi_{sn}(x,y)e^{ik_n z} + \displaystyle\sum_{n'} \frac{r_{n'n}(E)}{\sqrt{2\pi\hbar\upsilon_{sn'}}}\phi_{sn'}(x,y)e^{-ik_n z}, \ n, z \in s, \\ \displaystyle\sum_{m} \frac{t_{mn}(E)}{\sqrt{2\pi\hbar\upsilon_{pm}}}\phi_{pm}(x,y)e^{ik'_m z}, \ p \neq s, \ m, z \in p. \end{cases} \tag{2.154}$$

The current through the terminal s, flowing in the direction to the scattering region, is given by the following expression

$$I_s = e\sum_n \left[\int_0^\infty \upsilon_s(n,k_z) f_s(n,k_z)\frac{dk_z}{2\pi} + \int_{-\infty}^0 \upsilon_s(n,k_z)\sum_{pm}|S_{sn,pm}|^2 f_p(m,k_z)\frac{dk_z}{2\pi}\right], \tag{2.155}$$

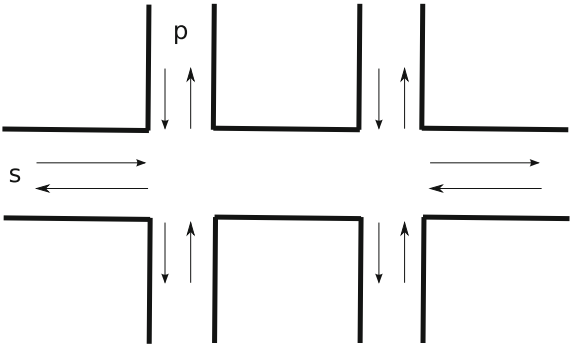

Fig. 2.15 Example of a multi-terminal system

here s, p are the terminal indices, n, m are the channel indices. The first term is the current of the electrons incoming from the s electrode, the second term is the current of electrons reflected and transmitted from other electrodes. Changing to the energy integration, we get finally

$$I_s = \frac{e}{h}\int_{-\infty}^{\infty}\sum_{n,pm}\left[\delta_{sp}\delta_{nm} - |S_{sn,pm}|^2\right] f_p(E)dE. \tag{2.156}$$

Let us introduce the transmission and reflection functions

$$T_{sp} = \sum_{nm}|S_{sn,pm}|^2 = \sum_{nm}|t_{sn,pm}|^2, \quad R_{ss} = \sum_{nn'}|S_{sn,sn'}|^2, \tag{2.157}$$

by definition $T_{ss} = R_{ss}$. Then, the current gets the form

$$I_s = \frac{e}{h}\int_{-\infty}^{\infty}\left[(N_s - R_{ss})f_s(E) - \sum_{p\neq s}T_{sp}f_p(E)\right]dE, \tag{2.158}$$

or, equivalently,

$$I_s = \frac{e}{h}\int_{-\infty}^{\infty}\left[N_s f_s(E) - \sum_{p}T_{sp}f_p(E)\right]dE, \tag{2.159}$$

or, equivalently

$$I_s = \frac{e}{h}\sum_{p}\int_{-\infty}^{\infty}\left[T_{ps}f_s(E) - T_{sp}f_p(E)\right]dE. \tag{2.160}$$

From the unitarity the following sum rule can be obtained

$$\sum_{p}T_{sp} = \sum_{p}T_{ps} = N_s. \tag{2.161}$$

From time-reversal in the presence of a magnetic field $\mathbf{H}$

$$\sum_{p\neq s}T_{sp}(\mathbf{H}) = \sum_{p\neq s}T_{ps}(-\mathbf{H}). \tag{2.162}$$

2.4.2 Büttiker Conductance Formalism

Following Büttiker [9, 10], we formulate the elegant formulas, which allow to calculate the currents and voltages in the linear regime. We start from the current expression (2.160). For small voltages it holds that:

$$G_{sp} = \frac{e^2}{h} \int_{-\infty}^{\infty} T_{sp}(E) \left(-\frac{\partial f_0}{\partial E} \right) dE, \tag{2.163}$$

$$I_s = \sum_p \left[G_{ps} V_s - G_{sp} V_p \right]. \tag{2.164}$$

In the time-reversal case these formulas take the usual multi-channel form. For example, the formulas (2.133) and (2.134) can be rewritten as

$$I_s = \frac{e^2}{h} \sum_p T_{sp} \left(V_s - V_p \right) = \frac{e^2}{h} \sum_{s \neq p} T_{sp} V_{sp}, \tag{2.165}$$

$$G_{sp} = \frac{e^2}{h} T_{sp} = \frac{e^2}{h} \mathrm{Tr} \left(\hat{t}_{sp} \hat{t}_{sp}^{\dagger} \right). \tag{2.166}$$

In equilibrium $I_s = 0$, but the potentials V_s can have some constant value because of gauge invariance $V_s = V_0 \neq 0$. Thus, we obtain the sum rule

$$\sum_p G_{ps} = \sum_p G_{sp}. \tag{2.167}$$

This shows, that the current can be equivalently written as

$$I_s = \sum_p G_{sp} \left[V_s - V_p \right]. \tag{2.168}$$

There is also the alternative representation

$$I_s = \sum_p G'_{sp} V_p, \tag{2.169}$$

where the conductances $\hat{G}'$ are defined by the following $M \times M$ matrix

$$\hat{G}' = \frac{e^2}{h} \begin{bmatrix} N_1 - R_{11} & -T_{12} & \cdots & -T_{1M} \\ -T_{21} & N_2 - R_{22} & \cdots & -T_{2M} \\ \vdots & \cdots & \ddots & \vdots \\ -T_{M1} & \cdots & \cdots & N_M - R_{MM} \end{bmatrix}. \tag{2.170}$$

The conductances G and G' are related in an obvious way, and can be used equivalently. The sum rule for $\hat{G}'$ is

$$\sum_p G'_{ps} = 0 \;\Rightarrow\; G'_{ss} = -\sum_{p\neq s} G'_{ps}. \tag{2.171}$$

Before discussing the applications of this current formula, we should introduce the notion of a *voltage probe*. The voltage probe is any terminal, in which the zero current is preserved, $I_s = 0$. In spite of zero current, such terminal influences the current through other terminals. The physical reason is that the electrons can enter the electrode and return back, but after phase randomization. Thus, the voltage probe can be used not only for voltage measurement, but also for introducing a decoherence into the system.

3-Terminal Conductance

Consider, as an example, a three-terminal junction (Fig. 2.16). Let the terminal 3 to be a voltage probe: $I_3 = 0$, $I_1 = -I_2 = I$, $V_1 - V_2 = V$. We have the following equations

$$I_3 = G_{31}(V_3 - V_1) + G_{32}(V_3 - V_2) = 0, \tag{2.172}$$

$$I = G_{12}V + G_{13}(V_1 - V_3) = G_{21}V - G_{23}(V_2 - V_3). \tag{2.173}$$

We can also choose $V_1 = V$, $V_2 = 0$, then

$$V_3 = \frac{G_{31}}{G_{31} + G_{32}} V. \tag{2.174}$$

This voltage is not small in the limit $G_{31}, G_{32} \ll G_{12}$, when the third electrode is used for unperturbed voltage measurement. The current is

$$I = \left[G_{12} + \frac{G_{13}G_{32}}{G_{31} + G_{32}} \right] V, \tag{2.175}$$

it is not perturbed when $G_{31}, G_{32} \to 0$ and we get simply 2-terminal Landauer conductance $V = G_{12}V$, but at finite coupling to the third electrode, the current between electrodes 1 and 2 is changed. The first term in (2.175) is usual coherent transport between 1st and 2nd electrodes. Let us try to clarify the physical sense of the second contribution. To this end, assume that $G_{12} \to 0$ and we have only the second term. Then we can rewrite (2.175) in the following form

$$\frac{V}{I} = R = \frac{G_{13} + G_{32}}{G_{13}G_{32}} = \frac{1}{G_{13}} + \frac{1}{G_{32}} = R_{13} + R_{32}. \tag{2.176}$$

We got the result that the resistance of the system is just the sum of the classical serial resistances R_{13} and R_{32}! Somehow the answer corresponds to the case with no

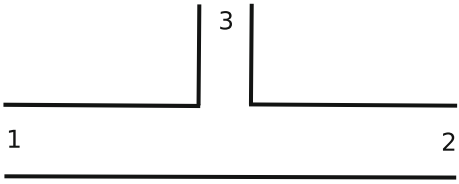

Fig. 2.16 Three-terminal junctions

quantum coherence between two junctions. Thus the Büttiker voltage probe works as a dephasing element.

4-Terminal Conductance

Consider finally the 4-terminal system (Fig. 2.17) and assume that electrodes 3 and 4 are weakly coupled voltage probes. In this case the current $I = I_1 = -I_2 \approx G_{12}V$. What is the voltage $V' = V_3 - V_4$? Neglecting G_{34} and G_{43} as the next-order small terms, we obtain (detailed calculations can be found in the book of D. K. Ferry and S. M. Goodnick [11], Sect. 3.9)

$$V' = \frac{T_{31}T_{42} - T_{32}T_{41}}{(T_{31} + T_{32})(T_{41} + T_{42})}V, \tag{2.177}$$

where we use transmissions instead of conductances. Now we assume that the scattering region is placed between 3rd and 4th terminals and is characterized by the transmission coefficient T and the reflection coefficient R if we have only electrodes 1 and 2. Transmissions from 1st to 3rd and from 4th to 2nd terminals are all equal and include two contributions: direct tunneling from 1st to 3rd and from 4th to 2nd with some small probability $\varepsilon \ll 1$ (because we assumed that electrodes 3 and 4 are weakly coupled) and tunneling after the reflection from the scattering region with the probability εR, thus the full transmission coefficients are $T_{31} = T_{42} = \varepsilon(1 + R)$. On the other hand, the probability to go from the 1st electrode to the 4th one and from the 2nd electrode to the 3rd is $T_{32} = T_{41} = \varepsilon T$. Collecting these expressions together and using $T + R = 1$, we obtain

$$V' = RV, \tag{2.178}$$

and

$$R_{12,34} = \frac{V'}{I} = \frac{h}{2e^2}\frac{R}{T}. \tag{2.179}$$

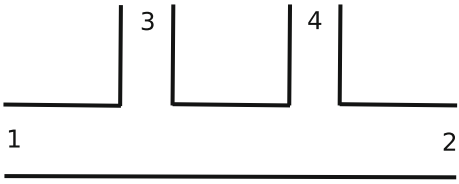

Fig. 2.17 Four-terminal junctions

We obtain the first Landauer formula (2.68). That confirms our understanding of this formula as a conductance for the 4-probe measurement inside the coherent conductor.

References

1. R. Landauer, IBM J. Res. Develop. **1**, 223 (1957)
2. R. Landauer, Phil. Mag. **21**, 863 (1970)
3. E.N. Economou, C.M. Soukoulis, Phys. Rev. Lett. **46**, 618 (1981)
4. D.S. Fisher, P.A. Lee, Phys. Rev. B **23**, 6851 (1981)
5. M. Büttiker, Phys. Rev. B **41**, 7906 (1990)
6. Y.V. Sharvin, JETP **21**, 655 (1965). [J. Exp. Theor. Fiz. **48**, 948 (1965)]
7. C.W.J. Beenakker, H. van Houten, in *Solid State Physics*, vol. 44, ed. by H. Ehrenreich, D. Turnbull (Academic Press, Boston, 1991)
8. H. Bruus, K. Flensberg, *Many-Body Quantum Theory in Condensed Matter Physics* (Oxford University Press, Oxford, 2004)
9. M. Büttiker, Phys. Rev. Lett. **57**, 1761 (1986)
10. M. Büttiker, IBM J. Res. Develop. **32**, 317 (1988)
11. D.K. Ferry, S.M. Goodnick, *Transport in Nanostructures* (Cambridge University Press, Cambridge, 1997)

Chapter 3
Green Functions

In this chapter we formulate the Landauer approach using the *Green function* (GF) formalism. It is a mathematically elegant and numerically effective method to describe quantum scattering and transport. In Sect. 3.1 we consider definitions and basic properties of *retarded* (and *advanced*) Green functions and discuss the relations between Schrödinger equation, wave functions, GFs, and the scattering matrix.

Atomic and molecular scale systems are naturally described by discrete-level models, based, for example, on atomic orbitals and molecular orbitals. For continuous systems with complex geometries and/or disorder, discretization is a first step towards numerical computational methods. Starting from discrete-level representations we come to *matrix* Green functions, being the main theoretical tool at nanoscale. On the other hand, electrodes are assumed to be infinitely large and have continuous energy spectrum. To include the electrode effects systematically, it is reasonable to start from the discrete-level representation for the whole system. It can be made with a help of the *tight-binding* (TB) model, which was proposed to describe quantum systems in which the localized electronic states play essential role, it is widely used as an alternative to the plane wave description of electrons in solids, and also as a method to calculate the electronic structure of molecules in quantum chemistry. All effects of the equilibrium electrodes can be included into the matrix equations for the central region through the *self-energies*. We consider the matrix formalism in general in Sect. 3.2 and the recursive method for long or complex systems in Sect. 3.3. Finally, calculation of self-energies for semi-infinite electrodes requires some special methods, which are considered in Sect. 3.4.

Note that Green functions introduced in this section are *single-particle GFs in non-interacting systems*. The extension of the technique to many-body systems with interactions will be considered in Chap. 7.

D.A. Ryndyk, *Theory of Quantum Transport at Nanoscale*,
Springer Series in Solid-State Sciences 184,
DOI 10.1007/978-3-319-24088-6_3

3.1 Green Functions and the Scattering Problem

3.1.1 Retarded and Advanced Green Functions

Green functions are known to be a convenient tool to solve linear differential equations, including the Schrödinger equation in quantum mechanics. Being completely equivalent to the Landauer scattering approach, the GF technique has the advantage that it calculates relevant transport quantities (e.g. transmission function) using effective numerical techniques. Besides, the Green function formalism is well adopted for atomic and molecular discrete-level systems and can be easily extended to include inelastic and many-body effects. First of all, we give the formal general definition and the basic properties of *retarded* and *advanced* Green functions (also called *propagators*).

Let us start from the time-dependent Schrödinger equation

$$i\hbar\frac{\partial|\Psi(t)\rangle}{\partial t} = \hat{H}|\Psi(t)\rangle. \tag{3.1}$$

In this section we use general Dirac notations $|\ldots\rangle$ for quantum states and general operator notations $\hat{.\,.}$ to show that the representation is arbitrary (coordinate and matrix representations considered below are special cases). The solution of this equation at time t can be written in terms of the solution at time t':

$$|\Psi(t)\rangle = \hat{U}(t,t')|\Psi(t')\rangle, \tag{3.2}$$

where $\hat{U}(t,t')$ is called the time-evolution operator.

Below we consider only the case of a time-independent Hermitian Hamiltonian $\hat{H}$, so that the eigenstates $|\Psi_n(t)\rangle = e^{-iE_nt/\hbar}|\Psi_n\rangle$ with energies E_n are found from the stationary Schrödinger equation

$$\hat{H}|\Psi_n\rangle = E_n|\Psi_n\rangle. \tag{3.3}$$

The eigenfunctions $|\Psi_n\rangle$ are orthogonal and normalized, for discrete energy levels[1]:

$$\langle\Psi_n|\Psi_m\rangle = \delta_{nm}, \tag{3.4}$$

and form a complete set of states ($\hat{I}$ is the unity operator)

$$\sum_n |\Psi_n\rangle\langle\Psi_n| = \hat{I}. \tag{3.5}$$

[1] $\langle\Psi_1|\Psi_2\rangle$ is the scalar product in the corresponding Hilbert space. The Kronecker delta $\delta_{nm} = 1$ if $n = m$, otherwise $\delta_{nm} = 0$. It is equivalent to the unity matrix I_{nm}.

For continuous spectrum the orthogonality condition is

$$\langle \Psi_k | \Psi_{k'} \rangle = \delta(k - k'), \tag{3.6}$$

and the completeness in the case of combined (discrete and continuous) spectrum is written explicitly as

$$\sum_n |\Psi_n\rangle\langle\Psi_n| + \int dk |\Psi_k\rangle\langle\Psi_k| = \hat{I}. \tag{3.7}$$

The time-evolution operator for a time-independent Hamiltonian can be written as

$$\hat{U}(t - t') = e^{-i(t-t')\hat{H}/\hbar}. \tag{3.8}$$

This formal solution is difficult to use directly in most cases, but one can obtain the useful eigenstate representation from it. From the identity $\hat{U} = \hat{U}\hat{I}$ and (3.3), (3.5), (3.8) it follows that[2]

$$\hat{U}(t - t') = \sum_n e^{-\frac{i}{\hbar}E_n(t-t')} |\Psi_n\rangle\langle\Psi_n|, \tag{3.9}$$

which demonstrates the superposition principle. The wave function at time t is

$$|\Psi(t)\rangle = \hat{U}(t, t')|\Psi(t')\rangle = \sum_n e^{-\frac{i}{\hbar}E_n(t-t')} \langle\Psi_n|\Psi(t')\rangle |\Psi_n\rangle, \tag{3.10}$$

where $\langle\Psi_n|\Psi(t')\rangle$ are the coefficients of the expansion of the initial function $|\Psi(t')\rangle$ in the basis of eigenstates.

It is equivalent and more convenient to introduce two *Green operators*, called also *propagators*, retarded $\hat{G}^R(t, t')$ and advanced $\hat{G}^A(t, t')$:

$$\hat{G}^R(t, t') = -\frac{i}{\hbar}\theta(t - t')\hat{U}(t, t') = -\frac{i}{\hbar}\theta(t - t')e^{-i(t-t')\hat{H}/\hbar}, \tag{3.11}$$

$$\hat{G}^A(t, t') = \frac{i}{\hbar}\theta(t' - t)\hat{U}(t, t') = \frac{i}{\hbar}\theta(t' - t)e^{-i(t-t')\hat{H}/\hbar}, \tag{3.12}$$

so that at $t > t'$ one has

$$|\Psi(t)\rangle = i\hbar\hat{G}^R(t - t')|\Psi(t')\rangle, \tag{3.13}$$

while at $t < t'$ it follows

$$|\Psi(t)\rangle = -i\hbar\hat{G}^A(t - t')|\Psi(t')\rangle. \tag{3.14}$$

[2]Note the property $f(\hat{H})|\Psi_n\rangle = f(E_n)|\Psi_n\rangle$ for any function f.

From the definition one can see that $G^R(t-t')=0$ at $t<t'$, $G^A(t-t')=0$ at $t'<t$, and[3]

$$\hat{G}^A(t,t')=\hat{G}^{R\dagger}(t',t). \tag{3.15}$$

We can conclude that retarded functions describe propagation into future, while advanced into past. Actually retarded and advanced propagators are related because of the time-symmetry of quantum mechanics (we neglect here any dissipation).

The operators $\hat{G}^R(t,t')$ at $t\geqslant t'$ and $\hat{G}^A(t,t')$ at $t\leqslant t'$ are the solutions of the equation

$$\left[i\hbar\frac{\partial}{\partial t}-\hat{H}\right]\hat{G}^{R(A)}(t,t')=\hat{I}\delta(t-t'), \tag{3.16}$$

with the boundary conditions $\hat{G}^R(t,t')=0$ at $t<t'$, $\hat{G}^A(t,t')=0$ at $t>t'$. Indeed, at $t>t'$ (3.13) satisfies the Schrödinger equation (3.1) due to (3.16). And integrating (3.16) from $t=t'-\eta$ to $t=t'+\eta$, where η is an infinitesimally small positive number $\eta=0^+$, one gets

$$\hat{G}^R(t+\eta,t')=\frac{1}{i\hbar}\hat{I}, \tag{3.17}$$

giving correct boundary condition at $t=t'$. Thus, if we know the retarded Green operator $\hat{G}^R(t,t')$, we can find the time-dependent wave function at any initial condition (and make many other useful things, as we will see below).

For a time-independent Hamiltonian the Green function is a function of the time difference $\tau=t-t'$, and one can consider the Fourier transform

$$\hat{G}^{R(A)}(E)=\int_{-\infty}^{\infty}\hat{G}^{R(A)}(\tau)e^{iE\tau/\hbar}d\tau. \tag{3.18}$$

This transform, however, can not be performed in all cases, because $G^{R(A)}(\tau)$ includes oscillating terms $e^{-\frac{i}{\hbar}E_n\tau}$. To avoid this problem we define the retarded Fourier transform

$$\hat{G}^R(E)=\lim_{\eta\to 0^+}\int_{-\infty}^{\infty}\hat{G}^R(\tau)e^{i(E+i\eta)\tau/\hbar}d\tau, \tag{3.19}$$

and the advanced one

$$\hat{G}^A(E)=\lim_{\eta\to 0^+}\int_{-\infty}^{\infty}\hat{G}^A(\tau)e^{i(E-i\eta)\tau/\hbar}d\tau. \tag{3.20}$$

where the limit $\eta\to 0$ is assumed in the end of calculation. With this addition the integrals are convergent. This definition is equivalent to the definition of a retarded

[3] $O^\dagger$ is the Hermitian conjugated operator, defined for operator $\hat{O}$ as $\langle\hat{O}\Psi|\Phi\rangle=\langle\Psi|\hat{O}^\dagger\Phi\rangle$.

(advanced) function as a function of complex energy variable at the upper (lower) part of the complex plain.

Applying this transform to (3.16), we get the equation for the retarded Green operator $\hat{G}^R(E)$

$$\left[(E+i\eta)\hat{I}-\hat{H}\right]\hat{G}^R(E)=\hat{I}, \tag{3.21}$$

or

$$\hat{G}^R(E)=\left[(E+i\eta)\hat{I}-\hat{H}\right]^{-1}. \tag{3.22}$$

The advanced operator $\hat{G}^A(E)$ is related to the retarded one through

$$\hat{G}^A(E)=\hat{G}^{R\dagger}(E). \tag{3.23}$$

It is possible to represent the Green function in the basis of the eigenstates $|\Psi_n\rangle$. Using the completeness property $\sum_n |\Psi_n\rangle\langle\Psi_n| = 1$, we obtain

$$\hat{G}^R(E)=\frac{1}{(E+i\eta)\hat{I}-\hat{H}}\sum_n|\Psi_n\rangle\langle\Psi_n|=\sum_n\frac{1}{(E+i\eta)\hat{I}-\hat{H}}|\Psi_n\rangle\langle\Psi_n|, \tag{3.24}$$

if we expand now $\left[(E+i\eta)\hat{I}-\hat{H}\right]^{-1}$ into a power series and use $\hat{H}\Psi_n = E_n\Psi_n$, we obtain the *eigenstate expansion*

$$\hat{G}^R(E)=\sum_n\frac{|\Psi_n\rangle\langle\Psi_n|}{E-E_n+i\eta}. \tag{3.25}$$

Note, that if we apply the ordinary inverse Fourier transform to $\hat{G}^R(E)$, we automatically obtain the retarded function

$$\hat{G}^R(\tau)=\int_{-\infty}^{\infty}\hat{G}^R(E)e^{-iE\tau/\hbar}\frac{dE}{2\pi\hbar}=-\frac{i}{\hbar}\theta(\tau)\sum_n e^{-\frac{i}{\hbar}E_n\tau}|\Psi_n\rangle\langle\Psi_n|. \tag{3.26}$$

Indeed, a simple pole in the complex E plain is at $E = E_n - i\eta$, the residue in this point determines the integral at $\tau > 0$ when the integration contour is closed through the lower half-plane, while at $\tau < 0$ the integration should be closed through the upper half-plane and the integral is zero.

3.1.2 Green Functions in the Coordinate Representation

The formalism of retarded Green functions is quite general and can be applied to quantum systems in an arbitrary representation. Below in this section we consider

the scattering problem in the coordinate representation for the wave function $|\Psi(t)\rangle \equiv \Psi(\boldsymbol{r}, t)$. The coordinate representation can be obtained from the general equations of the previous section, if one uses the position states $|\boldsymbol{r}\rangle$ (the eigenvectors of the position operator) as a basis. The orthonormality conditions are

$$\langle \boldsymbol{r}|\boldsymbol{r}'\rangle = \delta(\boldsymbol{r} - \boldsymbol{r}'), \tag{3.27}$$

$$\int d\boldsymbol{r}|\boldsymbol{r}\rangle\langle\boldsymbol{r}| = 1. \tag{3.28}$$

The scalar product is defined as $\langle \Phi|\Psi\rangle = \int \Phi^*(\boldsymbol{r})\Psi(\boldsymbol{r})d\boldsymbol{r}$, the unity operator is $\hat{I} = \delta(\boldsymbol{r} - \boldsymbol{r}')$.

The following transition rules relate the Dirac states and operators with the states and operators in the ordinary coordinate representation (time or energy variable is omitted):

$$\Psi(\boldsymbol{r}) = \langle \boldsymbol{r}|\Psi\rangle, \quad \Psi^*(\boldsymbol{r}) = \langle\Psi|\boldsymbol{r}\rangle, \tag{3.29}$$

$$\delta(\boldsymbol{r} - \boldsymbol{r}')\hat{H}(\boldsymbol{r}) = \langle \boldsymbol{r}|\hat{H}|\boldsymbol{r}'\rangle, \tag{3.30}$$

$$G^R(\boldsymbol{r}, \boldsymbol{r}') = \langle \boldsymbol{r}|\hat{G}^R|\boldsymbol{r}'\rangle, \tag{3.31}$$

$$\sum_n \Psi_n(\boldsymbol{r})\Psi_n^*(\boldsymbol{r}') = \delta(\boldsymbol{r} - \boldsymbol{r}'). \tag{3.32}$$

Applying these rules to (3.13), we obtain

$$\Psi(\boldsymbol{r}, t) = i\hbar \int d\boldsymbol{r}' G^R(\boldsymbol{r}, t, \boldsymbol{r}', t')\Psi(\boldsymbol{r}', t'), \tag{3.33}$$

where $G^R(\boldsymbol{r}, t, \boldsymbol{r}', t')$ is the retarded Green function, to be defined from the equation

$$\left[i\hbar\frac{\partial}{\partial t} - \hat{H}(\boldsymbol{r})\right] G^R(\boldsymbol{r}, t, \boldsymbol{r}', t') = \delta(\boldsymbol{r} - \boldsymbol{r}')\delta(t - t'), \tag{3.34}$$

where $\hat{H}(\boldsymbol{r})$ is the single-particle Hamiltonian

$$\hat{H}(\boldsymbol{r}) = -\frac{\hbar^2}{2m}\nabla^2 + V(\boldsymbol{r}). \tag{3.35}$$

The equation (3.34) is obtained from the operator equation (3.16), if one takes the matrix element $\langle \boldsymbol{r}|\ldots|\boldsymbol{r}'\rangle$ of the left and right parts of (3.16).

The equation for the stationary retarded Green function is

$$\left[E + i\eta - \hat{H}(\boldsymbol{r})\right] G^R(\boldsymbol{r}, \boldsymbol{r}', E) = \delta(\boldsymbol{r} - \boldsymbol{r}'). \tag{3.36}$$

This Green function corresponds to the Schrödinger equation

$$\left[-\frac{\hbar^2}{2m}\nabla^2 + V(\boldsymbol{r})\right]\Psi(\boldsymbol{r}) = E\Psi(\boldsymbol{r}). \tag{3.37}$$

Let us consider as an example the one dimensional GF for free electrons. The corresponding equation is

$$\left[E \pm i\eta + \frac{\hbar^2}{2m}\frac{\partial^2}{\partial x^2}\right] G^{R(A)}(x, x', E) = \delta(x - x'). \tag{3.38}$$

This equation has two exact solutions:

$$G_1(x - x', E) = -\frac{im}{\hbar^2 k} e^{ik|x-x'|}, \tag{3.39}$$

$$G_2(x - x', E) = \frac{im}{\hbar^2 k} e^{-ik|x-x'|}, \tag{3.40}$$

where $\hbar k = \sqrt{2m(E \pm i\eta)}$. Note, that k has an imaginary part, positive for retarded and negative for advanced Green functions:

$$k = \frac{\sqrt{2m(E \pm i\eta)}}{\hbar} = \frac{\sqrt{2mE}}{\hbar}\sqrt{1 \pm \frac{i\eta}{E}} \approx \frac{\sqrt{2mE}}{\hbar}\left(1 \pm \frac{i\eta}{2E}\right). \tag{3.41}$$

From the condition of being finite at infinity, we select $G_1(x - x', E)$ to be the retarded function ($\hbar k = \sqrt{2m(E + i\eta)}$) and $G_2(x - x', E)$ to be the advanced function ($\hbar k = \sqrt{2m(E - i\eta)}$). At the same time, we can consider x' as a position of the scatterer. From this point of view, $G_1(x - x', E)$ corresponds to the outgoing wave, while $G_2(x - x', E)$ for incoming.

The coordinate retarded function has many useful properties. In particular, it is related to the local density of states $\rho(\boldsymbol{r}, E)$, which can be determined as

$$\rho(\boldsymbol{r}, E) = \sum_n |\Psi_n(\boldsymbol{r})|^2 \delta(E - E_n). \tag{3.42}$$

On the other hand, from (3.25) we get the eigenstate expansion

$$G^R(\boldsymbol{r}, \boldsymbol{r}', E) = \sum_n \frac{\langle \boldsymbol{r}|\Psi_n\rangle\langle\Psi_n|\boldsymbol{r}'\rangle}{E - E_n + i\eta} = \sum_n \frac{\Psi_n(\boldsymbol{r})\Psi_n^*(\boldsymbol{r}')}{E - E_n + i\eta}, \tag{3.43}$$

or for the coinciding coordinates $\boldsymbol{r} = \boldsymbol{r}'$:

$$G^R(\boldsymbol{r},\boldsymbol{r},E)=\sum_n\frac{\langle\boldsymbol{r}|\Psi_n\rangle\langle\Psi_n|\boldsymbol{r}\rangle}{E-E_n+i\eta}=\sum_n\frac{|\Psi_n(\boldsymbol{r})|^2}{E-E_n+i\eta}. \tag{3.44}$$

Comparing these expressions and using the relation

$$\frac{1}{x\pm i\eta}=P\left(\frac{1}{x}\right)\mp i\pi\delta(x), \tag{3.45}$$

where P stands for the principal value in the case of integration, one obtains

$$\rho(\boldsymbol{r},E)=-\frac{1}{\pi}\mathrm{Im}\left\{G^R(\boldsymbol{r},\boldsymbol{r},E)\right\}. \tag{3.46}$$

It is also possible to show that the real and imaginary parts of $G^{R(A)}(E)$ are related through a Hilbert transformation

$$\mathrm{Re}\left\{G^{R(A)}(E)\right\}=\mp P\int_{-\infty}^{\infty}\frac{\mathrm{Im}\left\{G^{R(A)}(E')\right\}}{E-E'}\frac{dE'}{\pi}, \tag{3.47}$$

and the following representation holds:

$$G^{R(A)}(\boldsymbol{r},\boldsymbol{r},E)=\int_{-\infty}^{\infty}\frac{\rho(\boldsymbol{r},E')dE'}{E-E'\pm i\eta}. \tag{3.48}$$

3.1.3 Lippmann-Schwinger Equation

Using Green functions, we can reformulate the scattering theory. Assume that our system can be divided into an unperturbed part with the Hamiltonian $\hat{H}_0$ and the perturbation $\hat{V}$, both time-independent:

$$\hat{H}=\hat{H}_0+\hat{V}. \tag{3.49}$$

This decomposition can be naturally done for scattering of particles in free space, where $\hat{H}_0$ includes only (the operators of) kinetic energies and $\hat{V}$ is the scattering potential. For quantum junctions $\hat{H}_0$ can be taken for infinite electrodes and $\hat{V}$ should then describe all possible scattering events between electrodes and channels. Usually it is difficult to formulate such a problem explicitly, but the analysis is important for qualitative understanding.

Writing the time-dependent equation (3.16) for the full Hamiltonian $\hat{H}=\hat{H}_0+\hat{V}$ and for $\hat{H}_0$ only:

$$\left[i\hbar\frac{\partial}{\partial t}-\hat{H}_0-\hat{V}\right]\hat{G}^R(t,t_0)=\hat{I}\delta(t-t_0), \tag{3.50}$$

$$\left[i\hbar\frac{\partial}{\partial t}-\hat{H}_0\right]\hat{G}_0^R(t,t_0)=\hat{I}\delta(t-t_0), \tag{3.51}$$

combining these equations together and integrating over the time we get the Lippmann-Schwinger equation for the Green functions in two different forms:

$$\hat{G}^R(t-t_0)=\hat{G}_0^R(t-t_0)+\int_{t_0}^{t}\hat{G}_0^R(t-t')\hat{V}\hat{G}^R(t'-t_0)dt', \tag{3.52}$$

or

$$\hat{G}^R(t-t_0)=\hat{G}_0^R(t-t_0)+\int_{t_0}^{t}\hat{G}^R(t-t')\hat{V}\hat{G}_0^R(t'-t_0)dt'. \tag{3.53}$$

Before going further we define the *incoming* state as a result of the time evolution of the initial state $\Psi_0(t_0)$ from the infinite past under the action of unperturbed Hamiltonian, in accordance with (3.13) it is determined by the Green function $\hat{G}_0(t-t_0)$ while the full scattering state is obtained by the full Green function $\hat{G}(t-t_0)$:

$$|\Psi^{in}(t)\rangle=i\hbar\lim_{t_0\to-\infty}\hat{G}_0^R(t-t_0)|\Psi_0(t_0)\rangle, \tag{3.54}$$

$$|\Psi(t)\rangle=i\hbar\lim_{t_0\to-\infty}\hat{G}^R(t-t_0)|\Psi_0(t_0)\rangle. \tag{3.55}$$

The sense of this procedure is to "clean" the time-dependent state from the transient contributions and stay only with the state supported by the boundary conditions.

Now we substitute (3.53) into (3.55) and replace the upper limit of integration over t by ∞, we can do that because $\hat{G}^R(t-t'<0)=0$. We obtain the Lippmann-Schwinger equation for the wave function:

$$|\Psi(t)\rangle=|\Psi^{in}(t)\rangle+\int_{-\infty}^{\infty}dt'\hat{G}^R(t-t')\hat{V}|\Psi^{in}(t')\rangle, \tag{3.56}$$

or (if we use (3.52) instead)

$$|\Psi(t)\rangle=|\Psi^{in}(t)\rangle+\int_{-\infty}^{\infty}dt'\hat{G}_0^R(t-t')\hat{V}|\Psi(t')\rangle. \tag{3.57}$$

Making the Fourier transform (3.19) we get the time-independent Lippmann-Schwinger equations, e.g. with the retarded functions

$$\hat{G}^R(E)=\hat{G}_0^R(E)+\hat{G}^R(E)\hat{V}\hat{G}_0^R(E), \tag{3.58}$$

$$|\Psi_E\rangle=|\Psi_E^{in}\rangle+\hat{G}^R(E)\hat{V}|\Psi_E^{in}\rangle. \tag{3.59}$$

or

$$\hat{G}^R(E) = \hat{G}_0^R(E) + \hat{G}_0^R(E)\hat{V}\hat{G}^R(E), \tag{3.60}$$

$$|\Psi_E\rangle = |\Psi_E^{in}\rangle + \hat{G}_0^R(E)\hat{V}|\Psi_E\rangle. \tag{3.61}$$

In the coordinate representation

$$\Psi_E(\boldsymbol{r}) = \Psi_E^{in}(\boldsymbol{r}) + \int d\boldsymbol{r}' G^R(\boldsymbol{r}, \boldsymbol{r}', E) V(\boldsymbol{r}') \Psi_E^{in}(\boldsymbol{r}'), \tag{3.62}$$

or

$$\Psi_E(\boldsymbol{r}) = \Psi_E^{in}(\boldsymbol{r}) + \int d\boldsymbol{r}' G_0^R(\boldsymbol{r}, \boldsymbol{r}', E) V(\boldsymbol{r}') \Psi_E(\boldsymbol{r}'). \tag{3.63}$$

Both equations describe the wave function as a superposition of incoming wave and all outgoing waves produced by this incoming wave. As a direct computational tool the Lippmann-Schwinger equations are useful in free space with localized scattering region or in rather simple geometries, when the unperturbed Green functions can be easily defined analytically.

Consider as an example scattering at the δ-potential $V(x) = \alpha\delta(x)$. The retarded Green function for free 1D electrons is given by (3.39):

$$G_0^R(x - x', E) = -\frac{im}{\hbar^2 k} e^{ik|x-x'|}. \tag{3.64}$$

Using the equation (3.63) we get ($\Psi^{in}(x) = e^{ikx}$):

$$\Psi(x) = e^{ikx} - \frac{im\alpha}{\hbar^2 k} \int dx' e^{ik|x-x'|} \delta(x') \Psi(x') = e^{ikx} - \frac{im\alpha}{\hbar^2 k} e^{ik|x|} \Psi(0). \tag{3.65}$$

Boundary conditions at infinity suggest that the solution has the form

$$\Psi(x) = A \begin{cases} e^{ikx} + re^{-ikx}, & x < 0, \\ te^{ikx}, & x > 0. \end{cases} \tag{3.66}$$

Substituting it into (3.65) for $x = +0$ and $x = -0$ we obtain the equations for the reflection amplitude r and the transmission amplitude t:

$$1 + r = 1 - \frac{im\alpha}{\hbar^2 k}(1 + r), \quad t = 1 - \frac{im\alpha}{\hbar^2 k} t, \tag{3.67}$$

with the solution

$$r = \frac{1}{i\frac{\hbar^2 k}{m\alpha} - 1}, \quad t = \frac{i\frac{\hbar^2 k}{m\alpha}}{i\frac{\hbar^2 k}{m\alpha} - 1}. \tag{3.68}$$

It is exactly the same result which we obtained solving the Schrödinger equation (2.29)–(2.36).

For more details about the Lippmann-Schwinger equations we recommend the book of M. Di Ventra [1], Sect. 3.4.

3.1.4 Fisher-Lee Relation Between S and G^R

Finally, let us establish the relation between the Green function $G^R(\boldsymbol{r}_1, \boldsymbol{r}_2, E)$ and the scattering matrix $\boldsymbol{S}$. Although we will not use it explicitly below (instead we derive more practical matrix formulas), it is important to demonstrate equivalence between the Landauer's scattering approach based on the wave function picture and the Green function formalism.

Let us start from a simple 1D case. The multi-channel scattering states (2.126), (2.127) become

$$\Psi_{LE}(z) = \begin{cases} \dfrac{1}{\sqrt{2\pi\hbar\upsilon_L}} e^{ikz} + \dfrac{r(E)}{\sqrt{2\pi\hbar\upsilon_L}} e^{-ikz}, & z < z_L, \\ \dfrac{t(E)}{\sqrt{2\pi\hbar\upsilon_R}} e^{ik'z}, & z > z_R. \end{cases} \tag{3.69}$$

$$\Psi_{RE}(z) = \begin{cases} \dfrac{1}{\sqrt{2\pi\hbar\upsilon_R}} e^{-ik'z} + \dfrac{r'(E)}{\sqrt{2\pi\hbar\upsilon_R}} e^{ik'z}, & z > z_R, \\ \dfrac{t'(E)}{\sqrt{2\pi\hbar\upsilon_L}} e^{-ikz}, & z < z_L. \end{cases} \tag{3.70}$$

where we keep different left and right velocities $\upsilon_L = \hbar k/m$, $\upsilon_R = \hbar k'/m$, $k(E)$ and $k'(E)$ can be different. These states form a full set of eigenstates and we can use the representation (3.43):

$$G^R(z, z', E) = \int_0^\infty \frac{\Psi_{LE_k}(z)\Psi^*_{LE_k}(z')}{E - E_k + i\eta} dE_k + \int_0^\infty \frac{\Psi_{RE_k}(z)\Psi^*_{RE_k}(z')}{E - E_k + i\eta} dE_k. \tag{3.71}$$

Let us calculate these integrals at $z \to \infty$, $z' \to -\infty$ taking into account that $t(E)r^*(E) + r'(E)t'^*(E) = 0$ from (2.53). Finally we get the relation between the retarded Green function and the transmission amplitude:

$$G^R(z, z', E) = \frac{-it(E)}{\hbar\sqrt{\upsilon_L\upsilon_R}} e^{ik'z - ikz'}, \tag{3.72}$$

or

$$t(E) = i\hbar\sqrt{\upsilon_L\upsilon_R} G^R(z, z', E) e^{-ik'z + ikz'}. \tag{3.73}$$

Now we can extend this approach to multi-channel and multi-terminal case. In the general case of multi-terminal scattering the wave functions in the leads, far from the scattering region, are determined by the asymptotic expressions (2.154). The Green functions for scattering from the electrode s into the electrode p at energy E are:

$$G^R(\boldsymbol{r}_p, \boldsymbol{r}_s, E) = \sum_{mn} \frac{-it_{mn}}{\hbar\sqrt{\upsilon_m \upsilon_n}} \phi_m(\boldsymbol{r}_p)\phi_n^*(\boldsymbol{r}_s) e^{-ik_m z_p - ik_n z_s}, \ m \in p, \ n \in s, \quad (3.74)$$

$$G^R(\boldsymbol{r}'_s, \boldsymbol{r}_s, E) = \sum_{n'n} \left[-\frac{i\delta_{n'n}}{\hbar\upsilon_n} - \frac{ir_{n'n}}{\hbar\sqrt{\upsilon_{n'}\upsilon_n}} \right] \phi_{n'}(\boldsymbol{r}'_s)\phi_n^*(\boldsymbol{r}_s) e^{-ik_{n'} z'_p - ik_n z_s}, \ n, n' \in s. \quad (3.75)$$

Making the inversion of these expressions and assuming the points with coordinates $z_s = z_p = 0$ in the leads (we are free to choose the beginning of coordinate axes), we get the Fisher-Lee relations [2] in the form:

$$t_{pm,sn} = i\hbar\sqrt{\upsilon_n \upsilon_m} \int d\boldsymbol{r}_s \int d\boldsymbol{r}_p \phi_m^*(\boldsymbol{r}_p) G^R(\boldsymbol{r}_p, \boldsymbol{r}_s)\phi_n(\boldsymbol{r}_s), \ p \neq s, \quad (3.76)$$

$$r_{sn',sn} = -\delta_{n'n} + i\hbar\sqrt{\upsilon_n \upsilon_{n'}} \int d\boldsymbol{r}_s \int d\boldsymbol{r}'_s \phi_{n'}^*(\boldsymbol{r}'_s) G^R(\boldsymbol{r}'_s, \boldsymbol{r}_s)\phi_n(\boldsymbol{r}_s), \quad (3.77)$$

or, combining both together,

$$S_{pm,sn} = -\delta_{ps}\delta_{mn} + i\hbar\sqrt{\upsilon_n \upsilon_m} \int d\boldsymbol{r}_s \int d\boldsymbol{r}_p \phi_m^*(\boldsymbol{r}_p) G^R(\boldsymbol{r}_p, \boldsymbol{r}_s)\phi_n(\boldsymbol{r}_s). \quad (3.78)$$

Using these expressions and (2.157) we can get the transmission function $T_{sp}(E)$ from the lead p into s:

$$T_{sp}(E) = \sum_{nm} |t_{sn,pm}|^2 = \int d\boldsymbol{r}_{p2} \int d\boldsymbol{r}_{p1} \int d\boldsymbol{r}_{s1} \int d\boldsymbol{r}_{s2} \Gamma_p(\boldsymbol{r}_{p2}, \boldsymbol{r}_{p1}) G^R(\boldsymbol{r}_{p1}, \boldsymbol{r}_{s1}) \Gamma_s(\boldsymbol{r}_{s1}, \boldsymbol{r}_{s2}) G^A(\boldsymbol{r}_{s2}, \boldsymbol{r}_{p2}), \quad (3.79)$$

where we introduced the functions

$$\Gamma_s(\boldsymbol{r}_{s1}, \boldsymbol{r}_{s2}) = \hbar \sum_n \upsilon_n \phi_n(\boldsymbol{r}_{s1})\phi_n^*(\boldsymbol{r}_{s2}), \quad (3.80)$$

which describe the properties of the s-th electrode and are independent from other electrodes.

3.2 Matrix Green Functions

3.2.1 Matrix (Tight-Binding, Lattice) Hamiltonian

Before we considered only continuous quantum systems described by wave functions in real space. However, the nanoscale systems are typically *discrete-level* systems due to spatial quantization in quantum dots and molecules or importance of atomistic structure. From here on our focus will be on the systems described by the *matrix Hamiltonians*

$$\boldsymbol{H} = \begin{pmatrix} H_{11} & H_{12} & \cdots & H_{1N} \\ H_{21} & H_{22} & \cdots & H_{2N} \\ \vdots & \vdots & \ddots & \vdots \\ H_{N1} & H_{N2} & \cdots & H_{NN} \end{pmatrix}. \tag{3.81}$$

Actually, any Hamiltonian of this type has some basis states $|i\rangle$, $i = 1, \ldots, N$ in its origin. The physical nature of these states is not important from mathematical point of view, but we note that the matrix structure appears as a result of matrix element calculation of some Hamiltonian $\langle i|\hat{H}|j\rangle$, and the vector wave function

$$\boldsymbol{\Psi} = \begin{pmatrix} c_1 \\ c_2 \\ \vdots \\ c_N \end{pmatrix} \tag{3.82}$$

represents the coefficients of the expansion

$$|\Psi\rangle = \sum_i c_i |i\rangle. \tag{3.83}$$

The Hamilton operator can be written also using the basis states and matrix elements (3.81) as

$$\hat{H} = \sum_{ij} |i\rangle H_{ij} \langle j|. \tag{3.84}$$

The eigenstates Ψ_n are to be found from the matrix Schrödinger equation

$$\boldsymbol{H}\boldsymbol{\Psi}_n = E_n \boldsymbol{\Psi}_n. \tag{3.85}$$

Let us consider some typical systems, for which the matrix method is appropriate starting point.

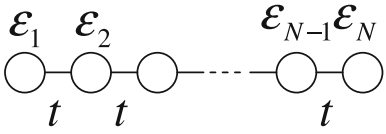

Fig. 3.1 A linear chain of sites

The simplest example is a single quantum dot, in the basis formed by the *eigenstates*, the corresponding Hamiltonian is diagonal:

$$\boldsymbol{H} = \begin{pmatrix} \varepsilon_1 & 0 & 0 & \cdots & 0 \\ 0 & \varepsilon_2 & 0 & \cdots & 0 \\ \vdots & \ddots & \ddots & \ddots & \vdots \\ 0 & \cdots & 0 & \varepsilon_{N-1} & 0 \\ 0 & \cdots & 0 & 0 & \varepsilon_N \end{pmatrix}. \tag{3.86}$$

We can write it also, using Dirac notations and second quantization, as

$$\hat{H} = \sum_i |i\rangle \varepsilon_i \langle i| = \sum_i \varepsilon_i d_i^\dagger d_i. \tag{3.87}$$

The next typical example is a linear chain of single-state sites with only nearest-neighbor couplings (Fig. 3.1)

$$\boldsymbol{H} = \begin{pmatrix} \varepsilon_1 & t & 0 & \cdots & 0 \\ t & \varepsilon_2 & t & \cdots & 0 \\ \vdots & \ddots & \ddots & \ddots & \vdots \\ 0 & \cdots & t & \varepsilon_{N-1} & t \\ 0 & \cdots & 0 & t & \varepsilon_N \end{pmatrix}. \tag{3.88}$$

Two important ways to obtain discrete Hamiltonians are the tight-binding approximation and discretization of the Scrödinger equation (or the equivalent equations for Green functions) using finite differences and discretized space grid (lattice) instead of derivatives in continuous space.

Tight-Binding Model

The main idea of the method is to represent the wave function of a particle as a linear combination of some known *localized* states $\psi_\alpha(\boldsymbol{r}, \sigma)$, where α denote the set of quantum numbers, and σ is the spin index (for example, atomic orbitals, in this particular case the method is called LCAO—linear combination of atomic orbitals)

$$\psi(\xi) = \sum_\alpha c_\alpha \psi_\alpha(\xi), \tag{3.89}$$

here and below we use $\xi \equiv (\boldsymbol{r}, \sigma)$ to denote both spatial coordinates and spin.

Using the Dirac notations $|\alpha\rangle \equiv \psi_\alpha(\xi)$ and assuming that $\psi_\alpha(\xi)$ are orthonormal functions $\langle\alpha|\beta\rangle = \delta_{\alpha\beta}$ we can write the *single-particle tight-binding Hamiltonian* in the Hilbert space formed by $\psi_\alpha(\xi)$

$$\hat{H} = \sum_\alpha (\varepsilon_\alpha + e\varphi_\alpha)|\alpha\rangle\langle\alpha| + \sum_{\alpha\beta} t_{\alpha\beta}|\alpha\rangle\langle\beta|, \tag{3.90}$$

the first term in this Hamiltonian describes the states with energies ε_α, φ_α is the electrical potential, the second term should be included if the states $|\alpha\rangle$ are not eigenstates of the Hamiltonian. In the TB model $t_{\alpha\beta}$ is the hopping matrix element between states $|\alpha\rangle$ and $|\beta\rangle$, which is nonzero, as a rule, for nearest neighbor sites. The two-particle interaction is described by the Hamiltonian

$$\hat{H} = \sum_{\alpha\beta,\delta\gamma} V_{\alpha\beta,\delta\gamma}|\alpha\rangle|\beta\rangle\langle\delta|\langle\gamma|, \tag{3.91}$$

in the two-particle Hilbert space, and so on.

The energies and hopping matrix elements in this Hamiltonian can be calculated as matrix elements of the single-particle real-space Hamiltonian $\hat{h}(\xi)$:

$$\varepsilon_{\alpha\beta} = \varepsilon_\alpha\delta_{\alpha\beta} + t_{\alpha\beta}(1 - \delta_{\alpha\beta}) = \int \psi^*_\alpha(\xi)\hat{h}(\xi)\psi_\beta(\xi)d\xi. \tag{3.92}$$

We combined in this expression the energies and hopping terms into one energy matrix $\varepsilon_{\alpha\beta}$ with the matrix elements of the single-particle Hamiltonian

$$H_{\alpha\beta} \equiv \varepsilon_{\alpha\beta} = \begin{cases} \varepsilon_\alpha + e\varphi_\alpha, & \alpha = \beta, \\ t_{\alpha\beta}, & \alpha \neq \beta. \end{cases} \tag{3.93}$$

This approach was developed originally as an approximate method, if the wave functions of isolated atoms are taken as a basis wave functions $\psi_\alpha(\xi)$, but also can be formulated exactly with the help of Wannier functions. Only in the last case the expansion (3.89) and the Hamiltonian (3.90) are exact, but some extension to the arbitrary basis functions is possible. The method is useful to calculate the conductance of complex quantum systems in combination with *ab initio* methods. It is particular important to describe small molecules, when the atomic orbitals form the basis.

Finally, in the second quantized form the tight-binding Hamiltonian is

$$\hat{H} = \sum_\alpha (\varepsilon_\alpha + e\varphi_\alpha)\, c^\dagger_\alpha c_\alpha + \sum_{\alpha\neq\beta} t_{\alpha\beta} c^\dagger_\alpha c_\beta. \tag{3.94}$$

The formalism of second quantization we will use in the second part devoted to advanced methods.

In the mathematical sense, the TB model represents also a discrete (grid) version of the continuous Schrödinger equation, thus it is routinely used in numerical calculations.

Consider, as an example, the one-dimensional Schrödinger equation with the Hamiltonian

$$\hat{H}(x) = -\frac{\hbar^2}{2m}\frac{d^2}{dx^2} + V(x). \tag{3.95}$$

For numerical calculation we introduce the discrete lattice of sites with coordinates $x_i = ai,\ i \in Z$, a is the lattice constant. The continuous functions are replaced by their values in points x_i:

$$\Psi(x) \Rightarrow \Psi_i, \quad V(x) \Rightarrow V_i, \tag{3.96}$$

the derivatives are approximated by the finite differences[4]

$$\frac{d}{dx}\Psi(x) \Rightarrow \left(\frac{d}{dx}\Psi(x)\right)_i = \frac{\Psi_{i+1} - \Psi_i}{a}, \tag{3.97}$$

$$\left(\frac{d^2}{dx^2}\Psi(x)\right)_i = \frac{1}{a}\left[\left(\frac{d}{dx}\Psi(x)\right)_i - \left(\frac{d}{dx}\Psi(x)\right)_{i-1}\right] = \frac{\Psi_{i+1} - 2\Psi_i + \Psi_{i-1}}{a^2}. \tag{3.98}$$

Introducing $t = \dfrac{\hbar^2}{2ma}$, we get the TB Hamiltonian

$$\hat{H} = \sum_i \Big[(2t + V_i)|i\rangle\langle i| - t|i\rangle\langle i-1| - t|i\rangle\langle i+1|\Big]. \tag{3.99}$$

This Hamiltonian in the matrix form is

$$\boldsymbol{H} = \begin{pmatrix} \ddots & -t & 0 & 0 & \ddots \\ -t & 2t + V_{i-1} & -t & 0 & 0 \\ 0 & -t & 2t + V_i & -t & 0 \\ 0 & 0 & -t & 2t + V_{i+1} & -t \\ \ddots & 0 & 0 & -t & \ddots \end{pmatrix}. \tag{3.100}$$

[4]Note, that we consider here the simplest possible discretization scheme.

3.2.2 Retarded Single-Particle Matrix Green Function

The solution of single-particle quantum problems, formulated with the help of a matrix Hamiltonian, is possible along the usual line of finding the wave-functions on a lattice, solving the Schrödinger equation (3.85). The other method, namely matrix Green functions, considered in this section, was found to be more convenient for transport calculations, especially when interactions are included.

The retarded single-particle matrix Green function

$$\boldsymbol{G}^R(E) = \begin{pmatrix} G_{11} & G_{12} & \cdots & G_{1N} \\ G_{21} & G_{22} & \cdots & G_{2N} \\ \vdots & \vdots & \ddots & \vdots \\ G_{N1} & G_{N2} & \cdots & G_{NN} \end{pmatrix} \tag{3.101}$$

is determined by the equation

$$[(E + i\eta)\boldsymbol{I} - \boldsymbol{H}]\,\boldsymbol{G}^R = \boldsymbol{I}, \tag{3.102}$$

where η is an infinitesimally small positive number $\eta = 0^+$.

For an isolated non-interacting system the Green function is simply obtained after the matrix inversion

$$\boldsymbol{G}^R(E) = [(E + i\eta)\boldsymbol{I} - \boldsymbol{H}]^{-1}. \tag{3.103}$$

All general properties of GFs, discussed above, are applicable also for matrix GFs. For example, the local density of states in state α at energy E is determined by

$$\rho_\alpha(E) = -\frac{1}{\pi}\mathrm{Im}G^R_{\alpha\alpha}(E). \tag{3.104}$$

For simple quantum dot Hamiltonian (3.87) the matrix Green function is easily found to be

$$G^R_{\alpha\beta}(E) = \frac{\delta_{\alpha\beta}}{E - \varepsilon_\alpha + i\eta}. \tag{3.105}$$

Let us consider the example of a two-level system with the Hamiltonian

$$\boldsymbol{H} = \begin{pmatrix} \varepsilon_1 & t \\ t & \varepsilon_2 \end{pmatrix}. \tag{3.106}$$

The retarded GF is

$$\boldsymbol{G}^R(E) = \frac{1}{(E + i\eta - \varepsilon_1)(E + i\eta - \varepsilon_2) - t^2} \begin{pmatrix} E + i\eta - \varepsilon_2 & t \\ t & E + i\eta - \varepsilon_1 \end{pmatrix}. \tag{3.107}$$

The tight-binding and lattice Hamiltonians are applied as well to consider the semi-infinite leads. Although the matrices are formally infinitely-dimensional in this case, we shall show below, that the problem is reduced to the finite-dimensional problem for the quantum system of interest, and the semi-infinite leads can be integrated out.

For more details about the lattice Hamiltonians and Green functions we recommend the book of D.K. Ferry and S.M. Goodnick [3], Sect. 3.8.

3.2.3 Electrode Self-Energies

Now let us consider the case, when the system of interest is coupled to the electrodes and forms the nanojunction (Fig. 3.2). We assume here that the electrodes are also described by the tight-binding model and by the matrix GFs. Actually, the semi-infinite contacts should be described by the matrix of infinite dimension. We shall consider the semi-infinite contacts later. As usually, we assume, that the electrodes are equilibrium (with possibly different electrochemical potentials), and the central region includes leads and scatterer.

Let us present the full Hamiltonian of the considered system in the following block form

$$\boldsymbol{H} = \begin{pmatrix} \boldsymbol{H}_L & \boldsymbol{V}_{LC} & 0 \\ \boldsymbol{V}_{CL} & \boldsymbol{H}_C & \boldsymbol{V}_{CR} \\ 0 & \boldsymbol{V}_{RC} & \boldsymbol{H}_R \end{pmatrix}, \tag{3.108}$$

where $\boldsymbol{H}_L$, $\boldsymbol{H}_C$, and $\boldsymbol{H}_R$ are the matrix Hamiltonians of the left electrode, the central region, and the right electrode respectively. And the off-diagonal terms describe the coupling to the electrodes. Here we neglect the direct coupling between the electrodes. The Hamiltonian should be Hermitian, such that

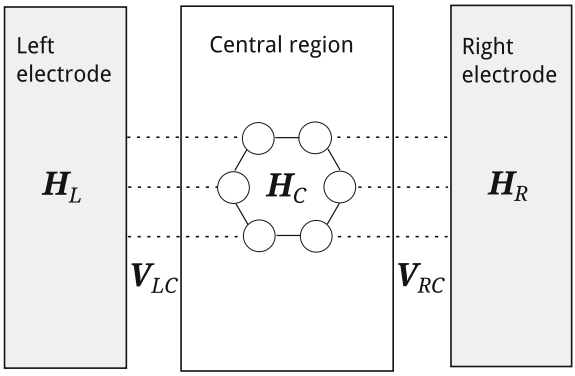

Fig. 3.2 A quantum system coupled to the *left* and *right* equilibrium electrodes

$$\boldsymbol{V}_{CL} = \boldsymbol{V}_{LC}^{\dagger}, \quad \boldsymbol{V}_{CR} = \boldsymbol{V}_{RC}^{\dagger}. \tag{3.109}$$

The equation (3.102) can be written as

$$\begin{pmatrix} \boldsymbol{E} - \boldsymbol{H}_L & -\boldsymbol{V}_{LC} & 0 \\ -\boldsymbol{V}_{LC}^{\dagger} & \boldsymbol{E} - \boldsymbol{H}_C & -\boldsymbol{V}_{RC}^{\dagger} \\ 0 & -\boldsymbol{V}_{RC} & \boldsymbol{E} - \boldsymbol{H}_R \end{pmatrix} \begin{pmatrix} \boldsymbol{G}_L & \boldsymbol{G}_{LC} & 0 \\ \boldsymbol{G}_{CL} & \boldsymbol{G}_C & \boldsymbol{G}_{CR} \\ 0 & \boldsymbol{G}_{RC} & \boldsymbol{G}_R \end{pmatrix} = \boldsymbol{I}, \tag{3.110}$$

where we introduce the matrix $\boldsymbol{E} = (E + i\eta)\boldsymbol{I}$, and represent the matrix Green function in a convenient form, the notation of retarded function is omitted in intermediate formulas. Now our first goal is to find the system Green function $\boldsymbol{G}_C$ which defines all quantities of interest. From the matrix equation (3.110)

$$(\boldsymbol{E} - \boldsymbol{H}_L)\,\boldsymbol{G}_{LC} - \boldsymbol{V}_{LC}\boldsymbol{G}_C = 0, \tag{3.111}$$

$$-\boldsymbol{V}_{LC}^{\dagger}\boldsymbol{G}_{LC} + (\boldsymbol{E} - \boldsymbol{H}_C)\,\boldsymbol{G}_C - \boldsymbol{V}_{RC}^{\dagger}\boldsymbol{G}_{RC} = \boldsymbol{I}, \tag{3.112}$$

$$-\boldsymbol{V}_{RC}\boldsymbol{G}_C + (\boldsymbol{E} - \boldsymbol{H}_R)\,\boldsymbol{G}_{RC} = 0. \tag{3.113}$$

From the first and the third equations one has

$$\boldsymbol{G}_{LC} = (\boldsymbol{E} - \boldsymbol{H}_L)^{-1}\,\boldsymbol{V}_{LC}\boldsymbol{G}_C, \tag{3.114}$$

$$\boldsymbol{G}_{RC} = (\boldsymbol{E} - \boldsymbol{H}_R)^{-1}\,\boldsymbol{V}_{RC}\boldsymbol{G}_C, \tag{3.115}$$

and substituting it into the second equation we arrive at the equation

$$(\boldsymbol{E} - \boldsymbol{H}_C - \boldsymbol{\Sigma})\,\boldsymbol{G}_C = \boldsymbol{I}, \tag{3.116}$$

where we introduce the *electrode self-energy* (which should be also called retarded)

$$\boldsymbol{\Sigma} = \boldsymbol{V}_{LC}^{\dagger}\,(\boldsymbol{E} - \boldsymbol{H}_L)^{-1}\,\boldsymbol{V}_{LC} + \boldsymbol{V}_{RC}^{\dagger}\,(\boldsymbol{E} - \boldsymbol{H}_R)^{-1}\,\boldsymbol{V}_{RC}. \tag{3.117}$$

Finally, we found, that the retarded GF of a nanosystem coupled to the leads is determined by the expression (we restore the R notation for retarded functions)

$$\boldsymbol{G}_C^R(E) = \left[\boldsymbol{E} - \boldsymbol{H}_C - \boldsymbol{\Sigma}^R\right]^{-1}, \tag{3.118}$$

the effects of the leads are included through the self-energy.

Here we should stress the important property of the self-energy (3.117), it is determined only by the coupling Hamiltonians $\boldsymbol{V}_{sC}$ and the retarded GFs of the *isolated* leads $\boldsymbol{G}_s^R$ $(s = L, R)$

$$\boldsymbol{G}_s^R = (\boldsymbol{E} - \boldsymbol{H}_s)^{-1}, \tag{3.119}$$

$$\boldsymbol{\Sigma}_s^R = \boldsymbol{V}_{sC}^\dagger (\boldsymbol{E} - \boldsymbol{H}_s)^{-1} \boldsymbol{V}_{sC} = \boldsymbol{V}_{sC}^\dagger \boldsymbol{G}_s^R \boldsymbol{V}_{sC}, \tag{3.120}$$

or, in index notation,

$$\boldsymbol{\Sigma}_{s;\alpha\beta}^R = \sum_{\delta\gamma} \left(\boldsymbol{V}_{sC}^\dagger\right)_{\alpha\delta} G_{s;\delta\gamma}^R V_{s;\gamma\beta} = \sum_{\delta\gamma} V_{s;\delta\alpha}^* V_{s;\gamma\beta} G_{s;\delta\gamma}^R. \tag{3.121}$$

It means, that the contact self-energy is independent of the state of the nanosystem itself and describes completely the influence of the electrodes. Later we shall see that this property is also conserved for interacting central systems, if the leads are still non-interacting.

The extension from two-electrode to multi-electrode case is straightforward, the self-energies ($s = 1, \ldots, N$) are given by the formulas (3.119)–(3.121) and $\boldsymbol{\Sigma}^R$ in (3.118) is the sum over all electrodes

$$\boldsymbol{\Sigma}^R = \sum_s \boldsymbol{\Sigma}_s^R. \tag{3.122}$$

3.2.4 *Transmission Function and Current*

Now we want to calculate the current through a junction. We assume, as before, that the electrodes are equilibrium, and there is the voltage V applied between the left and right electrodes. The calculation of the current in a general case is more convenient to perform using the full power of the nonequilibrium Green function method. Here we present a simplified approach, valid for non-interacting systems only.

First, we consider a very simple approach, following Paulsson [4]. Let us come back to the Schrödinger equation in the matrix representation (3.85), and write it in the following form

$$\begin{pmatrix} \boldsymbol{H}_L^0 & \boldsymbol{V}_{LS} & 0 \\ \boldsymbol{V}_{LS}^\dagger & \boldsymbol{H}_C^0 & \boldsymbol{V}_{RS}^\dagger \\ 0 & \boldsymbol{V}_{RS} & \boldsymbol{H}_R^0 \end{pmatrix} \begin{pmatrix} \boldsymbol{\Psi}_L \\ \boldsymbol{\Psi}_C \\ \boldsymbol{\Psi}_R \end{pmatrix} = E \begin{pmatrix} \boldsymbol{\Psi}_L \\ \boldsymbol{\Psi}_C \\ \boldsymbol{\Psi}_R \end{pmatrix}, \tag{3.123}$$

where $\boldsymbol{\Psi}_L$, $\boldsymbol{\Psi}_C$, and $\boldsymbol{\Psi}_R$ are vector wave functions of the left lead, the central system, and the right lead correspondingly.

Now we find the solution in the scattering form (which is difficult to call true scattering because we do not define explicitly the geometry of the leads). Namely, in the left lead $\boldsymbol{\Psi}_L = \boldsymbol{\Psi}_L^0 + \boldsymbol{\Psi}_L^1$, where $\boldsymbol{\Psi}_L^0$ is the eigenstate of $\boldsymbol{H}_L^0$, and is considered as known initial wave. The "reflected" wave $\boldsymbol{\Psi}_L^1$, as well as the transmitted wave in the right lead $\boldsymbol{\Psi}_R$, appear only as a result of the interaction between subsystems. The main trick is, that we find a *retarded* solution.

Solving the equation (3.123) with these conditions, the solution is

$$\boldsymbol{\Psi}_L = \left(1 + \boldsymbol{G}_L^{0R} \boldsymbol{V}_{LS} \boldsymbol{G}_C^R \boldsymbol{V}_{LS}^\dagger\right) \boldsymbol{\Psi}_L^0, \tag{3.124}$$

$$\boldsymbol{\Psi}_R = \boldsymbol{G}_R^{0R} \boldsymbol{V}_{RS} \boldsymbol{G}_C^R \boldsymbol{V}_{LS}^\dagger \boldsymbol{\Psi}_L^0 \tag{3.125}$$

$$\boldsymbol{\Psi}_C = \boldsymbol{G}_C^R \boldsymbol{V}_{LS}^\dagger \boldsymbol{\Psi}_L^0. \tag{3.126}$$

The physical sense of this expressions is quite transparent, they describe the quantum amplitudes of the scattering processes. Three functions $\boldsymbol{\Psi}_L$, $\boldsymbol{\Psi}_C$, and $\boldsymbol{\Psi}_R$ are equivalent together to the scattering state in the Landauer-Büttiker theory. Note, that $\boldsymbol{G}_C^R$ here is the full GF of the nanosystem including the lead self-energies.

Now the next step. We want to calculate the current. The partial (for some particular eigenstate $\boldsymbol{\Psi}_{L\lambda}^0$) current from the lead to the system is

$$j_{s=L,R} = \frac{ie}{\hbar} \left(\boldsymbol{\Psi}_s^\dagger \boldsymbol{V}_{sC} \boldsymbol{\Psi}_C - \boldsymbol{\Psi}_C^\dagger \boldsymbol{H}_{sC}^\dagger \boldsymbol{\Psi}_s\right). \tag{3.127}$$

To calculate the total current we should substitute the expressions for the wave functions (3.124)–(3.126), and summarize all contributions [4]. As a result the Landauer formula is obtained. We present the calculation for the transmission function. First, after substitution of the wave functions we have for the partial current through the system

$$\begin{aligned} j_\lambda = j_L = -j_R &= -\frac{ie}{\hbar} \left(\boldsymbol{\Psi}_R^\dagger \boldsymbol{V}_{RS} \boldsymbol{\Psi}_C - \boldsymbol{\Psi}_C^\dagger \boldsymbol{H}_{RS}^\dagger \boldsymbol{\Psi}_R\right) \\ &= -\frac{ie}{\hbar} \left(\boldsymbol{\Psi}_L^{0\dagger} \boldsymbol{V}_{LS} \boldsymbol{G}_C^A \boldsymbol{V}_{RS}^\dagger \left(\boldsymbol{G}_R^{0\dagger} - \boldsymbol{G}_R^0\right) \boldsymbol{V}_{RS} \boldsymbol{G}_C^R \boldsymbol{V}_{LS}^\dagger \boldsymbol{\Psi}_L^0\right) \\ &= \frac{e}{\hbar} \left(\boldsymbol{\Psi}_L^{0\dagger} \boldsymbol{V}_{LS} \boldsymbol{G}_C^A \boldsymbol{\Gamma}_R \boldsymbol{G}_C^R \boldsymbol{V}_{LS}^\dagger \boldsymbol{\Psi}_L^0\right). \end{aligned} \tag{3.128}$$

Here we introduce and use for the first time the new function (matrix)

$$\boldsymbol{\Gamma}_s = i \left(\boldsymbol{\Sigma}_s^R - \boldsymbol{\Sigma}_s^A\right), \tag{3.129}$$

called the *level-width function*.

The full current of all possible left eigenstates is given by

$$I = \sum_\lambda j_\lambda = \sum_\lambda \frac{e}{\hbar} \left(\boldsymbol{\Psi}_{L\lambda}^{0\dagger} \boldsymbol{V}_{LS} \boldsymbol{G}_C^A \boldsymbol{\Gamma}_R \boldsymbol{G}_C^R \boldsymbol{H}_{LS}^\dagger \boldsymbol{\Psi}_{L\lambda}^0\right) f_L(E_\lambda), \tag{3.130}$$

the distribution function $f_L(E_\lambda)$ describes the population of the left states, the distribution function of the right lead is absent here, because we consider only the current from the left to the right.

The same current is given by the Landauer formula through the transmission function $T(E)$

$$I = \frac{e}{h}\int_{-\infty}^{\infty} T(E) f_L(E) dE. \tag{3.131}$$

If one compares these two expressions for the current, the transmission function at some energy is obtained as

$$\begin{aligned} T(E) &= 2\pi \sum_{\lambda} \delta(E - E_\lambda) \left(\boldsymbol{\Psi}_{L\lambda}^{0\dagger} \boldsymbol{V}_{LS} \boldsymbol{G}_C^A \boldsymbol{\Gamma}_R \boldsymbol{G}_C^R \boldsymbol{V}_{LS}^\dagger \boldsymbol{\Psi}_{L\lambda}^0 \right) \\ &= 2\pi \sum_{\lambda} \sum_{\delta} \delta(E - E_\lambda) \left(\boldsymbol{\Psi}_{L\lambda}^{0\dagger} \boldsymbol{V}_{LS} \boldsymbol{\Psi}_\delta \right) \left(\boldsymbol{\Psi}_\delta^\dagger \boldsymbol{G}_C^A \boldsymbol{\Gamma}_R \boldsymbol{G}_C^R \boldsymbol{V}_{LS}^\dagger \boldsymbol{\Psi}_{L\lambda}^0 \right) \\ &= \sum_{\delta} \left(\boldsymbol{\Psi}_\delta^\dagger \boldsymbol{G}_C^A \boldsymbol{\Gamma}_R \boldsymbol{G}_C^R \boldsymbol{V}_{LS}^\dagger \left(2\pi \sum_{\lambda} \delta(E - E_\lambda) \boldsymbol{\Psi}_{L\lambda}^0 \boldsymbol{\Psi}_{L\lambda}^{0\dagger} \right) \boldsymbol{V}_{LS} \boldsymbol{\Psi}_\delta \right) \\ &= \mathrm{Tr}\left(\boldsymbol{\Gamma}_L \boldsymbol{G}_C^A \boldsymbol{\Gamma}_R \boldsymbol{G}_C^R \right). \end{aligned} \tag{3.132}$$

To evaluate the sum in brackets we used the eigenfunction expansion (3.162) for the left contact.

We obtained a new representation for the transmission function, which is very convenient for numerical calculations

$$T(E) = \mathrm{Tr}\left(\boldsymbol{t}\boldsymbol{t}^\dagger \right) = \mathrm{Tr}\left(\boldsymbol{\Gamma}_L(E) \boldsymbol{G}^R(E) \boldsymbol{\Gamma}_R(E) \boldsymbol{G}^A(E) \right). \tag{3.133}$$

If one compares this expression with (3.79), obtained from the Fisher-Lee relation, it becomes clear that our new formula is the discretized version of (3.79) and the function $\Gamma_s(\boldsymbol{r}_{s1}, \boldsymbol{r}_{s2})$ is analog of the level-width function. Indeed, one can calculate the self-energy explicitly from the wave functions of a semi-infinite electrode. It means that (3.133) can be derived from the Landauer approach directly.

Finally, one important remark, at finite voltage the diagonal energies in the Hamiltonians $\boldsymbol{H}_L^0$, $\boldsymbol{H}_C^0$, and $\boldsymbol{H}_R^0$ are shifted $\varepsilon_\alpha \to \varepsilon_\alpha + e\varphi_\alpha$. Consequently, the energy dependencies of the self-energies defined by (3.121) are also changed and the lead self-energies are voltage dependent. However, it is convenient to define the self-energies using the Hamiltonians at zero voltage, in that case the voltage dependence should be explicitly shown in the transmission formula

$$T(E) = \mathrm{Tr}\left[\tilde{\boldsymbol{\Gamma}}_L(E - e\varphi_L) \boldsymbol{G}^R(E) \tilde{\boldsymbol{\Gamma}}_R(E - e\varphi_R) \boldsymbol{G}^A(E) \right], \tag{3.134}$$

where φ_R and φ_L are electrical potentials of the right and left leads.

3.3 Recursive Method

3.3.1 Dyson Equation

The recursive Green function method is an approach to calculate the Green functions of multi-component systems if the Green functions of isolated subsystems and the coupling matrices between subsystems are known. Starting at one end of the system (usually one of the electrodes), the subsystems are added one by one, finally the Green function of the whole system can be found. It is a convenient way to calculate the relevant Green function components for large complex systems which can be divided into many connected parts. From computational point of view the recursive method can be much faster than direct solution of the equations for large systems.

The method is based on the Dyson equation[5] for the full Green function $\boldsymbol{G}$, the Green function for a disconnected system $\boldsymbol{G}_0$ and the coupling matrix $\boldsymbol{V}$:

$$\boldsymbol{G} = \boldsymbol{G}_0 + \boldsymbol{G}_0 \boldsymbol{V} \boldsymbol{G}. \tag{3.135}$$

The full GF is defined by the full Hamiltonian $\boldsymbol{H} = \boldsymbol{H}_0 + \boldsymbol{V}$: $(\boldsymbol{E} - \boldsymbol{H})\boldsymbol{G} = \boldsymbol{I}$, the GF of the particular parts of the system is defined as $(\boldsymbol{E} - \boldsymbol{H}_0)\boldsymbol{G}_0 = \boldsymbol{I}$. Comparing this two equations, it is easy to get (3.135). The advantage of the Dyson equation is that if one connects an additional external system to the system of interest, it is enough to know the Green function of this external system (independently of how it was calculated) and the coupling matrix. Note, that this procedure works only for non-interacting systems or as a perturbation in $\boldsymbol{V}$ for interacting systems, otherwise $\boldsymbol{V}$ should be replaced by a more general self-energy. However, the recursive method can be applied to interacting systems in combination with the iterative procedure.

Consider how this equation works if we couple two systems with Green functions $\boldsymbol{G}_A^0$ and $\boldsymbol{G}_B^0$ (Fig. 3.3), note that we do not need any explicit Hamiltonian for the subsystems A and B, they can be connected to an arbitrary number of other systems and electrodes through corresponding self-energies. The functions $\boldsymbol{G}_A^0$ and $\boldsymbol{G}_B^0$ are defined in the subspaces A and B with the numbers of states N_A and N_B respectively, the full matrices $\boldsymbol{G}$, $\boldsymbol{G}_0$, $\boldsymbol{V}$ have the dimensions $(N_A + N_B) \times (N_A + N_B)$, and we write the equation (3.135) as

$$\begin{pmatrix} \boldsymbol{G}_A & \boldsymbol{G}_{AB} \\ \boldsymbol{G}_{BA} & \boldsymbol{G}_B \end{pmatrix} = \begin{pmatrix} \boldsymbol{G}_A^0 & 0 \\ 0 & \boldsymbol{G}_B^0 \end{pmatrix} + \begin{pmatrix} \boldsymbol{G}_A^0 & 0 \\ 0 & \boldsymbol{G}_B^0 \end{pmatrix} \begin{pmatrix} 0 & \boldsymbol{V}_{AB} \\ \boldsymbol{V}_{BA} & 0 \end{pmatrix} \begin{pmatrix} \boldsymbol{G}_A & \boldsymbol{G}_{AB} \\ \boldsymbol{G}_{BA} & \boldsymbol{G}_B \end{pmatrix}, \tag{3.136}$$

where $\boldsymbol{V}_{AB}$ is the coupling matrix between subsystems with the dimensions $N_A \times N_B$. We are interested in calculation of the function $\boldsymbol{G}^A$ describing the subsystem A and

[5] The Dyson equation considered here is a particular case of the general Dyson equation for interacting systems. It is actually equivalent to the Lippmann-Schwinger equation (3.60) in the scattering theory.

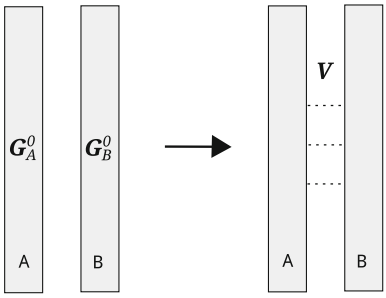

Fig. 3.3 Two subsystems A and B with known Green functions are connected by the coupling $\boldsymbol{V}$ forming the system $A + B$

$\boldsymbol{G}_{BA}$ describing mixing between subsystems A and B. After simple calculations we get

$$\left(\left(\boldsymbol{G}_A^0\right)^{-1} - \boldsymbol{V}_{AB}\boldsymbol{G}_B^0\boldsymbol{V}_{BA}\right)\boldsymbol{G}_A = \left(\left(\boldsymbol{G}_A^0\right)^{-1} - \boldsymbol{\Sigma}_{AB}\right)\boldsymbol{G}_A = \boldsymbol{I}, \tag{3.137}$$

$$\boldsymbol{G}_{BA} = \boldsymbol{G}_B^0\boldsymbol{V}_{BA}\boldsymbol{G}_A. \tag{3.138}$$

We reproduce in a more general way the calculation of the self-energy (3.120)

$$\boldsymbol{\Sigma}_{AB} = \boldsymbol{V}_{AB}\boldsymbol{G}_B^0\boldsymbol{V}_{BA}, \tag{3.139}$$

introduced by the system B into the system A.

As an other example we prove that the multi-electrode self-energy (3.122) is a sum of the self-energies for particular electrodes. Assume that we add one more electrode with the Green function (of the isolated electrode) $\boldsymbol{G}_s$ through the coupling matrix $\boldsymbol{V}_{sC}$. The Green function of the system before is $\boldsymbol{G}_C^{(0)} = [\boldsymbol{E} - \boldsymbol{H}_C - \boldsymbol{\Sigma}^{(0)}]^{-1}$, with $\boldsymbol{\Sigma}^{(0)}$ being the self-energy of all electrodes coupled earlier. Using the equation (3.137) we get

$$\left(\left(\boldsymbol{G}_C^0\right)^{-1} - \boldsymbol{V}_{Cs}\boldsymbol{G}_s\boldsymbol{V}_{sC}\right)\boldsymbol{G}_C = \left(\boldsymbol{E} - \boldsymbol{H}_C - \boldsymbol{\Sigma}^{(0)} - \boldsymbol{\Sigma}_{Cs}\right)\boldsymbol{G}_C = \boldsymbol{I}, \tag{3.140}$$

so that the new self-energy is $\boldsymbol{\Sigma} = \boldsymbol{\Sigma}^{(0)} + \boldsymbol{\Sigma}_{Cs}$.

3.3.2 *Recursive Method for 1D Systems*

Direct calculation of the retarded Green function by means of matrix inversion (3.118) may be computationally intractable for large systems. In the particularly important case of "long" systems with high aspect ratio and short range coupling between base orbitals (important examples are carbon nanotubes and nanoribbons) the central system can be divided into many parts (slices) with only neighbor coupling

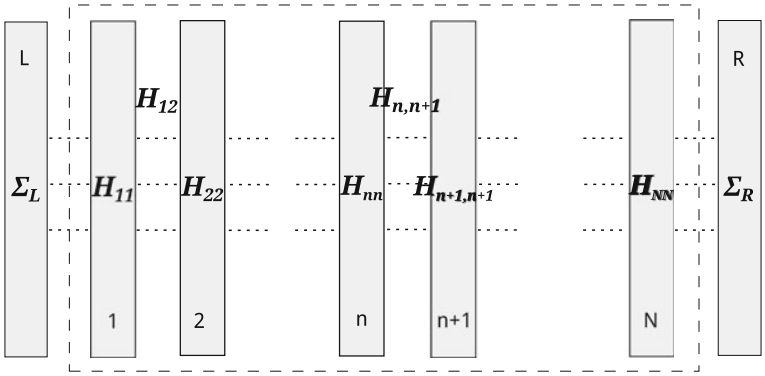

Fig. 3.4 The central region (in the *dashed* box) divided into N slices

between slices (Fig. 3.4), namely $\boldsymbol{H}_{i,i+1}$ is the coupling of slice i and $(i+1)$. The Hamiltonian has a tridiagonal form:

$$\boldsymbol{H} = \begin{pmatrix} \boldsymbol{H}_{11} & \boldsymbol{H}_{12} & 0 & \cdots & 0 \\ \boldsymbol{H}_{21} & \boldsymbol{H}_{22} & \boldsymbol{H}_{23} & \cdots & \cdots \\ 0 & \boldsymbol{H}_{32} & \boldsymbol{H}_{33} & & 0 \\ \vdots & \vdots & \ddots & \ddots & \boldsymbol{H}_{NN-1} \\ 0 & \cdots & 0 & \boldsymbol{H}_{N-1N} & \boldsymbol{H}_{NN} \end{pmatrix}, \tag{3.141}$$

Besides, we assume here that 1-st and N-th slices are coupled to the left and right electrodes by the self-energies $\boldsymbol{\Sigma}_L$ and $\boldsymbol{\Sigma}_R$ respectively.

The Green function $\boldsymbol{G}$ can be represented as a matrix in the "slice space" with the elements being matrices in the basis of corresponding slices:

$$\boldsymbol{G} = \begin{pmatrix} \boldsymbol{G}_{11} & \boldsymbol{G}_{12} & \boldsymbol{G}_{13} & \cdots & \boldsymbol{G}_{1N} \\ \boldsymbol{G}_{21} & \boldsymbol{G}_{22} & \boldsymbol{G}_{23} & \cdots & \boldsymbol{G}_{2N} \\ \boldsymbol{G}_{31} & \boldsymbol{G}_{32} & \boldsymbol{G}_{33} & \cdots & \boldsymbol{G}_{3N} \\ \vdots & \vdots & \vdots & \ddots & \vdots \\ \boldsymbol{G}_{N1} & \boldsymbol{G}_{N2} & \boldsymbol{G}_{N3} & \cdots & \boldsymbol{G}_{NN} \end{pmatrix}. \tag{3.142}$$

The full Green function can be found from the equation

$$(\boldsymbol{E} - \boldsymbol{H} - \boldsymbol{\Sigma})\, \boldsymbol{G} = \boldsymbol{I}, \tag{3.143}$$

where the electrode self-energy has only two components in slice space: $\boldsymbol{\Sigma}_{11} = \boldsymbol{\Sigma}_L$ and $\boldsymbol{\Sigma}_{NN} = \boldsymbol{\Sigma}_R$.

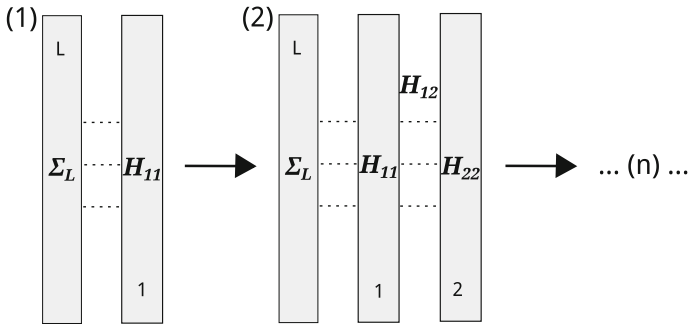

Fig. 3.5 Two first steps of the recursive method "from the left"

Usually the calculation of all elements is not required. Indeed, substituting (3.142) into the expressions for the transmission function (3.133) and the local density of states (3.104) and taking into account that only first and last slices are coupled to the electrodes ($\boldsymbol{\Gamma}_L$ has only one nonzero element $\boldsymbol{\Gamma}_{L,11} = -2\mathrm{Im}\,\boldsymbol{\Sigma}_L$ and $\boldsymbol{\Gamma}_{R,NN} = -2\mathrm{Im}\,\boldsymbol{\Sigma}_R$), we find[6]

$$T(E) = \mathrm{Tr}(\boldsymbol{\Gamma}_L \boldsymbol{G}_{1N} \boldsymbol{\Gamma}_R \boldsymbol{G}_{1N}^{\dagger}), \tag{3.144}$$

$$\rho(E) = \sum_{i=1}^{N} \rho_i(E) = -\frac{1}{\pi} \sum_{i=1}^{N} \mathrm{Im}(\mathrm{Tr}\, \boldsymbol{G}_{ii}). \tag{3.145}$$

As one can see, for transmission and current calculation only $\boldsymbol{G}_{1N}$ is required, for DOS calculation also all $\boldsymbol{G}_{ii}$.

The Green functions can be calculated starting from any end, first we consider the direction of recursion from left to right (forward recursion). At the first step the Green function $\boldsymbol{G}_{11}^{\rightarrow(1)}$ is

$$\boldsymbol{G}_{11}^{\rightarrow(1)} = [\boldsymbol{E} - \boldsymbol{H}_{11} - \boldsymbol{\Sigma}_L]^{-1}, \tag{3.146}$$

this function is not the function $\boldsymbol{G}_{11}$ in (3.142), it is just the function of the first slice connected to the left electrode (Fig. 3.5). We repeat this procedure N times for functions $\boldsymbol{G}_{ii}^{\rightarrow(i)}$ and $\boldsymbol{G}_{1i}^{\rightarrow(i)}$, for $2 \le i \le N$:

$$\boldsymbol{G}_{ii}^{\rightarrow(i)} = \left[\boldsymbol{E} - \boldsymbol{H}_{ii} - \boldsymbol{\Sigma}_R \delta_{iN} - \boldsymbol{H}_{i,i-1} \boldsymbol{G}_{i-1,i-1}^{\rightarrow(i-1)} \boldsymbol{H}_{i-1,i}\right]^{-1}, \tag{3.147}$$

$$\boldsymbol{G}_{1i}^{\rightarrow(i)} = \boldsymbol{G}_{1,i-1}^{\rightarrow(i-1)} \boldsymbol{H}_{i-1,i} \boldsymbol{G}_{ii}^{\rightarrow(i)}. \tag{3.148}$$

[6] All Green functions considered here are retarded Green functions, the index ^{R} is omitted. $\boldsymbol{G}^{\dagger}$ is equivalent to an advanced function.

The equation (3.147) follows from (3.137). To get the equation (3.148) we consider the Dyson equation (3.135) taken $\boldsymbol{G}_0$ before connecting of the ith slice as (we show only the elements calculated by the forward method):

$$\boldsymbol{G}_0 = \begin{pmatrix} \boldsymbol{G}_{11}^{\rightarrow(1)} & \boldsymbol{G}_{12}^{\rightarrow(2)} & \cdots & \boldsymbol{G}_{1,i-1}^{\rightarrow(i-1)} & 0 \\ & \boldsymbol{G}_{22}^{\rightarrow(2)} & & & 0 \\ & & \ddots & & \\ & & & \boldsymbol{G}_{i-1,i-1}^{\rightarrow(i-1)} & \vdots \\ 0 & 0 & \cdots & 0 & \boldsymbol{G}_{ii}^{(0)} \end{pmatrix}. \tag{3.149}$$

And the coupling matrix $\boldsymbol{V}$ has only elements $\boldsymbol{V}_{i-1,i} = \boldsymbol{H}_{i-1,i}$ and $\boldsymbol{V}_{i,i-1} = \boldsymbol{H}_{i,i-1}$. From the first line and i-th column of (3.135) we get immediately the equation (3.148).

At each step we get the Green function of the i-th slice $\boldsymbol{G}_{ii}^{\rightarrow(i)}$ and the propagator between the first and the i-th slice $\boldsymbol{G}_{1i}^{\rightarrow i}$ for the system connected up to the i-th slice to the left electrode. At the last step we get $\boldsymbol{G}_{1N}^{\rightarrow(N)}$, which is the true function $\boldsymbol{G}_{1N}$ and is sufficient to calculate the transmission function, as can be seen from (3.144).

Additional computational effort is required to calculate the density of states (3.145), as one needs all diagonal elements $\boldsymbol{G}_{ii}$, and during the recursion from left to right we got only intermediate functions $\boldsymbol{G}_{ii}^{\rightarrow(i)}$ for partial systems. To get other slice Green functions we will apply the backward recursion, for $N \geq i \geq 1$:

$$\boldsymbol{G}_{NN}^{\leftarrow(N)} = [\boldsymbol{E} - \boldsymbol{H}_{NN} - \boldsymbol{\Sigma}_R]^{-1}, \tag{3.150}$$

$$\boldsymbol{G}_{ii}^{\leftarrow(i)} = \left[\boldsymbol{E} - \boldsymbol{H}_{ii} - \boldsymbol{\Sigma}_L \delta_{i1} - \boldsymbol{H}_{i,i+1} \boldsymbol{G}_{i+1,i+1}^{\leftarrow(i+1)} \boldsymbol{H}_{i+1,i}\right]^{-1}, \tag{3.151}$$

in the end of this procedure we get the right answer for $\boldsymbol{G}_{11}$, as well as in the forward recursion we obtained $\boldsymbol{G}_{NN}$, all other $\boldsymbol{G}_{ii}$ for $1 < i < N$ are calculated as:

$$\boldsymbol{G}_{ii} = \left[\boldsymbol{E} - \boldsymbol{H}_{ii} - \boldsymbol{H}_{i,i-1} \boldsymbol{G}_{i-1,i-1}^{\rightarrow(i-1)} \boldsymbol{H}_{i-1,i} - \boldsymbol{H}_{i,i+1} \boldsymbol{G}_{i+1,i+1}^{\leftarrow(i+1)} \boldsymbol{H}_{i+1,i}\right]^{-1}. \tag{3.152}$$

This is just the Dyson equation for slice i with the left and right self-energies. Actually the first part in this expression is already calculated $\left[\boldsymbol{G}_{ii}^{\rightarrow(i)}\right]^{-1}$. So that we can rewrite this expression as

$$\boldsymbol{G}_{ii} = \boldsymbol{G}_{ii}^{\rightarrow(i)} \left[\boldsymbol{I} - \boldsymbol{G}_{ii}^{\rightarrow(i)} \boldsymbol{H}_{i,i+1} \boldsymbol{G}_{i+1,i+1}^{\leftarrow(i+1)} \boldsymbol{H}_{i+1,i}\right]^{-1}. \tag{3.153}$$

For long systems with short range interactions the time required for calculation scales as $M^3 N$, where $M \times M$ are typical dimensions of one slice matrix (the typical time of matrix inversion is M^3). If one uses the inversion for the whole system it scales as $(MN)^3$ which is much larger for large N.

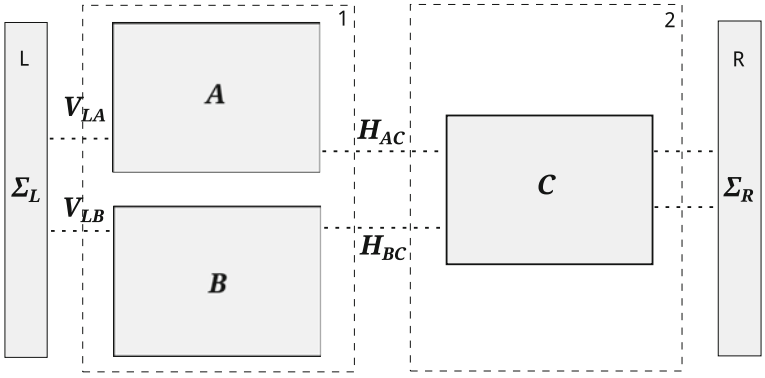

Fig. 3.6 Example of a multi-connected system

3.3.3 Multi-connected Systems

In the case of 2D and 3D multi-connected systems the recursive method in the form discussed above can be applied if the system is divided into slices with several subsystems in every slice. Alternatively, the Dyson equation can be applied to multi-connected systems with Green functions of isolated subsystems included into $\boldsymbol{G}_0$ and all couplings between subsystems into $\boldsymbol{V}$.

Consider as an example three subsystems between two electrodes (Fig. 3.6). The fist slice consists of subsystems A and B, the second of subsystem C. The self-energy $\boldsymbol{\Sigma}_L$ should be calculated for the system $A + B$. It has a general non-diagonal form, as well as the Green function of the system $A + B$ connected to the electrode, which should be determined from the Dyson equation:

$$\begin{pmatrix} \boldsymbol{G}_A & \boldsymbol{G}_{AB} \\ \boldsymbol{G}_{BA} & \boldsymbol{G}_B \end{pmatrix}^{\rightarrow(1)} = \begin{pmatrix} \boldsymbol{G}^0_A & 0 \\ 0 & \boldsymbol{G}^0_B \end{pmatrix} + \begin{pmatrix} \boldsymbol{G}^0_A & 0 \\ 0 & \boldsymbol{G}^0_B \end{pmatrix} \begin{pmatrix} \boldsymbol{\Sigma}_{AA} & \boldsymbol{\Sigma}_{AB} \\ \boldsymbol{\Sigma}_{BA} & \boldsymbol{\Sigma}_{BB} \end{pmatrix} \begin{pmatrix} \boldsymbol{G}_A & \boldsymbol{G}_{AB} \\ \boldsymbol{G}_{BA} & \boldsymbol{G}_B \end{pmatrix}^{\rightarrow(1)}, \tag{3.154}$$

this equation replaces the equation (3.146). The functions $\boldsymbol{G}_A$ and $\boldsymbol{G}_B$ are not independent and should be calculated simultaneously.

Let us consider in detail how the off-diagonal components appear. Following the previous approach we consider the coupling of systems A and B to the "left" system L. The equation equivalent to (3.136) is:

$$\begin{pmatrix} \boldsymbol{G}_A & \boldsymbol{G}_{AB} & \boldsymbol{G}_{AC} \\ \boldsymbol{G}_{BA} & \boldsymbol{G}_B & \boldsymbol{G}_{BC} \\ \boldsymbol{G}_{LA} & \boldsymbol{G}_{LB} & \boldsymbol{G}_L \end{pmatrix} = \begin{pmatrix} \boldsymbol{G}^0_A & 0 & 0 \\ 0 & \boldsymbol{G}^0_B & 0 \\ 0 & 0 & \boldsymbol{G}^0_L \end{pmatrix} + \begin{pmatrix} \boldsymbol{G}^0_A & 0 & 0 \\ 0 & \boldsymbol{G}^0_B & 0 \\ 0 & 0 & \boldsymbol{G}^0_L \end{pmatrix} \begin{pmatrix} 0 & 0 & \boldsymbol{V}_{AL} \\ 0 & 0 & \boldsymbol{V}_{BL} \\ \boldsymbol{V}_{LA} & \boldsymbol{V}_{LB} & 0 \end{pmatrix} \begin{pmatrix} \boldsymbol{G}_A & \boldsymbol{G}_{AB} & \boldsymbol{G}_{AL} \\ \boldsymbol{G}_{BA} & \boldsymbol{G}_B & \boldsymbol{G}_{BL} \\ \boldsymbol{G}_{LA} & \boldsymbol{G}_{LB} & \boldsymbol{G}_L \end{pmatrix}, \tag{3.155}$$

note that A and B are coupled to L, but there is no direct coupling between A and B. From this equation one gets (3.154) with the self-energy

$$\begin{pmatrix} \boldsymbol{\Sigma}_{AA} & \boldsymbol{\Sigma}_{AB} \\ \boldsymbol{\Sigma}_{BA} & \boldsymbol{\Sigma}_{BB} \end{pmatrix} = \begin{pmatrix} \boldsymbol{V}_{AL}\boldsymbol{G}_L^0\boldsymbol{V}_{LA} & \boldsymbol{V}_{AL}\boldsymbol{G}_L^0\boldsymbol{V}_{LB} \\ \boldsymbol{V}_{BL}\boldsymbol{G}_L^0\boldsymbol{V}_{LA} & \boldsymbol{V}_{BL}\boldsymbol{G}_L^0\boldsymbol{V}_{LB} \end{pmatrix}. \tag{3.156}$$

The diagonal elements reproduce (3.139), and the off-diagonal elements describe mutual influence of the systems A and B. Even if there is no direct coupling between A and B (if this coupling $\boldsymbol{V}_{AB}$ is present, it should be also included in (3.155)), the effective coupling is established through the electrode.

The Green functions of A and B are calculated from (3.154). At the second step the Green function of the system C is determined as:

$$\boldsymbol{G}_C = \left[\boldsymbol{E} - \boldsymbol{H}_C - \boldsymbol{\Sigma}_R - \boldsymbol{H}_{CA}\boldsymbol{G}_A^{\rightarrow(1)}\boldsymbol{H}_{AC} - \boldsymbol{H}_{CB}\boldsymbol{G}_B^{\rightarrow(1)}\boldsymbol{H}_{BC}\right]^{-1}. \tag{3.157}$$

For large systems with many elements and complex topology, the application of the recursive method starts to be cumbersome. It seems that the methods based on the direct solution of the Dyson equation in a subsystem space should be preferable.

3.4 Semi-infinite Electrodes

3.4.1 Surface Green Function

Previously in this chapter we introduced the electrode self-energies $\boldsymbol{\Sigma}_s$, which are determined by (3.120), (3.121). Now let us discuss in more detail how these self-energies can be calculated. The problem is that electrodes are usually assumed to be infinitely large at least in one direction. The direct matrix inversion (3.119) can not be performed in this case because the matrix has infinite size and the spectrum of an infinitely large system is continuous.

To proceed, we refine the model of electrodes and introduce the concept of *surface Green function*. First of all, one should note that usually (actually in all relevant cases) the electrode-to-system coupling $\boldsymbol{V}_{sC}$ in the spatially localized (tight-binding) basis is nonzero only for limited number of close to the surface basis orbitals. We consider a semi-infinite electrode (Fig. 3.7) as a series of equivalent blocks with the Hamiltonian $\boldsymbol{H}_0$ and interblock neighbor couplings $\boldsymbol{H}_1$. We assume that the size of the block is large enough to fulfill two conditions:

(i) only couplings between neighbor blocks can be taken into account. The Hamiltonian of such an electrode is of the standard tridiagonal form:

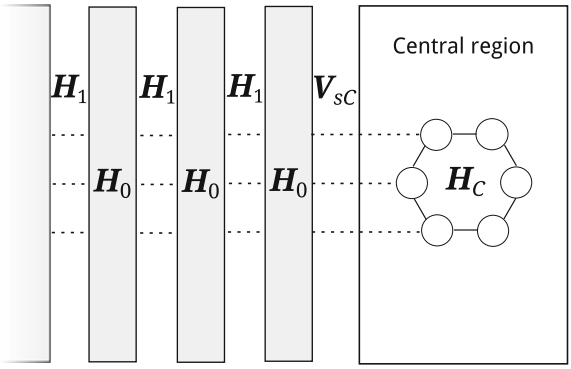

Fig. 3.7 A quantum system coupled to a semi-infinite 1D electrode

$$\boldsymbol{H} = \begin{pmatrix} \boldsymbol{H}_0 & \boldsymbol{H}_1 & 0 & 0 & \cdots \\ \boldsymbol{H}_1^\dagger & \boldsymbol{H}_0 & \boldsymbol{H}_1 & 0 & \cdots \\ 0 & \boldsymbol{H}_1^\dagger & \boldsymbol{H}_0 & \boldsymbol{H}_1 & \cdots \\ 0 & 0 & \boldsymbol{H}_1^\dagger & \boldsymbol{H}_0 & \ddots \\ \vdots & \vdots & \vdots & \ddots & \ddots \end{pmatrix}, \tag{3.158}$$

(ii) the central system is coupled only to the edge block. It means that the coupling matrix has the form

$$\boldsymbol{V}_{sC} = \begin{pmatrix} \tilde{\boldsymbol{V}}_{sC} & 0 & 0 & \cdots \\ 0 & 0 & 0 & \cdots \\ 0 & 0 & 0 & \cdots \\ \vdots & \vdots & \vdots & \ddots \end{pmatrix}. \tag{3.159}$$

The Green function $\boldsymbol{G}_s^R$ is of a general type (not periodic):

$$\boldsymbol{G}_s^R = \begin{pmatrix} \tilde{\boldsymbol{G}}_s^R & \boldsymbol{G}_{12} & \boldsymbol{G}_{13} & \cdots \\ \boldsymbol{G}_{21} & \boldsymbol{G}_{22} & \boldsymbol{G}_{23} & \cdots \\ \boldsymbol{G}_{31} & \boldsymbol{G}_{32} & \boldsymbol{G}_{33} & \cdots \\ \vdots & \vdots & \vdots & \ddots \end{pmatrix}. \tag{3.160}$$

We introduce here the Green function of the edge block (rigorously, it is the part of the Green function corresponding to the basis of the edge block) $\tilde{\boldsymbol{G}}_s^R$ and call it surface Green function. Because of the condition (ii) the self-energy is determined by $\tilde{\boldsymbol{G}}_s^R$ only, namely

$$\boldsymbol{\Sigma}_s^R = \tilde{\boldsymbol{V}}_{sC}^\dagger \tilde{\boldsymbol{G}}_s^R \tilde{\boldsymbol{V}}_{sC}, \tag{3.161}$$

Thus, our aim is to calculate the surface Green function $\tilde{\boldsymbol{G}}_s^R$, all other parts of the matrix (3.160) are irrelevant.

We consider two different approaches to this problem: first the analytical solution, and second the numerical iterative method.

3.4.2 Analytical Solution

To proceed, we use the relation between the Green function and the eigenfunctions Ψ_λ of a system, which are solutions of the Schrödinger equation (3.85). Let us define $\Psi_\lambda(\alpha) \equiv c_\lambda$ in the eigenstate $|\lambda\rangle$ in the sense of definition (3.82), then

$$G^R_{\alpha\beta}(\varepsilon) = \sum_\lambda \frac{\Psi_\lambda(\alpha)\Psi^*_\lambda(\beta)}{\varepsilon + i\eta - E_\lambda}, \tag{3.162}$$

where α is the TB state (site) index, λ denotes the eigenstate, E_λ is the energy of the eigenstate. The summation in this formula can be easily replaced by integration in the case of a continuous spectrum. It is important to notice, that the eigenfunctions $\Psi_\lambda(\alpha)$ should be calculated for the semi-infinite lead separately, because the Green function of the isolated lead is entering into the contact self-energy.

For example, for the semi-infinite 1D chain of single-state sites ($n, m = 1, 2, \ldots$) we write

$$G^R_{nm}(\varepsilon) = \int_{-\pi}^{\pi} \frac{dk}{2\pi} \frac{\Psi_k(n)\Psi^*_k(m)}{\varepsilon + i\eta - E_k}, \tag{3.163}$$

with the eigenfunctions $\Psi_k(n) = \sqrt{2}\sin kn$, and energies $E_k = \varepsilon_0 + 2t\cos k$.

Let us consider a simple situation, when the nanosystem is coupled only to the end site of the 1D lead (Fig. 3.8). From (3.120) we obtain the matrix elements of the self-energy

$$\Sigma_{\alpha\beta} = V^*_{1\alpha} V_{1\beta} G^{0R}_{11}, \tag{3.164}$$

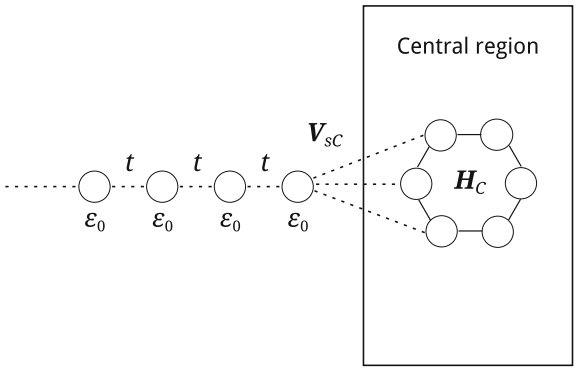

Fig. 3.8 A semi-infinite 1D chain coupled to the system's central region

where the matrix element $V_{1\alpha}$ describes the coupling between the end site of the lead ($n = m = 1$) and the state $|\alpha\rangle$ of the nanosystem.

To make clear the main physical properties of the lead self-energy, let us analyze in detail the semi-infinite 1D lead with the Green function (3.163). The integral can be calculated analytically

$$G_{11}^{R}(\varepsilon) = \frac{1}{\pi}\int_{-\pi}^{\pi} \frac{\sin^2 k dk}{\varepsilon + i\eta - \varepsilon_0 - 2t\cos k} = -\frac{\exp(iK(\varepsilon))}{t}, \tag{3.165}$$

where $K(\varepsilon)$ is determined from $\varepsilon = \varepsilon_0 + 2t\cos K$. Finally, we obtain the following expressions for the real and imaginary part of the self-energy

$$\mathrm{Re}\,\Sigma_{\alpha\alpha} = \frac{|V_{1\alpha}|^2}{t}\left(\kappa - \sqrt{\kappa^2 - 1}\,[\theta(\kappa - 1) - \theta(-\kappa - 1)]\right), \tag{3.166}$$

$$\mathrm{Im}\,\Sigma_{\alpha\alpha} = -\frac{|V_{1\alpha}|^2}{t}\sqrt{1 - \kappa^2}\,\theta(1 - |\kappa|), \tag{3.167}$$

$$\kappa = \frac{\varepsilon - \varepsilon_0}{2t}. \tag{3.168}$$

The real and imaginary parts of the self-energy, given by these expressions, are shown in Fig. 3.9. There are several important general conclusion that we can make looking at the formulas and the curves.

(i) The self-energy is a complex function, the real part describes the energy shift of the level, and the imaginary part describes broadening. The *finite* imaginary part appears as a result of the continuous spectrum in the leads. The imaginary part determines the level-width function

$$\Gamma = i\left(\Sigma - \Sigma^{\dagger}\right). \tag{3.169}$$

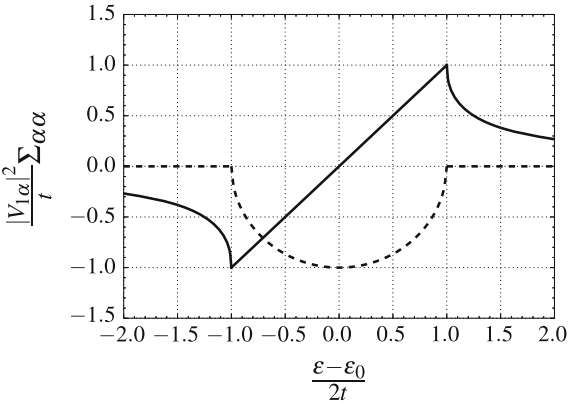

Fig. 3.9 Real (*solid line*) and imaginary (*dashed line*) parts of the electrode self-energy as a function of energy for a one-band one-dimensional lead

(ii) In the wide-band limit ($t \to \infty$), at the energies $\varepsilon - \varepsilon_0 \ll t$, it is possible to neglect the real part of the self-energy, and the only effect of the leads is level broadening. So that the self-energy of the left (right) lead is

$$\Sigma_{L(R)} = -i\frac{\Gamma_{L(R)}}{2}. \tag{3.170}$$

These expressions we will use soon in Sect. 3.5.

3.4.3 The Iterative Method for 1D Electrodes

In the case when analytical calculation of the electrode Green function is not possible, a numerical approach can be used. We consider the iterative method suggested in [5]. Here we first consider a 1D electrode: semi-infinite in one direction, but finite in other directions. The Hamiltonian in this case has the form (3.158) with all block matrices $\boldsymbol{H}_0$, $\boldsymbol{H}_1$ being finite-size, so that usual matrix inversion operations can be used for particular blocks.

We start from the exact equations for the elements of the Green function matrix (3.160), function $\tilde{\boldsymbol{G}} \equiv \boldsymbol{G}_{11}$ is the surface Green function,

$$(\boldsymbol{E} - \boldsymbol{H}_0)\tilde{\boldsymbol{G}} = \boldsymbol{I} + \boldsymbol{H}_1\boldsymbol{G}_{21}, \tag{3.171}$$

$$(\boldsymbol{E} - \boldsymbol{H}_0)\boldsymbol{G}_{p1} = \boldsymbol{H}_1^{\dagger}\boldsymbol{G}_{p-1,1} + \boldsymbol{H}_1\boldsymbol{G}_{p+1,1}, \ \ p \geqslant 2, \tag{3.172}$$

this infinite system of equations can be truncated to give the approximate answer. The convenient and numerically stable way to do it uses the following renormalization idea. Let us substitute the expression for $\boldsymbol{G}_{21}$ from the second equation into the first one:

$$\left(\boldsymbol{E} - \boldsymbol{H}_0 - \boldsymbol{H}_1(\boldsymbol{E} - \boldsymbol{H}_0)^{-1}\boldsymbol{H}_1^{\dagger}\right)\tilde{\boldsymbol{G}} = \boldsymbol{I} + \boldsymbol{H}_1(\boldsymbol{E} - \boldsymbol{H}_0)^{-1}\boldsymbol{H}_1\boldsymbol{G}_{31}, \tag{3.173}$$

at the same time we rewrite (3.172) for only odd numbers $p = 3, 5, \ldots$:

$$\left(\boldsymbol{E} - \boldsymbol{H}_0 - \boldsymbol{H}_1(\boldsymbol{E} - \boldsymbol{H}_0)^{-1}\boldsymbol{H}_1^{\dagger} - \boldsymbol{H}_1^{\dagger}(\boldsymbol{E} - \boldsymbol{H}_0)^{-1}\boldsymbol{H}_1\right)\tilde{\boldsymbol{G}}_{p,1} = \\ \boldsymbol{H}_1^{\dagger}(\boldsymbol{E} - \boldsymbol{H}_0)^{-1}\boldsymbol{H}_1^{\dagger}\boldsymbol{G}_{p-2,1} + \boldsymbol{H}_1(\boldsymbol{E} - \boldsymbol{H}_0)^{-1}\boldsymbol{H}_1\boldsymbol{G}_{p+2,1}. \tag{3.174}$$

The structure of these equations is similar to the initial one, but they describe only odd slices. All even blocks participate through the renormalized coupling $\boldsymbol{H}_1' = \boldsymbol{H}_1(\boldsymbol{E} - \boldsymbol{H}_0)^{-1}\boldsymbol{H}_1$. If we change the numbering defining new Green functions at $k > 1$ as $\boldsymbol{G}'_{k,1} = \boldsymbol{G}_{2k-1,1}$: $\boldsymbol{G}'_{2,1} = \boldsymbol{G}_{3,1}$, $\boldsymbol{G}'_{3,1} = \boldsymbol{G}_{5,1}$, etc., and redefine the functions

$$\boldsymbol{A} = \boldsymbol{H}_1, \tag{3.175}$$
$$\boldsymbol{B} = \boldsymbol{H}_1^{\dagger}, \tag{3.176}$$
$$\boldsymbol{C} = \boldsymbol{E} - \boldsymbol{H}_0, \tag{3.177}$$
$$\boldsymbol{D} = \boldsymbol{E} - \boldsymbol{H}_0, \tag{3.178}$$

with the following transformation

$$\boldsymbol{A}' = \boldsymbol{A}\boldsymbol{D}^{-1}\boldsymbol{A}, \tag{3.179}$$
$$\boldsymbol{B}' = \boldsymbol{B}\boldsymbol{D}^{-1}\boldsymbol{B}, \tag{3.180}$$
$$\boldsymbol{C}' = \boldsymbol{C} - \boldsymbol{A}\boldsymbol{D}^{-1}\boldsymbol{B}, \tag{3.181}$$
$$\boldsymbol{D}' = \boldsymbol{D} - \boldsymbol{A}\boldsymbol{D}^{-1}\boldsymbol{B} - \boldsymbol{B}\boldsymbol{D}^{-1}\boldsymbol{A}, \tag{3.182}$$

we arrive at the (3.171), (3.172) with renormalized parameters. Note that $\boldsymbol{C}$ and $\boldsymbol{D}$ are the same in the beginning, but are transformed differently. Repeating the procedure n times, we obtain the equations

$$\boldsymbol{C}^{(n)}\tilde{\boldsymbol{G}} = \boldsymbol{I} + \boldsymbol{A}^{(n)}\boldsymbol{G}_{21}^{(n)}, \tag{3.183}$$
$$\boldsymbol{D}^{(n)}\boldsymbol{G}_{k1}^{(n)} = \boldsymbol{B}^{(n)}\boldsymbol{G}_{k-1,1}^{(n)} + \boldsymbol{A}^{(n)}\boldsymbol{G}_{k+1,1}^{(n)},\ k \geqslant 2, \tag{3.184}$$

The Green functions at each step are related to the functions of the initial problem, e.g. $\boldsymbol{G}_{21}^{(n)} = \boldsymbol{G}_{2^n+1}$, but the first (surface) Green function $\boldsymbol{G}_{11}$ is not changed by this transformation.

In the limit $n \to \infty$ one gets $\boldsymbol{A}^{(n)} \to 0$ and $\tilde{\boldsymbol{G}} = \left(\boldsymbol{C}^{(n)}\right)^{-1}$. The physical sense of this procedure is that the effective interaction for larger and larger distance between the blocks (at each step the number of "passive" slices between "active" is doubled) decreases and finally can be neglected. In practice, a large enough number of iterations should be done, the convergence criteria is small enough value of $\boldsymbol{A}^{(n)}$.

3.4.4 The Iterative Method for 2D and 3D Electrodes

In the case of 2D (for example graphene) or 3D (usual metal and semiconductor) electrodes the iterative method should be combined with k-sampling in the directions perpendicular to the surface. We assume here an ideal semi-infinite electrode formed from the blocks with the Hamiltonian $\boldsymbol{H}_0$ and coupling dependent on the distance between blocks $\boldsymbol{H}_{\Delta n \Delta m \Delta l}$.

$$\boldsymbol{H} = \sum_{nml,n'm'l'} \boldsymbol{H}_{nml,n'm'l'},\ n \in [0,\infty],\ m,l \in [-\infty,\infty] \tag{3.185}$$

$$\boldsymbol{\Psi}_{nml} = \sum_{k_x k_y} \boldsymbol{\Psi}_{n\boldsymbol{k}} e^{ik_x m + ik_y l},\ k_x, k_y \in [-\pi,\pi] \tag{3.186}$$

$$\sum_{nml,n'm'l'} \boldsymbol{H}_{nml,n'm'l'} \boldsymbol{\Psi}_{n'\boldsymbol{k}} e^{ik_x m' + ik_y l'} = E_{\boldsymbol{k}} \boldsymbol{\Psi}_{n\boldsymbol{k}} e^{ik_x m + ik_y l} \tag{3.187}$$

$$\sum_{n'} \boldsymbol{H}_{n-n',\boldsymbol{k}} \boldsymbol{\Psi}_{n'\boldsymbol{k}} = E_{\boldsymbol{k}} \boldsymbol{\Psi}_{n\boldsymbol{k}}, \tag{3.188}$$

where we introduced the k-dependent Hamiltonian

$$\boldsymbol{H}_{n-n',\boldsymbol{k}} = \sum_{\Delta m \Delta l} \boldsymbol{H}_{n-n',\Delta m \Delta l} e^{ik_x \Delta m + ik_y \Delta l}. \tag{3.189}$$

Now we assume that only neighbouring blocks in z-direction are coupled and introduce the Hamiltonians $\boldsymbol{H}_0^k = \boldsymbol{H}_{0,\boldsymbol{k}}$ and $\boldsymbol{H}_1^k = \boldsymbol{H}_{1,\boldsymbol{k}}$. We reduced the problem to the previously considered 1D case, which can be solved by the iterative method. Thus for any $\boldsymbol{k}$ we obtain the surface Green function $\tilde{\boldsymbol{G}}^k$.

The last thing to do is to calculate the surface Green function $\tilde{\boldsymbol{G}}_{ml,m'l'}(E)$ which takes all states into account. Using the eigenvalue expansion (3.25) and the Fourier representation (3.186) one gets:

$$G_{nml,n'm'l'}(E) = \sum_{\boldsymbol{k}} \left[\sum_{\lambda} \frac{|\boldsymbol{\Psi}_{n\boldsymbol{k}}^{\lambda}\rangle\langle\boldsymbol{\Psi}_{n'\boldsymbol{k}}^{\lambda}|}{E + i\eta - E_{\boldsymbol{k}}^{\lambda}} \right] e^{ik_x(m-m') + ik_y(l-l')} \tag{3.190}$$

$$\tilde{\boldsymbol{G}}_{ml,m'l'}(E) = \sum_{\boldsymbol{k}} \tilde{\boldsymbol{G}}^k e^{ik_x(m-m') + ik_y(l-l')}, \tag{3.191}$$

or

$$\tilde{\boldsymbol{G}}_{\Delta m \Delta l}(E) = \sum_{\boldsymbol{k}} \tilde{\boldsymbol{G}}^k e^{ik_x \Delta m + ik_y \Delta l} \tag{3.192}$$

The surface Green function within one block is given simply by $\sum_{\boldsymbol{k}} \tilde{\boldsymbol{G}}^k$.

3.5 Resonant Transport

We can now analyze the basic features of coherent transport through discrete-level systems and some general properties described by the retarded Green function (3.118):

$$\boldsymbol{G}_C^R(E) = \left[\boldsymbol{E} - \boldsymbol{H}_C - \boldsymbol{\Sigma}^R\right]^{-1} = \left[\boldsymbol{E} - \boldsymbol{H}_C - \boldsymbol{\Sigma}_L^R - \boldsymbol{\Sigma}_R^R\right]^{-1}, \tag{3.193}$$

the transmission function (3.133):

$$T(E) = \mathrm{Tr}\left(\boldsymbol{\Gamma}_L(E)\boldsymbol{G}_C^R(E)\boldsymbol{\Gamma}_R(E)\boldsymbol{G}_C^A(E)\right), \tag{3.194}$$

clarify the physical sense of the self-energy (3.120):

$$\boldsymbol{\Sigma}_{s=L(R)}^R = \boldsymbol{V}_{sC}^\dagger \boldsymbol{G}_s^R \boldsymbol{V}_{sC}, \tag{3.195}$$

$$\Sigma_{s=L(R);\alpha\beta}^R = \sum_{\delta\gamma}\left(\boldsymbol{V}_{sC}^\dagger\right)_{\alpha\delta} G_{s;\delta\gamma}^R V_{s;\gamma\beta} = \sum_{\delta\gamma} V_{s;\delta\alpha}^* V_{s;\gamma\beta} G_{s;\delta\gamma}^R, \tag{3.196}$$

and the level-width function (3.129):

$$\boldsymbol{\Gamma}_s = i\left(\boldsymbol{\Sigma}_s^R - \boldsymbol{\Sigma}_s^A\right). \tag{3.197}$$

We introduce also one new important function, the *spectral function (matrix)*:

$$\boldsymbol{A} = i\left(\boldsymbol{G}^R - \boldsymbol{G}^A\right). \tag{3.198}$$

Comparing this expression with (3.104) one can see that $A_{\alpha\alpha}(E) = 2\pi\rho_{\alpha\alpha}(E)$ describes the local density of states.

The level-width function can be in principle complex, for example in the situations with the external magnetic filed, but we will consider only the cases with a real $\boldsymbol{\Gamma}$. Moreover, we assume that $\boldsymbol{\Gamma}$ is symmetric matrix $\Gamma_{\alpha\beta} = \Gamma_{\beta\alpha}$ and determines the imaginary part of $\boldsymbol{\Sigma}^R$:

$$\boldsymbol{\Gamma} = i\left(\boldsymbol{\Sigma}^R - \boldsymbol{\Sigma}^A\right) = -2\mathrm{Im}\,\boldsymbol{\Sigma}^R, \quad \boldsymbol{\Sigma}^R = \mathrm{Re}\,\boldsymbol{\Sigma}^R - \frac{i}{2}\boldsymbol{\Gamma}. \tag{3.199}$$

To understand the meaning of these functions, let us consider some simple examples of *resonant transport*, which take place for small couplings to the electrodes and energies close to the eigenenergies of the isolated system.

3.5.1 Single-Level Model

The simplest, but important case of resonant tunneling is transmission through a single level (Fig. 3.10). We already considered it in Chap. 2 as the limiting case of transmission through a double-barrier potential and obtained the Lorentzian-shape formula (2.66). Now we get the same result using the Green function method. In the wide-band limit the energy independent electrode self-energies are

$$\Sigma^R = \Sigma_L^R + \Sigma_R^R, \quad \Sigma_L^R = -i\frac{\Gamma_L}{2}, \quad \Sigma_R^R = -i\frac{\Gamma_R}{2}, \tag{3.200}$$

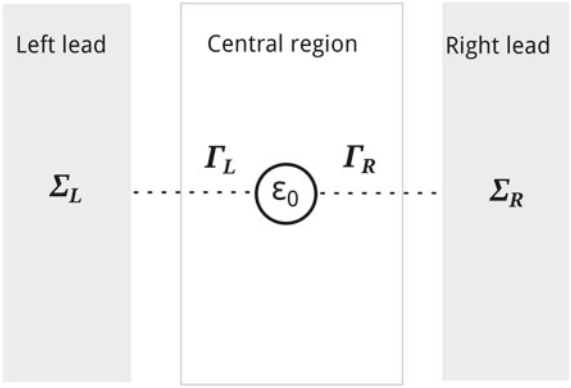

Fig. 3.10 The single-level model

and for the retarded and advanced Green functions one gets (ε_0 is the energy of the level):

$$G^R(E) = \frac{1}{E - \varepsilon_0 - \Sigma^R} = \frac{1}{E - \varepsilon_0 + i(\Gamma_L + \Gamma_R)/2}, \tag{3.201}$$

$$G^A(E) = \frac{1}{E - \varepsilon_0 - i(\Gamma_L + \Gamma_R)/2}. \tag{3.202}$$

which gives the spectral function

$$A(E) = -2\mathrm{Im}G^R = \frac{\Gamma_L + \Gamma_R}{(E - \varepsilon_0)^2 + (1/4)(\Gamma_L + \Gamma_R)^2} = \frac{\Gamma}{(E - \varepsilon_0)^2 + \Gamma^2/4}, \tag{3.203}$$

with $\Gamma = \Gamma_L + \Gamma_R$. This function is shown in Fig. 3.11 at three values of $\Gamma = 1, 2, 4$. It is nicely seen that Γ determines the width of the curve at half-height.

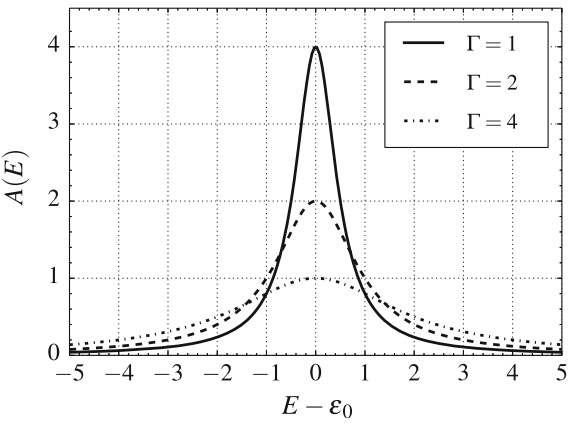

Fig. 3.11 The spectral function for the single-level model

Now using the general expression (3.194) we obtain the transmission function, recovering the result (2.66) generalized for asymmetric coupling:

$$T(E) = \frac{\Gamma_L \Gamma_R}{[E - \varepsilon_0]^2 + (\Gamma_L + \Gamma_R)^2/4}. \tag{3.204}$$

This curve has the same Lorentzian shape as the spectral function. Interesting feature of the transmission for symmetric junctions ($\Gamma_L = \Gamma_R$) is that its maximum value at $E = \varepsilon_0$ is always unity, even for very weak coupling.

It is useful to have some expressions to estimate current and conductance in the limiting cases.

At Zero Temperature

Note that the spin degeneracy is not taken into account and the Fermi distribution functions are assumed in the electrodes. The conductance at the Fermi energy is

$$G = \frac{e^2}{h} T(E_F) = \frac{e^2}{h} \frac{\Gamma_L \Gamma_R}{(E_F - \varepsilon_0)^2 + (\Gamma_L + \Gamma_R)^2/4}, \tag{3.205}$$

with the maximum at $\varepsilon_0 = E_F$, we assume that the Fermi level is fixed by the electrodes and the energy of the level ε_0 is the parameter which can be changed. The maximum value of conductance is

$$G_{max} = \frac{e^2}{h} \frac{4\Gamma_L \Gamma_R}{(\Gamma_L + \Gamma_R)^2}. \tag{3.206}$$

It is interesting that for symmetric junction ($\Gamma_L = \Gamma_R$) it is always e^2/h independently of the value of Γ_L. For weaker coupling to the electrodes, exactly at the resonance the conductance is always the same, but the width of the resonance is decreasing.

The other useful formula is the exact expression for the current at finite voltage

$$I(V) = \frac{e}{h} \frac{2\Gamma_L \Gamma_R}{\Gamma_L + \Gamma_R} \left[\arctan\left(\frac{(1-\eta)eV - \varepsilon_0}{(\Gamma_L + \Gamma_R)/2} \right) + \arctan\left(\frac{\eta eV + \varepsilon_0}{(\Gamma_L + \Gamma_R)/2} \right) \right], \tag{3.207}$$

if one assumes the linear shift of the energy level with voltage $\tilde{\varepsilon}_0(V) = \varepsilon_0 + \eta eV$.

The saturation current at large voltage is

$$I_{max} = \frac{e}{h} \frac{2\pi \Gamma_L \Gamma_R}{\Gamma_L + \Gamma_R} = \frac{e}{\hbar} \frac{\Gamma_L \Gamma_R}{\Gamma_L + \Gamma_R}. \tag{3.208}$$

At Finite Temperature

The linear conductance is given by

$$G(T) = \frac{e^2}{h}\frac{1}{4T}\int_{-\infty}^{\infty}\left[\frac{\Gamma_L\Gamma_R}{(E-\varepsilon_0)^2+(\Gamma_L+\Gamma_R)^2/4}\right]\frac{dE}{\cosh^2(E/(2T))}. \tag{3.209}$$

The off-resonant conductance at $|\varepsilon_0| \gg \Gamma_L + \Gamma_R, T$ is

$$G = \frac{e^2}{h}\frac{\Gamma_L\Gamma_R}{\varepsilon_0^2}. \tag{3.210}$$

At weak coupling $\Gamma_L, \Gamma_R \ll T$ one gets

$$G = \frac{e^2}{h}\frac{\pi\Gamma_L\Gamma_R}{\Gamma_L+\Gamma_R}\frac{1}{T\cosh^2(\varepsilon_0/(2T))}. \tag{3.211}$$

These simple formulas are useful to estimate the currents and conductances.

3.5.2 Two-Level Model, Interference

The other example (Fig. 3.12) is the two-level model (3.106):

$$\boldsymbol{H} = \begin{pmatrix} \varepsilon_1 & t \\ t & \varepsilon_2 \end{pmatrix}, \tag{3.212}$$

we will consider the diagonal in level indices self-energies in the wide-band limit

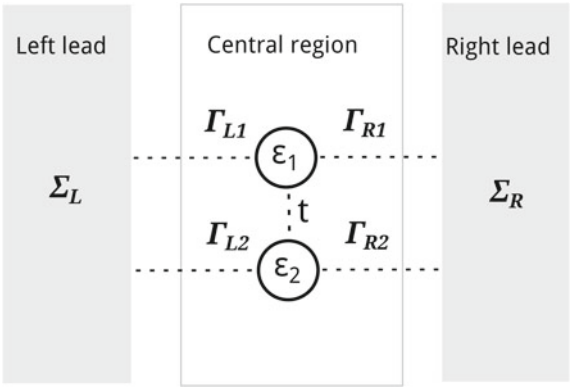

Fig. 3.12 Two-level model

$$\boldsymbol{\Sigma}_L = \begin{pmatrix} -\frac{i}{2}\Gamma_{L1} & 0 \\ 0 & -\frac{i}{2}\Gamma_{L2} \end{pmatrix}, \quad \boldsymbol{\Sigma}_R = \begin{pmatrix} -\frac{i}{2}\Gamma_{R1} & 0 \\ 0 & -\frac{i}{2}\Gamma_{R2} \end{pmatrix}. \tag{3.213}$$

The expression for the Green function we obtain from (3.107) by replacing η with the corresponding $\Gamma_1 = (\Gamma_{L1} + \Gamma_{R1})/2$ or $\Gamma_2 = (\Gamma_{L2} + \Gamma_{R2})/2$:

$$\boldsymbol{G}^R(E) = \frac{1}{(E + i\Gamma_1 - \varepsilon_1)(E + i\Gamma_2 - \varepsilon_2) - t^2} \begin{pmatrix} E + i\Gamma_2 - \varepsilon_2 & t \\ t & E + i\Gamma_1 - \varepsilon_1 \end{pmatrix}. \tag{3.214}$$

This model describes several important limiting cases:

(i) the parallel coupling: $\Gamma_{L1} = \Gamma_{L2}$ and $\Gamma_{R1} = \Gamma_{R2}$, in this case the levels are equivalently coupled to the electrodes and the current flows between the electrodes through both levels, also at $t = 0$;

(ii) the sequential coupling:

$$\boldsymbol{\Sigma}_L = \begin{pmatrix} -\frac{i}{2}\Gamma_{L1} & 0 \\ 0 & 0 \end{pmatrix}, \quad \boldsymbol{\Sigma}_R = \begin{pmatrix} 0 & 0 \\ 0 & -\frac{i}{2}\Gamma_{R2} \end{pmatrix}, \tag{3.215}$$

in this case the current flows consequently through the first and the second level. At $t = 0$ there is no current;

(iii) T-junction:

$$\boldsymbol{\Sigma}_L = \begin{pmatrix} -\frac{i}{2}\Gamma_{L1} & 0 \\ 0 & 0 \end{pmatrix}, \quad \boldsymbol{\Sigma}_R = \begin{pmatrix} -\frac{i}{2}\Gamma_{R1} & 0 \\ 0 & 0 \end{pmatrix}, \tag{3.216}$$

in this case only first level is coupled to the electrodes, the second level participates in transport only through coupling t to the first level.

Also other configurations are possible. For different couplings to the electrodes the transmission shows qualitatively different behavior.

Consider first symmetric parallel coupling with $\Gamma_{L1} = \Gamma_{R1} = \Gamma_{L2} = \Gamma_{R2} = \Gamma/2$, thus $\Gamma_1 = \Gamma_2 = \Gamma/2$, which in the case of the uncoupled levels ($t = 0$) gives the same broadening as for the single-level model above. The spectral function $A(E) = A_{11} + A_{22} = -2\mathrm{Im}(G^R_{11} + G^R_{22})$ is presented in Fig. 3.13 at $\Gamma = 1$, $\varepsilon_1 = -2$, $\varepsilon_2 = 2$ and three values of $t = 0, 2, 3$. The dashed curve ($t = 0$) is just a superposition of two spectral functions for two independent levels. At finite interaction between basis states ($t = 2, 3$) we observe the shift of the level positions, they reflect now the positions of the eigenenergies $E_{1,2}$, and also some change of width. The transmission function looks again similar to the spectral function.

In all examples we considered so far, the resonant transmission functions have the Lorentzian (Breit-Wigner) form with the maxima corresponding to the eigenenergies of the central system and broadening being dependent by the coupling to the electrodes (the level-width functions). Situation can be very different if the interference effects are more important. Consider, for example, the T-junction case when the second state is not coupled to the electrodes: $\Gamma_{L2} = \Gamma_{R2} = 0$. We assume also that the first level is symmetrically coupled to the electrodes $\Gamma_{L1} = \Gamma_{R1}$ (Fig. 3.14).

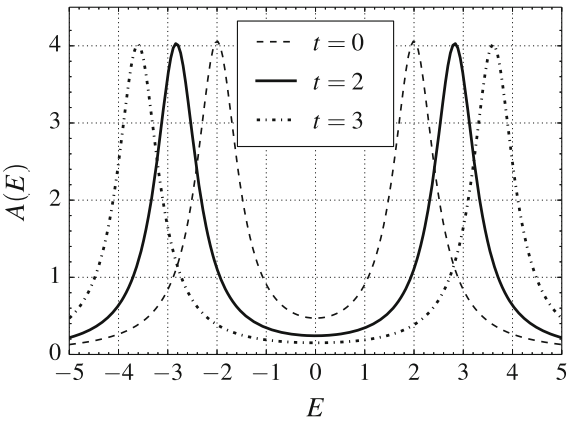

Fig. 3.13 The spectral function for the symmetric two-level model at $\Gamma_1 = 1$, $\varepsilon_1 = -2$, $\varepsilon_2 = 2$ and three values of $t = 0$ (*dashed line*), $t = 2$ (*solid line*), and $t = 3$ (*dotted line*)

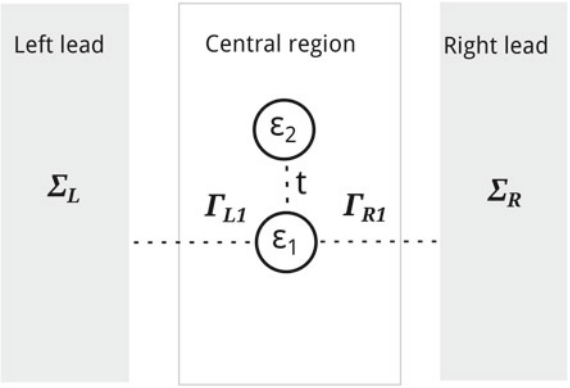

Fig. 3.14 The T-shape two-level junction

The spectral function is shown in Fig. 3.15. The second peak is much thinner because the second level is not directly coupled to the electrodes and broadening is possible only indirectly through the first level. Thus the level broadening is smaller for smaller t. The form of the peaks is still Lorentz-like.

More interesting is the transmission function shown in Fig. 3.16 at different inter-level couplings t. First of all, at $t = 0$ (dashed line) the transmission is nonzero only though the first level, the second level in this case is completely disconnected from the electrodes. Note that the spectral function takes the form $A(\varepsilon) \propto \delta(E - \varepsilon_2)$ near the energy of the second level. At finite t the transmission appears near the energy of the second level (actually near the energy E_2 of the second eigenstate), but the *shape* of the resonance is not Lorentzian! Moreover, the transmission is exactly zero at the energy of the second level ε_2 independently of other parameters!

Qualitatively, the transmission can be exactly zero at some energy in the case of *destructive interference*, when the amplitudes for transmission for two paths have the same absolute values, but opposite sign because of the phase shift equal to π. In our case the first path is the direct path through the first level, and the second path is

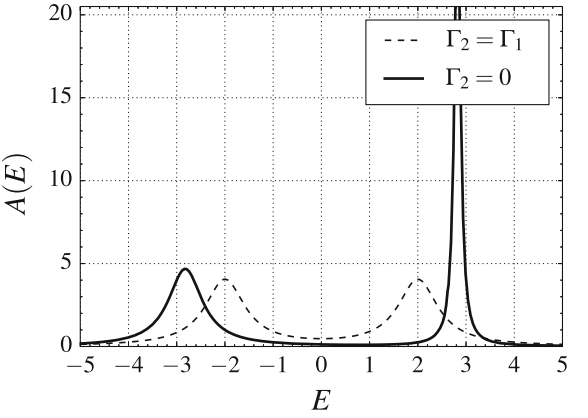

Fig. 3.15 The spectral function for the T-shape two-level junction at $t = 2$, $\varepsilon_1 = -2$, $\varepsilon_2 = 2$, $\Gamma_1 = 1$ (*solid line*). The case $\Gamma_1 = \Gamma_2 = 1$, $t = 0$ is shown by *dashed line*

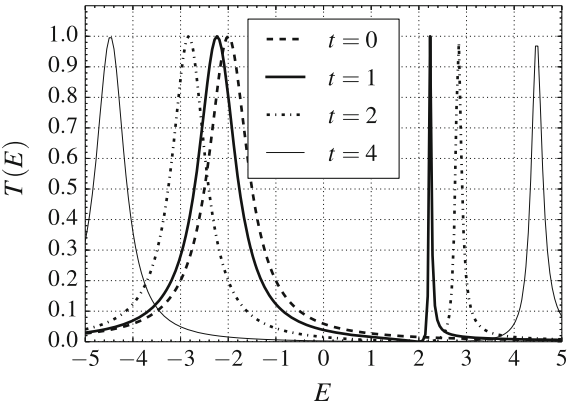

Fig. 3.16 Transmission for the T-shape two-level junction at $\Gamma_1 = 1$, $\varepsilon_1 = -2$, $\varepsilon_2 = 2$, $t = 0$ (*dashed line*), $t = 1$ (*solid line*), $t = 2$ (*dotted line*), $t = 4$ (*thin solid line*)

the path from the left electrode to the first level, then to the second level, back to the first and finally to the right electrode. This situation is also called *antiresonance*.

Consider the analytic expression for the transmission function (which is quite easy to calculate in this case)

$$T(E) = \frac{\Gamma_1}{\left[E - \varepsilon_1 - \dfrac{t^2}{E - \varepsilon_2}\right]^2 + \Gamma_1^2}. \tag{3.217}$$

At $t = 0$ the Breit-Wigner resonance is reproduced. At small t the antiresonance is strongly pronounced because the second resonant maximum is only slightly shifted from the antiresonant point $E = \varepsilon_2$. At larger t the second maximum is shifted to larger energies, the shape of this peak is more and more Lorentzian and the antiresonant feature is disappearing.

References

1. M. Di Ventra, *Electrical Transport in Nanoscale Systems* (Cambridge University Press, Cambridge, 2008)
2. D.S. Fisher, P.A. Lee, Phys. Rev. B **23**, 6851 (1981)
3. D.K. Ferry, S.M. Goodnick, *Transport in Nanostructures* (Cambridge University Press, Cambridge, 1997)
4. M. Paulsson, cond-mat/0210519 (2002)
5. M.P. Lopez Sancho, J.M. Lopez Sancho, J. Rubio, J. Phys. F: Met. Phys. **15**, 851 (1985)

Chapter 4
Tunneling

The Landauer-Büttiker scattering method, considered in the previous chapters, can be easily applied only in the case of noninteracting electrons and without inelastic scattering. Besides, it requires full quantum mechanical solution of the scattering problem and can be cumbersome for real geometries. The Green function formalism is a better starting point for generalization of the scattering approach, but its application is limited by available approximations for interacting systems. In the case of *weak coupling to the electrodes*, the other approach, known as the method of Tunneling (or Transfer) Hamiltonian, plays an important role, and is widely used in solid-state theory to describe tunneling effects in superconductors, ferromagnets, semiconductor quantum dots, and other nanostructures. The important advantage of this method is that it is combined easily with powerful methods of many-body theory for interacting systems. On the other hand, it is very convenient even for noninteracting electrons, when the coupling between subsystems is weak, and tunneling processes can be described by rather simple matrix elements.

In Sect. 4.1 we start from quantum mechanical description of tunneling through a planar barrier and consider different limiting cases. Then we introduce the Tunneling Hamiltonian method and apply it to calculation of the tunneling current. The important example of tunneling current calculation is the Tersoff-Hamann theory for scanning tunneling microscopy, considered in this section. In the following Sect. 4.2 we consider sequential tunneling in multi-barrier structures, first we consider the noninteracting transport, then we formulate the master equation approach for sequential tunneling through interacting systems. This formalism is used in Chaps. 5 and 6 to describe Coulomb blockade phenomena and electron-vibron (polaron) effects.

D.A. Ryndyk, *Theory of Quantum Transport at Nanoscale*,
Springer Series in Solid-State Sciences 184,
DOI 10.1007/978-3-319-24088-6_4

4.1 Tunneling (Transfer) Hamiltonian Method

4.1.1 Planar Barrier

The starting point to consider tunneling phenomena is coherent transmission through a single barrier (coherent here means that there are no inelastic processes inside the barrier, but they can be present in the electrodes and between the barriers in multi-barrier systems). This problem is formally equivalent to the scattering problem in Chap. 2, but now we will focus on the case of weakly transmitted barriers and corresponding approximations.

Previously we considered only (quasi-) 1D motion, here we first extend the analysis to planar barriers in three-dimensional case. In 3D the scattering can be still one-dimensional for ideal barriers, but in general it is more complicated. The two limiting cases are: (i) momentum-conserving tunneling through an ideal barrier with the potential dependent only on z coordinate and independent from the parallel wave number $\boldsymbol{k}_{\parallel}$ (Fig. 4.1) and (ii) diffusive tunneling through strongly inhomogeneous barrier, when the incident plane wave is transmitted as (and reflected into) many waves with different $\boldsymbol{k}_{\parallel}$ (Fig. 4.2). In the framework of the Landauer-Büttiker approach the change of $\boldsymbol{k}_{\parallel}$ is equivalent to multi-channel scattering.

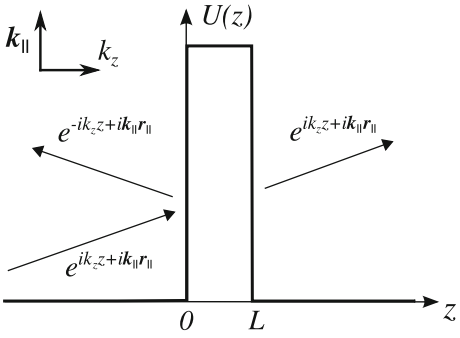

Fig. 4.1 Momentum-conserving tunneling through a planar barrier

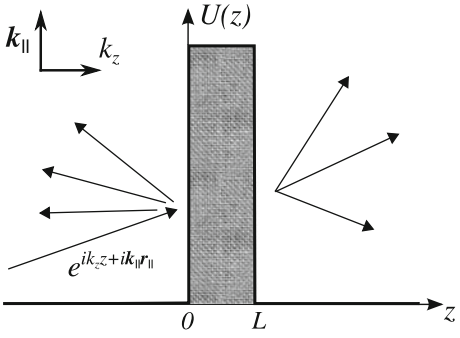

Fig. 4.2 Diffusive tunneling through a planar barrier

Momentum-conserving tunneling can be observed in clean semiconductor heterostructures, the diffusive tunneling is typical for tunnel junctions between metal electrodes with an amorphous oxide insulator as a barrier.

Momentum-Conserving Tunneling

As we already discussed in Sect. 2.1, in (ideal) layered systems the wave function at the energy E is represented as ($\boldsymbol{k}_\parallel \equiv (k_x, k_y)$)

$$\Psi_E(\boldsymbol{r}) = \sum_{\boldsymbol{k}_\parallel} e^{i(k_x x + k_y y)} \psi_{\boldsymbol{k}_\parallel E}(z). \tag{4.1}$$

The initial 3D problem is reduced in this case to a 1D problem for the function $\psi_{\boldsymbol{k}_\parallel E}(z)$.

Consider first the rectangular barrier, for which the exact expression can be obtained. We follow the notations of Sect. 2.1.3. The potential can be written as:

$$U(z) = \begin{cases} 0, & z < -L/2, \\ U_0, & -L/2 < z < L/2, \\ 0, & z > L/2. \end{cases} \tag{4.2}$$

The wave function is given by

$$\psi(z) = \begin{cases} A_+ e^{ikz} + A_- e^{-ikz}, & z < -L/2 \\ C_1 e^{-\kappa z} + C_2 e^{\kappa z}, & -L/2 < z < L/2 \\ B_- e^{ikz} + B_+ e^{-ikz}, & z > L/2 \end{cases} \tag{4.3}$$

where

$$k = \frac{\sqrt{2mE_z}}{\hbar}, \tag{4.4}$$

$$\kappa = \frac{\sqrt{2m(U_0 - E_z)}}{\hbar}. \tag{4.5}$$

The transmission function is given by

$$T(E_z < U_0) = \frac{4k^2\kappa^2}{(k^2 + \kappa^2)^2 \sinh^2(L\kappa) + 4k^2\kappa^2}, \tag{4.6}$$

$$T(E_z > U_0) = \frac{4k^2k'^2}{(k^2 - k'^2)^2 \sin^2(Lk') + 4k^2k'^2}. \tag{4.7}$$

$k' = i\kappa$

Consider the energy dependence of the transmission coefficient $T(E_z)$ being presented in Fig. 4.3. One can see that at low energies the transmission becomes very small, it is actually the tunneling limit. At small energies $E_z \ll U_0$ (and

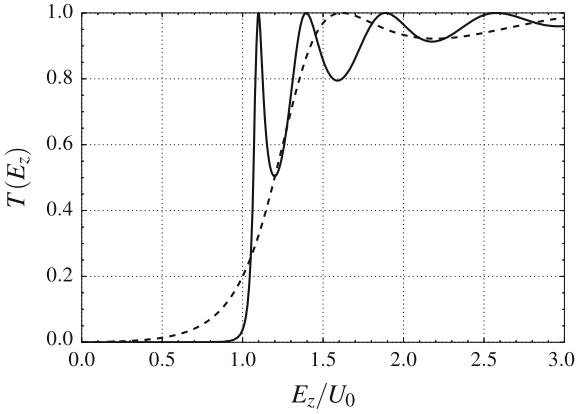

Fig. 4.3 Transmission coefficient as a function of energy for symmetric rectangular barrier, *dashed line* is for smaller thickness

$\frac{2\sqrt{2mU_0}}{\hbar}L \gg 1$) one gets explicitly

$$T(E_z) = \frac{16E_z}{U_0}\exp\left(-\frac{2\sqrt{2mU_0}}{\hbar}L\right). \tag{4.8}$$

This expression demonstrates two general features of tunneling: the exponential dependence on barrier amplitude and thickness, and linear energy dependence. The linear energy dependence can be proven to be true for all localized in space one-dimensional barriers, e.g. the barriers having sharp enough edges.

The other known approximation for tunneling probability is the Wentzel-Kramers-Brillouin approximation. It gives

$$T(E_z) = \exp\left(-\int_0^L \frac{2\sqrt{2mU(z)}}{\hbar}dz\right) \tag{4.9}$$

in the limit of very smooth potential, when the quasi-classical approximation is valid in all space except of the reflection point. In the WKB approximation the tunneling transmission coefficient is constant at low energies, opposite to (4.8). For real barriers the energy dependence is somewhere between those limiting cases. Note however, that for very thin potential barriers the tunneling approximation does not exist, see the transmission coefficient for the $\delta-$potential (2.35).

Diffusive tunneling can not be described by a 1D transmission coefficient, we will consider it later in the next section.

4.1.2 Tunneling Hamiltonian

The main idea of the method (known also as Transfer Hamiltonian) is to represent the Hamiltonian of the system (we consider first a single contact between two electrodes)

as a sum of three parts: "left" $\hat{H}_L$, "right" $\hat{H}_R$, and "tunneling" $\hat{H}_T$

$$\hat{H} = \hat{H}_L + \hat{H}_R + \hat{H}_T, \tag{4.10}$$

$\hat{H}_L$ and $\hat{H}_R$ determine "left" $|Lk\rangle$ and "right" $|Rq\rangle$ states

$$\hat{H}_L \psi_k(\xi) = E_k \psi_k(\xi), \tag{4.11}$$
$$\hat{H}_R \psi_q(\xi) = E_q \psi_q(\xi), \tag{4.12}$$

below in this section we use the index k for left states and the index q for right states. $\hat{H}_T$ determines "transfer" between these states and is *defined* through matrix elements $V_{kq} = \langle Lk|\hat{H}_T|Rq\rangle$. With these definitions the single-particle tunneling Hamiltonian is

$$\hat{H} = \sum_{k\in L} E_k |k\rangle\langle k| + \sum_{q\in R} E_q |q\rangle\langle q| + \sum_{kq} \left[V_{qk}|q\rangle\langle k| + V^*_{qk}|k\rangle\langle q|\right]. \tag{4.13}$$

The idea to use the Tunneling Hamiltonian was introduced by Bardeen [1], developed by Harrison [2], and formulated in most familiar second quantized form by Cohen, Falicov, and Phillips [3]. In spite of many very successful applications of this method, it was many times criticized for its phenomenological character and incompleteness, beginning from the work of Prange [4]. However, in the same work Prange showed that the Tunneling Hamiltonian is well defined in the sense of the perturbation theory. These developments and discussions were summarized by Duke [5]. Note, that the formulation equivalent to the method of the Tunneling Hamiltonian can be derived exactly from the tight-binding approach (see below in this section).

"Separability and Non-orthogonality" Discussion

Now we want to consider the following question: is it possible to find left $\psi_k(\xi)$ and right $\psi_q(\xi)$ states in such a way, that they form one system of orthonormal states $|kq\rangle = |k\rangle \otimes |q\rangle$, which are eigenstates of the Hamiltonian $\hat{H}_L + \hat{H}_R$? Note that in any case we want to keep the complete description of any left state with only the left basis functions $\psi_k(\xi)$, without "right" contribution. And the same for any right state.

If we find such a system of states $|kq\rangle$, then the Hamiltonian (4.13) is a complete and consistent model. Unfortunately, in general it is impossible. To understand the problem, let us consider a double-well potential (Fig. 4.4), for which a system of *orthogonal* states can be easy built. Using the exact even $\psi_e(z)$ and odd $\psi_o(z)$ eigenstates (for simplicity we consider only two states with lowest energies), we can define orthogonal left and right states as

$$\psi_{r,l}(z) = \frac{\psi_e(z) \pm \psi_o(z)}{\sqrt{2}}. \tag{4.14}$$

It is problematic, however, to consider these states as the left and right states in the method of tunneling Hamiltonian, because left (right) state $\psi_l(z)$ ($\psi_r(z)$) does

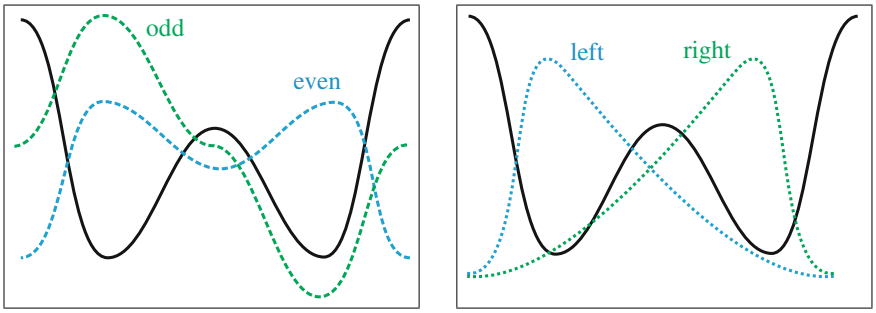

Fig. 4.4 *Even-odd* and *left-right* basis in a double-well potential

not define completely the state in the left (right) part of the system, there is some contribution of the right (left) state. This is quite a general problem for geometrical barriers dividing a system into two parts: left states should propagate through the barrier into the "wrong" right part of the system.

The other objection against the orthogonal basis is that in this case it is difficult to find the limit of usual perturbative quantum tunneling. Indeed, in the standard theory of quantum tunneling the probability of tunneling $P_{k\to q} = \Gamma^{\rightarrow}_{qk} t$ is *proportional to time*, and $\Gamma^{\rightarrow}_{qk}$ is the transition rate form the left (k) to the right (q). So that the current can be defined as the tunneling rate multiplied by charge. Moreover, the single particle transition rate is determined by Fermi's golden rule

$$\Gamma^{\rightarrow}_{qk} = \frac{2\pi}{\hbar}|V_{qk}|^2\delta(E_k - E_q). \tag{4.15}$$

Consider the exact solution for "tunneling" between left and right states in a two-level model.

In the basis of the orthogonal $\psi_{r,l}(z)$ states introduced above. We take these states as a two-level basis

$$|l\rangle \equiv \begin{pmatrix} 0 \\ 1 \end{pmatrix}, \quad |r\rangle \equiv \begin{pmatrix} 1 \\ 0 \end{pmatrix}, \tag{4.16}$$

E_L and E_R are left and right energies, we assume that the potential is symmetric ($E_R = E_L = E$).

These states are eigenstates of the diagonal Hamiltonian

$$\hat{H}_0 = \begin{pmatrix} E & 0 \\ 0 & E \end{pmatrix}. \tag{4.17}$$

It is important that $|l\rangle$ and $|r\rangle$ are two eigenstates of the same Hamiltonian, thus it is the case of the orthonormal combined left-right basis.

Now if we take into account *tunneling between these states* with characteristic matrix element V, the Hamiltonian and eigenstates take the form

$$\hat{H} = \begin{pmatrix} E & V \\ V & E \end{pmatrix}: \quad \tilde{\psi}_e = \frac{1}{\sqrt{2}} \begin{pmatrix} 1 \\ 1 \end{pmatrix}, \quad \tilde{\psi}_o = \frac{1}{\sqrt{2}} \begin{pmatrix} 1 \\ -1 \end{pmatrix}, \tag{4.18}$$

$\tilde{\psi}_e$ and $\tilde{\psi}_o$ are the even and odd eigenstates described below with energies

$$\tilde{E}_{e,o} = E \mp V. \tag{4.19}$$

Now the time-dependent solution in the basis of the left-right states is

$$\Psi(t) = \begin{pmatrix} c_r \\ c_l \end{pmatrix} = \frac{c_e}{\sqrt{2}} e^{-i\tilde{E}_e t} \begin{pmatrix} 1 \\ 1 \end{pmatrix} + \frac{c_o}{\sqrt{2}} e^{-i\tilde{E}_o t} \begin{pmatrix} 1 \\ -1 \end{pmatrix}, \tag{4.20}$$

and the populations of left and right states oscillate in time.

Now let us consider at $t = 0$ the initial state of the system with a particle in the left state $\Psi(0) = \begin{pmatrix} 0 \\ 1 \end{pmatrix}$. Then we find the probability of tunneling

$$P_{l\to r} = |c_r|^2 = \frac{1}{2}\left(1 - \cos 2Vt\right), \tag{4.21}$$

at small times

$$P_{l\to r} = |c_r|^2 = V^2 t^2. \tag{4.22}$$

Tunneling in the sense of Fermi's golden rule can not be described by this exact solution! It seems that if we take at $t = 0$ such a orthogonal left state, in fact it gives significant contribution to the probability to find the particle at the right ("wrong") side of the barrier, already taken into account the probability, which should be given by the golden rule otherwise [4]. Of course, one can say that our result is the consequence of the normalization condition $|c_l|^2 + |c_r|^2 = 1$ which should be omitted if we want to consider stationary tunneling current using perturbation theory. But it means that the Hamiltonian (4.13) is not complete and some additional assumptions are needed.

For example, to calculate the stationary tunneling current between two metals with different electro-chemical potentials (constant voltage) we should assume, in the same way as in the scattering approach, that left and right states are permanently populated by reservoirs and the distribution functions of these states are not changed.

Finally we can make the following conclusions:

1. There is some difficulty in dividing the system into the left and right parts. If the exact wave functions of the whole system are used, then the corresponding exact left (right) states do not form separately the complete basis for the left (right) part. The states which form such a complete left basis can be nonorthogonal to the states which form a complete right basis.
2. Left and right orthogonal states do not describe tunneling in a proper way. At least if we consider the Hamiltonian (4.13) without additional assumptions. Basically we should assume that (4.13) is not a true Hamiltonian, but some formal combina-

tion of independent Hamiltonians describing left and right states with tunneling Hamiltonian, which describes *only transfer of electrons* in the way consistent with the perturbation theory. In the next section we follow this way of thinking.

3. The problem exists only in a general case of some potential barrier. The case when possible (effective) electronic states are restricted, as in the tight-binding model, is considered below, and in this case the Transfer Hamiltonian is well defined.

The Second Quantization Form

For applications, especially together with a many-body technique, it is convenient to represent the Tunneling Hamiltonian (4.13) in the second quantized form. We introduce creation and annihilation *Schrödinger* operators $c^{\dagger}_{Lk}$, c_{Lk}, $c^{\dagger}_{Rq}$, c_{Rq}. Using the usual rules we obtain

$$\hat{H} = \hat{H}_L\left(\left\{c_k^{\dagger}; c_k\right\}\right) + \hat{H}_R\left(\left\{c_q^{\dagger}; c_q\right\}\right) + \hat{H}_T\left(\left\{c_k^{\dagger}; c_k; c_q^{\dagger}; c_q\right\}\right), \tag{4.23}$$

$$\hat{H} = \sum_k (\varepsilon_k + e\varphi_L(t))c_k^{\dagger}c_k + \sum_q (\varepsilon_q + e\varphi_R(t))c_q^{\dagger}c_q + \sum_{kq}\left[V_{qk}c_q^{\dagger}c_k + V_{qk}^{*}c_k^{\dagger}c_q\right]. \tag{4.24}$$

It is assumed that left c_k and right c_q operators describe independent states and are anticommutative. For nonorthogonal states of the Hamiltonian $\hat{H}_L + \hat{H}_R$ it is not exactly the case. But if we consider $\hat{H}_L$ and $\hat{H}_R$ as two independent Hamiltonians with independent Hilbert spaces we resolve this problem. Thus we again should consider (4.24) not as a true Hamiltonian, but as the formal expression describing current between left and right states. In the weak coupling case the small corrections to the commutation relations are of the order of $|V_{qk}|$ and can be neglected. If the tight-binding formulation is possible, (4.24) is exact within the framework of this formulation. In general the method of tunneling Hamiltonian can be considered as a *phenomenological* microscopic approach, which was proved to give reasonable results in many cases, e.g. in description of tunneling between superconductors and Josephson effect.

Exact Formulation Based on the Tight-Binding Model

The problems with the orthogonality of the left-right states, considered in the previous section, exist only in continuous systems, when we try to introduce the orthogonal states for the tunneling through a potential barrier. Here we show, that if one starts from the tight-binding formulation, then the tunneling Hamiltonian is simply reformulation of a TB Hamiltonian without any approximation.

Indeed, the tight-binding model assumes that the left and right states can be clear separated, also when they are orthogonal. The difference with the continuous case is, that we restrict the Hilbert space introducing the tight-binding model, so that the solution is not exact in the sense of the continuous Schrödinger equation. But, in fact, we only consider physically relevant states, neglecting high-energy states not participating in transport.

Compare the tunneling Hamiltonian (4.13) and the tight-binding Hamiltonian (3.90), divided into left and right parts

$$\hat{H} = \sum_{\alpha\beta\in L} \tilde{\varepsilon}_{\alpha\beta}|\alpha\rangle\langle\beta| + \sum_{\delta\gamma\in R} \tilde{\varepsilon}_{\delta\gamma}|\delta\rangle\langle\gamma| + \sum_{\alpha\in L,\,\delta\in R} \left[V_{\delta\alpha}|\delta\rangle\langle\alpha| + V^*_{\delta\alpha}|\alpha\rangle\langle\delta|\right]. \quad (4.25)$$

The first two terms are the Hamiltonians of the left and right parts, the third term describes the left-right (tunneling) coupling. The equivalent matrix representation of this Hamiltonian is

$$\boldsymbol{H} = \begin{pmatrix} \boldsymbol{H}^0_L & \boldsymbol{H}_{LR} \\ \boldsymbol{H}^\dagger_{LR} & \boldsymbol{H}^0_R \end{pmatrix}. \quad (4.26)$$

The Hamiltonians (4.13) and (4.25) are essentially the same, only the first one is written in the eigenstate basis $|k\rangle$, $|q\rangle$, while the second in the tight-binding basis $|\alpha\rangle$, $|\beta\rangle$ of the left lead and $|\delta\rangle$, $|\gamma\rangle$ of the right lead. Now we want to transform the TB Hamiltonian (4.25) into the eigenstate representation.

Canonical transformation from the tight-binding (atomic orbitals) representation to the eigenstate (molecular orbitals) representation plays an important role, and we consider it in detail. Assume, that we find two unitary matrices $\mathbf{S}_L$ and $\mathbf{S}_R$, such that the Hamiltonians of the left part $\boldsymbol{H}^0_L$ and of the right part $\boldsymbol{H}^0_R$ can be diagonalized by the canonical transformations

$$\bar{\boldsymbol{H}}^0_L = \mathbf{S}^{-1}_L \boldsymbol{H}^0_L \mathbf{S}_L, \quad (4.27)$$

$$\bar{\boldsymbol{H}}^0_R = \mathbf{S}^{-1}_R \boldsymbol{H}^0_R \mathbf{S}_R. \quad (4.28)$$

The left and right eigenstates can be written as

$$|k\rangle = \sum_\alpha S_{Lk\alpha}|\alpha\rangle, \quad (4.29)$$

$$|q\rangle = \sum_\delta S_{Rq\delta}|\delta\rangle, \quad (4.30)$$

and the first two free-particle terms of the Hamiltonian (4.13) are reproduced. The tunneling terms can be transformed as

$$\bar{\boldsymbol{H}}_{LR} = \mathbf{S}^{-1}_L \boldsymbol{H}_{LR} \mathbf{S}_R, \quad (4.31)$$

$$\bar{\boldsymbol{H}}^\dagger_{LR} = \mathbf{S}^{-1}_R \boldsymbol{H}^\dagger_{LR} \mathbf{S}_L, \quad (4.32)$$

or explicitly

$$\sum_{\alpha\in L,\,\delta\in R} V_{\delta\alpha}|\delta\rangle\langle\alpha| = \sum_{kq} V_{qk}|q\rangle\langle k|, \quad (4.33)$$

where

$$V_{qk} = \sum_{\alpha \in L,\, \delta \in R} V_{\delta\alpha} S_{L\alpha k} S_{R\delta q}. \tag{4.34}$$

The last expressions solve the problem of transformation of the tight-binding matrix elements into tunneling matrix elements.

4.1.3 Bardeen's Matrix Elements

From the previous consideration it is clear that the left $\psi_k(\xi)$ states can be considered as nonorthogonal to the right $\psi_q(\xi)$ states. In this case we can choose left and right states which form two *independent* complete systems, this is the main idea of the method of tunneling Hamiltonian. In this section we show that both of the above mentioned problems can be overcome if we apply consistently the perturbation theory to calculate matrix elements V_{qk} and tunneling current.

Consider here the one-dimensional problem described by the Hamiltonian ($\hbar = 1$)

$$\hat{H} = -\frac{1}{2m}\frac{d^2}{dz^2} + U(z), \tag{4.35}$$

with potential barrier (Fig. 4.5)

$$U(z) = \begin{cases} 0, & z < -a, \\ U_0, & -a < z < a, \\ 0, & z > a. \end{cases} \tag{4.36}$$

The left and right states are defined as the eigenstates in the two different step-function potentials

$$U_{left}(z) = \begin{cases} 0, & z < -a, \\ U_0, & z > -a, \end{cases} \tag{4.37}$$

$$U_{right}(z) = \begin{cases} U_0, & z < a, \\ 0, & z > a. \end{cases} \tag{4.38}$$

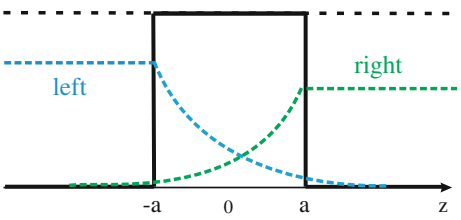

Fig. 4.5 Schematic picture of the nonorthogonal *left* and *right* states

These eigenstates are obviously not orthogonal. We restrict consideration to the case when energies of all contributing states are well below the maximum of the barrier. Hamiltonian (4.35) coincides with the left Hamiltonian at $z < a$, and with the right Hamiltonian at $z > -a$, so that

$$\hat{H}\psi_k(z) = E_k\psi_k(z), \quad z < a, \tag{4.39}$$

$$\hat{H}\psi_q(z) = E_q\psi_q(z), \quad z > -a, \tag{4.40}$$

k and q are the wave numbers outside barriers.

Now consider tunneling of the left state k into right states q using time-dependent perturbation theory. We find the solution of the time dependent Schrödinger equation

$$i\frac{\partial\Psi(t)}{\partial t} = \hat{H}\Psi(t), \tag{4.41}$$

with the Hamiltonian (4.35), and wave function

$$\Psi(t) = \psi_k e^{-iE_k t} + \sum_q a_q(t)\psi_q e^{-iE_q t}, \tag{4.42}$$

we assume that

$$a_q(0) = 0, \quad |a_q(t)| \ll 1.$$

Further calculation is the standard time-dependent perturbation theory. The answer is

$$\frac{da_q(t)}{dt} = -i\int_{-\infty}^{\infty}\psi_q^*(z)(\hat{H} - E_k)\psi_k dz e^{-i(E_k - E_q)t}, \tag{4.43}$$

at $t \to \infty$ (it is assumed, however, that t is not too large and $|a_q(t)| \ll 1$)

$$|a(t)|^2 = \frac{2\pi}{\hbar}|V_{qk}|^2\delta(E_k - E_q)t, \tag{4.44}$$

$$V_{qk} = \int_{-\infty}^{\infty}\psi_q^*(z)(\hat{H} - E_k)\psi_k(z)dz. \tag{4.45}$$

The last expression determines the tunneling matrix element, now we want to transform it into more convenient form. From (4.39) it follows that integrand $\psi_q^*(z)(\hat{H} - E_k)\psi_k(z)$ is identically zero at $z < a$, so we first change the down limit of integration to z_1 placed inside the barrier between $-a$ and a

$$V_{qk} = \int_{z_1}^{\infty}\psi_q^*(z)(\hat{H} - E_k)\psi_k(z)dz. \tag{4.46}$$

Then we add to the integrand the expression $\psi_k(z)(\hat{H} - E_q)\psi_q^*(z)$ which is identically zero at $z > z_1 > -a$ because of (4.40)

$$V_{qk} = \int_{z_1}^{\infty} \left[\psi_q^*(z)(\hat{H} - E_k)\psi_k(z) - \psi_k(z)(\hat{H} - E_q)\psi_q^*(z)\right] dz. \tag{4.47}$$

Now, taken into account that V_{qk} is nonzero only for $E_k = E_q$, we can exclude energies, as well as potentials $U(z)$ from this expression, and obtain

$$V_{qk} = \int_{z_1}^{\infty} \left[\psi_q^*(z)\left(-\frac{1}{2m}\frac{d^2}{dz^2}\right)\psi_k(z) - \psi_k(z)\left(-\frac{1}{2m}\frac{d^2}{dz^2}\right)\psi_q^*(z)\right] dz, \tag{4.48}$$

and after integration we obtain finally (here $\hbar$ is restored)

$$V_{qk} = -i\hbar J_{qk}, \tag{4.49}$$

$$J_{qk} = -\frac{i\hbar}{2m}\left[\psi_q^*(z)\frac{d}{dz}\psi_k(z) - \psi_k(z)\frac{d}{dz}\psi_q^*(z)\right]_{-a<z<a}, \tag{4.50}$$

or

$$V_{qk} = \frac{\hbar^2}{2m}\left[\psi_k(z)\frac{d}{dz}\psi_q^*(z) - \psi_q^*(z)\frac{d}{dz}\psi_k(z)\right]_{-a<z<a}. \tag{4.51}$$

This expression determines explicitly the matrix element as the overlap of left and right wave functions. Due to the properties of the one-dimensional Schrödinger equation any point z inside the barrier can be taken if $E_k = E_q$ (the condition actually determines the relation between k and q in (4.44), it is a consequence of the current conservation in the barrier.

4.1.4 Current Through a Planar Junction

Since the probability of tunneling is given by the usual expression (4.44), the current from the state k into the state q is given by the golden rule

$$I_{k\to q} = e\Gamma_{qk} = \frac{2\pi e}{\hbar}|V_{qk}|^2 f_L(k)\,(1 - f_R(q))\,\delta(E_k - E_q), \tag{4.52}$$

the probability $(1 - f_R(E_q))$ that the right state is unoccupied should be included, it is different from the scattering approach because left and right states are two independent states!

Then we write the total current as the sum of all partial currents from left states to right states and vice versa (note that the terms $f_L(k)f_R(q)$ are cancelled)

$$I = \frac{2\pi e}{\hbar} \sum_{kq} |V_{qk}|^2 \left[f_L(k) - f_R(q) \right] \delta(E_q - E_k). \tag{4.53}$$

For tunneling between two equilibrium leads the distribution functions are simply Fermi-Dirac functions

$$f(k) = f^0(E_k) = \frac{1}{\exp\left(\dfrac{E_k - \tilde{\mu}}{T} \right) + 1}, \tag{4.54}$$

and current can be finally written in the well known form[1]

$$I = \frac{e}{h} \int_{-\infty}^{\infty} T(E, V) \left[f_L(E - eV) - f_R(E) \right] dE, \tag{4.55}$$

with

$$T(E, V) = (2\pi)^2 \sum_{qk} |V_{kq}|^2 \delta(E - E_k - eV) \delta(E - E_q). \tag{4.56}$$

This expression is equivalent to the Landauer formula (2.140), but the transmission function is related now to the tunneling matrix element.

The Second Quantization Form

Now let us calculate the tunneling current as the time derivative of the number of particles operator in the left lead $\hat{N}_L = \sum_k c_k^\dagger c_k$. Current from the left to right contact is

$$I(t) = -e \left\langle \left(\frac{dN_L}{dt} \right) \right\rangle_S = -\frac{ie}{\hbar} \left\langle \left[\hat{H}_T, N_L \right]_- \right\rangle_S, \tag{4.57}$$

where $\langle ... \rangle_S$ is the average over time-dependent Schrödinger state. $\hat{N}_L$ commute with both left and right Hamiltonians, but not with the tunneling Hamiltonian

$$\left[\hat{H}_T, N_L \right]_- = \sum_{k'} \sum_{kq} \left[\left(V_{qk} c_q^\dagger c_k + V_{qk}^* c_q c_k^\dagger \right) c_{k'}^\dagger c_{k'} \right]_-, \tag{4.58}$$

using commutation relations

$$c_k c_{k'}^\dagger c_{k'} - c_{k'}^\dagger c_{k'} c_k = c_k c_{k'}^\dagger c_{k'} + c_{k'}^\dagger c_k c_{k'} = (c_k c_{k'}^\dagger + \delta_{kk'} - c_k c_{k'}^\dagger) c_{k'} = \delta_{kk'} c_k,$$

we obtain

$$I(t) = \frac{ie}{\hbar} \sum_{kq} \left[V_{qk} \left\langle c_q^\dagger c_k \right\rangle_S - V_{qk}^* \left\langle c_k^\dagger c_q \right\rangle_S \right]. \tag{4.59}$$

[1] To do this one should multiply the integrand on $1 = \int \delta(E - E_q) dE$.

Now we switch to the Heisenberg picture, and average over initial time-independent *equilibrium* state

$$\left\langle \hat{O}(t) \right\rangle = Sp\left(\hat{\rho}_{eq}\hat{O}(t)\right), \quad \hat{\rho}_{eq} = \frac{e^{-H_{eq}/T}}{Sp\left(e^{-H_{eq}/T}\right)}. \tag{4.60}$$

One obtains

$$I(t) = \frac{ie}{\hbar}\sum_{kq}\left[V_{qk}\left\langle c_q^\dagger(t)c_k(t)\right\rangle - V_{qk}^*\left\langle c_k^\dagger(t)c_q(t)\right\rangle\right]. \tag{4.61}$$

It can be finally written as

$$I(t) = \frac{2e}{\hbar}\mathrm{Im}\left(\sum_{kq}V_{qk}\rho_{kq}(t)\right) = \frac{2e}{\hbar}\mathrm{Re}\left(\sum_{kq}V_{qk}G_{kq}^<(t,t)\right).$$

We define "left-right" density matrix or more generally the lesser Green function

$$G_{kq}^<(t_1,t_2) = i\left\langle c_q^\dagger(t_2)c_k(t_1)\right\rangle.$$

Later we show that these expressions for the tunneling current give the same answer as was obtained above by the golden rule in the case of noninteracting leads.

Momentum-Conserving Tunneling

When the parallel momentum is not changed, we can represent the square of the tunneling matrix element as

$$|V_{kk'}|^2 = t_c(k_z,k_z',\boldsymbol{k}_\parallel)\delta(\boldsymbol{k}_\parallel - \boldsymbol{k}_\parallel'). \tag{4.62}$$

Function $t_c(k_z,k_z',\boldsymbol{k}_\parallel)$ is determined by the shape of the barrier. One can consider only positive values of k_z and k_z' because states $k_z > 0$ (incident wave) and $k_z < 0$ (reflected wave) with the same energy form together an initial state for tunneling.

Then one has for the current

$$I = \frac{2\pi e}{\hbar}\int\frac{d^3k}{(2\pi)^3}\int\frac{d^3k'}{(2\pi)^3}t_c(k_z,k_z',\boldsymbol{k}_\parallel)\delta(\boldsymbol{k}_\parallel - \boldsymbol{k}_\parallel')\left[f(k) - f(k')\right]\delta(\varepsilon_{k'} - \varepsilon_k - eV)$$

$$= \frac{e}{2\pi\hbar}\int\frac{d^2k_\parallel}{(2\pi)^2}\int\frac{dk_z}{2\pi}\int\frac{dk_z'}{2\pi}t_c(k_z,k_z',\boldsymbol{k}_\parallel)\left[f(k_z,\boldsymbol{k}_\parallel) - f(k_z',\boldsymbol{k}_\parallel)\right]\delta(\varepsilon_k - \varepsilon_k - eV). \tag{4.63}$$

Assuming simple free particle dispersion of quasiparticles

$$\varepsilon \equiv \varepsilon_k = \frac{\hbar^2 k^2}{2m} = \frac{\hbar^2 k_\parallel^2}{2m} + \frac{\hbar^2 k_z^2}{2m} = \xi + \frac{\hbar^2 k_z^2}{2m}, \tag{4.64}$$

and taking here that $\xi = \dfrac{\hbar^2 k_\parallel^2}{2m} = const$ (integration over $\boldsymbol{k}_\parallel$ we perform in the end of the calculation), we obtain the following expressions

$$d\varepsilon = \frac{\hbar^2}{m} k_z dk_z, \;\; k_z = \sqrt{\frac{2m}{\hbar^2}}\sqrt{\varepsilon - \xi}, \;\; \Rightarrow \;\; dk_z = \frac{\sqrt{m}}{\hbar\sqrt{2}} \frac{d\varepsilon}{\sqrt{\varepsilon - \xi}}, \tag{4.65}$$

and for the current

$$\begin{aligned} I &= \frac{em}{2(2\pi)^3\hbar^3} \int \frac{d^2 k_\parallel}{(2\pi)^2} \int_\xi^\infty d\varepsilon \int_\xi^\infty d\varepsilon' t_c(k_z, k_z', \boldsymbol{k}_\parallel) \frac{\left[f(\varepsilon) - f(\varepsilon')\right] \delta(\varepsilon' - \varepsilon - eV)}{\sqrt{\varepsilon - \xi}\sqrt{\varepsilon' - \xi'}} \\ &= \frac{em}{2(2\pi)^3\hbar^3} \int \frac{d^2 k_\parallel}{(2\pi)^2} \int_{-\infty}^\infty d\varepsilon \left[f(\varepsilon) - f(\varepsilon + eV)\right] \frac{t_c(k_z, k_z')\theta\left(\varepsilon - \xi\right)\theta\left(\varepsilon + eV - \xi\right)}{\sqrt{\varepsilon - \xi}\sqrt{\varepsilon + eV - \xi}}. \end{aligned} \tag{4.66}$$

This expression can be written in well known Landauer-like form

$$I = \frac{e}{h} \int_{-\infty}^\infty d\varepsilon \left[f(\varepsilon) - f(\varepsilon + eV)\right] \int \frac{d^2 k_\parallel}{(2\pi)^2} T(\varepsilon, \boldsymbol{k}_\parallel), \tag{4.67}$$

with

$$T(\varepsilon, \boldsymbol{k}_\parallel) = \frac{m}{2(2\pi)^2\hbar^2} \frac{t_c(k_z, k_z', \boldsymbol{k}_\parallel)\theta\left(\varepsilon - \xi\right)\theta\left(\varepsilon + eV - \xi\right)}{\sqrt{\varepsilon - \xi}\sqrt{\varepsilon + eV - \xi}}, \tag{4.68}$$

and finally

$$I = \frac{e}{h} \int_{-\infty}^\infty T(\varepsilon) \left[f(\varepsilon) - f(\varepsilon + eV)\right] d\varepsilon, \tag{4.69}$$

with

$$T(\varepsilon) = \int \frac{d^2 k_\parallel}{(2\pi)^2} T(\varepsilon, \boldsymbol{k}_\parallel) = \frac{m^2}{2(2\pi)^3\hbar^4} \int_0^\infty d\xi \frac{t_c(k_z, k_z', \boldsymbol{k}_\parallel)\theta\left(\varepsilon - \xi\right)\theta\left(\varepsilon + eV - \xi\right)}{\sqrt{\varepsilon - \xi}\sqrt{\varepsilon + eV - \xi}}. \tag{4.70}$$

Now let us consider two model approximations:

$$t_c(k_z, k_z', \boldsymbol{k}_\parallel) = t_{c1} k_z k_z', \tag{4.71}$$

which corresponds to a smooth (quasiclassical) barrier, and

$$t_c(k_z, k_z', \boldsymbol{k}_\parallel) = t_{c2}(k_z k_z')^2, \tag{4.72}$$

which corresponds to a rectangular barrier. We take into account only low-k_z behaviour of the matrix element, which is the most essential because of $1/k_z \propto 1/\sqrt{\varepsilon - \xi}$ factors in the transmission coefficient. In these models one obtains.

In the model C1 ($t_c \propto k_z k_z'$):

$$\begin{aligned} T^{C1}(\varepsilon) &= \frac{m^3 t_{c1}}{(2\pi)^3 \hbar^6} \int_0^\infty d\xi \theta\left(\varepsilon - \xi\right) \theta\left(\varepsilon + eV - \xi\right) \\ &= \frac{m^3 t_{c1}}{(2\pi)^3 \hbar^6} \max\left[0, \min\left(\varepsilon, \varepsilon + eV\right)\right]. \end{aligned} \tag{4.73}$$

In the model C2 ($t_c \propto (k_z k_z')^2$):

$$\begin{aligned} T^{C2}(\varepsilon) &= \frac{2m^4 t_{c2}}{(2\pi)^3 \hbar^8} \int_0^{\xi_m} \sqrt{\varepsilon - \xi}\sqrt{\varepsilon + eV - \xi}\, d\xi, \\ \xi_m &= \max\left[0, \min\left(\varepsilon, \varepsilon + eV\right)\right]. \end{aligned} \tag{4.74}$$

Before discussing these results we calculate the current for diffusive tunneling.

Diffusive Tunneling

For diffusive tunneling the matrix element is independent on momentum (note that the energy conservation is guaranteed by the δ-function in the expression for the current)

$$|V_{kk}|^2 = t_d. \tag{4.75}$$

For the current one obtains

$$I = \frac{2\pi e}{\hbar} \int \frac{d^3k}{(2\pi)^3} \int \frac{d^3k'}{(2\pi)^3} t_d \left[f(k) - f(k')\right] \delta(\varepsilon_{k'} - \varepsilon_k - eV). \tag{4.76}$$

In this expression the matrix element is constant and the distribution functions of electrodes are assumed to be functions of energy $\varepsilon \equiv \varepsilon_k$, so that one can introduce the density of states $\rho(\varepsilon)$ through the expression

$$\int \frac{d^3k}{(2\pi)^3} = \frac{1}{2} \int \rho(\varepsilon) d\varepsilon, \tag{4.77}$$

the $1/2$ appears here because the integration is going only over positive values of k_z and k_z'.

Assuming again free particle dispersion (4.64), one gets the following relations

$$d\varepsilon = \frac{\hbar^2}{m} k dk, \quad k = \sqrt{\frac{2m}{\hbar^2}}\sqrt{\varepsilon} \quad \Rightarrow \quad dk = \frac{\sqrt{m}}{\hbar\sqrt{2}} \frac{d\varepsilon}{\sqrt{\varepsilon}}, \tag{4.78}$$

$$d^3k \to 4\pi k^2 dk \;\Rightarrow\; \int \frac{d^3k}{(2\pi)^3} = \frac{1}{2}\int \rho(\varepsilon)d\varepsilon = \int \frac{\sqrt{2}m^{3/2}}{(2\pi)^2\hbar^3}\sqrt{\varepsilon}d\varepsilon, \tag{4.79}$$

and for the current

$$I = \frac{\pi e t_d}{2\hbar}\int_{-\infty}^{\infty} \rho_L(\varepsilon)\rho_R(\varepsilon + eV)\,[f(\varepsilon) - f(\varepsilon + eV)]\,d\varepsilon, \tag{4.80}$$

or in the Landauer form

$$I = \frac{e}{h}\int_{-\infty}^{\infty} T(\varepsilon)\,[f(\varepsilon) - f(\varepsilon + eV)]\,d\varepsilon, \tag{4.81}$$

with (*model D*)

$$T^D(\varepsilon) = \pi^2 t_d \rho_L(\varepsilon)\rho_R(\varepsilon + eV) = \frac{m^3 t_d}{2\pi^2\hbar^6}\sqrt{\varepsilon}\sqrt{\varepsilon + eV}\,\theta(\varepsilon)\theta(\varepsilon + eV). \tag{4.82}$$

The expression (4.80) is the standard formula for the tunneling current.

For tunneling junctions between metals, when the energy dependence of the density of states can be neglected and the distribution functions in the electrodes can be approximated by the step functions, the current-voltage dependence becomes Ohmic $V = R_T I$ with the tunneling resistance

$$R_T = \frac{2\hbar}{\pi e^2 t_d \rho_L(\varepsilon)\rho_R(\varepsilon)}. \tag{4.83}$$

We see that for momentum-conserving tunneling the expressions are more complex and are not simply proportional to the density of state. However, for metals the main contribution to the current is from the energies near the Fermi energy, thus one can neglect the energy dependence of matrix elements.

4.1.5 Tersoff-Hamann Theory of STM

Scanning tunneling microscopy (STM) is based on the effect of electron tunneling between the sample surface (or some structures on the surface) and the metal tip.

Bardeen's formula (4.51) can be easily generalized to the 3D case:

$$V_{qk} = \frac{\hbar^2}{2m}\int_S \left[\psi_k(\boldsymbol{r})\frac{\partial}{\partial \boldsymbol{r}}\psi_q^*(\boldsymbol{r}) - \psi_q^*(\boldsymbol{r})\frac{\partial}{\partial \boldsymbol{r}}\psi_k(\boldsymbol{r})\right]_S d\boldsymbol{S}. \tag{4.84}$$

The integral is taken over the separating surface $\boldsymbol{S}$ placed in the vacuum gap between tip and sample. As in 1D case, the integral is independent from the exact position of this surface.

Both tip and sample wave functions satisfy the Schrödinger equation $\nabla^2\psi = \kappa^2\psi$ in the vacuum region. In the Tersoff-Hamann theory it is assumed that only one atomic orbital of s type predominantly participates in tunneling [6, 7]. We write this wave function in the tunneling gap using the Green function as

$$\psi_{tip}(\boldsymbol{r}) = \frac{C\hbar^2}{m\kappa} G(\boldsymbol{r}), \quad \left(-\nabla^2 + \kappa^2\right) G(\boldsymbol{r}) = \frac{2m}{\hbar^2}\delta(\boldsymbol{r} - \boldsymbol{r}_0), \quad \kappa = \frac{\sqrt{2mW}}{\hbar}, \tag{4.85}$$

where κ is the decay constant, W is the work function of the tip, C is the constant depending on the details of tip material and geometry. Substituting this wave function into (4.84) and changing surface integration to volume integration, one derives the following expression

$$\begin{aligned} V_k &= \frac{C\hbar^4}{2m^2\kappa} \int_S \left[\psi_k(\boldsymbol{r}) \frac{\partial}{\partial \boldsymbol{r}} G(\boldsymbol{r}) - G(\boldsymbol{r}) \frac{\partial}{\partial \boldsymbol{r}} \psi_k(\boldsymbol{r}) \right]_S d\boldsymbol{S} \\ &= \frac{C\hbar^4}{2m^2\kappa} \int \left[\psi_k(\boldsymbol{r}) \nabla^2 G(\boldsymbol{r}) - G(\boldsymbol{r}) \nabla^2 \psi_k(\boldsymbol{r}) \right] d\boldsymbol{r}^3 = -\frac{C\hbar^2}{m\kappa} \psi_k(\boldsymbol{r}_0). \end{aligned} \tag{4.86}$$

We found that the matrix element between tip s-state and some surface state k is determined only by the wave function of the surface state in the space point of the center of the s-state. The tunneling current

$$I = \propto \int_{-\infty}^{\infty} \rho_{sample}(\boldsymbol{r}_0, \varepsilon + eV) \left[f(\varepsilon) - f(\varepsilon + eV) \right] d\varepsilon, \tag{4.87}$$

is determined by the local density of states of the sample in the point of the edge tip atom $\rho_{sample}(\boldsymbol{r}_0, \varepsilon) = \sum_k |\psi_k(\boldsymbol{r}_0)|^2 \delta(\varepsilon - \varepsilon_k)$.

This approach can be extended to other types of atomic wave functions for the tip apex: $p, d, \ldots$ [8]

4.2 Sequential Tunneling

Up to now in this chapter we considered the tunneling between two electrodes, in this section let us come back to our favorite problem—transport through a quantum system. There are two limiting cases of single-particle tunneling: *coherent tunneling* and *sequential tunneling*. Coherent tunneling is usual quantum-mechanical transmission through two barriers or more complex structures. We considered coherent resonant transport in Sect. 3.5. In the sequential tunneling picture electrons tunnel through the first barrier, then lose their phase memory (coherence) as a result of some inelastic scattering processes, and after that tunnel through the second barrier independently of the first tunneling event. Still, we can consider this type of tunneling as resonant if the distance between energy levels in the central region is much larger than the level broadening.

4.2.1 Sequential Tunneling Through a Single Level

Assume that a noninteracting nanosystem is coupled weakly to a thermal bath (in addition to the leads). The effect of the thermal bath is to break phase coherence of the electron inside the system during some time τ_{ph}, called *decoherence or phase-breaking time*. τ_{ph} is an important time-scale in the theory, it should be compared to the so-called "tunneling time"—the characteristic time for the electron to go from the nanosystem to the lead, which can be estimated as an inverse level-width function Γ^{-1}. So that the criteria of sequential tunneling is

$$\Gamma \tau_{ph} \ll 1. \tag{4.88}$$

The finite decoherence time is due to some inelastic scattering mechanism inside the system, but typically this time is smaller than the energy relaxation time τ_ε, and the distribution function of electrons inside the system can be in nonequilibrium (if the finite voltage is applied). This transport regime is well known in semiconductor superlattices and quantum-cascade structures.

In the sequential tunneling regime the tunneling events between the left lead and the nanosystem and between the nanosystem and the right lead are independent and the current from the left (right) lead to the nanosystem is given by the golden rule expression (4.53). Let us modify it to the case of tunneling from the lead to a *single level* $|\alpha\rangle$ of a quantum system

$$I = \frac{2\pi e}{\hbar} \sum_k |V_{\alpha k}|^2 \left[f(k) - P_\alpha \right] \delta(E_\alpha - E_k), \tag{4.89}$$

where we introduce the probability P_α to find the electron in the state $|\alpha\rangle$ with the energy E_α.

4.2.2 Rate Equations for Noninteracting Systems

The rate equation method is a simple approach base on the balance of incoming and outgoing currents. Assuming that the contacts are in equilibrium we obtain for the left and right currents

$$I_{i=L(R)} = e \frac{\Gamma_{i\alpha}}{\hbar} \left[f_i^0(E_\alpha) - P_\alpha \right], \tag{4.90}$$

where

$$\Gamma_{i\alpha} = 2\pi \sum_k |V_{\alpha k}|^2 \delta(E_\alpha - E_k). \tag{4.91}$$

In the stationary state $I = I_L = -I_R$, and from this condition the level population P_α is found to be

$$P_\alpha = \frac{\Gamma_{L\alpha} f_L^0(E_\alpha) + \Gamma_{R\alpha} f_R^0(E_\alpha)}{\Gamma_{L\alpha} + \Gamma_{R\alpha}}, \tag{4.92}$$

with the current

$$I = \frac{e}{\hbar} \frac{\Gamma_{L\alpha}\Gamma_{R\alpha}}{\Gamma_{L\alpha} + \Gamma_{R\alpha}} \big(f_L^0(E_\alpha) - f_R^0(E_\alpha)\big). \tag{4.93}$$

At large voltage and low temperature it becomes

$$I_{max} = \frac{e}{\hbar} \frac{\Gamma_L \Gamma_R}{\Gamma_L + \Gamma_R}. \tag{4.94}$$

It is interesting to note that this expression is exactly the same, as one can obtain for coherent tunneling through a single level without any scattering. It should be not forgotten, however, that we did not take into account additional level broadening due to scattering.

4.2.3 The Basis of Many-Body Eigenstates

Assume that the central system is described by some model Hamiltonian, for example the Hubbard model

$$\hat{H}_C = \sum_{\alpha\beta} \tilde{\varepsilon}_{\alpha\beta} \hat{d}_\alpha^\dagger \hat{d}_\beta + \frac{1}{2} \sum_{\alpha\beta} U_{\alpha\beta} \hat{n}_\alpha \hat{n}_\beta, \tag{4.95}$$

where $\tilde{\varepsilon}_{\alpha\beta}$ are the bare energies of electron states, including the shifts due to external voltage, $\hat{n}_\alpha = \hat{d}_\alpha^\dagger \hat{d}_\alpha$ are the density operators.

The coupling to the leads is described by the tunneling Hamiltonian:

$$\hat{H}_T = \sum_{s=L,R} \sum_{k\sigma,\alpha} \left(V_{sk\sigma,\alpha}^* c_{sk\sigma}^\dagger d_\alpha + V_{sk\sigma,\alpha} d_\alpha^\dagger c_{sk\sigma} \right), \tag{4.96}$$

and the Hamiltonians of the left and right leads are

$$\hat{H}_{s=L(R)} = \sum_{k\sigma} \tilde{\varepsilon}_{sk\sigma} c_{sk\sigma}^\dagger c_{sk\sigma}, \tag{4.97}$$

k is the index of a state, σ is spin.

The starting point of the QME method is transformation from the basis of single-particle states into the basis of many-body states $|\lambda\rangle$. Thus we obtain the Hamiltonian

$$\hat{H} = \sum_{\lambda} E_{\lambda} |\lambda\rangle\langle\lambda| \quad + \sum_{s=L,R;k\sigma;\lambda\lambda'} \left[T_{sk\sigma,\lambda\lambda'} |\lambda\rangle\langle\lambda'| c_{sk\sigma} + T^{*}_{sk\sigma,\lambda\lambda'} |\lambda'\rangle\langle\lambda| c^{\dagger}_{sk\sigma} \right] \tag{4.98}$$

with tunneling matrix elements

$$T_{sk\sigma,\lambda\lambda'} = \sum_{\alpha} V_{sk\sigma,\alpha} \langle\lambda| \hat{d}^{\dagger}_{\alpha} |\lambda'\rangle. \tag{4.99}$$

4.2.4 Master Equation in the Basis of Many-Body Eigenstates

Now let us formulate briefly a more general approach to transport through interacting nanosystems weakly coupled to the leads in the sequential tunneling regime, namely the master equation method. Assume, that the system can be in several states $|\lambda\rangle$, which are the eigenstates of an isolated system and introduce the distribution function P_{λ}—the probability to find the system in the state $|\lambda\rangle$. Note, that these states are *many-particle* states, for example for a two-level quantum dot the possible states are $|\lambda\rangle = |00\rangle$, $|10\rangle$, $|01\rangle$, and $|11\rangle$. The first state is empty dot, the second and the third with one electron, and the last one is the double occupied state. The other non-electronic degrees of freedom can be introduced on the same ground in this approach. The only restriction is that some full set of eigenstates should be used

$$\sum_{\lambda} P_{\lambda} = 1. \tag{4.100}$$

Then, the kinetic (master) equation can be written as

$$\frac{dP_{\lambda}}{dt} = \sum_{\lambda'} \left(\Gamma^{\lambda\lambda'} P_{\lambda'} - \Gamma^{\lambda'\lambda} P_{\lambda} \right), \tag{4.101}$$

where the first term describes tunneling transition *into the state* $|\lambda\rangle$, and the second term—tunneling transition *out of the state* $|\lambda\rangle$.

In the stationary case the probabilities are determined from

$$\sum_{\lambda'} \Gamma^{\lambda\lambda'} P_{\lambda'} = \sum_{\lambda'} \Gamma^{\lambda'\lambda} P_{\lambda}. \tag{4.102}$$

For noninteracting electrons the transition rates are determined by the single-electron tunneling rates, and are nonzero only for the transitions between the states with the number of electrons different by one. For example, transition from the state $|\lambda'\rangle$ with empty electron level α into the state $|\lambda\rangle$ with filled state α is described by

$$\hbar\Gamma^{n_\alpha=1\ n_\alpha=0} = \Gamma_{L\alpha} f_L^0(E_\alpha) + \Gamma_{R\alpha} f_R^0(E_\alpha), \tag{4.103}$$

where $\Gamma_{L\alpha}$ and $\Gamma_{R\alpha}$ are left and right level-width functions (4.91).

For interacting electrons the calculation is a little bit more complicated. One should establish the relation between *many-particle* eigenstates of the system and *single-particle* tunneling. To do this, let us note, that the states $|\lambda\rangle$ and $|\lambda'\rangle$ in the golden rule formula (4.106) are actually the states of the whole system, including the leads. We denote the initial and final states as

$$|i\rangle = |\hat{k}_i, \lambda'\rangle = |\hat{k}_i\rangle|\lambda'\rangle, \tag{4.104}$$

$$|f\rangle = |\hat{k}_f, \lambda\rangle = |\hat{k}_f\rangle|\lambda\rangle, \tag{4.105}$$

where $\hat{k}$ is the occupation of the single-particle states in the lead. The parameterization is possible, because we apply the perturbation theory, and isolated lead and nanosystem are independent.

The next step is to treat tunneling as a perturbation. Following this idea, the transition rates $\Gamma^{\lambda\lambda'}$ from the state λ' to the state λ are calculated using the Fermi golden rule

$$\Gamma^{fi} = \frac{2\pi}{\hbar} \left|\left\langle f|\hat{H}_T|i\right\rangle\right|^2 \delta(E_f - E_i). \tag{4.106}$$

The important point is, that the leads are actually in the equilibrium mixed state, the single electron states are populated with probabilities, given by the Fermi-Dirac distribution function. Taking into account all possible single-electron tunneling processes, we obtain the incoming tunneling rate

$$\Gamma_{in}^{\lambda\lambda'} = \frac{2\pi}{\hbar} \sum_{sk\sigma} f_s^0(E_{sk\sigma}) \left|\langle s\bar{k}, \lambda \left|\bar{H}_T\right| sk, \lambda'\rangle\right|^2 \delta(E_{\lambda'} + E_{sk\sigma} - E_\lambda), \tag{4.107}$$

where we use the short-hand notations: $|sk, \lambda'\rangle$ is the state with occupied k-state in the s-th lead, while $|s\bar{k}, \lambda\rangle$ is the state with unoccupied k-state in the s-th lead, and all other states are assumed to be unchanged, E_λ is the energy of the state λ .

To proceed, we introduce the following Hamiltonian, describing single electron tunneling and changing of the nanosystem state

$$\hat{H}_T = \sum_{k\lambda\lambda'} \left[T_{k,\lambda\lambda'} c_k X^{\lambda\lambda'} + T^*_{k,\lambda\lambda'} c_k^\dagger X^{\lambda'\lambda} \right], \tag{4.108}$$

the Hubbard operators $X^{\lambda\lambda'} = |\lambda\rangle\langle\lambda'|$ describe transitions between eigenstates of the nanosystem.

Substituting this Hamiltonian one obtains

$$\Gamma_{in}^{\lambda\lambda'} = \frac{2\pi}{\hbar} \sum_{sk\sigma} f_s^0(E_{sk\sigma}) \left|T_{sk\sigma,\lambda\lambda'}\right|^2 \delta(E_{\lambda'} + E_{sk\sigma} - E_\lambda). \tag{4.109}$$

The probabilities P_λ are found from the master equation:

$$\frac{dP_\lambda}{dt} = \sum_{\lambda'} \left(\Gamma^{\lambda\lambda'} P_{\lambda'} - \Gamma^{\lambda'\lambda} P_\lambda \right), \tag{4.110}$$

$$\Gamma^{\lambda\lambda'} = \sum_{s=L,R;\sigma} \left[\gamma^{s\sigma}_{\lambda\lambda'} f^0_\sigma(E_\lambda - E_{\lambda'} - e\varphi_s) + \gamma^{s\sigma}_{\lambda'\lambda} \left(1 - f^0_\sigma(E_{\lambda'} - E_\lambda - e\varphi_s)\right) \right], \tag{4.111}$$

$$\begin{aligned} \gamma^{s\sigma}_{\lambda\lambda'} &= \frac{2\pi}{\hbar} \sum_k T_{sk\sigma,\lambda\lambda'} T^*_{sk\sigma,\lambda\lambda'} \delta(E_\lambda - E_{\lambda'} - \tilde{\varepsilon}_{sk\sigma}) \\ &= \frac{2\pi}{\hbar} \sum_{\alpha\beta k} V_{sk\sigma,\beta} \langle\lambda|\hat{d}^\dagger_\beta|\lambda'\rangle V^*_{sk\sigma,\alpha} \langle\lambda'|\hat{d}_\alpha|\lambda\rangle \delta(E_\lambda - E_{\lambda'} - \tilde{\varepsilon}_{sk\sigma}) \\ &= \frac{2\pi}{\hbar} \sum_{\alpha\beta} \Gamma_{s\sigma,\alpha\beta}(E_\lambda - E_{\lambda'}) \langle\lambda|\hat{d}^\dagger_\beta|\lambda'\rangle \langle\lambda'|\hat{d}_\alpha|\lambda\rangle. \end{aligned} \tag{4.112}$$

In the wide-band limit one has $\hbar\gamma^{s\sigma}_{\lambda\lambda'} = 2\pi\rho_0 |T_{s\sigma,\lambda\lambda'}|^2$. The current (from the left or right lead to the system) is

$$I_{i=L,R}(t) = e \sum_{\lambda\lambda'} \left(\Gamma^{\lambda\lambda'}_{i\,in} P_{\lambda'} - \Gamma^{\lambda\lambda'}_{i\,out} P_{\lambda'} \right). \tag{4.113}$$

$$I_{s=L,R} = e \sum_{\lambda\lambda';\sigma} \left[\gamma^{s\sigma}_{\lambda\lambda'} f^0_\sigma(E_\lambda - E_{\lambda'} - e\varphi_s) P_{\lambda'} - \gamma^{s\sigma}_{\lambda\lambda'} \left(1 - f^0_\sigma(E_\lambda - E_{\lambda'} - e\varphi_s)\right) P_\lambda \right]. \tag{4.114}$$

This system of equations solves the transport problem in the sequential tunneling regime.

References

1. J. Bardeen, Phys. Rev. Lett. **6**, 57 (1961)
2. W.A. Harrison, Phys. Rev. **123**, 85 (1961)
3. M.H. Cohen, L.M. Falicov, J.C. Phillips, Phys. Rev. Lett. **8**, 316 (1962)
4. R.E. Prange, Phys. Rev. **131**, 1083 (1963)
5. C.B. Duke, *Tunneling in Solids* (Academic Press, New York, 1969). Chapter VII
6. J. Tersoff, D.R. Hamann, Phys. Rev. Lett. **50**, 1998 (1983)
7. J. Tersoff, D.R. Hamann, Phys. Rev. B **31**, 805 (1985)
8. C. Julian Chen, *Introduction to Scanning Tunneling Microscopy* (Oxford University Press, 1993)

Chapter 5
Electron-Electron Interaction and Coulomb Blockade

In this chapter we start to consider the effects of electron-electron interaction. In the case of weak coupling to the electrodes or weak coupling between the parts of the system, the discreteness of electron charge is important and transport is described mainly as a sequence of tunneling events (*single-electron tunneling*). A competition between tunneling and Coulomb repulsion leads to suppression of the current known as *Coulomb blockade*.

At the beginning (Sect. 5.1) we introduce the models of electron-electron interaction and important parameters. We introduce the Hubbard-Anderson model taking into account density-density Coulomb repulsion of electrons in different single-particle states (this model is used later) and more simple constant-interaction model when the energy is dependent only on the full charge of the system. All calculations in this chapter a based on this model.

In the Sects. 5.2 and 5.3 we consider Coulomb blockade in the systems with dense energy spectrum (metal grains or large quantum dots). Two basic models are considered: single-electron box and single-electron transistor. The modification of this theory in the case of quantum dots with discrete energy levels is presented in the Sect. 5.4. *Cotunneling*, which is the tunneling process involving simultaneous transfer of two (or more) electrons, is described briefly in the Sect. 5.5.

5.1 Electron-Electron Interaction in Nanosystems

5.1.1 Single-Electron Tunneling: Charging Energy

In tunneling through nanosystems, which are weakly coupled to the leads (see below the condition of weak coupling (5.19)), the discreteness of the electronic charge starts to be important. For example, the sequential tunneling assumes that an electron from the left lead jumps into the system, stays here some time, and then jumps into the right lead. In the noninteracting case the probabilities of both processes

D.A. Ryndyk, *Theory of Quantum Transport at Nanoscale*,
Springer Series in Solid-State Sciences 184,
DOI 10.1007/978-3-319-24088-6_5

are determined by the tunneling matrix elements and actual distribution functions of electrons, and are restricted by the Pauli principle only. However, if we include Coulomb interaction between electrons, the situation changes drastically. Even a single electron produces some extra charges just after the tunneling event (Fig. 5.1). Coulomb repulsion increases the energy, which is necessary for tunneling into the system, and determines the effective energy levels for additional electrons. As a result, electrons pass through such a system one-by-one (because if the system is occupied by one extra electron, the second one does not have enough energy to go here), and the current is suppressed at low temperatures and low voltages (Coulomb blockade).

Let us start from the case of a relatively large system with dense energy spectrum (it can be a metallic grain or a large quantum dot with many electrons, Fig. 5.1). The energy required to add one electron *from the zero-energy level (zero-temperature Fermi-level in the leads)* to the system is called *addition energy* (we assume that in equilibrium the Fermi level in the leads and the quasi-Fermi level in the grain are equal). If only the electrostatic energy is taken into account it is

$$\Delta E_N^+(N \to N+1) = E(N+1) - E(N), \tag{5.1}$$

where $E(N)$ is the electrostatic energy of a system with N electrons, which is determined for large enough isolated systems by the capacitance C:

$$E(N) = \frac{Q^2}{2C} = \frac{e^2(N-N_0)^2}{2C}, \tag{5.2}$$

where $-eN_0$ is the ionic positive charge, compensating the electronic charge eN. This approximation is reasonable only for the large number of electrons N, $N_0 \gg 1$.

The *minimal* energy required to add one electron to the neutral system is called *charging energy*

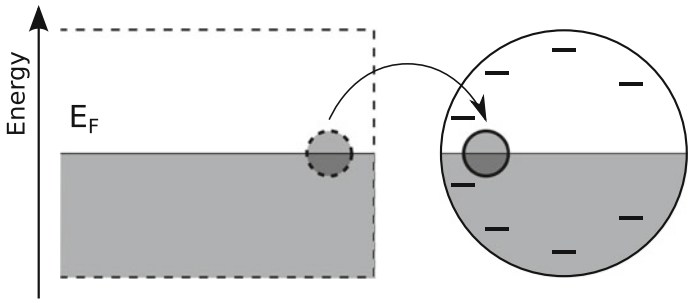

Fig. 5.1 Charging during electron tunneling to a small metal grain

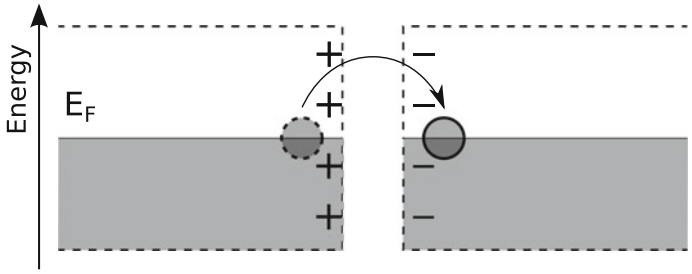

Fig. 5.2 Charging during electron tunneling in a tunnel junction

$$E_C = \Delta E^+_{N_0}(N_0 \to N_0 + 1) = \frac{e^2}{2C}. \tag{5.3}$$

If we want to add the second electron, the addition energy

$$\Delta E^+_{N_0+1}(N_0 + 1 \to N_0 + 2) = \frac{3e^2}{2C}, \tag{5.4}$$

is required, and so on. We can say that in this case the discrete energy levels are formed by the Coulomb interaction, in spite of the fact that the initial energy spectrum is dense (quasi-continuous).

The single-electron charging effects are observed not only in transport through small grains, but also in single tunnel junctions (Fig. 5.2).

The charging energy is an important energy scale. Let us estimate it in some typical cases. The classical expression for the capacitance of the usual oxide tunneling junction is $C = \varepsilon S/(4\pi d)$, where $\varepsilon \approx 10$ is the dielectric constant of the oxide, $S \approx (100\,\text{nm})^2$ is the area of the junction, and $d \approx 10\,\text{Å}$ is the thickness of the oxide layer. With these typical parameters the capacitance is $C \approx 10^{-15}$ F, which corresponds to the charging energy $E_C \approx 10^{-4}$ eV and temperature $T \sim 1$ K. This means that in metallic junctions the charging effects can be observed at sub-Kelvin temperatures. However, for nanoscale metallic particles, semiconductor quantum dots, and single molecules the charging energy, and corresponding temperature, can be orders of magnitude larger.

5.1.2 Discrete Energy Levels

The first important energy scale in small systems is the charging energy E_C, the second one is the energy level spacing $\Delta\epsilon$ between the eigenstates of a system. In metallic islands and semiconductor quantum dots the level spacing is determined by the geometrical size, because the discrete energy levels are formed as a result of spatial quantization of quasiparticles. It can be estimated using the free-electron

expression near the Fermi surface. For example, in a 3D system with characteristic size L the level spacing can be approximated by

$$\Delta\epsilon(\epsilon_F) \sim \frac{\pi^2\hbar^2}{mk_F L^3}, \tag{5.5}$$

here m is the effective mass, k_F is the Fermi wave-vector.

In smaller systems, like small quantum dots, multi quantum dot systems, and single molecules, the energy spectrum is more complex and the level spacing (or, more precisely, the energy spectrum ϵ_λ itself) should be calculated from the microscopic model. In this case the interactions can not be neglected and the level spacing $\Delta\epsilon$ can not be unambiguously distinguished from the charging energy E_C. In the limit of small single molecules the charging energy is, in fact, the same as the ionization energy, which in turn is related to the energy spectrum $E(q, \lambda)$ of the isolated molecule, where q is the charge state, and λ is the eigenstate *in this charge state*. Finally, for nanosystems we understand the charging energy as the minimal energy required to add one electron to the neutral system, and the level spacing as the typical energy difference between two levels of the system in the same charge state.

The consideration in this chapter is devoted mostly to the case of the dense energy spectrum $\Delta\epsilon \ll E_C$, when the directness of the energy levels can be neglected or taken into account within the simplified models.

It is reasonable to note here, that the last very important energy scale is the temperature T. Both discrete energy spectrum and charging effects can be observed only if the temperature is lower, than the corresponding energy scales

$$T \ll \Delta\epsilon, \quad T \ll E_C. \tag{5.6}$$

5.1.3 Hubbard-Anderson and Constant-Interaction Models

To take into account both discrete energy levels of a system and the electron-electron interaction, it is convenient to start from the general Hamiltonian

$$\hat{H} = \sum_{\alpha\beta} \tilde{\epsilon}_{\alpha\beta} d_\alpha^\dagger d_\beta + \frac{1}{2} \sum_{\alpha\beta\gamma\delta} V_{\alpha\beta,\gamma\delta} d_\alpha^\dagger d_\beta^\dagger d_\gamma d_\delta. \tag{5.7}$$

The first term of this Hamiltonian is a free-particle discrete-level model (3.94) with $\tilde{\epsilon}_{\alpha\beta}$ including electrical potentials. And the second term describes all possible interactions between electrons and is equivalent to the real-space Hamiltonian

$$\hat{H}_{ee} = \frac{1}{2} \int d\xi \int d\xi' \hat{\psi}^\dagger(\xi) \hat{\psi}^\dagger(\xi') V(\xi, \xi') \hat{\psi}(\xi') \hat{\psi}(\xi), \tag{5.8}$$

where $\hat{\psi}(\xi)$ are field operators

$$\hat{\psi}(\xi) = \sum_{\alpha} \psi_{\alpha}(\xi) d_{\alpha}, \tag{5.9}$$

$\psi_{\alpha}(\xi)$ are the basis single-particle functions, we remind, that spin quantum numbers are included in α, and spin indices are included in $\xi \equiv \boldsymbol{r}, \sigma$ as variables.

The matrix elements are defined as

$$V_{\alpha\beta,\gamma\delta} = \int d\xi \int d\xi' \psi^*_{\alpha}(\xi) \psi^*_{\beta}(\xi') V(\xi, \xi') \psi_{\gamma}(\xi) \psi_{\delta}(\xi'). \tag{5.10}$$

For pair Coulomb interaction $V(|\boldsymbol{r}|)$ the matrix elements are

$$V_{\alpha\beta,\gamma\delta} = \sum_{\sigma\sigma'} \int d\boldsymbol{r} \int d\boldsymbol{r}' \psi^*_{\alpha}(\boldsymbol{r}, \sigma) \psi^*_{\beta}(\boldsymbol{r}', \sigma') V(|\boldsymbol{r} - r'|) \psi_{\gamma}(\boldsymbol{r}, \sigma) \psi_{\delta}(\boldsymbol{r}', \sigma'). \tag{5.11}$$

Assume now, that the basis states $|\alpha\rangle$ are the states with definite spin quantum number σ_{α}. It means, that only one spin component of the wave function, namely $\psi_{\alpha}(\sigma_{\alpha})$ is nonzero, and $\psi_{\alpha}(\bar{\sigma}_{\alpha}) = 0$. In this case the only nonzero matrix elements are those with $\sigma_{\alpha} = \sigma_{\gamma}$ and $\sigma_{\beta} = \sigma_{\delta}$, they are

$$V_{\alpha\beta,\gamma\delta} = \int d\boldsymbol{r} \int d\boldsymbol{r}' \psi^*_{\alpha}(\boldsymbol{r}) \psi^*_{\beta}(\boldsymbol{r}') V(|\boldsymbol{r} - r'|) \psi_{\gamma}(\boldsymbol{r}) \psi_{\delta}(\boldsymbol{r}'). \tag{5.12}$$

In the case of delocalized basis states $\psi_{\alpha}(\boldsymbol{r})$, the main matrix elements are those with $\alpha = \gamma$ and $\beta = \delta$, because the wave functions of two different states with the same spin are orthogonal in real space and their contribution is small. It is also true for the systems with localized wave functions $\psi_{\alpha}(\boldsymbol{r})$, when the overlap between two different states is weak. In these cases it is enough to replace the interacting part by the Hubbard Hamiltonian, describing only density-density interaction

$$\hat{H}_H = \frac{1}{2} \sum_{\alpha \neq \beta} U_{\alpha\beta} \hat{n}_{\alpha} \hat{n}_{\beta}. \tag{5.13}$$

With the Hubbard interaction constants defined as

$$U_{\alpha\beta} = \int d\boldsymbol{r} \int d\boldsymbol{r}' |\psi_{\alpha}(\boldsymbol{r})|^2 |\psi_{\beta}(\boldsymbol{r}')|^2 V(|\boldsymbol{r} - r'|). \tag{5.14}$$

In the limit of a single-level quantum dot (which is, however, a two-level system because of spin degeneration) we get the Anderson impurity model (AIM)

$$\hat{H}_{AIM} = \sum_{\sigma=\uparrow\downarrow} \epsilon_{\sigma} d^{\dagger}_{\sigma} d_{\sigma} + U \hat{n}_{\uparrow} \hat{n}_{\downarrow}. \tag{5.15}$$

The other important limit is the constant interaction model (CIM), which is valid when many levels interact with similar energies, assuming $U_{\alpha\beta} = U$ for any states α and β

$$\hat{H}_{AH} = \frac{1}{2}\sum_{\alpha\neq\beta} U_{\alpha\beta}\hat{n}_\alpha\hat{n}_\beta \approx \frac{U}{2}\left(\sum_\alpha \hat{n}_\alpha\right)^2 - \frac{U}{2}\left(\sum_\alpha \hat{n}_\alpha^2\right) = \frac{U\hat{N}(\hat{N}-1)}{2}, \quad (5.16)$$

where we used $\hat{n}^2 = \hat{n}$, for large N it is equivalent to (5.2).

Thus, the CIM reproduces the charging energy considered above, and the Hamiltonian of an isolated system is

$$\hat{H}_{CIM} = \sum_{\alpha\beta} \tilde{\epsilon}_{\alpha\beta} d_\alpha^\dagger d_\beta + E(N). \quad (5.17)$$

Note, that the equilibrium compensating charge density can be easily introduced into the Hubbard Hamiltonian

$$\hat{H}_H = \frac{1}{2}\sum_{\alpha\neq\beta} U_{\alpha\beta}\left(\hat{n}_\alpha - \bar{n}_\alpha\right)\left(\hat{n}_\beta - \bar{n}_\beta\right), \quad (5.18)$$

and at $N \gg 1$ we obtain the electrostatic energy (5.2) with $C = e^2/U$.

5.2 Single-Electron Box

The simplest nanosystem, where the effects of single charge tunneling are important, is the single-electron box (SEB), a metallic island with dense electron spectrum coupled to the lead by a weak tunneling contact with the capacitance C_L and the resistance R_L (Fig. 5.3). Weak coupling means, that the tunneling resistance R_T of the junction is rather high

$$R_T \gg R_K = \frac{h}{e^2} \simeq 25.8\,\mathrm{k}\Omega, \quad (5.19)$$

the R_K is a resistance quantum (it is defined only by the fundamental constants). Note, that this resistance is well known from the Landauer-Büttiker theory, where it plays the role of the *minimum resistance* of a single quantum channel. Thus, we understand now better the limits of weak ($R_T \gg R_K$) and strong ($R_T \leq R_K$) tunneling.

We allow also to apply some voltage V_{GL} to the system through the gate capacitance C_G. The circuit is broken in this place, and the current can not flow though a system. The gate capacitance C_G is "true" capacitance, while the tunnel junction includes the classical capacitance C_L and quantum "possibility to tunnel" (shown

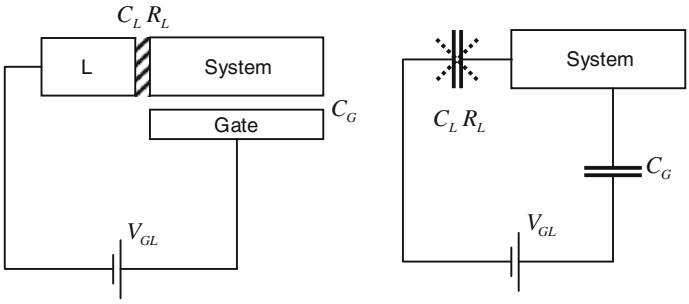

Fig. 5.3 A single-electron box and its electrical scheme

by the cross). It is *not* equivalent to a classical resistance, in particular, the finite voltage at the capacitance C_L does not imply necessarily the current through the tunnel junction.

Now let us consider the following question: what is the charge state of the SEB at arbitrary voltage V_{GL}? The important point is, that if the condition (5.19) is satisfied, the probability of tunneling is small, and electrons can be considered as localized inside the system almost all time. Therefore, the electronic charge of the SEB is quantized and is always en with integer n. However, the voltage V_{GL} is arbitrary and tries to charge the capacitance by the charge $C_G V_{GL}$, which is not possible in general. The solution, found by the system, is to create two charges: Q_L at the capacitance of the tunneling contact and Q_G at the gate capacitance, in such a way that

$$Q_L + Q_G = en,$$

and the voltage is also divided between capacitances as

$$V_{GL} = \frac{Q_L}{C_L} - \frac{Q_G}{C_G}.$$

From these two equations the charges Q_L and Q_G are easily defined as

$$Q_L = \frac{C_L C_G}{C_L + C_G}\left(\frac{en}{C_G} + V_{GL}\right), \tag{5.20}$$

$$Q_G = \frac{C_L C_G}{C_L + C_G}\left(\frac{en}{C_L} - V_{GL}\right). \tag{5.21}$$

Now we need the free energy of the system as a function of the electron number n with the gate voltage V_{GL} as an external parameter. It allows to determine the ground state, and the probabilities of the states with different n, which are given by the Gibbs distribution. The problem is, that when the charge en is changed, the charges Q_L and Q_G are also changed and the external source makes the work $-V_{GL} dQ_G$, note

that here the asymmetry between true capacitance C_G and the junction capacitance C_L plays the role. After the Legendre transformation the free energy $E^*(n)$ is

$$E^*(n) = \frac{Q_L^2}{2C_L} + \frac{Q_G^2}{2C_G} + Q_G V_{GL}, \tag{5.22}$$

where $C = C_L + C_G$. Substituting (5.20) and (5.21) in this expression, we obtain

$$E^*(n) = \frac{(en)^2}{2C} + \frac{C_G V_{GL}}{C}(en) + \frac{C_L C_G V_{GL}^2}{2C}. \tag{5.23}$$

Neglecting the last irrelevant term independent on n, we get the free electrostatic energy of a SEB with $n = N - N_0$ excess electrons:

$$E^*(n) = \frac{e^2(n + Q^*/e)^2}{2C}, \tag{5.24}$$

where $Q^* = C_G V_{GL}$ is determined by the gate voltage and is *non-integer* in the units of the elementary charge e.

This expression can be obtained alternatively from the simple argument, that the full energy of the system is the sum of its own electrostatic energy and the energy of the charge ne in the external potential. Indeed, the first term in the formula (5.23) is the electrostatic energy of the isolated system, and the second term is the electrostatic energy in the external potential $(C_G/C)V_{GL}$ in relation to the potential of the left lead. The full potential difference (voltage V_{LS}) between the system and the left lead is (from (5.20))

$$V_{LS} = \frac{Q_L}{C_L} = \frac{en}{C} + \frac{C_G V_{GL}}{C}, \tag{5.25}$$

where the first term is the electrical potential produced by the charge of the island with capacitance C, and the second term is produced by the external voltage. Integrating it over the charge ne we obtain the free energy (5.23).

We plot the energy $E^*(n)$ as a function of the gate charge Q^* at different n (the negative electron charge $e = -|e|$ is taken into account explicitly) in the Fig. 5.4. This picture shows, that the state with minimal energy is changed with Q^*. The neutral state $n = 0$ is stable at $-0.5 < Q^*/|e| < 0.5$ and so on.

At zero temperature (and neglecting "quantum fluctuations", e.g. treating n as a classical variable) the number of electrons is given by the minimum of the energy (5.24). By increasing of the gate voltage, the state of the SEB is changed from n to $n + 1$ in the degeneracy points $Q^*/|e| = n + 0.5$. Now let us consider the average number of electrons in the box $\langle n \rangle$ as a function of the gate voltage.

At finite temperature the probability $p(n)$ of different n is given by the Gibbs distribution

$$p(n) = \frac{1}{Z} \exp\left(-\frac{E^*(n)}{T}\right), \tag{5.26}$$

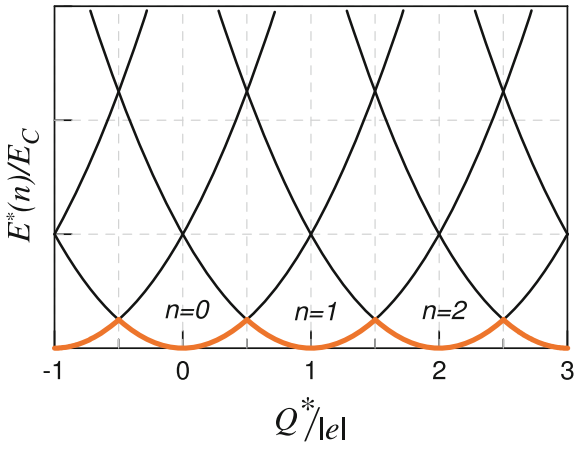

Fig. 5.4 The electrostatic energy $E(n)$ of a single-electron box as a function of the gate voltage for the states with different number n of excess electrons. The thick line shows the states with minimum energy

where the normalization coefficient is determined from the condition

$$\sum_n p(n) = 1. \tag{5.27}$$

The average number of electrons is

$$\langle n \rangle = \sum_n np(n) = \frac{1}{Z} \sum_n n \exp\left(-\frac{E^*(n)}{T}\right). \tag{5.28}$$

The results of calculation at different temperatures are shown in Fig. 5.5. We see, quite obviously, that the steps are smeared with temperature and disappear almost completely at $T \approx E_C$, in agreement with the estimate (5.6).

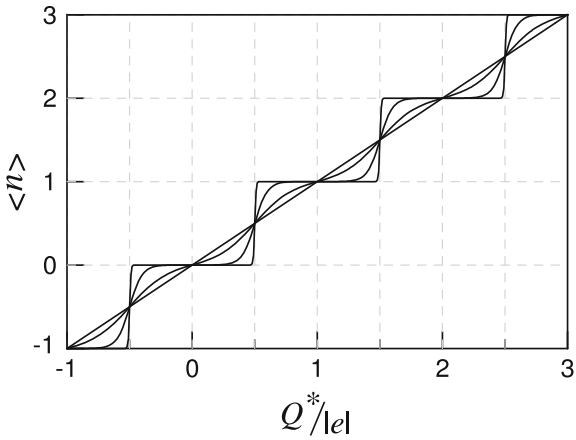

Fig. 5.5 The average number of electrons $\langle n \rangle$ in a single-electron box as a function of the gate voltage at different temperatures $T = 0.01E_C$ (steps), $T = 0.1E_C$, $T = 0.3E_C$, $T = E_C$ (*nearly linear*)

5.3 Single-Electron Transistor

Now we come back to transport problems. Consider the system between two leads coupled by two weak tunneling contacts (Fig. 5.6). When there is also a third electrode (gate), the system is called single-electron transistor.

The electrostatic energy of the central region is given by the same formula (5.24) with the gate charge Q^* determined by the combination of all voltages applied to a system and the full capacitance is

$$C = C_G + C_L + C_R. \tag{5.29}$$

The addition energy to increase the number of electrons from n to $n+1$ is

$$\Delta E_n^+(n \to n+1) = E^*(n+1) - E^*(n) = \frac{e^2}{C}\left(n + \frac{1}{2} + \frac{Q^*}{e}\right). \tag{5.30}$$

At zero bias voltage the system is equivalent to the single-electron box with two contacts instead of one, and the minimum energy, as well as the average number of excess electrons, are defined in the same way. At finite bias voltage $V = V_L - V_R$ the current flows through the system. To calculate this current we use the sequential tunneling approach and master equation, valid in the limit of weak system-to-lead coupling (see Sect. 4.2). To describe the transport we should calculate the nonequilibrium probability $p(n)$ of different states n, which is not described now by the Gibbs distribution as for the single-electron box. First of all, let us determine the transition rates in the sequential tunneling regime.

5.3.1 *Tunneling Transition Rates*

The transition rate is determined by the golden-rule expression. For example, the transition from the state $|n\rangle$ to the state $|n+1\rangle$ due to the coupling to the left lead, is determined by the full probability of tunneling of one electron from any state $|k\rangle$

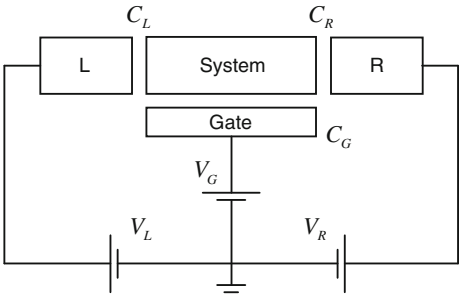

Fig. 5.6 A single-electron transistor

in the left lead to any single-particle state $|\alpha\rangle$:

$$\begin{aligned}\Gamma_L^{n+1\,n} &= \frac{2\pi}{\hbar}\left|\left\langle n+1|\hat{H}_{TL}|n\right\rangle\right|^2 \delta(E_i - E_f) \\ &= \frac{2\pi}{\hbar}\sum_{k\alpha}|V_{k\alpha}|^2\, f_k\,(1-f_\alpha)\,\delta(E_\alpha + \Delta E_n^+ - E_k),\end{aligned} \tag{5.31}$$

the sum here is over all electronic states $|k\rangle$ in the left lead and all single-particle states $|\alpha\rangle$ in the system in the sense of the constant-interaction model (5.17), and $\hat{H}_{TL}$ is the part of the tunneling Hamiltonian describing coupling to the left lead. All single-particle states are assumed to be thermalized and incoherent. The Fermi distribution functions f_k and $(1 - f_\alpha)$ describe probability for the state $|k\rangle$ to be occupied, and for the state $|\alpha\rangle$ to be unoccupied. In such a way we take into account that the state denoted as $|n\rangle$ is, in fact, a mixed state of many single-particle states. We assume also for simplicity that the energy relaxation time is fast enough and the distribution of particles inside the system is equilibrium (but not the distribution $p(n)$ of the different charge states!).

Analogously, the transition from the state $|n\rangle$ to the state $|n-1\rangle$ is determined by the probability of tunneling of one electron from the state with n electrons to the left lead

$$\begin{aligned}\Gamma_L^{n-1\,n} &= \frac{2\pi}{\hbar}\left|\left\langle n-1|\hat{H}_{TL}|n\right\rangle\right|^2 \delta(E_i - E_f) \\ &= \frac{2\pi}{\hbar}\sum_{k\alpha}|V_{k\alpha}|^2\, f_\alpha\,(1-f_k)\,\delta(E_\alpha + \Delta E_{n-1}^+ - E_k).\end{aligned} \tag{5.32}$$

Changing to the energy integration, we obtain

$$\Gamma_L^{n+1\,n} = \int dE_1 \int dE_2 \Gamma_L(E_1, E_2)\, f_L^0(E_1)\left(1 - f_S^0(E_2)\right)\delta(E_2 + \Delta E_n^+ - E_1), \tag{5.33}$$

where

$$\Gamma_{i=L,R}(E_1, E_2) = \frac{2\pi}{\hbar}\sum_{k\alpha}|V_{\alpha,ik}|^2\delta(E_1 - E_\alpha)\delta(E_2 - E_k). \tag{5.34}$$

Further simplification is possible in the wide-band limit, assuming that $\Gamma_{i=L,R}(E_1, E_2)$ is energy-independent. Finally, we arrive at

$$\Gamma_{i=L,R}^{n+1\,n} = (G_i/e^2) f(\Delta E_n^+ + eV_{iS}), \tag{5.35}$$

where G_i is the tunneling conductance

$$G_{i=L,R} = \frac{4\pi e^2}{\hbar} N_i(0) N_S(0) |V|^2, \tag{5.36}$$

with the densities of states $N_i(0)$ and $N_S(0)$, and $f(E)$ is

$$f(E) = \frac{E}{\exp\left(\frac{E}{T}\right) - 1}. \tag{5.37}$$

In the same way for the transition from n to $n-1$ we get

$$\Gamma^{n-1\,n}_{i=L,R} = (G_i/e^2) f(-\Delta E^{+}_{n-1} - eV_{iS}). \tag{5.38}$$

5.3.2 Master Equation

Now we can write the classical master equation for the probability $p(n,t)$ to find a state with n electrons

$$\begin{aligned}\frac{dp(n,t)}{dt} = &\left(\Gamma_L^{n\,n-1} + \Gamma_R^{n\,n-1}\right) p(n-1,t) + \left(\Gamma_L^{n\,n+1} + \Gamma_R^{n\,n+1}\right) p(n+1,t) \\ &- \left(\Gamma_L^{n-1\,n} + \Gamma_L^{n+1\,n} + \Gamma_R^{n-1\,n} + \Gamma_R^{n+1\,n}\right) p(n,t),\end{aligned} \tag{5.39}$$

where the transitions rates are calculated previously (5.35), (5.38). Introducing the short-hand notations

$$\Gamma^{n\,n-1} = \Gamma_L^{n\,n-1} + \Gamma_R^{n\,n-1},$$

$$\Gamma^{n\,n+1} = \Gamma_L^{n\,n+1} + \Gamma_R^{n\,n+1},$$

we arrive at

$$\frac{dp(n,t)}{dt} = \Gamma^{n\,n-1} p(n-1,t) + \Gamma^{n\,n+1} p(n+1,t) - \left(\Gamma^{n-1\,n} + \Gamma^{n+1\,n}\right) p(n,t). \tag{5.40}$$

The structure of this equation is completely clear. The first two terms describe transfer of one electron from the leads to the system (if the state before tunneling is $|n-1\rangle$) or from the system to the leads (if the initial state is $|n+1\rangle$), in both cases the final state is $|n\rangle$, thus raising the probability $p(n)$ to find this state. The last term in (5.40) describes tunneling from the state $|n\rangle$ into $|n-1\rangle$ or $|n+1\rangle$.

The current (from the left or right lead to the system) is

$$J_{i=L,R}(t) = e \sum_n \left(\Gamma_i^{n+1\,n} - \Gamma_i^{n-1\,n} \right) p(n,t). \tag{5.41}$$

In the stationary case the solution of the master equation (5.40) is given by the recursive relation (which is actually the stationary balance equation between $|n\rangle$ and $|n-1\rangle$ states).

$$\Gamma^{n-1\,n} p(n) = \Gamma^{n\,n-1} p(n-1). \tag{5.42}$$

It can be solved very easily numerically, one can start from an *arbitrary* value for one of the $p(n)$, then calculate all other $p(n)$ going up and down in n to some fixed limiting number, and, finally, normalize all the $p(n)$ to satisfy the condition (5.27).

Below we present the numerical solution in two cases: for conductance in the limit of low voltage, and for the voltage-current curves. The transport is blocked at low temperature and low voltage because of the non-zero addition energy (5.30).

5.3.3 Conductance: CB Oscillations

Consider first the conductance of a system as a function of the gate voltage V_G (gate charge Q^*). The result is shown in Fig. 5.7. The conductance has a maximum in the degeneracy points $Q^*/|e| = n + 0.5$, when the addition energy (5.30) vanishes. Between these points the conductance is very small at low temperatures, because the electron can not overcome the Coulomb energy, the effect was nick-named "Coulomb blockade".

The phenomena can be described within the noninteracting particle picture, if we notice, that the charging energy produce, in fact, discrete energy levels, while the

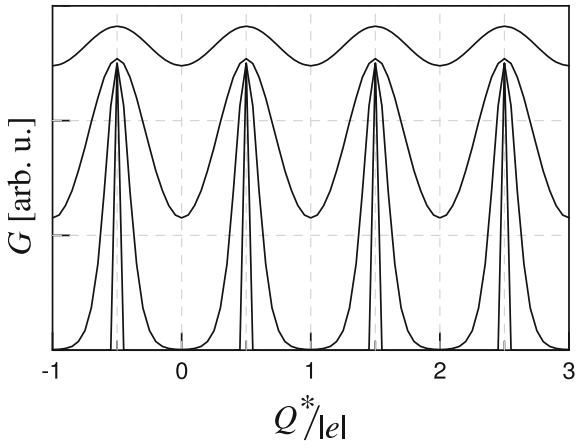

Fig. 5.7 Conductance oscillations as a function of the gate voltage at different temperatures $T = 0.01E_C$, $T = 0.1E_C$, $T = 0.3E_C$, $T = 0.5E_C$ (*upper curve*)

gate voltage works as a potential changing the position of the levels up and down in energy. The maximum of the conductance is observed when this induced discrete level is in resonance with the Fermi levels in the leads. This single-particle picture (or better to say analogy), however, should be used with care. The problem is that this single-particle level is fictional and corresponds, in fact, to a superposition of two many-particle states with different number of electrons. In the degeneracy point the probabilities $p(n)$ and $p(n+1)$ of the states with different number of electrons are equal. This circumstance shows that the Coulomb blockade is essentially many-particle phenomena, and the mean-field (Hartree-Fock) approximation can not be used to describe it. Later we shall see, that it is a consequence of the degeneracy of a single-particle spectrum.

At higher temperatures, the oscillations are smeared and completely disappear at $T \sim E_C$, the effect is analogous to the charge quantization in a single-electron box.

5.3.4 Current-Voltage Curve: Coulomb Staircase

Now let us discuss the signatures of Coulomb blockade at finite voltage. The results of calculations are presented in Fig. 5.8 for symmetric ($G_L = G_R$) system, and in Fig. 5.9 for asymmetric one. First of all, the gap (called Coulomb gap) is seen clearly at low temperatures and low voltages, that is another manifestation of Coulomb blockade. In agreement with conductance calculation, this gap is closed in the degeneracy points, where the linear current-voltage relation is reproduced at low voltages. At higher temperatures the gap is smeared and linear behaviour is restored.

The other characteristic feature, seen at higher voltages and more pronounced in the asymmetric case, is called Coulomb staircase (Fig. 5.9) and is observed due to the participation of higher charge states in transport at higher voltage. For example,

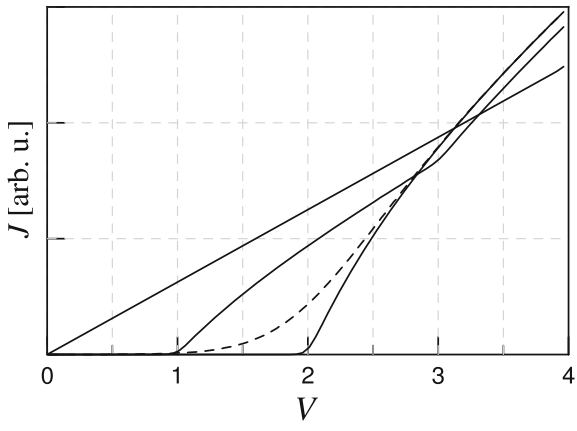

Fig. 5.8 Coulomb blockade: voltage-current curves of a symmetric junction at low temperature ($T = 0.01E_C$) and different gate voltages $V_G = 0$, $V_G = 0.25E_C$, and $V_G = 0.5E_C$. *Dashed line* shows the change at higher temperature $T = 0.1E_C$. Voltage is in units of $E_C/|e|$

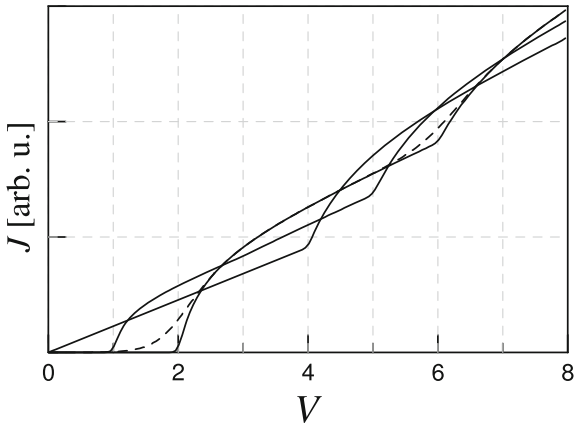

Fig. 5.9 Coulomb staircase: voltage-current curves of an asymmetric junction at low temperature ($T = 0.01E_C$) at different gate voltages $V_G = 0$, $V_G = 0.25E_C$, and $V_G = 0.5E_C$. *Dashed line* shows the change at higher temperature $T = 0.1E_C$. Voltage is in units of $E_C/|e|$

if $V_G = 0$ the transport is blocked at low voltage and the current appears only at $|e|V/2 > E_C$ ($V/2$ because the bias voltage is divided between the left and right contacts) when the Coulomb gap is overcome and the electron can go through the state $|n = 1\rangle$. At higher voltage $|e|V/2 > 3E_C$ the state $|n = 2\rangle$ becomes available, and so on.

The general formula for the threshold voltages of the n-th step is

$$V_n = \pm\frac{2(2n-1)E_C}{|e|}. \tag{5.43}$$

The amplitude of the steps is decaying with n and at large voltage the Ohmic behaviour is reproduced.

5.3.5 Contour Plots. Stability Diagrams

To analyze the experiments, the contour plots of the current $J(V, V_G)$ (Fig. 5.10) and the differential conductance $dJ/dV(V, V_G)$ (Fig. 5.11) are very useful. The characteristic structures of Coulomb blockade (so-called Coulomb diamonds) are well pronounced in these pictures.

The white rhombic-shaped regions are the regions of Coulomb blockade. At zero temperature there is no current, one state with n electrons is stable with respect to tunneling. For example, near the point $V = V_G = 0$ the state $n = 0$ is stable. If one changes the gate voltage, the other charge states become stable. At large enough bias voltage the stability is lost and sequential tunneling events produce a finite current. The contour plots, as well as schematic representations of the boundaries of the stability region in the (V, V_G) plane, are often called *stability diagrams*.

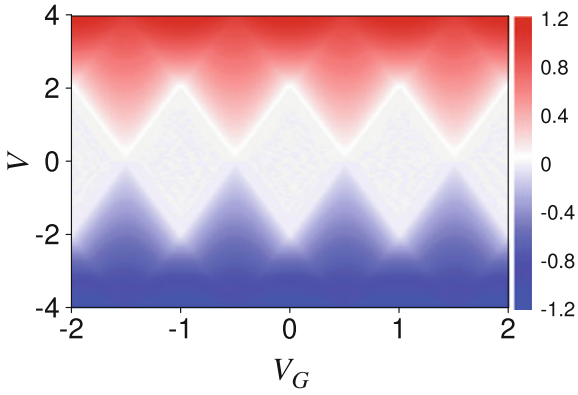

Fig. 5.10 Contour plot of the current

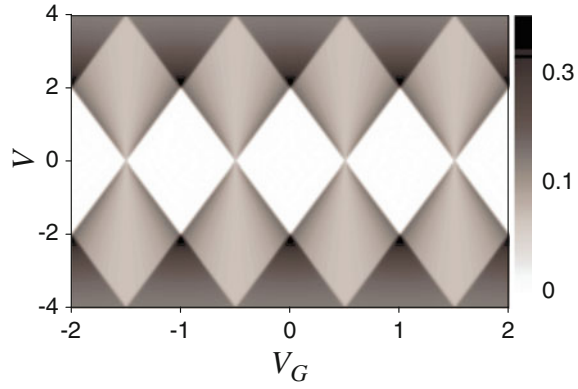

Fig. 5.11 Contour plot of the differential conductance

While both left and right tunneling events should be suppressed, there are two stability conditions, obtained directly from the tunneling rates (5.35), (5.38)

$$|e|\left(n-\frac{1}{2}\right) < C_G V_{GR} + C_R V < |e|\left(n+\frac{1}{2}\right), \tag{5.44}$$

$$|e|\left(n-\frac{1}{2}\right) < C_G V_{GL} - C_L V < |e|\left(n+\frac{1}{2}\right), \tag{5.45}$$

where $V = V_L - V_R$ is the bias voltage, and $V_{GL} = V_G - V_L$, $V_{GR} = V_G - V_R$ are the voltages between the gate and the leads.

These inequalities show that if the system leaves the stability region at finite bias voltage V, the new state with $n = n \pm 1$, which occurs as a result of tunneling through one junction, is also unstable with respect to tunneling through the other junction. As a result, the systems returns back to the state n, and the cycle is started again, thus the current flows through the system.

5.4 Coulomb Blockade in Quantum Dots

Here we want to consider the Coulomb blockade in intermediate-size quantum dots, where the typical energy level spacing $\Delta\epsilon$ is not too small to neglect it completely, but the number of levels is large enough, so that one can use the constant-interaction model (5.17), which we write in the eigenstate basis as

$$\hat{H}_{CIM} = \sum_{\alpha} \tilde{\epsilon}_{\alpha} d_{\alpha}^{\dagger} d_{\alpha} + E(n), \tag{5.46}$$

where the charging energy $E(n)$ is determined in the same way as previously, for example by the expression (5.16). Note, that for quantum dots it is not convenient to incorporate the gate voltage into the free electrostatic energy (5.24), as we did before for metallic islands, also the usage of classical capacitance is not well established, although for large quantum dots it is possible. Instead, we shift the energy levels in the dot $\tilde{\epsilon}_{\alpha} = \epsilon_{\alpha} + e\varphi_{\alpha}$ by the electrical potential

$$\varphi_{\alpha} = V_G + V_R + \eta_{\alpha}(V_L - V_R), \tag{5.47}$$

where η_{α} are some coefficients, dependent on geometry. This method can be easily extended to include any self-consistent effects on the mean-field level by the help of the Poisson equation (instead of classical capacitances). Besides, if all η_{α} are the same, our approach reproduces again the relevant part of the classical expressions (5.23), (5.24)

$$\hat{E}_{CIM} = \sum_{\alpha} \epsilon_{\alpha} n_{\alpha} + E(n) + en\varphi_{ext}. \tag{5.48}$$

The *addition energy* now depends not only on the charge of the molecule, but also on the state $|\alpha\rangle$, in which the electron is added

$$\Delta E_{n\alpha}^{+}(n, n_{\alpha} = 0 \to n+1, n_{\alpha} = 1) = E(n+1) - E(n) + \epsilon_{\alpha}. \tag{5.49}$$

We can assume in this case, that the single particle energies are additive to the charging energy, so that the full quantum eigenstate of the system is $|n, \hat{n}\rangle$, where the set $\hat{n} \equiv \{n_{\alpha}\}$ shows whether the particular single-particle state $|\alpha\rangle$ is empty or occupied. Some arbitrary state $\hat{n}$ looks like

$$\hat{n} \equiv \{n_{\alpha}\} \equiv \big(n_1, n_2, n_3, n_4, n_5, \ldots\big) = \big(1, 1, 0, 1, 0, \ldots\big). \tag{5.50}$$

Note, that the distribution $\hat{n}$ defines also $n = \sum_{\alpha} n_{\alpha}$. It is convenient, however, to keep notation n to remember about the charge state of a system, below we use both notations: $|n, \hat{n}\rangle$ and short one $|\hat{n}\rangle$ as equivalent.

The other important point is that the distribution function $f_n(\alpha)$ in the charge state $|n\rangle$ is not assumed to be in equilibrium, as previously (this condition is not specific to quantum dots with discrete energy levels, the distribution function in metallic islands

can also be in nonequilibrium. However, in the parameter range, typical for classical Coulomb blockade, the tunneling time is much smaller than the energy relaxation time, and quasiparticle nonequilibrium effects are usually neglected).

With these new assumptions, the theory of sequential tunneling is quite the same, as was considered in the previous section. The master equation (5.40) is replaced by

$$\frac{dp(n,\hat{n},t)}{dt} = \sum_{\hat{n}'} \left(\Gamma^{n\,n-1}_{\hat{n}\hat{n}'} p(n-1,\hat{n}',t) + \Gamma^{n\,n+1}_{\hat{n}\hat{n}'} p(n+1,\hat{n}',t) \right) - \sum_{\hat{n}'} \left(\Gamma^{n-1\,n}_{\hat{n}'\hat{n}} + \Gamma^{n+1\,n}_{\hat{n}'\hat{n}} \right) p(n,\hat{n},t) + I\left\{ p(n,\hat{n},t) \right\}, \tag{5.51}$$

where $p(n,\hat{n},t)$ is now the probability to find the system in the state $|n,\hat{n}\rangle$, $\Gamma^{n\,n-1}_{\hat{n}\hat{n}'}$ is the transition rate from the state with $n-1$ electrons and single level occupation $\hat{n}'$ into the state with n electrons and single level occupation $\hat{n}$. The sum is over all states $\hat{n}'$, which are different by one electron from the state $\hat{n}$. The last term is included to describe possible inelastic processes inside the system and relaxation to the equilibrium function $p_{eq}(n,\hat{n})$. In principle, it is not necessary to introduce such type of dissipation in calculation, because the current is in any case finite. But the dissipation may be important in large systems and at finite temperatures. Besides, it is necessary to describe the limit of classical single-electron transport, where the distribution function of particles is assumed to be in equilibrium. Below we shall not take into account this term, assuming that tunneling is more important.

While all considered processes are, in fact, single-particle tunneling processes, we arrive at

$$\frac{dp(\hat{n},t)}{dt} = \sum_{\beta} \left(\delta_{n_\beta 1} \Gamma^{n\,n-1}_{\beta} p(\hat{n}, n_\beta = 0, t) + \delta_{n_\beta 0} \Gamma^{n\,n+1}_{\beta} p(\hat{n}, n_\beta = 1, t) \right) - \sum_{\beta} \left(\delta_{n_\beta 1} \Gamma^{n-1\,n}_{\beta} + \delta_{n_\beta 0} \Gamma^{n+1\,n}_{\beta} \right) p(\hat{n},t), \tag{5.52}$$

where the sum is over single-particle states. The probability $p(\hat{n}, n_\beta = 0, t)$ is the probability of the state equivalent to $\hat{n}$, but without the electron in the state β. Consider, for example, the first term in the right part. Here the delta-function $\delta_{n_\beta 1}$ shows, that this term should be taken into account only if the single-particle state β in the many-particle state $\hat{n}$ is occupied, $\Gamma^{n\,n-1}_{\beta}$ is the probability of tunneling from the lead to this state, $p(\hat{n}, n_\beta = 0, t)$ is the probability of the state $\hat{n}'$, from which the system can come into the state $\hat{n}$.

The transition rates are defined by the same golden rule expressions, as before (5.31), (5.32), but with explicitly shown single-particle state α

$$\Gamma^{n+1\,n}_{L\alpha} = \frac{2\pi}{\hbar} \left| \left\langle n+1, n_\alpha = 1 | \hat{H}_{TL} | n, n_\alpha = 0 \right\rangle \right|^2 \delta(E_i - E_f) = \frac{2\pi}{\hbar} \sum_k |V_{k\alpha}|^2 f_k \delta(\Delta E^+_{n\alpha} - E_k), \tag{5.53}$$

$$\Gamma_{L\alpha}^{n-1\,n} = \frac{2\pi}{\hbar}\left|\left\langle n-1, n_\alpha = 0|\hat{H}_{TL}|n, n_\alpha = 1\right\rangle\right|^2 \delta(E_i - E_f)$$
$$= \frac{2\pi}{\hbar}\sum_k |V_{k\alpha}|^2\,(1-f_k)\,\delta(\Delta E^+_{n-1\,\alpha} - E_k), \tag{5.54}$$

there is no occupation factors $(1-f_\alpha)$, f_α because this state is assumed to be empty in the sense of the master equation (5.52). The energy of the state is now included into the addition energy.

Using again the level-width function

$$\Gamma_{i=L,R\,\alpha}(E) = \frac{2\pi}{\hbar}\sum_k |V_{ik,\alpha}|^2\delta(E - E_k). \tag{5.55}$$

we obtain

$$\Gamma_\alpha^{n+1\,n} = \Gamma_{L\alpha} f_L^0(\Delta E^+_{n\alpha}) + \Gamma_{R\alpha} f_R^0(\Delta E^+_{n\alpha}), \tag{5.56}$$
$$\Gamma_\alpha^{n-1\,n} = \Gamma_{L\alpha}\left(1 - f_L^0(\Delta E^+_{n-1\,\alpha})\right) + \Gamma_{R\alpha}\left(1 - f_R^0(\Delta E^+_{n-1\,\alpha})\right). \tag{5.57}$$

Finally, the current from the left or right contact to a system is

$$J_{i=L,R} = e\sum_\alpha\sum_{\hat{n}} p(\hat{n})\Gamma_{i\alpha}\left(\delta_{n_\alpha 0} f_i^0(\Delta E^+_{n\alpha}) - \delta_{n_\alpha 1}(1 - f_i^0(\Delta E^+_{n\alpha}))\right). \tag{5.58}$$

The sum over α takes into account all possible single particle tunneling events, the sum over states $\hat{n}$ summarize probabilities $p(\hat{n})$ of these states.

5.4.1 Linear Conductance

The linear conductance can be calculated analytically [1, 2]. Here we present the final result:

$$G = \frac{e^2}{T}\sum_\alpha\sum_{n=1}^{\infty}\frac{\Gamma_{L\alpha}\Gamma_{R\alpha}}{\Gamma_{L\alpha}+\Gamma_{R\alpha}} P_{eq}(n, n_\alpha = 1)\left[1 - f^0(\Delta E^+_{n-1\,\alpha})\right], \tag{5.59}$$

where $P_{eq}(n, n_\alpha = 1)$ is the joint probability that the quantum dot contains n electrons and the level α is occupied

$$P_{eq}(n, n_\alpha = 1) = \sum_{\hat{n}} p_{eq}(\hat{n})\delta\left(n - \sum_\beta n_\beta\right)\delta_{n_\alpha 1}, \tag{5.60}$$

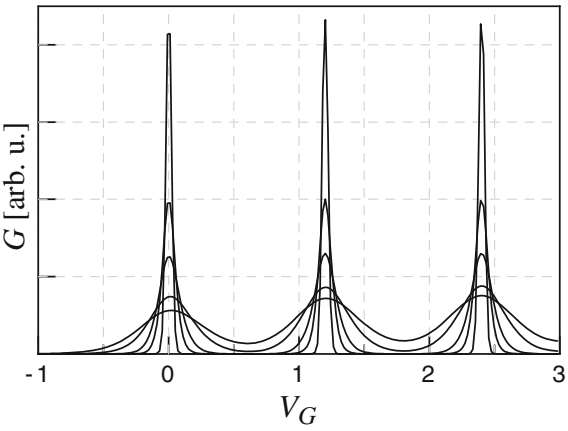

Fig. 5.12 Linear conductance of a multi-level quantum dot as a function of the gate voltage at different temperatures $T = 0.01E_C$, $T = 0.03E_C$, $T = 0.05E_C$, $T = 0.1E_C$, $T = 0.15E_C$ (*lower curve*)

and the equilibrium probability (distribution function) is determined by the Gibbs distribution in the grand canonical ensemble:

$$p_{eq}(\hat{n}) = \frac{1}{Z} \exp\left[-\frac{1}{T}\left(\sum_{\alpha} \tilde{\epsilon}_{\alpha} + E(n)\right)\right]. \tag{5.61}$$

A typical behaviour of the conductance as a function of the gate voltage at different temperatures is shown in Fig. 5.12. In the resonant tunneling regime at low temperatures $T \ll \Delta\epsilon$ the peak height is strongly temperature-dependent. It is changed by classical temperature dependence (constant height) at $T \gg \Delta\epsilon$.

5.4.2 *Transport at Finite Bias Voltage*

At finite bias voltage we find new manifestations of the interplay between single-electron tunneling and resonant free-particle tunneling.

Let us consider the curve of the differential conductance (Fig. 5.13). First of all, the Coulomb staircase is reproduced, which is more pronounced than for metallic islands, because the density of states is limited by the available single-particle states and the current is saturated. Besides, small additional steps due to discrete energy levels appear. This characteristic behaviour is possible for large enough dots with $\Delta\epsilon \ll E_C$. If the level spacing is of the order of the charging energy $\Delta\epsilon \sim E_C$, the Coulomb blockade steps and discrete-level steps look the same, but their statistics (position and height distribution) is determined by the details of the single-particle spectrum and interactions [3].

Finally, let us consider the contour plot of the differential conductance (Fig. 5.14). It is essentially different from those for the metallic island (Fig. 5.11). First, it is not

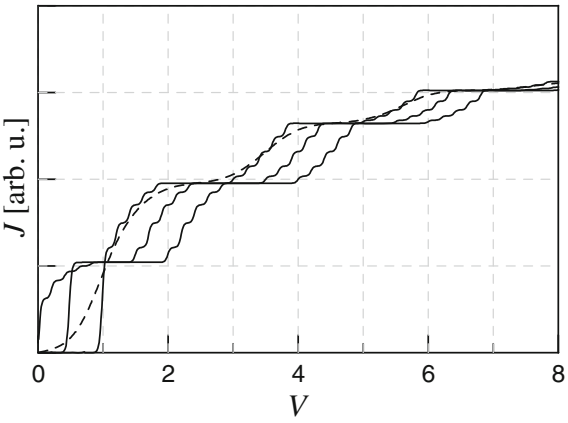

Fig. 5.13 Coulomb staircase of a multi-level quantum dot

symmetric in the gate voltage, because the energy spectrum is restricted from the bottom, and at negative bias all the levels are above the Fermi-level (the electron charge is negative, and a negative potential means a positive energy shift). Nevertheless, existing stability patterns are of the same origin and form the same structure. The qualitatively new feature is additional lines correspondent to the additional discrete-level steps in the voltage-current curves. In general, the current and conductance of quantum dots demonstrate all typical features of discrete-level systems: current steps, and conductance peaks. Without Coulomb interaction the usual picture of resonant tunneling is reproduced. In the limit of dense energy spectrum $\Delta\epsilon \to 0$ the sharp single-level steps are merged into the smooth Coulomb staircase.

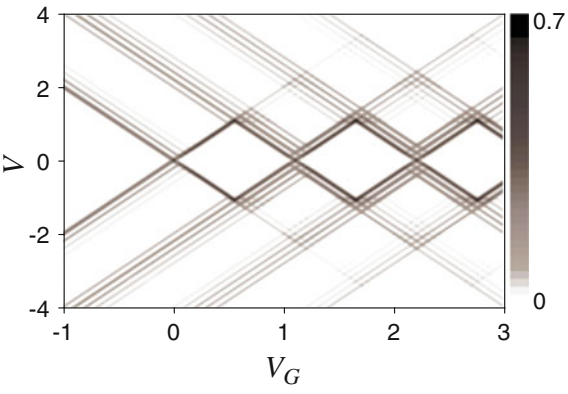

Fig. 5.14 Contour plot of the differential conductance of a multi-level quantum dot

5.5 Cotunneling

Until now we have considered only the sequential tunneling regime, which is described by the first-order perturbation in tunneling. At low temperatures the sequential tunneling is suppressed by the Coulomb blockade (except the degeneracy points), and the conductance of the system become exponentially small. In this case the second-order processes start to be important. These processes include the events, when two electrons *with different energy* participate in tunneling simultaneously (so-called *inelastic cotunneling*), or one electron tunnels coherently twice (*elastic cotunneling*), which is equivalent, however, to the simultaneous tunneling of two electrons *with the same energy*. Note, that both terms "inelastic" and "elastic" have no relation to the presence or absence of the additional inelastic interactions inside the system.

The standard second-order perturbation theory yields the transition rate from some initial state $|i\rangle$ to some final state $|f\rangle$

$$\Gamma^{(2)}_{i\to f} = \frac{2\pi}{\hbar}\left|\sum_{\lambda}\frac{\left\langle f\left|\hat{H}_T\right|\lambda\right\rangle\left\langle\lambda\left|\hat{H}_T\right|i\right\rangle}{E_\lambda - E_i}\right|^2 \delta(E_i - E_f). \tag{5.62}$$

The intermediate states $|\lambda\rangle$ are virtual states with $E_\lambda > E_i$. In this point we already assume that the system is in the Coulomb blockade regime with fixed number of electrons n, and the temperature is low $T \ll \Delta E^+_n$, because in the opposite case thermally excited quasiparticles in the leads can overcome the energy barrier, and the sequential tunneling through high-energy states will determine the current.

Before considering the particular cases, let us perform all possible general calculations in (5.62). First of all, the tunneling Hamiltonian is the sum of left and right parts, we are interested only in the processes, which transfer electrons from the left to the right, and include one tunneling through the right junction and one tunneling through the left junction. Then, the initial state is a mixed state with different probabilities for the states $|k\rangle$ and $|q\rangle$ to be occupied or empty, following the tunneling theory we introduce the sum over all possible configurations of the initial state with corresponding occupation probabilities (distribution functions) $f^0_L(E_k)$ and $f^0_R(E_q)$. Thus, we obtain

$$\begin{aligned}\Gamma^{(2)}_{L\to R} = \frac{2\pi}{\hbar}\sum_{k\in L, q\in R} f^0_L(E_k)\left(1 - f^0_R(E_q)\right)\delta(E_i - E_f)\\ \times\left|\sum_{\lambda}\frac{\left\langle f_q\left|\hat{H}_{TR}\right|\lambda\right\rangle\left\langle\lambda\left|\hat{H}_{TL}\right|i_k\right\rangle + \left\langle f_q\left|\hat{H}_{TL}\right|\lambda\right\rangle\left\langle\lambda\left|\hat{H}_{TR}\right|i_k\right\rangle}{E_\lambda - E_i}\right|^2.\end{aligned} \tag{5.63}$$

The intermediate states $|\lambda\rangle$ are the states with one extra electron (or without one electron, i.e. with one extra hole) in the central system. Note, that the only thing we

assume is that the *charge* of the central system is the same in the initial and the final states (and $\pm e$ in the virtual intermediate state). However the *state* and *energy* of the central system can change after the tunneling event. In the last case the process is called *inelastic cotunneling*.

Up to now, all our calculations are general, now it is reasonable to consider separately the contributions of inelastic and elastic cotunneling.

5.5.1 Inelastic Cotunneling

Consider the final state as the state with one electron transferred from the state k in the left lead to the state q in the right lead with the change of the state of the system from $|\lambda_i\rangle$ with electron in the state α and empty state β to $|\lambda_f\rangle$ with electron removed from α to β

$$\left| f \right\rangle = c_q^\dagger c_k d_\beta^\dagger d_\alpha \left| i \right\rangle, \tag{5.64}$$

the energy conservation implies that

$$E_i = E_k + E_\alpha = E_f = E_q + E_\beta. \tag{5.65}$$

Due to mutual incoherence of these states, not the amplitudes, but the probabilities of different events should be summarized. Below we neglect all cross-terms with different indices λ, and apply

$$\left| \sum X_\lambda \right|^2 = \sum |X_\lambda|^2 . \tag{5.66}$$

In the metallic dots we can assume that the distribution over internal single-particle states is in equilibrium, and obtain

$$\Gamma_{in}^{(2)n} = \frac{2\pi}{\hbar} \sum_{k\in L, q\in R} \sum_{\alpha\beta} \left(\frac{1}{E_\beta + \Delta E_n^+ - E_k} + \frac{1}{E_q - \Delta E_{n-1}^+ - E_\alpha} \right)^2 |V_{\alpha q}|^2 |V_{\beta k}|^2$$
$$\times f_L^0(E_k) \left(1 - f_R^0(E_q)\right) \left(1 - f_S^0(E_\beta)\right) f_S^0(E_\alpha) \delta(E_k + E_\alpha - E_q - E_\beta). \tag{5.67}$$

The two terms in this expression correspond to two physical processes. The first one describes the jump (virtual!) of the extra electron from the state k in the left lead into the state β in the system, and then the *other* electron jumps through the second junction from the state α into the state q in the right lead (Fig. 5.15b). In the second process (Fig. 5.15d) first the electron jumps *from the system* into the right lead, and then the second electron jumps from the left lead. All other matrix elements of the tunneling Hamiltonians in the expression (5.63) are zero. The distribution functions describe as usually the probabilities of necessary occupied or empty states.

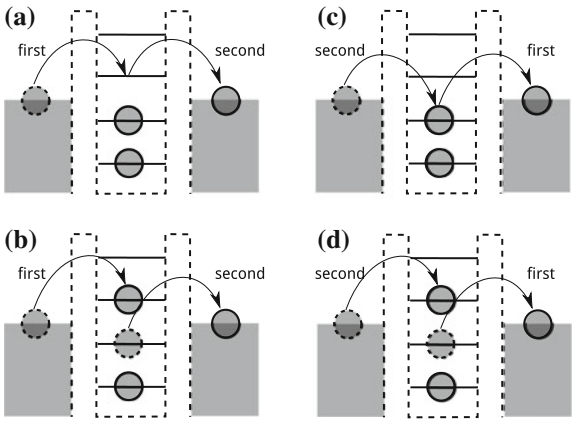

Fig. 5.15 Cotunneling processes, elastic **a**, **c** and inelastic **b**, **d**. Note that the "first" and "second" tunneling events are virtual and determine the virtual intermediate state $|\lambda\rangle$

In the wide-band limit with energy independent matrix elements we arrive at

$$\Gamma_{in}^{(2)n} = \frac{\hbar G_L G_R}{2\pi e^4} \int dE_k \int dE_q \int dE_\alpha \int dE_\beta f_L^0(E_k)\left(1 - f_S^0(E_\beta)\right) f_S^0(E_\alpha)\left(1 - f_R^0(E_q)\right) \times \left(\frac{1}{E_\beta + \Delta E_n^+ - E_k} + \frac{1}{E_q - \Delta E_{n-1}^+ - E_\alpha}\right)^2 \delta(E_k + E_\alpha - E_q - E_\beta). \tag{5.68}$$

At zero temperature the integrals in this expression can be evaluated analytically [5, 6].

The current is determined by the balance between forward and backward tunneling rates

$$J(V) = e\left(\Gamma_{in}^{(2)n}(V) - \Gamma_{in}^{(2)n}(-V)\right). \tag{5.69}$$

At finite temperatures and small voltage $V \ll \Delta E_n^+, \Delta E_{n-1}^+$, the analytical solution for the current is

$$J_{in} = \frac{\hbar G_L G_R}{12\pi e^3}\left(\frac{1}{\Delta E_n^+} - \frac{1}{\Delta E_{n-1}^+}\right)^2 \left[(eV)^2 + (2\pi T)^2\right] V. \tag{5.70}$$

The linear conductance can be estimated as

$$G \sim \frac{h}{e^2} G_L G_R \left(\frac{T}{E_C}\right)^2. \tag{5.71}$$

5.5.2 Elastic Cotunneling

So-called elastic cotunneling is a result of the second-order process excluded in previous consideration, namely

$$\Gamma_{el}^{(2)n} = \frac{2\pi}{\hbar} \sum_{k\in L, q\in R} \left| \sum_{\alpha\beta} \left(\frac{V_{\alpha q}^* V_{\beta k}}{E_\beta + \Delta E_n^+ - E_k} + \frac{V_{\alpha q}^* V_{\beta k}}{E_q - \Delta E_{n-1}^+ - E_\alpha} \right) \right|^2 \times f_L^0(E_k) \left(1 - f_R^0(E_q)\right) \delta(E_k - E_q). \tag{5.72}$$

For metallic dots the result of calculation is

$$\Gamma_{el}^{(2)n} = \frac{2\pi}{\hbar} \sum_{kq\alpha\beta} V_{\beta k} V_{\alpha k}^* V_{q\beta} V_{q\alpha}^* f_L^0(E_k) \left(1 - f_R^0(E_q)\right) \times F(E_\alpha, E_k, E_q) F(E_\beta, E_k, E_q) \delta(E_k - E_q), \tag{5.73}$$

$$F(E, E_k, E_q) = \frac{1 - f^0(E)}{E + \Delta E_n^+ - E_k} + \frac{f^0(E)}{E + \Delta E_{n-1}^+ - E_q}. \tag{5.74}$$

We shall not go into further details here and refer to the original publications. Elastic cotunneling though metallic dots is usually much smaller than inelastic, because the number of states available for elastic proces is small. It can be important only at very low temperatures and voltages, because it is linear in voltage at zero temperature, while the inelastic cotunneling is nonlinear (5.71).

Note once more, that the expressions for cotunneling current obtained above are valid only in the Coulomb blockade regime far from the degeneracy points (where the maxima of conductance are observed), when the sequential tunneling is suppressed, voltage and temperature are not very large.

References

1. C.W.J. Beenakker, Phys. Rev. B **44**, 1646 (1991)
2. H. van Houten, C.W.J. Beenakker, A.A.M. Staring, in *Single Charge Tunneling. NATO ASI Series B*, Vol. 294, ed. by H. Grabert, M.H. Devoret (Plenum, 1992), p. 167
3. J. von Delft, D.C. Ralph, Phys. Rep. **345**, 61 (2001)
4. I. Aleiner, P. Brouwer, L. Glazman, Phys. Rep. **358**(56), 309 (2002)
5. D.V. Averin, Y.V. Nazarov, *Macroscopic Quantum Tunneling of Charge and Co-tunneling*, *NATO ASI Series B*, vol. 294, chap. 6, (Plenum, 1992), p. 217
6. G. Schön, in *Quantum Dissipation and Transport* (Wiley-VCH, Heidelberg, 1998)

Chapter 6
Vibrons and Polarons

The second (after electron-electron interaction) ingredient of the nanoscale transport models are vibrons and electron-vibron interactions. It is especially important in molecular junctions because molecules are relatively flexible and vibrational effects are observed at current-voltage curves being one of the spectroscopic tools, and also can be significant at finite voltage producing some effects, for example the vibrational heating and switching.

In this chapter we consider basic electron-vibron phenomena. First we introduce vibrons (local vibrations, space localized version of phonons) and obtain a linear electron-vibron Hamiltonian in Sect. 6.1.

In Sect. 6.2 we consider the inelastic electron tunneling spectroscopy (IETS) for weak electron-vibron interaction and its description within the Persson-Baratoff model of inelastic STM spectroscopy.

In next sections we address the problem of strong electron-vibron interaction (polaron transport). In Sect. 6.3 we consider a polaron weakly and strongly coupled to the electrodes. We use canonical (Lang-Firsov) transformation to get the exact many-body eigenstates for isolated polarons.

In Sect. 6.4 we consider the exactly solvable case of inelastic tunneling through the polaron state in the single-particle approximation. In this approximation the Fermi see of electrons in the electrodes is ignored and only scattering of one electron is considered. The result can be used for tunneling at large energies, when the effect of other electrons can be neglected.

Finally in Sect. 6.5 we obtain the master equation for sequential tunneling and discuss the phenomena of Franck-Condon blockade.

D.A. Ryndyk, *Theory of Quantum Transport at Nanoscale*,
Springer Series in Solid-State Sciences 184,
DOI 10.1007/978-3-319-24088-6_6

6.1 Electron-Vibron Interaction in Nanosystems

6.1.1 Linear Vibrons

Vibrons are quantum local vibrations of nanosystems (Fig. 6.1), especially important in flexible molecules. In the linear regime the small displacements of the system can be expressed as linear combinations of the coordinates of the normal modes x_q, which are described by a set of independent linear oscillators with the Hamiltonian

$$\hat{H}_V^{(0)} = \sum_q \left(\frac{\hat{p}_q^2}{2m_q} + \frac{1}{2} m_q \omega_q^2 \hat{x}_q^2 \right). \tag{6.1}$$

The parameters m_q are determined by the microscopic theory, and $\hat{p}_q$ ($\hat{p}_q = -i\hbar \frac{\partial}{\partial x_q}$ in the x-representation) is the momentum conjugated to $\hat{x}_q$, $\left[\hat{x}_q, \hat{p}_q\right]_- = i\hbar$.

Let us outline briefly a possible way to calculate the normal modes of a molecule, and the relation between the positions of individual atoms and collective variables. We assume, that the atomic configuration of a system is determined mainly by the elastic forces, which are insensitive to the *transport* electrons. The dynamics of this system is determined by the *atomic* Hamiltonian

$$\hat{H}_{at} = \sum_n \frac{P_n^2}{2M_n} + W\left(\{\mathbf{R}_n\}\right), \tag{6.2}$$

where $W\left(\{\mathbf{R}_n\}\right)$ is the elastic energy, which includes also the static external forces and can be calculated by some *ab initio* method. Now define new generalized variables q_i with corresponding momentum p_i (as the generalized coordinates not only atomic positions, but also any other convenient degrees of freedom can be considered, for example, molecular rotations, center-of-mass motion, etc.)

$$\hat{H}_{at} = \sum_i \frac{p_i^2}{2m_i} + W\left(\{q_i\}\right), \tag{6.3}$$

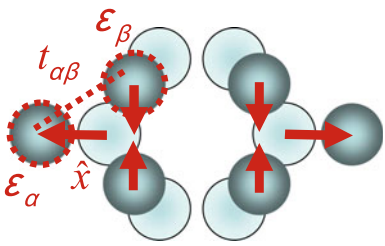

Fig. 6.1 A local molecular vibration. The *empty circles* show the equilibrium positions of the atoms. The energies ε_α, ε_β and the overlap integral $t_{\alpha\beta}$ are perturbed

and "masses" m_i, which should be considered as some parameters. The equilibrium coordinates q_i^0 are defined from the energy minimum, the set of equations is

$$\frac{\partial W\left(\{q_i^0\}\right)}{\partial q_i} = 0. \tag{6.4}$$

The equations for linear oscillations are obtained from the next order expansion in the deviations $\Delta q_i = q_i - q_i^0$

$$\hat{H}_{at} = \sum_i \frac{p_i^2}{2m_i} + \sum_{ij} \frac{\partial^2 W\left(\{q_j^0\}\right)}{\partial q_i \partial q_j} \Delta q_i \Delta q_j. \tag{6.5}$$

This Hamiltonian describes a set of coupled oscillators. Finally, applying the canonical transformation from Δq_i to new variables x_q (q is now the index of independent modes)

$$x_q = \sum_i C_{qi} q_i \tag{6.6}$$

we derive the Hamiltonian (6.1) together with the frequencies ω_q of vibrational modes.

It is useful to introduce the creation and annihilation operators

$$a_q^\dagger = \frac{1}{\sqrt{2}} \left(\sqrt{\frac{m_q \omega_q}{\hbar}} \hat{x}_q + \frac{i}{\sqrt{m_q \omega_q \hbar}} \hat{p}_q \right), \tag{6.7}$$

$$a_q = \frac{1}{\sqrt{2}} \left(\sqrt{\frac{m_q \omega_q}{\hbar}} \hat{x}_q - \frac{i}{\sqrt{m_q \omega_q \hbar}} \hat{p}_q \right), \tag{6.8}$$

in this representation the Hamiltonian of free vibrons is ($\hbar = 1$)

$$\hat{H}_V^{(0)} = \sum_q \omega_q a_q^\dagger a_q. \tag{6.9}$$

We consider only free noninteracting vibrons. In some cases it can be important to take into account the anharmonicity of vibrons, which takes place if the energy W ($\{\mathbf{R}_n\}$) is not a quadratic function. Thus, the next order expansion in $\Delta q_i = q_i - q_i^0$ should be calculated. This term gives additional terms to (6.9), which include several vibron operators and describe vibron-vibron interactions.

6.1.2 Electron-Vibron Hamiltonian

A system without vibrons is described as before by a basis set of states $|\alpha\rangle$ with energies ε_α and inter-state overlap integrals $t_{\alpha\beta}$, the model Hamiltonian of a noninteracting system is

$$\hat{H}_C^{(0)} = \sum_\alpha \left(\varepsilon_\alpha + e\varphi_\alpha(t)\right) d_\alpha^\dagger d_\alpha + \sum_{\alpha\neq\beta} t_{\alpha\beta} d_\alpha^\dagger d_\beta, \tag{6.10}$$

where $d_\alpha^\dagger$,d_α are creation and annihilation operators in the states $|\alpha\rangle$, and $\varphi_\alpha(t)$ is the (self-consistent) electrical potential (5.47). The index α is used to mark single-electron states (atomic orbitals) including the spin degree of freedom.

To establish the Hamiltonian describing the interaction of electrons with vibrons in nanosystems, we can start from the generalized Hamiltonian

$$\hat{H}_C = \sum_\alpha \tilde{\varepsilon}_\alpha \left(\{x_q\}\right) d_\alpha^\dagger d_\alpha + \sum_{\alpha\neq\beta} t_{\alpha\beta} \left(\{x_q\}\right) d_\alpha^\dagger d_\beta, \tag{6.11}$$

where the parameters are some functions of the vibronic normal coordinates x_q. Note that we consider now only the electronic states, which were excluded previously from the Hamiltonian (6.2), it is important to prevent double counting.

Expanding to the first order near the equilibrium state we obtain

$$\hat{H}_{ev} = \sum_\alpha \sum_q \frac{\partial \tilde{\varepsilon}_\alpha(0)}{\partial x_q} x_q d_\alpha^\dagger d_\alpha + \sum_{\alpha\neq\beta} \sum_q \frac{\partial t_{\alpha\beta}(0)}{\partial x_q} x_q d_\alpha^\dagger d_\beta, \tag{6.12}$$

where $\tilde{\varepsilon}_\alpha(0)$ and $t_{\alpha\beta}(0)$ are unperturbed values of the energy and the overlap integral. In the quantum limit the normal coordinates should be treated as operators, and in the second-quantized representation the interaction Hamiltonian is

$$\hat{H}_{ev} = \sum_{\alpha\beta} \sum_q \lambda_{\alpha\beta}^q (a_q + a_q^\dagger) d_\alpha^\dagger d_\beta. \tag{6.13}$$

This Hamiltonian is similar to the usual electron-phonon Hamiltonian, but the vibrations are like localized phonons and q is an index labeling them, not the wave-vector. We include both diagonal coupling, which describes a change of the electrostatic energy with the distance between atoms, and the off-diagonal coupling, which describes the dependence of the matrix elements $t_{\alpha\beta}$ over the distance between atoms.

The full Hamiltonian

$$\hat{H} = \hat{H}_C^0 + \hat{H}_V + \hat{H}_L + \hat{H}_R + \hat{H}_T \tag{6.14}$$

is the sum of the noninteracting Hamiltonian $\hat{H}_C^0$, the Hamiltonians of the leads $\hat{H}_{R(L)}$, the tunneling Hamiltonian $\hat{H}_T$ describing the system-to-lead coupling, the vibron Hamiltonian $\hat{H}_V$ including electron-vibron interaction and coupling of vibrations to the environment (describing dissipation of vibrons).

Vibrons and the electron-vibron coupling are described by the Hamiltonian ($\hbar = 1$)

$$\hat{H}_V = \sum_q \omega_q a_q^\dagger a_q + \sum_{\alpha\beta} \sum_q \lambda_{\alpha\beta}^q (a_q + a_q^\dagger) d_\alpha^\dagger d_\beta + \hat{H}_{env}. \tag{6.15}$$

The first term represents free vibrons with the energy $\hbar\omega_q$. The second term is the electron-vibron interaction. The remaining part $\hat{H}_{env}$ describes dissipation of vibrons due to interaction with other degrees of freedom, we do not consider the details in this chapter.

The Hamiltonians of the right (R) and left (L) leads read as usual

$$\hat{H}_{i=L(R)} = \sum_{k\sigma} (\varepsilon_{ik\sigma} + e\varphi_i) c_{ik\sigma}^\dagger c_{ik\sigma}, \tag{6.16}$$

φ_i are the electrical potentials of the leads. Finally, the tunneling Hamiltonian

$$\hat{H}_T = \sum_{i=L,R} \sum_{k\sigma,\alpha} \left(V_{ik\sigma,\alpha} c_{ik\sigma}^\dagger d_\alpha + V_{ik\sigma,\alpha}^* d_\alpha^\dagger c_{ik\sigma} \right) \tag{6.17}$$

describes the hopping between the leads and the molecule. A direct hopping between two leads is neglected.

The simplest example of the considered model is a single-level model (Fig. 6.2) with the Hamiltonian

$$\hat{H} = \tilde{\varepsilon}_0 d^\dagger d + \omega_0 a^\dagger a + \lambda \left(a^\dagger + a\right) d^\dagger d + \sum_{ik} \left[\tilde{\varepsilon}_{ik} c_{ik}^\dagger c_{ik} + V_{ik} c_{ik}^\dagger d + h.c. \right], \tag{6.18}$$

where the first and the second terms describe free electron state and free vibron, the third term is electron-vibron interaction, and the rest is the Hamiltonian of the leads and tunneling coupling ($i = L, R$ is the lead index).

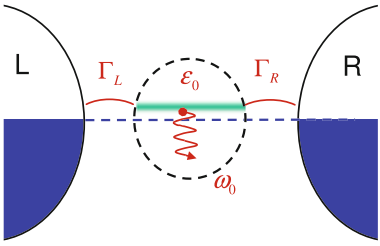

Fig. 6.2 Single-level electron-vibron model

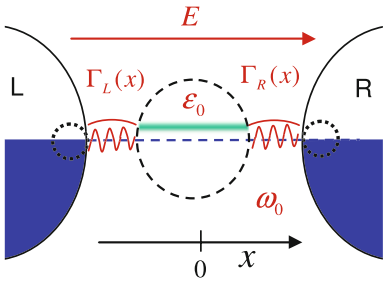

Fig. 6.3 A center-of-mass vibration

The other important case is a center-of-mass motion of molecules between the leads (Fig. 6.3). Here not the internal overlap integrals, but the coupling to the leads $V_{ik\sigma,\alpha}(x)$ is fluctuating. This model is easily reduced to the general model (6.15), if we consider additionally two not flexible states in the left and right leads (two atoms most close to a system), to which the central system is coupled (shown by the dotted circles).

The tunneling Hamiltonian includes x-dependent matrix elements, considered in linear approximation

$$H_T = \sum_{i=L,R} \sum_{k\sigma,\alpha} \left(V_{ik\sigma,\alpha}(\hat{x}) c^\dagger_{ik\sigma} d_\alpha + h.c. \right), \tag{6.19}$$

$$V_{L,R}(x) = V_0 e^{\mp \hat{x}/L} \approx V_0 \left(1 \mp \frac{\hat{x}}{L} \right). \tag{6.20}$$

Consider now a single-level molecule ($\alpha \equiv 0$) and extend our system, including two additional states from the left ($\alpha \equiv l$) and right ($\alpha \equiv r$) sides of a molecule, which are coupled to the central state through x-dependent matrix elements, and to the leads in a usual way through $\Gamma_{L(R)}$. Then the Hamiltonian is of linear electron-vibron type

$$\hat{H}_{M+V} = \sum_{\alpha=l,0,r} (\varepsilon_\alpha + e\varphi_\alpha) d^\dagger_\alpha d_\alpha + t_l (d^\dagger_l d_0 + h.c.) + t_r (d^\dagger_r d_0 + h.c.)$$
$$+ \omega_0 a^\dagger a + (a + a^\dagger) \left(\lambda_0 d^\dagger_0 d_0 - \lambda_l (d^\dagger_l d_0 + h.c.) + \lambda_r (d^\dagger_r d_0 + h.c.) \right). \tag{6.21}$$

6.2 Inelastic Electron Tunneling Spectroscopy (IETS)

We start from the case of weak electron-vibron interaction, when the perturbation theory can be used. The observed change of the voltage-current curve is small in this case. Nevertheless, the inelastic effects play an important role, being the powerful method of tunneling spectroscopy. The characteristic features of the inelastic

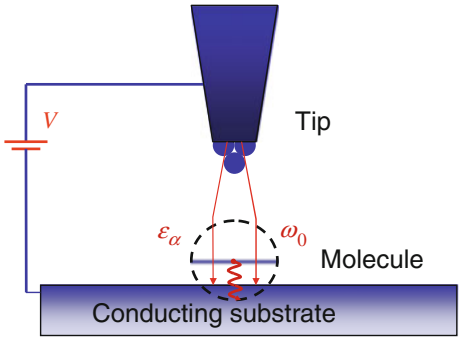

Fig. 6.4 The Persson-Baratoff model of the STM-to-molecule junction

electron scattering can be used to determine the frequencies of vibrons and identify the quantum system (any single molecule has the unique vibronic spectrum).

To demonstrate the peculiarities of the IETS of single molecules, we consider the Persson-Baratoff [1] model of the STM spectroscopy (Fig. 6.4). In this model, the system (molecule) is assumed to be strongly coupled to a substrate, so that any electron state $|\alpha\rangle$ of the system can be included into the basis set of the system + substrate states $|q\rangle$, the system is always in equilibrium and the wave function $|\alpha\rangle$ is defined by the projection

$$|\alpha\rangle = \sum_q \langle q|\alpha\rangle |q\rangle. \tag{6.22}$$

The state $|\alpha\rangle$, and therefore the states $|q\rangle$, are coupled to the states $|k\rangle$ of the STM tip by the usual tunneling Hamiltonian

$$\hat{H}_T = \sum_{kq} \left(V_{kq} c_k^\dagger c_q + V_{kq}^* c_q^\dagger c_k \right). \tag{6.23}$$

The problem is reduced to the tunneling from the "left" $|k\rangle$ to the "right" $|q\rangle$ states, but the state $|\alpha\rangle$ is coupled to a vibron with frequency ω_0, this coupling leads to a new inelastic channel of tunneling.

The electron-vibron Hamiltonian is

$$\hat{H}_{ev} = \lambda(a + a^\dagger) d_\alpha^\dagger d_\alpha = \lambda(a + a^\dagger) \sum_{qq'} \langle q'|\alpha\rangle\langle\alpha|q\rangle c_{q'}^\dagger c_q = \lambda(a + a^\dagger) \sum_{qq'} V_{q'q}^v c_{q'}^\dagger c_q. \tag{6.24}$$

Assuming that both the tunneling coupling and the electron-vibron interaction are weak, we can apply the perturbation theory to the Hamiltonian $\hat{H} = \hat{H}_0 + \hat{H}_1$

$$\hat{H}_0 = \sum_k \tilde{\varepsilon}_k c_k^\dagger c_k + \sum_q \tilde{\varepsilon}_q c_q^\dagger c_q + \omega_0 a^\dagger a, \tag{6.25}$$

$$\hat{H}_1 = \hat{H}_T + \hat{H}_{ev}. \tag{6.26}$$

The many-particle eigenstates $|\hat{k}, \hat{q}, m\rangle$ of the Hamiltonian $\hat{H}_0$ are characterized by three sets of quantum numbers: $\hat{k}$ is the occupation of the single particle states $|k\rangle$ in the tip (see (5.50)), $\hat{q}$ is the occupation of states $|q\rangle$ in the substrate, and m is the number of vibrons.

The transition rate from some initial state $|i\rangle$ into a final state $|f\rangle$ up to a second order in the perturbation Hamiltonian $\hat{H}_1$ is

$$\Gamma_{i\to f}^{(1+2)} = \frac{2\pi}{\hbar}\left|\left\langle f\left|\hat{H}_1\right|i\right\rangle + \sum_{\lambda}\frac{\left\langle f\left|\hat{H}_1\right|\lambda\right\rangle\left\langle\lambda\left|\hat{H}_1\right|i\right\rangle}{E_i - E_\lambda + i\eta}\right|^2 \delta(E_i - E_f). \tag{6.27}$$

What are possible final states $|\hat{k}_f, \hat{q}_f, m_f\rangle$ for a given initial state $|\hat{k}_i, \hat{q}_i, m_i\rangle$? The only nonzero *single-particle* matrix elements of the operators $\hat{H}_T$ and $\hat{H}_{ve}$ are

$$\langle q, m|\hat{H}_T|k, m\rangle = \langle q, m|V_{qk}c_q^\dagger c_k|k, m\rangle = V_{qk}, \tag{6.28}$$

the tunneling Hamiltonian transfer the electrons between left and right states, and does not change the number of vibrons,

$$\langle q, m+1|\hat{H}_{ev}|q', m\rangle = \langle q, m+1|\lambda(a+a^\dagger)V_{qq'}^v c_q^\dagger c_{q'}|q', m\rangle = \lambda\sqrt{m+1}V_{qq'}^v, \tag{6.29}$$

$$\langle q, m-1|\hat{H}_{ev}|q', m\rangle = \langle q, m-1|\lambda(a+a^\dagger)V_{qq'}^v c_q^\dagger c_{q'}|q', m\rangle = \lambda\sqrt{m}V_{qq'}^v, \tag{6.30}$$

the matrix elements of the electron-vibron Hamiltonian describe the inelastic scattering of electrons in the substrate with emission (absorption) of one vibron.

To apply the rate formula (6.27) we should take into account the incoherence and equilibrium distribution of electrons in the leads, which means that all initial states $|\hat{k}_i, \hat{q}_i, m_i\rangle$, as well as all final states $|\hat{k}_f, \hat{q}_f, m_f\rangle$, are incoherent and probabilities should be summarized instead of quantum amplitudes. The total tunneling rate of one electron from the tip (left) to the substrate (right) is a sum of all possible single-electron events.

For the elastic processes we get

$$\Gamma_{L\to R}^{(el)} = \frac{2\pi}{\hbar}\sum_{k\in L, q\in R}\left|V_{qk}\right|^2 f_L^0(E_k)\left(1 - f_R^0(E_q)\right)\delta(E_k - E_q), \tag{6.31}$$

and for the inelastic processes with emission of one vibron ($m \to m+1$)

$$\Gamma^{(in)}_{L\to R} = \frac{2\pi}{\hbar}\lambda^2 \sum_{k\in L, q\in R}\sum_m f^0_L(E_k)\left(1 - f^0_R(E_q)\right) f^0_B(m\omega_0)\delta(E_k - E_q - \omega_0) \times \left|\sum_{q'} \frac{\sqrt{m+1}V^v_{qq'}V_{q'k}}{E_k - E_{q'} + i\eta}\right|^2. \tag{6.32}$$

The tunneling rate for the inelastic process with absorption of one vibron ($m \to m-1$) is given by the same expression with $-\omega_0$ replaced by $+\omega_0$ in the delta-function, and $\sqrt{m+1}$ replaced by $\sqrt{m}$.

Now we restrict ourselves by the low temperatures $T \ll \omega_0$, so that thermally excited vibrons can be neglected, and assume that emitted vibrons are dissipated fast enough, in that case only one inelastic process with vibron emission is possible, which can be shown symbolically as

$$|k, 0\rangle \xrightarrow{\hat{H}_T} |q', 0\rangle \xrightarrow{\hat{H}_{ev}} |q, 1\rangle. \tag{6.33}$$

In this short-hand notation we show only the essential degrees of freedom, namely the electron from the initial state $|k\rangle$ in the tip tunnels into the state $|q'\rangle$ in the substrate (the first virtual transition), and then one vibron is emitted accompanied by the transition of the electron from the state $|q'\rangle$ into the final state $|q\rangle$. The first transition here is due to the tunneling Hamiltonian, and the second is due to the electron-vibron coupling.

The inelastic tunneling rate in this case is

$$\Gamma^{(in)}_{L\to R} = \frac{2\pi}{\hbar}\lambda^2 \sum_{k\in L, q\in R} f^0_L(E_k)\left(1 - f^0_R(E_q)\right)\delta(E_k - E_q - \omega_0) \times \left|\sum_{q'} \frac{V^v_{qq'}V_{q'k}}{E_k - E_{q'} + i\eta}\right|^2. \tag{6.34}$$

Making the natural assumption that the density of states in the tip ρ_{tip} is energy-independent near the Fermi-surface, and neglecting possible energy dependence of the tunneling and scattering matrix elements V_{kq} and $V_{qq'}$ we obtain the Persson-Baratoff formula for the inelastic differential conductance at finite voltage (we take $\varepsilon_F = 0$)

$$G(V) = \frac{ed\Gamma^{(in)}_{L\to R}}{dV} = \frac{4\pi e^2}{\hbar}\lambda^2|V|^2\rho_{tip}\rho_\alpha\,(eV - \omega_0)\left|\int d\varepsilon' \frac{\rho_\alpha(\varepsilon')}{\varepsilon' - eV - i\eta}\right|^2 \theta(eV - \omega_0), \tag{6.35}$$

note, that the voltage V is explicitly presented in this expression, and the density of states of the molecular level $\rho_\alpha(\varepsilon)$ is defined as

$$\rho_\alpha(\varepsilon) = \sum_q |\langle q|\alpha\rangle|^2 \delta(\varepsilon - \varepsilon_q). \tag{6.36}$$

The conductance can be calculated analytically if we assume the Lorentzian form for the molecular density of states

$$\rho_\alpha(\varepsilon) = \frac{\Gamma}{(\varepsilon - \varepsilon_\alpha)^2 + (\Gamma/2)^2}, \tag{6.37}$$

substituting this expression into (6.35) we find

$$G(V) = \frac{4\pi^3 e^2 \lambda^2 |V|^2 \rho_{tip}}{\hbar} \frac{\Gamma^3 \theta(eV - \omega_0)}{\left[(eV - \omega_0 - \varepsilon_\alpha)^2 + (\Gamma/2)^2\right]\left[(eV - \varepsilon_\alpha)^2 + (\Gamma/2)^2\right]^2}. \tag{6.38}$$

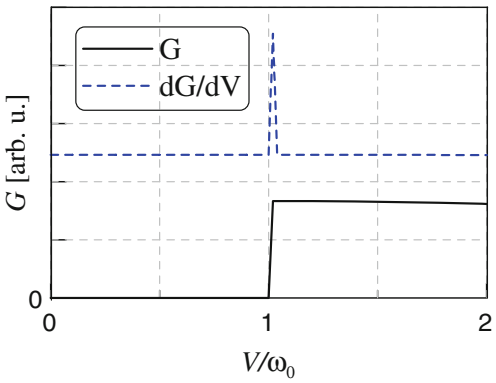

Fig. 6.5 The differential conductance and its derivative as a function of voltage for a broad density of states

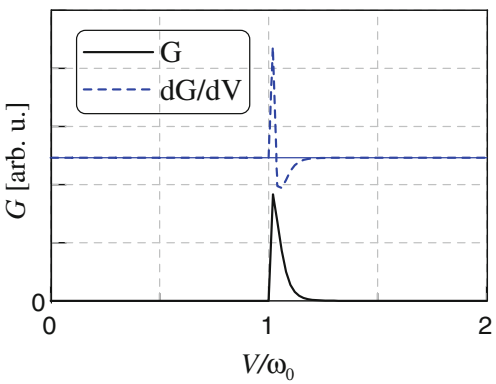

Fig. 6.6 The differential conductance and its derivative as a function of voltage at small broadening and $\omega_0 > \varepsilon_\alpha$

Now it is interesting to compare the inelastic conductance in two limiting cases, the broad molecular density of states (strong coupling to a substrate, Fig. 6.5), and small broadening (Fig. 6.6).

6.3 Local Polaron

Now let us start to consider the situation, when the electron-vibron interaction is strong. For an isolated system with the Hamiltonian, including only diagonal terms,

$$\hat{H}_{S+V} = \sum_{\alpha} \tilde{\varepsilon}_{\alpha} d_{\alpha}^{\dagger} d_{\alpha} + \sum_{q} \omega_q a_q^{\dagger} a_q + \sum_{\alpha} \sum_{q} \lambda_{\alpha}^{q} (a_q + a_q^{\dagger}) d_{\alpha}^{\dagger} d_{\alpha}, \tag{6.39}$$

the problem can be solved exactly. This solution, as well as the method of the solution (canonical transformation), plays an important role in the theory of electron-vibron systems, and we consider it in detail.

6.3.1 Canonical (Lang-Firsov) Transformation

Let's start from the simplest case. The single-level electron-vibron model is described by the Hamiltonian

$$\hat{H}_{S+V} = \tilde{\varepsilon}_0 d^{\dagger} d + \omega_0 a^{\dagger} a + \lambda \left(a^{\dagger} + a\right) d^{\dagger} d, \tag{6.40}$$

where the first and the second terms describe free electron state and free vibron, and the third term is the electron-vibron interaction.

This Hamiltonian is diagonalized by the canonical transformation (called "Lang-Firsov" or "polaron")

$$\bar{H} = \hat{S}^{-1} \hat{H} \hat{S}, \tag{6.41}$$

with

$$\hat{S} = \exp\left[-\frac{\lambda}{\omega_0} \left(a^{\dagger} - a\right) d^{\dagger} d\right], \tag{6.42}$$

the Hamiltonian (6.40) is transformed as

$$\bar{H}_{S+V} = \hat{S}^{-1} \hat{H}_{S+V} \hat{S} = \tilde{\varepsilon}_0 \bar{d}^{\dagger} \bar{d} + \omega_0 \bar{a}^{\dagger} \bar{a} + \lambda \left(\bar{a}^{\dagger} + \bar{a}\right) \bar{d}^{\dagger} \bar{d}, \tag{6.43}$$

it has the same form as (6.40) with new operators, it is a trivial consequence of the general property

$$\hat{S}^{-1}\left(\hat{f}_1\hat{f}_2\hat{f}_3\ldots\right)\hat{S} = (\hat{S}^{-1}\hat{f}_1\hat{S})(\hat{S}^{-1}\hat{f}_2\hat{S})(\hat{S}^{-1}\hat{f}_3\hat{S})\ldots = \bar{f}_1\bar{f}_2\bar{f}_3\ldots \tag{6.44}$$

and new single-particle operators are

$$\bar{a} = \hat{S}^{-1}a\hat{S} = a - \frac{\lambda}{\omega_0}d^\dagger d, \tag{6.45}$$

$$\bar{a}^\dagger = \hat{S}^{-1}a^\dagger\hat{S} = a^\dagger - \frac{\lambda}{\omega_0}d^\dagger d, \tag{6.46}$$

$$\bar{d} = \hat{S}^{-1}d\hat{S} = \exp\left[-\frac{\lambda}{\omega_0}\left(a^\dagger - a\right)\right]d, \tag{6.47}$$

$$\bar{d}^\dagger = \hat{S}^{-1}d^\dagger\hat{S} = \exp\left[\frac{\lambda}{\omega_0}\left(a^\dagger - a\right)\right]d^\dagger. \tag{6.48}$$

Substituting these expressions into (6.43) we get finally

$$\bar{H}_{S+V} = \left(\tilde{\varepsilon}_0 - \frac{\lambda^2}{\omega_0}\right)d^\dagger d + \omega_0 a^\dagger a. \tag{6.49}$$

We see that the electron-vibron Hamiltonian (6.40) is equivalent to the free-particle Hamiltonian (6.49). This equivalence means that any quantum state $|\bar{\psi}_\lambda\rangle$, obtained as a solution of the Hamiltonian (6.49) is one-to-one equivalent to the state $|\psi_\lambda\rangle$ as a solution of the initial Hamiltonian (6.40), with the same matrix elements for any operator

$$\langle\bar{\psi}_\lambda|\bar{f}|\bar{\psi}_\lambda\rangle = \langle\psi_\lambda|\hat{f}|\psi_\lambda\rangle, \tag{6.50}$$

$$\bar{f} = \hat{S}^{-1}\hat{f}\hat{S}, \tag{6.51}$$

$$|\bar{\psi}_\lambda\rangle = \hat{S}^{-1}|\psi_\lambda\rangle. \tag{6.52}$$

It follows immediately that the eigenstates of the free-particle Hamiltonian are

$$|\bar{\psi}_{nm}\rangle = |n = 0, 1; m = 0, 1, 2, \ldots\rangle = (d^\dagger)^n\frac{(a^\dagger)^m}{\sqrt{m!}}|0\rangle, \tag{6.53}$$

and the eigen-energies are

$$E(n, m) = \left(\tilde{\varepsilon}_0 - \frac{\lambda^2}{\omega_0}\right)n + \omega_0 m. \tag{6.54}$$

The eigenstates of the *initial* Hamiltonian (6.40) are

$$|\psi_{nm}\rangle = \hat{S}|\bar{\psi}_{nm}\rangle = e^{-\frac{\lambda}{\omega_0}(a^\dagger - a)d^\dagger d}(d^\dagger)^n\frac{(a^\dagger)^m}{\sqrt{m!}}|0\rangle, \tag{6.55}$$

with the same quantum numbers (n, m) and the same energies (6.54). This representation of the eigenstates demonstrates clearly the collective nature of the excitations, but it is inconvenient for practical calculations.

To conclude, after the canonical transformation we have two equivalent models: (1) the initial model (6.40) with the eigenstates (6.55); and (2) the *fictional* free-particle model (6.49) with the eigenstates (6.53). We shall call this second model *polaron representation*. The relation between the models is established by (6.50)–(6.52). It is also clear from the Hamiltonian (6.43), that the operators $\bar{d}^\dagger$, $\bar{d}$, $\bar{a}^\dagger$, and $\bar{a}$ describe the initial electrons and vibrons in the fictional model.

Note, that the problem can be solved by the same method in the multilevel case

$$\hat{H}_{S+V} = \sum_\alpha \tilde{\varepsilon}_\alpha d_\alpha^\dagger d_\alpha + \sum_q \omega_q a_q^\dagger a_q + \sum_\alpha \sum_q \lambda_\alpha^q (a_q + a_q^\dagger) d_\alpha^\dagger d_\alpha, \tag{6.56}$$

but not for the off-diagonal coupling.

The canonical transformation is then given by

$$\hat{S} = \exp\left[- \sum_{\alpha q} \frac{\lambda_\alpha^q}{\omega_0} \left(a_q^\dagger - a_q \right) d_\alpha^\dagger d_\alpha \right]. \tag{6.57}$$

6.3.2 Spectral Function

As it is clear from (6.55), the states without electrons $|0, m\rangle$ are the states with the definite number of vibrons in both models (both Hamiltonians are simply the same in this case), but the ground state of the system with one electron $|1, 0\rangle$ actually is a superposition of many vibrational states in the initial model. We can consider also the state $\bar{d}^\dagger |0, m\rangle$, which is the state with one electron and fixed number of vibrons in the initial model, and is *not the eigenstate* of this model. Expanding the state $|1, 0\rangle$ into the series

$$|1, 0\rangle = \sum_m c_m \bar{d}^\dagger |0, m\rangle, \tag{6.58}$$

we define the contribution of different vibronic states into the ground state with one electron

$$\rho_m = |c_m|^2 = \left| \langle 0, m | \bar{d} | 1, 0 \rangle \right|^2. \tag{6.59}$$

This function can be called spectral function (density of states) because it shows the contribution of states with different energy into the ground state.

To calculate the matrix element, we take

$$|1,0\rangle = d^\dagger|0\rangle, \tag{6.60}$$

$$|0,m\rangle = \frac{(a^\dagger)^m}{\sqrt{m!}}|0\rangle, \tag{6.61}$$

$$\bar{d} = e^{-\frac{\lambda}{\omega_0}(a^\dagger - a)}d, \tag{6.62}$$

and apply the Feynman's disentangling theorem

$$e^{A+B} = e^A e^B e^{-[A,B]_-/2}, \tag{6.63}$$

the theorem is valid when the commutator $[A, B]_-$ commutes itself with A and B, which is in our case

$$[A, B]_- = \left[-\frac{\lambda}{\omega_0}a^\dagger, \frac{\lambda}{\omega_0}a\right]_- = \left(\frac{\lambda}{\omega_0}\right)^2, \tag{6.64}$$

thus the theorem can be used. Now we can proceed with the calculation

$$\begin{aligned}\langle 0,m|\bar{d}|1,0\rangle =& \langle 0,m|e^{-\frac{\lambda}{\omega_0}(a^\dagger - a)}dd^\dagger|0\rangle = \\ & e^{-(\lambda/\omega_0)^2/2}\sum_{n=0}^{\infty}\sum_{n'=0}^{\infty}\left\langle 0,m\left|\left(-\frac{\lambda}{\omega_0}\right)^{n'}\frac{(a^\dagger)^{n'}}{n'!}\left(\frac{\lambda}{\omega_0}\right)^n\frac{(a)^n}{n!}\right|0\right\rangle,\end{aligned} \tag{6.65}$$

where we used the relation $dd^\dagger|0\rangle = (1 - d^\dagger d)|0\rangle = |0\rangle$, the Feynman's theorem, and expand the exponents into series. Obviously, the only nonzero contribution is from the term $n = 0, n' = m$. Finally we obtain

$$\langle 0,m|\bar{d}|1,0\rangle = \left(-\frac{\lambda}{\omega_0}\right)^m\frac{e^{-(\lambda/\omega_0)^2/2}}{\sqrt{m!}}, \tag{6.66}$$

and the density of states is

$$\rho_m = \left(\frac{\lambda}{\omega_0}\right)^{2m}\frac{e^{-(\lambda/\omega_0)^2}}{m!}. \tag{6.67}$$

6.3.3 Weak Coupling to the Metallic Lead

Before we considered an isolated system. Now assume that it is only very weakly coupled to the metallic lead (Fermi sea of electrons) with $\Gamma \ll \lambda^2/\omega_0$. The energy

spectrum is not changed, but the population of the system is determined by the equilibrium with the lead.

At zero temperature the system is in its ground state: neutral $|0, 0\rangle$ if $\tilde{\varepsilon} - \lambda^2/\omega_0 > 0$, and charged $|1, 0\rangle$ if $\tilde{\varepsilon} - \lambda^2/\omega_0 < 0$.

At finite temperature the probability to find the system in the state $|n, m\rangle$ is given by the Gibbs distribution

$$p(n, m) = \frac{1}{Z} \exp\left(-\frac{E(n, m)}{T}\right), \tag{6.68}$$

with the energy (6.54), the normalization coefficient is determined from the condition

$$\sum_{nm} p(n, m) = 1. \tag{6.69}$$

The average number of electrons is

$$\langle n \rangle = \sum_{m} p(1, m) = \frac{1}{Z} \sum_{m} \exp\left(-\frac{E(1, m)}{T}\right). \tag{6.70}$$

The situation in this case is completely the same as for the single-electron box, at temperature $T \sim |\tilde{\varepsilon} - \lambda^2/\omega_0|$ there are equal probabilities to find the system in neutral or charged state.

6.3.4 *Strong Coupling to the Metallic Lead*

Now consider the strong coupling to the lead $\Gamma \gg \lambda^2/\omega_0$. The energy spectrum is essentially modified in this case, and the simple arguments of the previous subsection can not be applied. The polaron transformation does not help, because the tunneling terms are nontrivially modified.

Let us consider the limit $\Gamma \gg \omega_0$. In that case the simple mean-field approximation can be used. Consider first the vibrons. While the frequency of vibrons is much smaller than the tunneling rate, vibrons see only the average electron charge density (the Born-Oppenheimer approximation). It means that the vibron Hamiltonian is coupled to the electron part only through the "mean field" $\langle n \rangle = \langle d^\dagger d \rangle$

$$\hat{H}_V = \omega_0 a^\dagger a + \lambda \langle n \rangle \left(a^\dagger + a\right). \tag{6.71}$$

The solution of this problem can be easily obtained by the equation-of-motion method

$$i\frac{\partial a}{\partial t} = \left[a, \hat{H}_V\right]_- = \omega_0 a + \lambda\langle n\rangle, \tag{6.72}$$

$$i\frac{\partial a^\dagger}{\partial t} = \left[a^\dagger, \hat{H}_V\right]_- = -\omega_0 a^\dagger - \lambda\langle n\rangle. \tag{6.73}$$

From these two equations we obtain in the stationary case

$$\langle a + a^\dagger\rangle = -\frac{2\lambda}{\omega_0}\langle n\rangle. \tag{6.74}$$

The self-consistent problem is obtained if we consider now the electron part of the Hamiltonian as a single-electron problem with the effective energy

$$\varepsilon^* = \tilde{\varepsilon}_0 - \lambda\langle a + a^\dagger\rangle = \tilde{\varepsilon}_0 - \frac{2\lambda^2}{\omega_0}\langle n\rangle, \tag{6.75}$$

taking the lead and tunneling into account we get

$$\hat{H}_e = \varepsilon^* d^\dagger d + \sum_{k\sigma}\varepsilon_{k\sigma}c^\dagger_{k\sigma}c_{k\sigma} + \sum_{k\sigma}\left(V_{ik\sigma}c^\dagger_{ik\sigma}d + V^*_{ik\sigma}d^\dagger c_{ik\sigma}\right). \tag{6.76}$$

The density of states is given by the Lorentzian

$$\rho(\varepsilon) = \frac{1}{2\pi}\frac{\Gamma}{(\varepsilon - \varepsilon^*)^2 + (\Gamma/2)^2}, \tag{6.77}$$

and the average number of electrons is

$$\langle n\rangle = \int_{-\infty}^{\infty}\rho(\varepsilon)f^0(\varepsilon)d\varepsilon, \tag{6.78}$$

where $f^0(\varepsilon)$ is the Fermi distribution function.

6.4 Inelastic Tunneling in the Single-Particle Approximation

In this section we consider a special case of a *single particle transmission* through an electron-vibron system. It means that we consider a system coupled to the leads, but without electrons in the leads. This can be considered equivalently as the limit of large electron level energy ε_0 (far from the Fermi surface in the leads).

6.4.1 The Inelastic Transmission Matrix

The inelastic *transmission matrix* $T(\varepsilon', \varepsilon)$ describes the probability that an electron with energy ε, incident from one lead, is transmitted with the energy ε' into a second lead. The transmission function can be defined as the total transmission probability

$$T(\varepsilon) = \int T(\varepsilon', \varepsilon) d\varepsilon'. \tag{6.79}$$

For a noninteracting single-level system the transmission matrix is

$$T^0(\varepsilon', \varepsilon) = \frac{\Gamma_R(\varepsilon)\Gamma_L(\varepsilon)\delta(\varepsilon - \varepsilon')}{(\varepsilon - \varepsilon_0 - \Lambda(\varepsilon))^2 + (\Gamma(\varepsilon)/2)^2}, \tag{6.80}$$

where $\Gamma(\varepsilon) = \Gamma_L(\varepsilon) + \Gamma_R(\varepsilon)$ is the level-width function, and $\Lambda(\varepsilon)$ is the real part of the self-energy.

To understand the general structure of the transmission matrix, let us consider again the polaron transformation (6.41) and (6.42) applied to the tunneling Hamiltonian

$$\hat{H}_T = \sum_{i=L,R} \sum_{k\sigma} \left(V_{ik\sigma} c^\dagger_{ik\sigma} d + V^*_{ik\sigma} d^\dagger c_{ik\sigma} \right) \tag{6.81}$$

The electron operators in the left and right leads $c_{ik\sigma}$ are not changed by this operation, but the dot operators d_α, $d^\dagger_\alpha$ are changed in accordance with (6.47) and (6.48). The transformed Hamiltonian is

$$\bar{H}_T = \sum_{i=L,R} \sum_{k\sigma} \left(V_{ik\sigma} e^{-\frac{\lambda}{\omega_0}(a^\dagger - a)} c^\dagger_{ik\sigma} d + V^*_{ik\sigma} e^{\frac{\lambda}{\omega_0}(a^\dagger - a)} d^\dagger c_{ik\sigma} \right). \tag{6.82}$$

Now we clearly see the problem: while the new dot Hamiltonian (6.49) is very simple and exactly solvable, the new tunneling Hamiltonian (6.82) is complicated. Moreover, instead of one linear electron-vibron interaction term, the exponent in (6.82) produces all powers of vibronic operators. Actually, we simply move the complexity from one place to the other. This approach works well, if the tunneling can be considered as a perturbation, we consider it in the next section. In the general case the problem is quite difficult, but in the single-particle approximation it can be solved exactly [2–4].

But first, we can do some general conclusions, based on the form of the tunneling Hamiltonian (6.82). Expanding the exponent in the same way as before, we get

$$\bar{H}_T = \sum_{i=L,R} \sum_{k\sigma} \left(V_{ik\sigma} c^\dagger_{ik\sigma} d \left[\alpha_0 + \sum_{m=1}^{\infty} \alpha_m \left((a^\dagger)^m + a^m \right) \right] + h.c. \right), \tag{6.83}$$

with the coefficients

$$\alpha_m = \left(-\frac{\lambda}{\omega_0}\right)^m \frac{e^{-(\lambda/\omega_0)^2/2}}{m!}. \tag{6.84}$$

This complex Hamiltonian has a very clear interpretation, the tunneling of one electron from the right to the left lead is accompanied by the excitation of vibrons. The energy conservation implies that

$$\varepsilon - \varepsilon' = \pm m\omega_0, \tag{6.85}$$

so that the inelastic tunneling with emission or absorption of vibrons is possible.

6.4.2 *Exact Solution in the Wide-Band Limit*

It is convenient to introduce the dimensionless electron-vibron coupling constant

$$g = \left(\frac{\lambda}{\omega_0}\right)^2. \tag{6.86}$$

At zero temperature the solution is

$$T(\varepsilon', \varepsilon) = \Gamma_L \Gamma_R e^{-2g} \sum_{m=0}^{\infty} \frac{g^m}{m!} \delta(\varepsilon - \varepsilon' - m\omega_0)$$
$$\times \left| \sum_{j=0}^{m} (-1)^j \frac{m!}{j!(m-j)!} \sum_{l=0}^{\infty} \frac{g^l}{l!} \frac{1}{\varepsilon - \varepsilon_0 + g\omega_0 - (j+l)\omega_0 + i\Gamma/2} \right|^2, \tag{6.87}$$

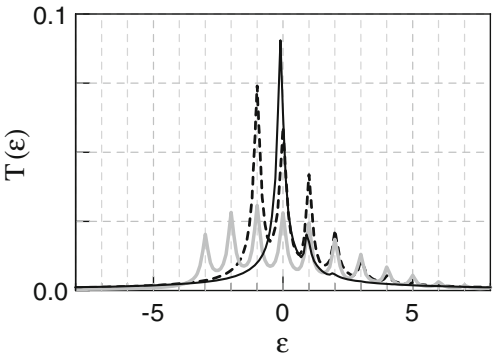

Fig. 6.7 Transmission function as a function of energy at different electron-vibron couplings: $g = 0.1$ (*thin solid line*), $g = 1$ (*dashed line*), and $g = 3$ (*thick solid line*), at $\Gamma = 0.1$

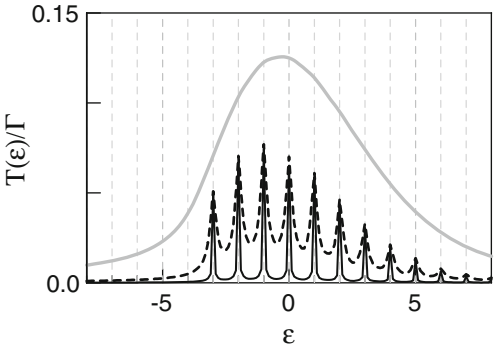

Fig. 6.8 Transmission function as a function of energy at different couplings to the leads: $\Gamma = 0.01$ (*thin solid line*), $\Gamma = 0.1$ (*dashed line*), and $\Gamma = 1$ (*thick solid line*), at $g = 3$.

the total transmission function $T(\varepsilon)$ is trivially obtained by integration over ε'. The representative results are presented in Figs. 6.7 and 6.8.

At finite temperature the general expression is too cumbersome, and we present here only the expression for the total transmission function

$$T(\varepsilon) = \frac{\Gamma_L \Gamma_R}{\Gamma} e^{-g(1+2n_\omega)} \int_{-\infty}^{\infty} dt \times \exp\left(-\frac{\Gamma}{2}|t| + i(\varepsilon - \varepsilon_0 + g\omega_0)t - g\left[(1+n_\omega)e^{-i\omega_0 t} + n_\omega e^{i\omega_0 t}\right]\right), \quad (6.88)$$

where n_ω is the equilibrium number of vibrons.

6.5 Sequential Inelastic Tunneling

When the system is weakly coupled to the leads, the polaron representation (6.49) and (6.82) is a convenient starting point. Here we consider how the sequential tunneling is modified by vibrons.

6.5.1 Master Equation

In the sequential tunneling regime the master equation for the probability $p(n, m, t)$ to find the system in one of the polaron eigenstates (6.53) can be written as

$$\frac{dp(n,m)}{dt} = \sum_{n'm'} \Gamma^{nn'}_{mm'} p(n', m') - \sum_{n'm'} \Gamma^{n'n}_{m'm} p(n, m) + I^V[p], \quad (6.89)$$

where the first term describes the tunneling transition *into the state* $|n, m\rangle$, and the second term – tunneling transition *out of the state* $|n, m\rangle$, $I^V[p]$ is the vibron scattering integral describing the relaxation to equilibrium. The transition rates $\Gamma^{nn'}_{mm'}$ should be found from the Hamiltonian (6.82).

Taking into account all possible single-electron tunneling processes, we obtain the incoming tunneling rate

$$\begin{aligned}\Gamma^{10}_{mm'} &= \frac{2\pi}{\hbar}\sum_{ik\sigma} f_i^0(E_{ik\sigma})\left|\left\langle i\bar{k}, 1, m\left|\bar{H}_T\right|ik, 0, m'\right\rangle\right|^2 \delta(E_{0m'} + E_{ik\sigma} - E_{1m}) \\ &= \frac{2\pi}{\hbar}\sum_{ik\sigma} f_i^0(E_{ik\sigma})\left|V_{ik\sigma}\right|^2 \left|\left\langle m\left|e^{\frac{\lambda}{\omega_0}(a^\dagger - a)}\right|m'\right\rangle\right|^2 \delta(E_{0m'} + E_{ik\sigma} - E_{1m}) \\ &= \sum_{i=L,R} \Gamma_i(E_{1m} - E_{0m'})\left|M_{mm'}\right|^2 f_i^0(E_{1m} - E_{0m'}),\end{aligned} \tag{6.90}$$

where

$$M_{mm'} = \left\langle m\left|e^{\frac{\lambda}{\omega_0}(a^\dagger - a)}\right|m'\right\rangle \tag{6.91}$$

is the Franck-Condon matrix element. We use usual short-hand notations: $|ik, n, m\rangle$ is the state with occupied k-state in the i-th lead, n electrons, and m vibrons, while $|i\bar{k}, n, m\rangle$ is the state with unoccupied k-state in the i-th lead, E_{nm} is the polaron energy (6.54).

Similarly, the outgoing rate is

$$\Gamma^{01}_{mm'} = \sum_{i=L,R} \Gamma_i(E_{1m'} - E_{0m})\left|M_{mm'}\right|^2 \left(1 - f_i^0(E_{1m'} - E_{0m})\right). \tag{6.92}$$

The current (from the left or right lead to the system) is

$$J_{i=L,R}(t) = e\sum_{mm'}\left(\Gamma^{10}_{imm'}p(0, m') - \Gamma^{01}_{imm'}p(1, m')\right). \tag{6.93}$$

The system of (6.89)–(6.93) solves the transport problem in the sequential tunneling regime.

6.5.2 *Franck-Condon Blockade*

Now let us consider some details of the tunneling at small and large values of the electro-vibron coupling constant (6.86). The matrix element (6.91) can be calculated analytically, it is symmetric in $m - m'$ and for $m < m'$ is

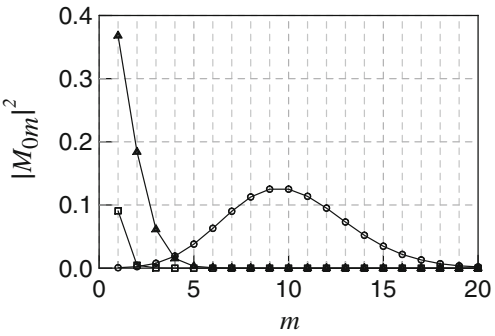

Fig. 6.9 Franck-Condon matrix elements M_{0m} for weak ($g = 0.1$, *squares*), intermediate ($g = 1$, *triangles*), and strong ($g = 10$, *circles*) electron-vibron interaction. *Lines* are the guides for eyes

$$M_{m<m'} = \sum_{l=0}^{m} \frac{(-g)^l \sqrt{m!m'!} e^{-g/2} g^{(m'-m)/2}}{l!(m-l)!(l+m'-m)!}. \tag{6.94}$$

The lowest order elements are

$$M_{0m} = e^{-g/2} \frac{g^{m/2}}{\sqrt{m!}}, \tag{6.95}$$

$$M_{11} = (1-g)e^{-g/2}, \tag{6.96}$$

$$M_{12} = \sqrt{2g}\left(1 - \frac{g}{2}\right) e^{-g/2} \ldots \tag{6.97}$$

The characteristic feature of these matrix elements is the so-called Franck-Condon blockade [5, 6], illustrated in Fig. 6.9 for the matrix element M_{0m}. From the picture, as well as from the analytical formulas, it is clear, that in the case of strong electron-vibron interaction the tunneling with small change of the vibron quantum number is suppressed exponentially, and only the tunneling through high-energy states is possible, which is also suppressed at low bias voltage and low temperature. Thus, the electron transport through a system (linear conductance) is very small.

There are several interesting manifestations of the Franck-Condon blockade.

The *life-time* of the state $|n, m\rangle$ is determined by the sum of the rates of all possible processes which change this state in the assumption that all other states are empty

$$\tau_{nm}^{-1} = \sum_{n'm'} \Gamma_{m'm}^{n'n}. \tag{6.98}$$

As an example, let us calculate the life-time of the neutral ground state $|0, 0\rangle$, which has the energy higher than the charged ground state $|1, 0\rangle$.

$$\tau_{00}^{-1} = \sum_{n'm'} \Gamma_{m'0}^{n'0} = \sum_{m} \sum_{i=L,R} \Gamma_i(E_{1m} - E_{00}) \, |M_{m0}|^2 \, f_i^0(E_{1m} - E_{00}). \tag{6.99}$$

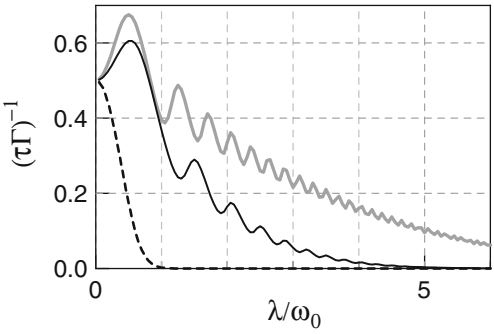

Fig. 6.10 The inverse life-time $(\tau_{00}\Gamma)^{-1}$ as a function of λ/ω_0 at different electron level position: $\varepsilon_0/\omega_0 = -5$ (*thin solid line*), $\varepsilon_0/\omega_0 = -1$ (*dashed line*), and $\varepsilon_0/\omega_0 = 5$ (*thick solid line*)

In the wide-band limit we obtain the simple analytical expression

$$\tau_{00}^{-1} = \Gamma \sum_m e^{-g} \frac{g^m}{m!} f^0 \left(\tilde{\varepsilon}_0 - \frac{\lambda^2}{\omega_0} + \omega_0 m \right). \tag{6.100}$$

The result of the calculation is shown in Fig. 6.10, it can be clearly seen that the tunneling from the state $|0, 0\rangle$ is suppressed in comparison with the bare tunneling rate Γ at large values of the electron-vibron interaction constant λ. Note that the charged state $|1, 0\rangle$ has lower energy and is also stable. However, at finite voltage the switch between two states is easy accessible through the excited vibron states. This *polaron memory effect* [7, 8] can be used to create nano-memory and nano-switches.

The other direct manifestation of the Franck-Condon blockade, the suppression of current at small bias voltages, was investigated by Koch et al. [5].

References

1. B.N.J. Persson, A. Baratoff, Phys. Rev. Lett. **59**, 339 (1987)
2. L.I. Glazman, R.I. Shekhter, Zh. Eksp. Teor. Fiz. **94**, 292 (1988) [Sov. Phys. JETP **67**, 163 (1988)]
3. N.S. Wingreen, K.W. Jacobsen, J.W. Wilkins, Phys. Rev. Lett. **61**, 1396 (1988)
4. N.S. Wingreen, K.W. Jacobsen, J.W. Wilkins, Phys. Rev. B **40**, 11834 (1989)
5. J. Koch, F. von Oppen, Phys. Rev. Lett. **94**, 206804 (2005)
6. J. Koch, M. Semmelhack, F. von Oppen, A. Nitzan, Phys. Rev. B **73**, 155306 (2006)
7. D.A. Ryndyk, P. D'Amico, G. Cuniberti, K. Richter, Phys. Rev. B **78**, 085409 (2008)
8. D.A. Ryndyk, P. D'Amico, K. Richter, Phys. Rev. B **81**, 115333 (2010)

Part II
Advanced Methods

Chapter 7
Nonequilibrium Green Functions

The Nonequilibrium Green Function (NGF) method is the most promising approach to describe quantum transport at nanoscale. The current through a nanosystem (as well as other observables) can be expressed with the help of NGFs. Before going to the explicit formulation of the method for transport through nanosystems, we discuss in this chapter the general properties of nonequilibrium Green functions and formulate the main equations.

First, in Sect. 7.1 we give the definitions of retarded, advanced, lesser, and greater Green functions and consider some simple examples, in particular the noninteracting case. We introduce Green functions of three different types: for fermions (electrons), for bosons and the special type for vibrons.

Then we include interactions and introduce the *interaction representation* in Sect. 7.2—the first important step to the diagrammatic approach. In Sect. 7.3 we discuss an important concept of the *Schwinger-Keldysh closed-time contour*, define the so-called *contour Green functions* and establish the relations between these functions and the real-time Green functions.

The rest of the chapter is devoted to the equations for NGFs within two approaches: *Equation of Motion method* (EOM) in Sect. 7.4 and the *Kadanoff-Baym-Keldysh method* in Sect. 7.5. We derive the expressions of the diagrammatic technique and come to the self-consistent equations in the integral and differential form.

D.A. Ryndyk, *Theory of Quantum Transport at Nanoscale*,
Springer Series in Solid-State Sciences 184,
DOI 10.1007/978-3-319-24088-6_7

7.1 Definition and Properties

7.1.1 Retarded (G^R) and Advanced (G^A) Functions

Definition

The retarded Green function for fermions is defined as[1]

$$G^R_{\alpha\beta}(t_1, t_2) = -i\theta(t_1 - t_2)\left\langle\left[c_\alpha(t_1), c^\dagger_\beta(t_2)\right]_+\right\rangle, \tag{7.1}$$

where $c^\dagger_\alpha(t)$, $c_\alpha(t)$ are creation and annihilation time-dependent (Heisenberg) operators, $[c, d]_+ = cd + dc$ is the anti-commutator, and $\langle \ldots \rangle$ denotes averaging over the initial equilibrium state.

We use notations α, β, ... to denote single-particle quantum states, the other possible notation is more convenient for bulk systems

$$G^R(x_1, x_2) = -i\theta(t_1 - t_2)\left\langle[c(x_1), c^\dagger(x_2)]_+\right\rangle, \tag{7.2}$$

where $x \equiv \boldsymbol{r}, t, \sigma, \ldots$ or $x \equiv \boldsymbol{k}, t, \sigma, \ldots$, etc. Some other types of notations can be found in the literature, they are equivalent.

The advanced function for fermions is defined as

$$G^A_{\alpha\beta}(t_1, t_2) = i\theta(t_2 - t_1)\left\langle\left[c_\alpha(t_1), c^\dagger_\beta(t_2)\right]_+\right\rangle. \tag{7.3}$$

Finally, retarded and advanced functions for *bosons* can be defined as

$$B^R_{\alpha\beta}(t_1, t_2) = -i\theta(t_1 - t_2)\left\langle\left[a_\alpha(t_1), a^\dagger_\beta(t_2)\right]_-\right\rangle, \tag{7.4}$$

$$B^A_{\alpha\beta}(t_1, t_2) = i\theta(t_2 - t_1)\left\langle\left[a_\alpha(t_1), a^\dagger_\beta(t_2)\right]_-\right\rangle, \tag{7.5}$$

where $a^\dagger_\alpha(t)$, $a_\alpha(t)$ are creation and annihilation boson operators, $[a, b]_- = ab - ba$ is the commutator.

Averaging

The average value of any operator $\hat{O}$ can be written as $\langle\hat{O}\rangle = \langle t|\hat{O}^S|t\rangle$ in the Schrödinger representation or $\langle\hat{O}\rangle = \langle 0|\hat{O}^H(t)|0\rangle$ in the Heisenberg representation, where $|0\rangle$ is some initial state. This initial state is in principle arbitrary, but in

[1] There are many equivalent notations used in the literature, some of them are $G_{\alpha\beta}(t_1, t_2)$, $G_{n\sigma,m\sigma'}(t_1, t_2)$, $G(x, t, x', t')$, $G(x_1, x_2)$, $G(1, 2)$, $\boldsymbol{G}\ldots$ We use different notations depending on the representation.

many-particle problems it is convenient to take this state as an equilibrium state, consequently without time-dependent perturbations we obtain usual equilibrium Green functions.

In accordance with this definition the Heisenberg operators $c_\alpha(t)$, $c^\dagger_\beta(t)$, etc. are equal to the time-independent Schrödinger operators at some initial time t_0: $c_\alpha(t_0) = c_\alpha$, etc. Density matrix of the system is assumed to be equilibrium at this time $\hat{\rho}(t_0) = \hat{\rho}_{eq}$. Usually we can take $t_0 = 0$ for simplicity, but if we want to use $t_0 \neq 0$ the transformation to the Heisenberg operators should be written as

$$\hat{f}^H(t) = e^{i\hat{H}(t-t_0)}\hat{f}^S e^{-i\hat{H}(t-t_0)}. \tag{7.6}$$

In fact, the initial conditions are not important because of dissipation (the memory about the initial state is completely lost after the relaxation time). However, in some pathological cases, for example for free noninteracting particles, the initial state determines the state at all times. Note also, that the initial conditions can be more conveniently formulated for Green functions itself, instead of corresponding initial conditions for operators or wave functions.

Nevertheless, thermal averaging is widely used and we define it here explicitly. If we introduce the basis of exact time-independent many-particle states $|n\rangle$ with energies E_n, the averaging over equilibrium states can be written as

$$\langle \hat{O} \rangle = \frac{1}{Z}\sum_n e^{-E_n/T}\left\langle n \left| \hat{O}^H(t) \right| n \right\rangle, \quad Z = \sum_n e^{-E_n/T}. \tag{7.7}$$

In the following when we use notations like $\left\langle \hat{O} \right\rangle$ or $\left\langle \Psi \left| \hat{O}(t) \right| \Psi \right\rangle$, we assume the averaging with the density matrix (density operator) $\hat{\rho}$

$$\left\langle \hat{O} \right\rangle = Sp\left(\hat{\rho}\hat{O}\right), \tag{7.8}$$

for equilibrium density matrix and Heisenberg operators it is equivalent to (7.7).

Time-Independent Case and Mixed Representation

Nonequilibrium Green functions are originally defined as the two-time functions $G(t_1, t_2)$. This complication is the price we pay for a possibility to consider time-dependent and moreover time-nonlocal phenomena with retarded interactions, memory, etc. In the stationary case without time-dependent external fields the Green functions depend only on time differences $G(t_1 - t_2) = G(\tau)$. In this case it is convenient to introduce the Fourier transform $G(\epsilon)$. We define it in the same way as before by the expression (3.19) for the retarded function:

$$G^R(\epsilon) = \lim_{\eta \to 0^+} \int_{-\infty}^{\infty} G^R(\tau) e^{i(\epsilon + i\eta)\tau/\hbar} d\tau, \tag{7.9}$$

and for the advanced one:

$$G^A(\epsilon) = \lim_{\eta \to 0^+} \int_{-\infty}^{\infty} G^A(\tau) e^{i(\epsilon - i\eta)\tau/\hbar} d\tau. \tag{7.10}$$

More generally, transformation (7.9) can be considered as the Laplace transformation with complex argument $z = \epsilon + i\eta$.

For slowly varying time processes the mixed representation (also called Wigner) $G(t, \epsilon)$ can be used with the same Fourier transform in time difference and the time $t = (t_1 + t_2)/2$.

Spectral Function

Finally, we introduce the important combination of retarded and advanced functions known as *spectral* or *spectral weight* function[2]

$$A_{\alpha\beta}(\epsilon) = i \left(G^R_{\alpha\beta}(\epsilon) - G^A_{\alpha\beta}(\epsilon) \right), \tag{7.11}$$

in equilibrium case the Fourie-transformed retarded and advanced functions are complex conjugate $G^A(\epsilon) = \left(G^R(\epsilon)\right)^*$, and $A_{\alpha\beta}(\epsilon) = -2\mathrm{Im} G^R_{\alpha\beta}(\epsilon)$.

For free fermions the spectral function is[3]

$$A_{\alpha\beta}(\epsilon) = -2\mathrm{Im} \left(\frac{\delta_{\alpha\beta}}{\epsilon - \epsilon_\alpha + i\eta} \right) = 2\pi \delta(\epsilon - \epsilon_\alpha) \delta_{\alpha\beta}. \tag{7.12}$$

The result is transparent—the function $A_{\alpha\beta}(\epsilon)$ is nonzero only at particle eigenenergies, such that

$$\rho(\epsilon) = \frac{1}{2\pi} \mathrm{Sp} A_{\alpha\beta}(\epsilon) = \frac{1}{2\pi} \sum_\alpha A_{\alpha\alpha}(\epsilon) = \sum_\alpha \delta(\epsilon - \epsilon_\alpha) \tag{7.13}$$

is the usual energy density of states. Note that the imaginary part $i\eta$ is necessary to obtain this result, thus it is not only a mathematical trick, but reflects the physical sense of the retarded Green function.

If we introduce the finite relaxation time τ, the Green function of free particles becomes

$$G^R_{\alpha\beta}(\tau) = -i\theta(\tau) e^{-i\epsilon_\alpha \tau - \gamma\tau} \delta_{\alpha\beta}, \tag{7.14}$$

[2] We already introduced the spectral function in Chap. 3, as well as some other functions, but repeat it here to keep consistency.

[3] We derive it later, see the Green function (7.52) for free fermions.

then the spectral function has the familiar Lorentzian form

$$A_{\alpha\beta}(\epsilon) = \frac{2\gamma\delta_{\alpha\beta}}{(\epsilon - \epsilon_\alpha)^2 + \gamma^2}. \tag{7.15}$$

Finally, spectral function has a special property, so-called *sum rule*, namely

$$\int_{-\infty}^{\infty} A_{\alpha\beta}(\epsilon)\frac{d\epsilon}{2\pi} = \delta_{\alpha\beta}. \tag{7.16}$$

7.1.2 Lesser ($G^<$) and Greater ($G^>$) Functions

Definition

Retarded and advanced functions, described before, determine the single-particle properties of the system, such as quasiparticle energy, broadening of the levels (lifetime), and density of states. These functions can be modified in nonequilibrium state, but most important *kinetic* properties, such as distribution function, charge, and current, are determined by the lesser Green function

$$G^<_{\alpha\beta}(t_1, t_2) = i\left\langle c^\dagger_\beta(t_2)c_\alpha(t_1)\right\rangle. \tag{7.17}$$

Indeed, the density matrix is the same as the equal-time lesser function

$$\rho_{\alpha\beta}(t) = \left\langle c^\dagger_\beta(t)c_\alpha(t)\right\rangle = -iG^<_{\alpha\beta}(t, t). \tag{7.18}$$

The number of particles in state $|\alpha\rangle$ (distribution function) is

$$n_\alpha(t) = \left\langle c^\dagger_\alpha(t)c_\alpha(t)\right\rangle = -iG^<_{\alpha\alpha}(t, t), \tag{7.19}$$

the tunneling current is

$$\begin{aligned} J(t) &= \frac{ie}{\hbar}\sum_{kq}\left[V_{qk}\left\langle c^\dagger_q(t)c_k(t)\right\rangle - V^*_{qk}\left\langle c^\dagger_k(t)c_q(t)\right\rangle\right] \\ &= \frac{2e}{\hbar}\mathrm{Re}\left(\sum_{kq} V_{qk}G^<_{kq}(t, t)\right). \end{aligned} \tag{7.20}$$

In addition to the lesser, the other (greater) function is used

$$G^>_{\alpha\beta}(t_1, t_2) = -i\left\langle c_\alpha(t_1)c^\dagger_\beta(t_2)\right\rangle. \tag{7.21}$$

For bosons, the lesser and greater functions are defined as

$$B^{<}_{\alpha\beta}(t_1, t_2) = -i \left\langle a^{\dagger}_{\beta}(t_2) a_{\alpha}(t_1) \right\rangle, \tag{7.22}$$

$$B^{>}_{\alpha\beta}(t_1, t_2) = -i \left\langle a_{\alpha}(t_1) a^{\dagger}_{\beta}(t_2) \right\rangle. \tag{7.23}$$

The name "lesser" originates from the time-ordered Green function, the main function in equilibrium theory, which can be calculated by the diagrammatic technique

$$G_{\alpha\beta}(t_1, t_2) = -i \left\langle T \left(c_{\alpha}(t_1) c^{\dagger}_{\beta}(t_2) \right) \right\rangle, \tag{7.24}$$

$$G_{\alpha\beta}(t_1, t_2) = \begin{cases} -i \left\langle c_{\alpha}(t_1) c^{\dagger}_{\beta}(t_2) \right\rangle \text{ if } t_1 > t_2 \Rightarrow \;\; G_{\alpha\beta} \equiv G^{>}_{\alpha\beta}, \\ i \left\langle c^{\dagger}_{\beta}(t_2) c_{\alpha}(t_1) \right\rangle \quad \text{if } t_1 < t_2 \Rightarrow \;\; G_{\alpha\beta} \equiv G^{<}_{\alpha\beta}, \end{cases} \tag{7.25}$$

here the additional sing minus appears for interchanging of fermionic creation-annihilation operators. Lesser means that $t_1 < t_2$.

7.1.3 Some Useful Relations

From the definitions it is clear that the retarded and advanced functions can be combined from lesser and greater functions

$$G^{R}_{\alpha\beta}(t_1, t_2) = \theta(t_1 - t_2) \left[G^{>}_{\alpha\beta}(t_1, t_2) - G^{<}_{\alpha\beta}(t_1, t_2) \right], \tag{7.26}$$

$$G^{A}_{\alpha\beta}(t_1, t_2) = \theta(t_2 - t_1) \left[G^{<}_{\alpha\beta}(t_1, t_2) - G^{>}_{\alpha\beta}(t_1, t_2) \right]. \tag{7.27}$$

The other useful relation is

$$G^{R}_{\alpha\beta}(t_1, t_2) - G^{A}_{\alpha\beta}(t_1, t_2) = G^{>}_{\alpha\beta}(t_1, t_2) - G^{<}_{\alpha\beta}(t_1, t_2), \tag{7.28}$$

and the symmetry relations

$$G^{<}_{\alpha\beta}(t_1, t_2) = -\left[G^{<}_{\beta\alpha}(t_2, t_1) \right]^{*}, \tag{7.29}$$

$$G^{>}_{\alpha\beta}(t_1, t_2) = -\left[G^{>}_{\beta\alpha}(t_2, t_1) \right]^{*}, \tag{7.30}$$

$$G^{A}_{\alpha\beta}(t_1, t_2) = \left[G^{R}_{\beta\alpha}(t_2, t_1) \right]^{*}. \tag{7.31}$$

The same relations hold in the mixed (Wigner) representation

$$G^{<}_{\alpha\beta}(t,\epsilon) = -\left[G^{<}_{\beta\alpha}(t,\epsilon)\right]^{*}, \tag{7.32}$$

$$G^{>}_{\alpha\beta}(t,\epsilon) = -\left[G^{>}_{\beta\alpha}(t,\epsilon)\right]^{*}, \tag{7.33}$$

$$G^{A}_{\alpha\beta}(t,\epsilon) = \left[G^{R}_{\beta\alpha}(t,\epsilon)\right]^{*}. \tag{7.34}$$

It can be written in the matrix representation using Hermitian conjugation †

$$\mathbf{G}^{<}(t,\epsilon) = -\mathbf{G}^{<\dagger}(t,\epsilon), \tag{7.35}$$

$$\mathbf{G}^{>}(t,\epsilon) = -\mathbf{G}^{>\dagger}(t,\epsilon), \tag{7.36}$$

$$\mathbf{G}^{A}(t,\epsilon) = \mathbf{G}^{R\dagger}(t,\epsilon). \tag{7.37}$$

Obviously, these relations are true also in the time-independent case.

7.1.4 Equilibrium Case. Fluctuation-Dissipation Theorem

Now we want to consider some general properties of interacting systems. In equilibrium the lesser function is not independent and is simply related to the spectral function by the relation

$$G^{<}_{\alpha\beta}(\epsilon) = i A_{\alpha\beta}(\epsilon) f^{0}(\epsilon). \tag{7.38}$$

This relation is important because it establishes an equilibrium initial condition for the nonequilibrium lesser function, and proposes a useful Ansatz if the equilibrium distribution function $f^0(\epsilon)$ is replaced by some unknown nonequilibrium function.

Here we prove this relation using the *Lehmann representation*—quite useful method in the theory of Green functions. The idea of the method is to use the exact many-particle eigenstates $|n\rangle$, even if they are not explicitly known.

Consider first the greater function. Using states $|n\rangle$ we represent this function as

$$\begin{aligned} G^{>}_{\alpha\beta}(t_1,t_2) &= -i\left\langle c_\alpha(t_1)c^{\dagger}_{\beta}(t_2)\right\rangle = -\frac{i}{Z}\sum_n \left\langle n\left| e^{-\hat{H}/T} c_\alpha(t_1)c^{\dagger}_{\beta}(t_2)\right| n\right\rangle \\ &= -\frac{i}{Z}\sum_{nm} e^{-E_n/T}\langle n|c_\alpha|m\rangle\langle m|c^{\dagger}_{\beta}|n\rangle e^{i(E_n-E_m)(t_1-t_2)}. \end{aligned} \tag{7.39}$$

In Fourier representation

$$G^{>}_{\alpha\beta}(\epsilon) = -\frac{2\pi i}{Z}\sum_{nm} e^{-E_n/T}\langle n|c_\alpha|m\rangle\langle m|c^{\dagger}_{\beta}|n\rangle\delta(E_n - E_m + \epsilon). \tag{7.40}$$

Similarly, for the lesser function we find

$$G^{<}_{\alpha\beta}(\epsilon) = \frac{2\pi i}{Z} \sum_{nm} e^{-E_m/T} \langle n|c^{\dagger}_{\beta}|m\rangle \langle m|c_{\alpha}|n\rangle \delta(E_m - E_n + \epsilon). \tag{7.41}$$

Now we can use these expressions to obtain some general properties of Green functions without explicit calculation of the matrix elements. By exchanging indices n and m in the expression (7.41) and taking into account that $E_m = E_n - \epsilon$ because of the delta-function, we see that

$$G^{>}_{\alpha\beta}(\epsilon) = -e^{-\epsilon/T} G^{<}_{\alpha\beta}(\epsilon). \tag{7.42}$$

From this expression and relation (7.26), which can be written as

$$A_{\alpha\beta}(\epsilon) = i \left[G^{>}_{\alpha\beta}(\epsilon) - G^{<}_{\alpha\beta}(\epsilon) \right] \tag{7.43}$$

we derive (7.38).

7.1.5 *Free Fermions*

Free-Particle Retarded Function for Fermions

Now consider the simplest possible example—the retarded Green function for free particles (fermions).

The free-particle Hamiltonian has an equivalent form if one uses Schrödinger or Heisenberg operators

$$\hat{H} = \sum_{\alpha} \epsilon_{\alpha} c^{\dagger}_{\alpha} c_{\alpha} = \sum_{\alpha} \epsilon_{\alpha} c^{\dagger}_{\alpha}(t) c_{\alpha}(t), \tag{7.44}$$

because (here we assume $t_0 = 0$)

$$c^{\dagger}_{\alpha}(t) c_{\alpha}(t) = e^{i\hat{H}t} c^{\dagger}_{\alpha} e^{-i\hat{H}t} e^{i\hat{H}t} c_{\alpha} e^{-i\hat{H}t} = e^{i\hat{H}t} c^{\dagger}_{\alpha} c_{\alpha} e^{-i\hat{H}t} = c^{\dagger}_{\alpha} c_{\alpha}, \tag{7.45}$$

where we used that $c^{\dagger}_{\alpha} c_{\alpha}$ is commutative with the Hamiltonian $\hat{H} = \sum_{\alpha} \epsilon_{\alpha} c^{\dagger}_{\alpha} c_{\alpha}$.

From the definitions (7.1) and (7.7) it follows that:

$$\begin{aligned} &\left\langle \left[c_{\alpha}(t_1), c^{\dagger}_{\beta}(t_2) \right]_{+} \right\rangle = \left\langle c_{\alpha}(t_1) c^{\dagger}_{\beta}(t_2) + c^{\dagger}_{\beta}(t_2) c_{\alpha}(t_1) \right\rangle \\ &= \left\langle e^{i\hat{H}t_1} c_{\alpha}(t_1) e^{-i\hat{H}t_1} e^{i\hat{H}t_2} c^{\dagger}_{\beta}(t_2) e^{-i\hat{H}t_2} + e^{i\hat{H}t_2} c^{\dagger}_{\beta}(t_2) e^{-i\hat{H}t_2} e^{i\hat{H}t_1} c_{\alpha}(t_1) e^{-i\hat{H}t_1} \right\rangle \\ &= e^{i\epsilon_{\beta}t_2 - i\epsilon_{\alpha}t_1} \left\langle c_{\alpha} c^{\dagger}_{\beta} + c^{\dagger}_{\beta} c_{\alpha} \right\rangle = e^{-i\epsilon_{\alpha}(t_1 - t_2)} \delta_{\alpha\beta}, \end{aligned} \tag{7.46}$$

$$G^R_{\alpha\beta}(t_1,t_2) = -i\theta(t_1-t_2)\left\langle\left[c_\alpha(t_1), c^\dagger_\beta(t_2)\right]_+\right\rangle$$
$$= -i\theta(t_1-t_2)e^{-i\epsilon_\alpha(t_1-t_2)}\delta_{\alpha\beta}, \tag{7.47}$$

where we used some obvious properties of the creation and annihilation operators and commutation relations.

We consider also the other method, based on the equations of motion for operators. From the Liouville–von Neuman equation we find (all c-operators are Heisenberg operators in the formula below, the time dependence (t) is omitted for shortness)

$$i\frac{dc_\alpha(t)}{dt} = [c_\alpha(t), H]_- = \sum_\beta \epsilon_\beta \left[c_\alpha, c^\dagger_\beta c_\beta\right]_-$$
$$= \sum_\beta \epsilon_\beta \left(c_\alpha c^\dagger_\beta c_\beta - c^\dagger_\beta c_\beta c_\alpha\right) = \sum_\beta \epsilon_\beta \left(c_\alpha c^\dagger_\beta c_\beta + c^\dagger_\beta c_\alpha c_\beta\right)$$
$$= \sum_\beta \epsilon_\beta \left(c_\alpha c^\dagger_\beta + c^\dagger_\beta c_\alpha\right) c_\beta = \sum_\beta \epsilon_\beta \delta_{\alpha\beta} c_\beta = \epsilon_\alpha c_\alpha(t), \tag{7.48}$$

so that Heisenberg operators for free fermions are

$$c_\alpha(t) = e^{-i\epsilon_\alpha t}c_\alpha(0), \quad c^\dagger_\alpha(t) = e^{i\epsilon_\alpha t}c^\dagger_\alpha(0). \tag{7.49}$$

Substituting these expressions into (7.1) we obtain again (7.47). Note also that if we take $t_0 \neq 0$, the Heisenberg operators for free fermions are

$$c_\alpha(t) = e^{-i\epsilon_\alpha(t-t_0)}c_\alpha(t_0), \quad c^\dagger_\alpha(t) = e^{i\epsilon_\alpha(t-t_0)}c^\dagger_\alpha(t_0), \tag{7.50}$$

but the result for the Green functions is just the same, because

$$\left\langle\left[c_\alpha(t_1), c^\dagger_\beta(t_2)\right]_+\right\rangle = -\left\langle c_\alpha(t_1)c^\dagger_\beta(t_2) + c^\dagger_\beta(t_2)c_\alpha(t_1)\right\rangle$$
$$= e^{i\epsilon_\beta(t_2-t_0)-i\epsilon_\alpha(t_1-t_0)}\left\langle c_\alpha c^\dagger_\beta + c^\dagger_\beta c_\alpha\right\rangle = e^{-i\epsilon_\alpha(t_1-t_2)}\delta_{\alpha\beta}. \tag{7.51}$$

It is interesting to make Fourier-transform of this function. In equilibrium the two-time function $G^R_{\alpha\beta}(t_1,t_2)$ is a function of the time difference only, so that we apply the transform (7.9). Adding an infinitely small positive complex part to ϵ is required to make this integral well defined in the upper limit (this is necessary for free particles without dissipation because function (7.47) oscillates at large times $\tau = t_1 - t_2$ and the integral (7.9) can not be calculated without $i\eta$ term). Then we obtain

$$G^R_{\alpha\beta}(\epsilon) = \frac{\delta_{\alpha\beta}}{\epsilon - \epsilon_\alpha + i\eta}. \tag{7.52}$$

This Green function looks exactly the same as the retarded matrix function (3.105) introduced in Chap. 3. It is not surprising, that the retarded Green functions of the NGF formalism for noninteracting systems are exactly the same as the single-particle retarded Green functions which we used before.

Free-Particle Lesser Function for Fermions

Now let us consider again free fermions. Heisenberg operators for free fermions are ($t_0 = 0$)

$$c_\alpha(t) = e^{-i\epsilon_\alpha t} c_\alpha(0), \quad c_\alpha^\dagger(t) = e^{i\epsilon_\alpha t} c_\alpha^\dagger(0). \tag{7.53}$$

Lesser function is

$$\begin{aligned} G^<_{\alpha\beta}(t_1, t_2) =& i \left\langle c_\beta^\dagger(t_2) c_\alpha(t_1) \right\rangle = i e^{i\epsilon_\beta t_2 - i\epsilon_\alpha t_1} \left\langle c_\beta^\dagger c_\alpha \right\rangle \\ &= i e^{-i\epsilon_\alpha (t_1 - t_2)} f^0(\epsilon_\alpha) \delta_{\alpha\beta}, \end{aligned} \tag{7.54}$$

one sees that contrary to the retarded function, the lesser function is proportional to the distribution function, in equilibrium this is the Fermi distribution function

$$f^0(\epsilon) = \frac{1}{e^{\frac{\epsilon-\mu}{T}} + 1}. \tag{7.55}$$

It is interesting to compare this answer with the result for *nonthermal* initial conditions. Assume that the initial state is described by the density matrix $\rho^0_{\alpha\beta} = \left\langle c_\beta^\dagger c_\alpha \right\rangle$, now with nonzero off-diagonal elements. The time dependence of the density matrix is given by

$$\rho_{\alpha\beta}(t) = e^{i(\epsilon_\beta - \epsilon_\alpha)t} \rho^0_{\alpha\beta}. \tag{7.56}$$

We obtain the well known result that off-diagonal elements oscillate in time.

Now define the Fourier-transform for the lesser function ($\tau = t_1 - t_2$)

$$G^<(\epsilon) = \int_{-\infty}^{\infty} G^<(\tau) e^{i[\epsilon + i\eta \mathrm{sign}(\tau)]\tau} d\tau, \tag{7.57}$$

note that here we use Fourie-transform with complicated term $i\eta \mathrm{sign}(\tau)$, which makes this transformation consistent with previously introduced transformations (7.9) for retarded ($\tau > 0$) and (7.10) advanced ($\tau < 0$) functions.

Applying this transformation to (7.54) we obtain

$$\begin{aligned} G^<_{\alpha\beta}(\epsilon) =& i f^0(\epsilon_\alpha) \delta_{\alpha\beta} \int_{-\infty}^{\infty} e^{+i[\epsilon - \epsilon_\alpha + i\eta \mathrm{sign}(\tau)]\tau} d\tau \\ &= 2\pi i f^0(\epsilon_\alpha) \delta(\epsilon - \epsilon_\alpha) \delta_{\alpha\beta}. \end{aligned} \tag{7.58}$$

For free fermions, the greater function is given by

$$G^{>}_{\alpha\beta}(t_1, t_2) = -ie^{-i\epsilon_\alpha(t_1-t_2)}(1 - f^0(\epsilon_\alpha))\delta_{\alpha\beta}, \tag{7.59}$$

$$G^{>}_{\alpha\beta}(\epsilon) = -2\pi i(1 - f^0(\epsilon_\alpha))\delta(\epsilon - \epsilon_\alpha)\delta_{\alpha\beta}. \tag{7.60}$$

7.1.6 Free Bosons

For free bosons the retarded and advanced functions are exactly the same and the lesser and the greater functions are similar, of course the distribution function now is the Bose function instead of Fermi-Dirac. We give here only the results of calculations:

$$B^R_{\alpha\beta}(t_1, t_2) = -i\theta(t_1 - t_2)e^{-i\epsilon_\alpha(t_1-t_2)}\delta_{\alpha\beta}, \tag{7.61}$$

$$B^A_{\alpha\beta}(t_1, t_2) = i\theta(t_2 - t_1)e^{-i\epsilon_\alpha(t_1-t_2)}\delta_{\alpha\beta}, \tag{7.62}$$

$$B^R_{\alpha\beta}(\epsilon) = \frac{\delta_{\alpha\beta}}{\epsilon - \epsilon_\alpha + i0}, \quad B^A_{\alpha\beta}(\epsilon) = \frac{\delta_{\alpha\beta}}{\epsilon - \epsilon_\alpha - i0}, \tag{7.63}$$

$$B^{<}_{\alpha\beta}(t_1, t_2) = -ie^{-i\epsilon_\alpha(t_1-t_2)}f^0_B(\epsilon_\alpha)\delta_{\alpha\beta}, \tag{7.64}$$

$$B^{>}_{\alpha\beta}(t_1, t_2) = -ie^{-i\epsilon_\alpha(t_1-t_2)}(1 + f^0_B(\epsilon_\alpha))\delta_{\alpha\beta}, \tag{7.65}$$

$$B^{<}_{\alpha\beta}(\epsilon) = -2\pi i f^0_B(\epsilon_\alpha)\delta(\epsilon - \epsilon_\alpha)\delta_{\alpha\beta}, \tag{7.66}$$

$$B^{>}_{\alpha\beta}(\epsilon) = -2\pi i(1 + f^0_B(\epsilon_\alpha))\delta(\epsilon - \epsilon_\alpha)\delta_{\alpha\beta}, \tag{7.67}$$

$$f^0_B(\epsilon) = \frac{1}{e^{\frac{\epsilon}{T}} - 1}. \tag{7.68}$$

7.1.7 Green Functions for Vibrons

As one can see from the Hamiltonian of the electron-vibron interaction (6.13), the relevant operator to describe vibrons is not an individual boson operator, but the density fluctuation operator $A_\alpha = a_\alpha + a^\dagger_\alpha$. Because of that all expressions for vibron functions are different from both fermion and usual boson functions discussed previously.

Definition

Using the Heisenberg density fluctuation operators $A_\alpha(t) = a_\alpha(t) + a_\alpha^\dagger(t)$, we define retarded, advanced, lesser, greater and Keldysh (explained later) Green functions for vibrons:

$$D^R_{\alpha\beta}(t_1, t_2) = -i\theta(t_1 - t_2)\left\langle \left[A_\alpha(t_1), A_\beta(t_2)\right]_- \right\rangle, \tag{7.69}$$

$$D^A_{\alpha\beta}(t_1, t_2) = i\theta(t_2 - t_1)\left\langle \left[A_\alpha(t_1), A_\beta(t_2)\right]_- \right\rangle, \tag{7.70}$$

$$D^<_{\alpha\beta}(t_1, t_2) = -i\left\langle A_\beta(t_2)A_\alpha(t_1)\right\rangle, \tag{7.71}$$

$$D^>_{\alpha\beta}(t_1, t_2) = D^<_{\beta\alpha}(t_2, t_1) = -i\left\langle A_\alpha(t_1)A_\beta(t_2)\right\rangle, \tag{7.72}$$

$$D^R_{\alpha\beta}(t_1, t_2) = \theta(t_1 - t_2)\left[D^>_{\alpha\beta}(t_1, t_2) - D^<_{\alpha\beta}(t_1, t_2)\right], \tag{7.73}$$

$$D^A_{\alpha\beta}(t_1, t_2) = \theta(t_2 - t_1)\left[D^<_{\alpha\beta}(t_1, t_2) - D^>_{\alpha\beta}(t_1, t_2)\right], \tag{7.74}$$

$$D^K_{\alpha\beta}(t_1, t_2) = D^<_{\alpha\beta}(t_1, t_2) + D^>_{\alpha\beta}(t_1, t_2). \tag{7.75}$$

Symmetry Relations

The symmetry relations are essentially different because of using commutators in the definition. The most important peculiarities are the special symmetries due to inversion of $\epsilon \Rightarrow -\epsilon$:

$$D^<_{\alpha\beta}(t_1, t_2) = -\left[D^<_{\beta\alpha}(t_2, t_1)\right]^*, \quad D^>_{\alpha\beta}(t_1, t_2) = -\left[D^>_{\beta\alpha}(t_2, t_1)\right]^*, \tag{7.76}$$

$$D^>_{\alpha\beta}(t_1, t_2) = D^<_{\beta\alpha}(t_2, t_1), \tag{7.77}$$

$$D^A_{\alpha\beta}(t_1, t_2) = \left[D^A_{\alpha\beta}(t_1, t_2)\right]^* = D^R{}_{\beta\alpha}(t_2, t_1) = \left[D^R_{\beta\alpha}(t_2, t_1)\right]^*. \tag{7.78}$$

In the mixed (Wigner) representation

$$D^<_{\alpha\beta}(t, \epsilon) = -\left[D^<_{\beta\alpha}(t, \epsilon)\right]^*, \quad D^>_{\alpha\beta}(t, \epsilon) = -\left[D^>_{\beta\alpha}(t, \epsilon)\right]^*, \tag{7.79}$$

$$D^>_{\alpha\beta}(t, \epsilon) = D^<_{\beta\alpha}(t, -\epsilon), \tag{7.80}$$

$$D^A_{\alpha\beta}(t, \epsilon) = \left[D^A_{\alpha\beta}(t, -\epsilon)\right]^* = D^R_{\beta\alpha}(t, -\epsilon) = \left[D^R_{\beta\alpha}(t, \epsilon)\right]^*. \tag{7.81}$$

In the matrix representation using Hermitian conjugation †

$$\mathbf{D}^<(t, \epsilon) = -\mathbf{D}^{<\dagger}(t, \epsilon), \quad \mathbf{D}^>(t, \epsilon) = -\mathbf{D}^{>\dagger}(t, \epsilon), \tag{7.82}$$

$$\mathbf{D}^>(t, \epsilon) = \mathbf{D}^{<\mathbf{T}}(t, -\epsilon), \tag{7.83}$$

$$\mathbf{D}^A(t, \epsilon) = \mathbf{D}^{A*}(t, -\epsilon) = \mathbf{D}^{R\mathbf{T}}(t, -\epsilon) = \mathbf{D}^{R\dagger}(t, \epsilon). \tag{7.84}$$

Free-Particle Functions

Free-particle functions also look significantly different:

$$D^R_{\alpha\beta}(t_1,t_2) = -i\theta(t_1-t_2)\left[e^{-i\epsilon_\alpha(t_1-t_2)} - e^{i\epsilon_\alpha(t_1-t_2)}\right]\delta_{\alpha\beta}, \tag{7.85}$$

$$D^A_{\alpha\beta}(t_1,t_2) = i\theta(t_2-t_1)\left[e^{-i\epsilon_\alpha(t_1-t_2)} - e^{i\epsilon_\alpha(t_1-t_2)}\right]\delta_{\alpha\beta}, \tag{7.86}$$

$$D^R_{\alpha\beta}(\epsilon) = \frac{\delta_{\alpha\beta}}{\epsilon-\epsilon_\alpha+i\eta} - \frac{\delta_{\alpha\beta}}{\epsilon+\epsilon_\alpha+i\eta}, \quad D^A_{\alpha\beta}(\epsilon) = \frac{\delta_{\alpha\beta}}{\epsilon-\epsilon_\alpha-i\eta} - \frac{\delta_{\alpha\beta}}{\epsilon+\epsilon_\alpha-i\eta}, \tag{7.87}$$

$$D^<_{\alpha\beta}(t_1,t_2) = -i\left[e^{-i\epsilon_\alpha(t_1-t_2)}f^0_B(\epsilon_\alpha) + e^{i\epsilon_\alpha(t_1-t_2)}(1+f^0_B(\epsilon_\alpha))\right]\delta_{\alpha\beta}, \tag{7.88}$$

$$D^<_{\alpha\beta}(\epsilon) = -2\pi i\left[f^0_B(\epsilon_\alpha)\delta(\epsilon-\epsilon_\alpha) + (1+f^0_B(\epsilon_\alpha))\delta(\epsilon+\epsilon_\alpha)\right]\delta_{\alpha\beta}, \tag{7.89}$$

$$D^>_{\alpha\beta}(\epsilon) = -2\pi i\left[f^0_B(\epsilon_\alpha)\delta(\epsilon+\epsilon_\alpha) + (1+f^0_B(\epsilon_\alpha))\delta(\epsilon-\epsilon_\alpha)\right]\delta_{\alpha\beta}, \tag{7.90}$$

$$f^0_B(\epsilon) = \frac{1}{e^{\epsilon/T}-1}, \tag{7.91}$$

$$f^0_B(-\epsilon) = -(1+f^0_B(\epsilon)). \tag{7.92}$$

We do not present the details of calculations here, they are exactly the same as we made for fermions. The differences originates from other definition of Green functions and other commutation relations for boson operators.

Finally the definition for the spectral function is the same:

$$A^D_{\alpha\beta}(\epsilon) = i\left(D^R_{\alpha\beta}(\epsilon) - D^A_{\alpha\beta}(\epsilon)\right). \tag{7.93}$$

For free vibrons the spectral function is

$$A^D_{\alpha\beta}(\epsilon) = 2\pi\left[\delta(\epsilon-\epsilon_\alpha)\delta_{\alpha\beta} - \delta(\epsilon+\epsilon_\alpha)\right]\delta_{\alpha\beta}. \tag{7.94}$$

The sum rule is

$$\int_{-\infty}^{\infty} A^D_{\alpha\beta}(\epsilon)\frac{d\epsilon}{2\pi} = 0. \tag{7.95}$$

It is obvious for free particles, and true for all spectral function because the spectral function is asymmetric in ϵ.

In equilibrium we have the following relations:

$$D^{<}_{\alpha\beta}(\epsilon) = -i A^{D}_{\alpha\beta}(\epsilon) f^{0}_{B}(\epsilon), \tag{7.96}$$

$$D^{>}_{\alpha\beta}(\epsilon) = -i A^{D}_{\alpha\beta}(\epsilon)(1 + f^{0}_{B}(\epsilon)), \tag{7.97}$$

$$D^{>}_{\alpha\beta}(\epsilon) = e^{\epsilon/T} D^{<}_{\alpha\beta}(\epsilon). \tag{7.98}$$

7.2 Interaction Representation

Previously we found that nonequilibrium Green functions can be quite easily calculated for free particles, and equations of motion for one-particle Green functions (the functions which are the averages of two creation-annihilation operators) can be formulated if we add interactions and time-dependent perturbations, but these equations include high-order Green functions (the averages of three, four, and larger number of operators). The equations can be truncated and formulated in terms of one-particle Green functions in some simple approximations. However, a systematic approach is needed to proceed with perturbation expansion and self-consistent methods (all together is known as *diagrammatic approach*). The main idea of the diagrammatic approach is to start from some "simple" Hamiltonian (usually for free particles), treating interactions and external fields as a perturbation, formulate perturbation expansion, and summarize all most important terms (diagrams) *in all orders of perturbation theory*. The result of such a procedure gives, in principle, a *nonperturbative* description (ordinary mean-field theory is the simplest example). The starting point of the method is the so-called *interaction representation*.

Let us consider the full Hamiltonian $\hat{H}$ as the sum of a *free-particle* time-independent part $\hat{H}_0$ and (possibly time-dependent) perturbation $\hat{V}(t)$ (note that this "perturbation" should not be necessarily small)

$$\hat{H} = \hat{H}_0 + \hat{V}(t). \tag{7.99}$$

We define new operators in *interaction representation* by

$$\hat{f}^{I}(t) = e^{i\hat{H}_0 t} \hat{f}^{S} e^{-i\hat{H}_0 t}, \tag{7.100}$$

where $\hat{f}^{S}$ is the time-independent Schrödinger operator. This is equivalent to the time-dependent Heisenberg operator, defined by the part $\hat{H}_0$ of the Hamiltonian. For a free-particle Hamiltonian $\hat{H}_0$ the operators $\hat{f}^{I}(t)$ can be calculated exactly.

A new wave function corresponding to (7.100) is

$$\Psi^{I}(t) = e^{i\hat{H}_0 t} \Psi^{S}(t). \tag{7.101}$$

It is easy to see that transformation (7.100), (7.101) is a unitary transformation and conserves the average value of any operator

$$\langle \Psi^S | \hat{f}^S | \Psi^S \rangle = \langle \Psi^I | \hat{f}^I | \Psi^I \rangle. \tag{7.102}$$

Substituting (7.101) into the ordinary Schrödinger equation, we derive the equation

$$i \frac{\partial \Psi^I}{\partial t} = \hat{V}^I(t) \Psi^I, \tag{7.103}$$

where $\hat{V}^I(t) = e^{i\hat{H}_0 t} \hat{V}^S(t) e^{-i\hat{H}_0 t}$ is in the interaction representation.

Equation (7.103) seems to be quite simple, however the operator nature of $\hat{V}$ makes this problem nontrivial. Indeed, consider a small time-step Δt. Then

$$\Psi(t + \Delta t) = \left[1 - i\hat{V}^S(t)\Delta t\right] \Psi(t) = \exp^{-i\hat{V}^S(t)\Delta t} \Psi(t), \tag{7.104}$$

linear in Δt term can be transformed into the exponent if we understand the exponential function of the operator in the usual way

$$\exp^{\hat{A}} = 1 + \hat{A} + \frac{1}{2!}\hat{A}^2 + \cdots + \frac{1}{n!}\hat{A}^n + \cdots, \tag{7.105}$$

and assume that only linear terms should be taken at $\Delta t \to 0$.

If we now repeat this procedure at times t_i with step Δt, we obtain finally

$$\Psi^I(t) = \hat{S}(t, t_0) \Psi^I(t_0), \tag{7.106}$$

with

$$\hat{S}(t, t_0) = \prod_{t_i = t_0}^{t} \exp\left(-i\hat{V}^I(t_i)\Delta t\right). \tag{7.107}$$

This product, however, is not simply $\exp\left(-i\int_{t_0}^{t} \hat{V}^I(t')dt'\right)$ in the limit $\Delta t \to 0$, because operators $\hat{V}^I(t')$ are not commutative at different times, and for two non-commutative operators $\hat{A}$ and $\hat{B}$ it holds that $e^{\hat{A}+\hat{B}} \neq e^{\hat{A}} e^{\hat{B}}$.

In the product (7.107) operators at earlier times should be applied first, before operators at later times. In the limit $\Delta t \to 0$ we obtain

$$\hat{S}(t, t_0) = T \exp\left(-i\int_{t_0}^{t} \hat{V}^I(t')dt'\right), \tag{7.108}$$

where T is the time-ordering operator ("-" for fermionic operators)

$$T\left(\hat{A}(t_1)\hat{B}(t_2)\right) = \begin{cases} \hat{A}(t_1)\hat{B}(t_2) & \text{if } t_1 > t_2, \\ \pm\hat{B}(t_2)\hat{A}(t_1) & \text{if } t_1 < t_2. \end{cases} \tag{7.109}$$

Of course, expression (7.108) is defined only in the sense of expansion (7.105). Consider for example the second-order term in the time-ordered expansion.

$$\begin{aligned} T\left[\int_{t_0}^{t} \hat{V}^I(t')dt'\right]^2 &= T\left[\int_{t_0}^{t} \hat{V}^I(t')dt' \int_{t_0}^{t} \hat{V}^I(t'')dt''\right] \\ &= \int_{t_0}^{t} dt' \int_{t_0}^{t'} dt'' \hat{V}^I(t')\hat{V}^I(t'') + \int_{t_0}^{t} dt'' \int_{t_0}^{t''} dt' \hat{V}^I(t'')\hat{V}^I(t'). \end{aligned} \tag{7.110}$$

If we exchange t' and t'' in the second integral, we see finally that

$$T\left[\int_{t_0}^{t} \hat{V}^I(t')dt'\right]^2 = 2\int_{t_0}^{t} dt' \int_{t_0}^{t'} dt'' \hat{V}^I(t')\hat{V}^I(t''). \tag{7.111}$$

Properties of $\hat{S}(t, t_0)$

$\hat{S}$ is the unitary operator and

$$\hat{S}^{-1}(t, t_0) = \hat{S}^{\dagger}(t, t_0) = \tilde{T}\exp\left(i\int_{t_0}^{t} \hat{V}^I(t')dt'\right), \tag{7.112}$$

where $\tilde{T}$ is time-anti-ordering operator. Some other important properties are

$$\hat{S}^{-1}(t, t_0) = \hat{S}(t_0, t), \tag{7.113}$$

$$\hat{S}(t_3, t_2)\hat{S}(t_2, t_1) = \hat{S}(t_3, t_1), \tag{7.114}$$

$$\hat{S}^{-1}(t_2, t_1)\hat{S}^{-1}(t_3, t_2) = \hat{S}^{-1}(t_3, t_1). \tag{7.115}$$

Finally, we need the expression of a Heisenberg operator, defined by the full Hamiltonian $\hat{H} = \hat{H}_0 + \hat{V}(t)$, through an operator in the interaction representation. The transformation, corresponding to (7.106), is given by

$$\hat{f}^H(t) = e^{-i\hat{H}_0 t_0}\hat{S}^{-1}(t, t_0)\hat{f}^I(t)\hat{S}(t, t_0)e^{i\hat{H}_0 t_0}, \tag{7.116}$$

and the state $\Psi^I(t_0)$ is related to the Heisenberg time-independent wave function by

$$\Psi^I(t_0) \equiv e^{i\hat{H}_0 t_0}\Psi^S(t_0) = e^{i\hat{H}_0 t_0}\Psi^H, \tag{7.117}$$

in accordance with our previous discussion of averaging we assume that at time $t = t_0$ Heisenberg operators coincide with time-independent Schrödinger operators $\hat{f}^H(t_0) = \hat{f}^S$, and Schrödinger wave function coincides at the same time with Heisenberg time-independent wave function $\Psi^S(t_0) = \Psi^H$. To avoid these additional exponents in (7.116) we can redefine the transformation to the interaction representation as

$$\hat{f}^I(t) = e^{i\hat{H}_0(t-t_0)}\hat{f}^S e^{-i\hat{H}_0(t-t_0)}, \tag{7.118}$$

in accordance with the transformation (7.6) for the time-independent Hamiltonian. Previously we showed that free-particle Green functions are not dependent on t_0 for equilibrium initial condition, if we want to consider some nontrivial initial conditions, it is easier to formulate these conditions directly for Green functions. Thus below we shall use relations

$$\hat{f}^H(t) = \hat{S}^{-1}(t, t_0)\hat{f}^I(t)\hat{S}(t, t_0), \tag{7.119}$$

and

$$\Psi^I(t_0) \equiv \Psi^S(t_0) = \Psi^H. \tag{7.120}$$

Green Functions in the Interaction Representation

Consider, for example, the lesser function

$$G^<_{\alpha\beta}(t_1, t_2) = i\left\langle c^\dagger_\beta(t_2)c_\alpha(t_1)\right\rangle = i\left\langle \Psi^H \left| c^\dagger_\beta(t_2)c_\alpha(t_1)\right| \Psi^H\right\rangle, \tag{7.121}$$

c-operators here are Heisenberg operators and they should be replaced by operators $c^I(t) \equiv \tilde{c}(t)$ in the interaction representation:

$$G^<_{\alpha\beta}(t_1, t_2) = i\left\langle \Psi^H \left| \hat{S}^{-1}(t_2, t_0)\tilde{c}^\dagger_\beta(t_2)\hat{S}(t_2, t_0)\hat{S}^{-1}(t_1, t_0)\tilde{c}_\alpha(t_1)\hat{S}(t_1, t_0)\right| \Psi^H\right\rangle. \tag{7.122}$$

Using properties of $\hat{S}$ operators, we rewrite this expression as

$$G^<_{\alpha\beta}(t_1, t_2) = i\left\langle \hat{S}(t_0, t_2)\tilde{c}^\dagger_\beta(t_2)\hat{S}(t_2, t_1)\tilde{c}_\alpha(t_1)\hat{S}(t_1, t_0)\right\rangle. \tag{7.123}$$

7.3 Schwinger-Keldysh Time Contour

7.3.1 Closed Time-Path Integration

Now let us introduce one useful trick, the so-called *closed time-path contour of integration*. First, note that the expression of the type

$$\hat{f}^H(t) = \hat{S}^{-1}(t,t_0)\hat{f}^I(t)\hat{S}(t,t_0) = \tilde{T}e^{i\int_{t_0}^{t}\hat{V}^I(t')dt'}\hat{f}^I(t)Te^{-i\int_{t_0}^{t}\hat{V}^I(t')dt'}, \quad (7.124)$$

can be written as

$$\hat{f}^H(t) = T_{C_t}\exp\left(-i\int_{C_t}\hat{V}^I(t')dt'\right)\hat{f}^I(t), \quad (7.125)$$

where the integral is taken along closed time contour from t_0 to t and then back from t to t_0

$$\int_{C_t}dt' = \int_{t_0}^{t}dt' + \int_{t}^{t_0}dt'. \quad (7.126)$$

The contour time-ordering operator T_{C_t} works along the contour C_t, it means that for times $t^{\rightarrow}$ it is usual time-ordering operator T, and for times $t^{\leftarrow}$ it is anti-time-ordering operator $\tilde{T}$. Symbolically

$$T_{C_t}\int_{C_t}dt' = T\int_{\rightarrow}dt' + \tilde{T}\int_{\leftarrow}dt'. \quad (7.127)$$

Consider now the application of this closed time-path contour to calculation of Green functions. It is convenient to start from the time-ordered function at $t_2 > t_1$

$$\left\langle T\left(\hat{B}(t_2)\hat{A}(t_1)\right)\right\rangle = \left\langle \hat{S}(t_0,t_2)\tilde{B}(t_2)\hat{S}(t_2,t_1)\tilde{A}(t_1)\hat{S}(t_1,t_0)\right\rangle, \quad (7.128)$$

here $\hat{A}(t)$ and $\hat{B}(t)$ are Heisenberg operators, $\tilde{A}(t)$ and $\tilde{B}(t)$ are operators in the interaction representation, and in the case of fermionic operators the additional minus should be added for any permutation of two operators.

Using the properties of the $\hat{S}$-operator, we transform this expression as

$$\left\langle \hat{S}(t_0,t_2)\tilde{B}(t_2)\hat{S}(t_2,t_1)\tilde{A}(t_1)\hat{S}(t_1,t_0)\right\rangle = \left\langle \hat{S}^{-1}(t_2,t_0)\tilde{B}(t_2)\hat{S}(t_2,t_1)\tilde{A}(t_1)\hat{S}(t_1,t_0)\right\rangle$$
$$= \left\langle \hat{S}^{-1}(\infty,t_0)\hat{S}(\infty,t_2)\tilde{B}(t_2)\hat{S}(t_2,t_1)\tilde{A}(t_1)\hat{S}(t_1,t_0)\right\rangle = \left\langle \hat{S}^{-1}T\left(\tilde{B}(t_2)\tilde{A}(t_1)\hat{S}\right)\right\rangle, \quad (7.129)$$

where we defined operator

$$\hat{S} = \hat{S}(\infty,t_0). \quad (7.130)$$

Using contour integration, it can be written as

$$\left\langle T\left(\hat{B}(t_2)\hat{A}(t_1)\right)\right\rangle = \left\langle T_C\left(\hat{S}_C\tilde{B}(t_2^{\rightarrow})\tilde{A}(t_1^{\rightarrow})\right)\right\rangle, \quad (7.131)$$

$$\hat{S}_C = T_C\exp\left(-i\int_C\hat{V}^I(t')dt'\right), \quad (7.132)$$

where the contour C goes from t_0 through t_1 and t_2, and back to t_0. If $t_2 > t_1$ it is obvious that contour ordering along $C^{\rightarrow}$ gives the terms from $\hat{S}(t_1, t_0)$ to $\hat{B}(t_2)$ in (7.128). The integral over the back path $C^{\leftarrow}$ gives

$$T_C \exp\left(-i \int_{\leftarrow} \hat{V}^I(t')dt'\right) = \tilde{T} \exp\left(-i \int_{t_2}^{t_0} \hat{V}^I(t')dt'\right)$$
$$= \tilde{T} \exp\left(i \int_{t_0}^{t_2} \hat{V}^I(t')dt'\right) = \hat{S}^{-1}(t_2, t_0) = \hat{S}(t_0, t_2). \tag{7.133}$$

For $t_2 < t_1$ the operators in (7.128) are reordered by T-operator and we again obtain (7.131).

The lesser and greater functions are not time-ordered and arguments of the operators are not affected by time-ordering operator. Nevertheless we can write such functions in the same form (7.131). The trick is to use one time argument from the forward contour and the other from the backward contour, for example

$$\left\langle \hat{B}(t_2)\hat{A}(t_1)\right\rangle = \left\langle T_C\left(\hat{S}_C \tilde{B}(t_2^{\leftarrow})\tilde{A}(t_1^{\rightarrow})\right)\right\rangle, \tag{7.134}$$

here the time t_1 is always before t_2.

7.3.2 Contour (Contour-Ordered) Green Function

Now we are able to define *contour* or *contour-ordered* Green function—the useful tool of Keldysh diagrammatic technique. The definition is similar to the previous one

$$G^C_{\alpha\beta}(\tau_1, \tau_2) = -i\left\langle T_C\left(c_\alpha(\tau_1)c^\dagger_\beta(\tau_2)\right)\right\rangle, \tag{7.135}$$

where, however, τ_1 and τ_2 are contour times. This function includes all nonequilibrium Green functions introduced before. Indeed, depending on contour position of times we obtain lesser, greater, or time-ordered functions (below we give different notations used in the literature)

$$G^C_{\alpha\beta}(\tau_1, \tau_2) = \begin{cases} \tau_1, \tau_2 \in C^{\rightarrow}: & -i\left\langle T c_\alpha(t_1)c^\dagger_\beta(t_2)\right\rangle \Longrightarrow G^{--} \text{ or } G^T(t_1, t_2), \\ \tau_1 \in C^{\leftarrow}, \tau_2 \in C^{\rightarrow}: & -i\left\langle c_\alpha(t_1)c^\dagger_\beta(t_2)\right\rangle \Longrightarrow G^{+-} \text{ or } G^{>}(t_1, t_2), \\ \tau_1 \in C^{\rightarrow}, \tau_2 \in C^{\leftarrow}: & i\left\langle c^\dagger_\beta(t_2)c_\alpha(t_1)\right\rangle \Longrightarrow G^{-+} \text{ or } G^{<}(t_1, t_2), \\ \tau_1, \tau_2 \in C^{\leftarrow}: & -i\left\langle \tilde{T} c_\alpha(t_1)c^\dagger_\beta(t_2)\right\rangle \Longrightarrow G^{++} \text{ or } G^{\tilde{T}}(t_1, t_2). \end{cases} \tag{7.136}$$

These four functions are not independent, from definitions it follows that

$$G^{<} + G^{>} = G^{T} + G^{\tilde{T}}, \tag{7.137}$$

and anti-Hermitian relations hold:

$$G^{T}_{\alpha\beta}(t_1, t_2) = -G^{T\,*}_{\beta\alpha}(t_2, t_1), \tag{7.138}$$
$$G^{<}_{\alpha\beta}(t_1, t_2) = -G^{<\,*}_{\beta\alpha}(t_2, t_1), \tag{7.139}$$
$$G^{>}_{\alpha\beta}(t_1, t_2) = -G^{>\,*}_{\beta\alpha}(t_2, t_1). \tag{7.140}$$

It is more convenient to use retarded and advanced functions instead of time-ordered functions. There is a number of ways to express G^R and G^A through above defined functions

$$G^{R} = \theta(t_1 - t_2)\left[G^{>} - G^{<}\right] = G^{T} - G^{<} = G^{>} - G^{\tilde{T}}, \tag{7.141}$$

$$G^{A} = \theta(t_2 - t_1)\left[G^{<} - G^{>}\right] = G^{T} - G^{>} = G^{<} - G^{\tilde{T}}. \tag{7.142}$$

This technique at real-time axes can be formulated for matrix functions

$$\check{G} = \begin{pmatrix} G^{++} & G^{+-} \\ G^{-+} & G^{--} \end{pmatrix}. \tag{7.143}$$

It is, however, more convenient to use the linear dependence of four functions and after the rotation in "Keldysh space" we get

$$\check{G} = \begin{pmatrix} G^{R} & G^{K} \\ 0 & G^{A} \end{pmatrix}, \tag{7.144}$$

where we obtain retarded ans advanced functions at the matrix diagonal and introduced new *Keldysh function* G^K

$$G^{K} = G^{>} + G^{<} = -i\langle[c_\alpha(t_1), c^{+}_{\beta}(t_2)]_{-}\rangle, \tag{7.145}$$
$$G^{<} = \tfrac{1}{2}G^{K} + \tfrac{i}{2}A. \tag{7.146}$$

7.3.3 Contour Green Function in the Interaction Representation

In the interaction representation one should repeat the calculations performed before and given the expressions (7.123), (7.128), and then replace usual times by contour times τ, so we obtain

$$\left\langle T_C\left(c_\alpha(\tau_1)c^\dagger_\beta(\tau_2)\right)\right\rangle = \left\langle T_C\left(\hat{S}(\tau_0,\tau_2)\tilde{c}^\dagger_\beta(\tau_2)\hat{S}(\tau_2,\tau_1)\tilde{c}_\alpha(\tau_1)\hat{S}(\tau_1,\tau_0)\right)\right\rangle. \tag{7.147}$$

Using contour integration, it can be written as

$$G^C_{\alpha\beta}(\tau_1,\tau_2) = -i\left\langle T_C\left(c_\alpha(\tau_1)c^\dagger_\beta(\tau_2)\right)\right\rangle = -i\left\langle T_C\left(\hat{S}_C\tilde{c}_\alpha(\tau_1)\tilde{c}^\dagger_\beta(\tau_2)\right)\right\rangle, \tag{7.148}$$

$$\hat{S}_C = T_C\exp\left(-i\int_C \hat{V}^I(t')dt'\right). \tag{7.149}$$

7.4 Nonequilibrium Equation of Motion Method

Now we start to consider the case of interacting nanosystems. Although it is possible to derive the *exact* expression for the current through an interacting central region (we consider it in Chap. 8), the problem to find the Green functions of the central region is sometimes highly nontrivial. At the present time there are several techniques developed to solve this problem.

The nonequilibrium equation of motion (NEOM) method is the simplest approximate approach. In spite of its simplicity, it is very useful in many cases, and is very convenient for numerical implementation. In this section we consider only a general formulation, some particular examples are considered further.

We start from the general definition of a Green function as the average of two Heisenberg operators $\hat{A}(t)$ and $\hat{B}(t)$, denoted as

$$\langle\langle \hat{A}(t_1), \hat{B}(t_2)\rangle\rangle^{R,A,<}.$$

The particular definitions of the averages for spectral and kinetic functions are

$$\left\langle\left\langle \hat{A}(t_1), \hat{B}(t_2)\right\rangle\right\rangle^R = -i\theta(t_1-t_2)\left\langle\left[\hat{A}(t_1), \hat{B}(t_2)\right]_\mp\right\rangle, \tag{7.150}$$

where upper sign here and below is for boson functions, lower sign for fermions,

$$\left\langle\left\langle \hat{A}(t_1), \hat{B}(t_2)\right\rangle\right\rangle^< = -i\left\langle\hat{A}(t_1), \hat{B}(t_2)\right\rangle. \tag{7.151}$$

The equations of motion for NGF are obtained from the Heisenberg equation of motion for operators

$$i\frac{\partial\hat{A}}{\partial t} = \left[\hat{A},\hat{H}\right]_- = \hat{A}\hat{H} - \hat{H}\hat{A}, \tag{7.152}$$

for any Heisenberg operator $\hat{A}(t)$. Here and below all Hamiltonians are *time-independent*. We consider the *stationary problem*.

7.4.1 Spectral (Retarded and Advanced) Functions

Let us start from a retarded function

$$\left\langle\!\left\langle \hat{A}(t_1), \hat{B}(t_2) \right\rangle\!\right\rangle^R = -i\theta(t_1 - t_2)\left\langle \left[\hat{A}(t_1), \hat{B}(t_2) \right]_{\mp} \right\rangle. \tag{7.153}$$

Taking the time derivative we obtain

$$i\frac{\partial}{\partial t_1}\left\langle\!\left\langle \hat{A}(t_1), \hat{B}(t_2) \right\rangle\!\right\rangle^R = \delta(t_1 - t_2)\left\langle \left[\hat{A}(t_1), \hat{B}(t_1) \right]_{\mp} \right\rangle + \left\langle\!\left\langle \left[\hat{A}(t_1), \hat{H} \right]_{-}, \hat{B}(t_2) \right\rangle\!\right\rangle^R, \tag{7.154}$$

where the first term originates from the time-derivative of the θ-function, and the (7.152) is used in the second term.

In the stationary case the Fourier transform can be used

$$(\epsilon + i\eta)\left\langle\!\left\langle \hat{A}, \hat{B} \right\rangle\!\right\rangle^R_\epsilon = \left\langle \left[\hat{A}, \hat{B} \right]_{\mp} \right\rangle + \left\langle\!\left\langle \left[\hat{A}, \hat{H} \right]_{-}, \hat{B} \right\rangle\!\right\rangle^R_\epsilon. \tag{7.155}$$

Now let us assume that the Hamiltonian can be divided into "free particle" and "interaction" parts $\hat{H} = \hat{H}_0 + \hat{H}_1$, and $[\hat{A}, \hat{H}_0]_- = \hat{\epsilon}_0\hat{A}$. (The simple example. For the free particle Hamiltonian $\hat{H}_0 = \sum_\beta \epsilon_\beta d^\dagger_\beta d_\beta$ and the operator $\hat{A} = d^\dagger_\alpha$ one has $[\hat{A}, \hat{H}_0]_- = \sum_\beta \epsilon_\beta [d^\dagger_\alpha, d^\dagger_\beta d_\beta]_- = \epsilon_\alpha d^\dagger_\alpha$, $\hat{\epsilon}_0 = \epsilon_\alpha$ is simply a number. In general, $\hat{\epsilon}_0$ is some time-independent operator). So that

$$(\epsilon + i\eta - \hat{\epsilon}_0)\left\langle\!\left\langle \hat{A}, \hat{B} \right\rangle\!\right\rangle^R_\epsilon = \left\langle \left[\hat{A}, \hat{B} \right]_{\mp} \right\rangle + \left\langle\!\left\langle \left[\hat{A}, \hat{H}_1 \right]_{-}, \hat{B} \right\rangle\!\right\rangle^R_\epsilon, \tag{7.156}$$

the second term includes interaction and can not be easy simplified.

It is convenient now to introduce the "free particle" function $\hat{g}^R_\epsilon$ as a solution of the equation

$$(\epsilon + i\eta - \hat{\epsilon}_0)\hat{g}^R_\epsilon = 1. \tag{7.157}$$

Now we multiply the right and left parts of (7.156) by $\hat{g}^R_\epsilon$. Using the function $\hat{g}^R(t) = \int \hat{g}^R_\epsilon e^{-i\epsilon t}\frac{d\epsilon}{2\pi}$ we can write the time-dependent solution of (7.154) as

$$\begin{aligned}\left\langle\!\left\langle \hat{A}(t_1), \hat{B}(t_2) \right\rangle\!\right\rangle^R &= \hat{g}^R(t_1 - t_2)\left\langle \left[\hat{A}(t_1), \hat{B}(t_1) \right]_{\mp} \right\rangle \\ &+ \int \hat{g}^R(t_1 - t')\left\langle\!\left\langle \left[\hat{A}(t'), \hat{H}_1 \right]_{-}, \hat{B}(t_2) \right\rangle\!\right\rangle^R dt'. \end{aligned} \tag{7.158}$$

7.4.2 EOM at the Schwinger-Keldysh Contour

The calculation of the lesser functions by the EOM technique requires some care. To demonstrate it let us compare the EOM for retarded and lesser functions of free particles.

The equation for $g^R_{\alpha\beta}$ is (assuming the diagonal matrix $\tilde{\epsilon}_{\alpha\beta}$)

$$(\epsilon + i\eta - \tilde{\epsilon}_\alpha)\, g^R_{\alpha\beta} = \delta_{\alpha\beta}, \tag{7.159}$$

from which the free-particle Green function is easily obtained.

At the same time for the lesser function we have the equation

$$(\epsilon - \tilde{\epsilon}_\alpha)\, g^<_{\alpha\beta} = 0, \tag{7.160}$$

from which, however, the free-particle lesser function $g^<_{\alpha\beta} = 2\pi f_0(\epsilon)\delta(\epsilon - \epsilon_\alpha)\delta_{\alpha\beta}$ can not be obtained.

The problem can be generally resolved by using the EOM on the Schwinger-Keldysh time contour. The contour-ordered Green function is defined as

$$\left\langle\!\left\langle \hat{A}(\tau_1), \hat{B}(\tau_2) \right\rangle\!\right\rangle^C = -i\left\langle T_C\left(\hat{A}(\tau_1), \hat{B}(\tau_2)\right)\right\rangle, \tag{7.161}$$

where $\hat{A}(\tau_1)$ and $\hat{B}(\tau_2)$ are two Heisenberg operators, defined along the contour.

Taking the time derivative we obtain the equation

$$i\frac{\partial}{\partial\tau_1}\left\langle\!\left\langle \hat{A}(\tau_1), \hat{B}(\tau_2) \right\rangle\!\right\rangle^C = \delta^c(\tau_1 - \tau_2)\left\langle\left[\hat{A}(\tau_1), \hat{B}(\tau_1)\right]_\mp\right\rangle + \left\langle\!\left\langle\left[\hat{A}(\tau_1), \hat{H}\right]_-, \hat{B}(\tau_2)\right\rangle\!\right\rangle^C, \tag{7.162}$$

in the stationary case this equation can be formally solved if one applies the Fourier transform along the contour, or perturbation expansion in the interaction representation (Niu et al. 1999). Using the free particle solution $\hat{g}^C(\tau_1 - \tau_2)$ we can write the time-dependent solution as

$$\begin{aligned}\left\langle\!\left\langle \hat{A}(\tau_1), \hat{B}(\tau_2) \right\rangle\!\right\rangle^C =& \hat{g}^C(\tau_1 - \tau_2)\left\langle\left[\hat{A}(\tau_1), \hat{B}(\tau_1)\right]_\mp\right\rangle \\ &+ \int \hat{g}^C(\tau_1 - \tau')\left\langle\!\left\langle\left[\hat{A}(\tau'), \hat{H}_1\right]_-, \hat{B}(\tau_2)\right\rangle\!\right\rangle^C d\tau'.\end{aligned} \tag{7.163}$$

7.4.3 Kinetic (Lesser) Function

Applying now the Langreth rules (see the next section for details), which shows, that from

$$C(\tau_1, \tau_2) = \int_C A(\tau_1, \tau_3) B(\tau_3, \tau_2) d\tau_3 \tag{7.164}$$

it follows

$$C^R(t_1, t_2) = \int A^R(t_1, t_3) B^R(t_3, t_2) dt_3, \tag{7.165}$$

$$C^<(t_1, t_2) = \int \left(A^R(t_1, t_3) B^R(t_3, t_2) + A^<(t_1, t_3) B^A(t_3, t_2) \right) dt_3, \tag{7.166}$$

we get (7.158) for the retarded function, and

$$\begin{aligned} \left\langle\!\left\langle \hat{A}(t_1), \hat{B}(t_2) \right\rangle\!\right\rangle^< &= \hat{g}^<(t_1 - t_2) \left\langle \left[\hat{A}(t_1), \hat{B}(t_1) \right]_\mp \right\rangle \\ &+ \int \hat{g}^R(t_1 - t') \left\langle\!\left\langle \left[\hat{A}(t'), \hat{H}_1 \right]_-, \hat{B}(t_2) \right\rangle\!\right\rangle^< dt' \\ &+ \int \hat{g}^<(t_1 - t') \left\langle\!\left\langle \left[\hat{A}(t'), \hat{H}_1 \right]_-, \hat{B}(t_2) \right\rangle\!\right\rangle^A dt' \end{aligned} \tag{7.167}$$

for the lesser function. And the Fourier transform is

$$\left\langle\!\left\langle \hat{A}, \hat{B} \right\rangle\!\right\rangle_\epsilon^< = \hat{g}_\epsilon^< \left\langle \left[\hat{A}, \hat{B} \right]_\mp \right\rangle + \hat{g}_\epsilon^R \left\langle\!\left\langle \left[\hat{A}, \hat{H}_1 \right]_-, \hat{B} \right\rangle\!\right\rangle_\epsilon^< + \hat{g}_\epsilon^< \left\langle\!\left\langle \left[\hat{A}, \hat{H}_1 \right]_-, \hat{B} \right\rangle\!\right\rangle_\epsilon^A. \tag{7.168}$$

7.5 Kadanoff-Baym-Keldysh Method

Now we review briefly the other approach. The Kadanoff-Baym-Keldysh method systematically extends the equilibrium many-body theory to the nonequilibrium case. Potentially, it is the most powerful approach. Below we give a simple introduction into the method, which is currently actively developed.

7.5.1 Perturbation Expansion and Diagrammatic Rules for Contour Functions

We found that Green functions can be written in the interaction representation with a help of the $\hat{S}$-operator. For example, the time-ordered fermionic Green function is

$$G^T_{\alpha\beta}(t_1, t_2) = -i \left\langle T \left(c_\alpha(t_1) c^\dagger_\beta(t_2) \right) \right\rangle = -i \left\langle \hat{S}^{-1} T \left(\tilde{c}_\alpha(t_1) \tilde{c}^\dagger_\beta(t_2) \hat{S} \right) \right\rangle, \tag{7.169}$$

using "usual" $\hat{S}$-operator

$$\hat{S} = \hat{S}(\infty, t_0) = T \exp\left(-i \int_{t_0}^{\infty} \hat{V}^I(t')dt'\right), \tag{7.170}$$

or

$$G^T_{\alpha\beta}(t_1, t_2) = -i\left\langle T_C \left(\tilde{c}_\alpha(t_1^{\rightarrow})\tilde{c}^\dagger_\beta(t_2^{\rightarrow})\hat{S}_C\right)\right\rangle, \tag{7.171}$$

using "contour" $\hat{S}_C$-operator

$$\hat{S}_C = T_C \exp\left(-i \int_C \hat{V}^I(t')dt'\right). \tag{7.172}$$

We first consider the zero temperature case, when one can set $t_0 = -\infty$,

$$\hat{S} = \hat{S}(\infty, -\infty) = T \exp\left(-i \int_{-\infty}^{\infty} \hat{V}^I(t')dt'\right), \tag{7.173}$$

and assume that interaction is switched on and switched off at $t \to +\infty$ *adiabatically*. This condition is necessary to prevent excitation of the system from its ground state. The other necessary condition is that the perturbation is time-independent in the Schrödinger representation. In this case if the initial state $|\Psi(t = -\infty)\rangle = |\Psi_0\rangle$ is the ground state (of free particles), then the final state $|\Psi(t = +\infty)\rangle = \hat{S}|\Psi^0\rangle = e^{i\theta}|\Psi^0\rangle$ is also the ground state, only the phase can be changed. Now, using the average value of the $\hat{S}$-operator

$$\langle\hat{S}\rangle = \langle\Psi^0|\hat{S}|\Psi^0\rangle = e^{i\theta}\langle\Psi^0|\Psi^0\rangle = e^{i\theta}, \tag{7.174}$$

we obtain

$$\hat{S}|\Psi^0\rangle = \langle\hat{S}\rangle|\Psi^0\rangle, \tag{7.175}$$

and

$$\langle\Psi^0|\hat{S}^{-1} = \frac{\langle\Psi^0|}{\langle\hat{S}\rangle}. \tag{7.176}$$

So that (7.169) can be written as

$$G^T_{\alpha\beta}(t_1, t_2) = -i\frac{\left\langle T\left(\tilde{c}_\alpha(t_1)\tilde{c}^\dagger_\beta(t_2)\hat{S}\right)\right\rangle}{\langle\hat{S}\rangle}. \tag{7.177}$$

Now we can expand the exponent (note that S-operator is defined only in the sense of this expansion)

$$\hat{S} = T \exp\left(-i \int_{-\infty}^{\infty} \hat{V}^I(t')dt'\right)$$
$$= T \sum_{n=0}^{\infty} \frac{(-i)^n}{n!} \int_{-\infty}^{\infty} dt_1' \ldots \int_{-\infty}^{\infty} dt_n' \, \hat{V}^I(t_1') \ldots \hat{V}^I(t_n'), \tag{7.178}$$

and numerator and denominator of the expression (7.177) are

$$\left\langle T\left(\tilde{c}_\alpha(t_1)\tilde{c}_\beta^\dagger(t_2)\hat{S}\right)\right\rangle$$
$$= \sum_{n=0}^{\infty} \frac{(-i)^n}{n!} \int_{-\infty}^{\infty} dt_1' \ldots \int_{-\infty}^{\infty} dt_n' \left\langle T\tilde{c}_\alpha(t_1)\tilde{c}_\beta^\dagger(t_2)\hat{V}^I(t_1') \ldots \hat{V}^I(t_n')\right\rangle, \tag{7.179}$$

$$\langle \hat{S} \rangle = \sum_{n=0}^{\infty} \frac{(-i)^n}{n!} \int_{-\infty}^{\infty} dt_1' \ldots \int_{-\infty}^{\infty} dt_n' \left\langle T\hat{V}^I(t_1') \ldots \hat{V}^I(t_n')\right\rangle. \tag{7.180}$$

These expressions are used to produce the perturbation series.

The main quantity to be calculated is the contour Green function

$$G(1,2) \equiv G^C_{\alpha\beta}(\tau_1, \tau_2) = -i\left\langle T_C\left(c_\alpha(\tau_1)c_\beta^\dagger(\tau_2)\right)\right\rangle, \tag{7.181}$$

where τ_1 and τ_2 are contour times. Here $1_c \equiv \alpha, \tau_1$.

The general diagrammatic rules for contour Green functions are exactly the same as in the usual zero-temperature technique (we call it standard rules). The correspondence between diagrams and analytical expressions is established in the following way:

1. Open bare electron line is $iG_0(1,2)$.
2. Closed bare electron line is $n_0(1) \equiv n_\alpha^{(0)}(\tau_1)$.
3. Bare interaction line is $-iv(1,2)$.
4. Self-energy is $-i\Sigma(1,2)$.
5. Integration over internal vertices, and other standard rules.

7.5.2 *Langreth Rules*

Although the basic equations and diagrammatic rules are formulated for contour Green functions, the solution of these equations and final results are much more transparent when represented by real-time spectral and kinetic functions.

As in the ordinary diagrammatic technique, the important role is played by the integration (summation) over space and contour-time arguments of Green functions, which is denoted as

$$\int d1_c \equiv \sum_{\alpha} \int_C d\tau_1. \tag{7.182}$$

After application of the Langreth rules [1], for real-time functions these integrals become

$$\int d1 \equiv \sum_{\alpha} \int_{-\infty}^{\infty} dt_1. \tag{7.183}$$

The Langreth rules show, for example, that from

$$C(\tau_1, \tau_2) = \int_C A(\tau_1, \tau_3) B(\tau_3, \tau_2) d\tau_3 \tag{7.184}$$

it follows

$$C^R(t_1, t_2) = \int A^R(t_1, t_3) B^R(t_3, t_2) dt_3, \tag{7.185}$$

$$C^<(t_1, t_2) = \int \left(A^R(t_1, t_3) B^<(t_3, t_2) + A^<(t_1, t_3) B^A(t_3, t_2) \right) dt_3. \tag{7.186}$$

The other important rules are: from

$$C(\tau_1, \tau_2) = A(\tau_1, \tau_2) B(\tau_1, \tau_2) \tag{7.187}$$

it follows

$$C^R(t_1, t_2) = A^R(t_1, t_2) B^R(t_1, t_2) + A^R(t_1, t_2) B^<(t_1, t_2) + A^<(t_1, t_2) B^R(t_1, t_2), \tag{7.188}$$

$$C^<(t_1, t_2) = A^<(t_1, t_2) B^<(t_1, t_2), \tag{7.189}$$

and from

$$C(\tau_1, \tau_2) = A(\tau_1, \tau_2) B(\tau_2, \tau_1) \tag{7.190}$$

it follows

$$C^R(t_1, t_2) = A^R(t_1, t_2) B^<(t_2, t_1) + A^<(t_1, t_2) B^A(t_2, t_1), \tag{7.191}$$

$$C^<(t_1, t_2) = A^<(t_1, t_2) B^>(t_2, t_1). \tag{7.192}$$

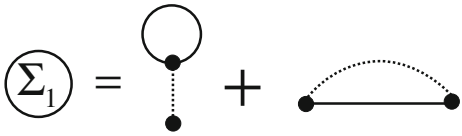

Fig. 7.1 Diagrammatic representation of the first-order self-energy

7.5.3 First-Order Self-Energy and Polarization Operator

Consider, as an example, the first order expression for the self-energy, shown in Fig. 7.1. Following the diagrammatic rules, we find

$$\Sigma_1(1,2) = \delta(1-2)\int v(1,3)n_0(3)d3 + iv(1,2)G_0(1,2), \tag{7.193}$$

where the first term is the Hartree contribution, which can be included into the unperturbed Green function $G_0(1,2)$. This expression is actually symbolic, and translation from contour (Keldysh-time) to real-time functions is necessary. Using the Langreth rules, one obtains

$$\begin{aligned}\Sigma_1^R(1,2) =& \delta(1^+-2)\int v^R(1,3)n_0(3,3)d3 + iv^R(1,2)G_0^R(1,2)\\ &+ iv^<(1,2)G_0^R(1,2) + iv^R(1,2)G_0^<(1,2),\end{aligned} \tag{7.194}$$

$$\Sigma_1^<(1,2) = iv^<(1,2)G_0^<(1,2). \tag{7.195}$$

There is no Hartree term for lesser function, because the times τ_1 and τ_2 are always at the different branches of the Keldysh contour, and the δ-function $\delta(\tau_1-\tau_2)$ is zero.

In the stationary case and using explicit matrix indices, we have, finally (here $\tau = t_1 - t_2$, not to mix with the Keldysh time)

$$\begin{aligned}\Sigma_{\alpha\beta}^{R(1)}(\tau) =& \delta(\tau^+)\delta_{\alpha\beta}\textstyle\sum_\gamma \tilde{v}_{\alpha\gamma}^R(0)n_\gamma^{(0)} + iv_{\alpha\beta}^R(\tau)G_{\alpha\beta}^{R(0)}\tau)\\ &+iv_{\alpha\beta}^<(\tau)G_{\alpha\beta}^{R(0)}(\tau) + iv_{\alpha\beta}^R(\tau)G_{\alpha\beta}^{<(0)}(\tau),\end{aligned} \tag{7.196}$$

$$\Sigma_{\alpha\beta}^{<(1)}(\tau) = iv_{\alpha\beta}^<(\tau)G_{\alpha\beta}^{<(0)}(\tau), \tag{7.197}$$

and we define the Fourier transform of the bare interaction

$$\tilde{v}_{\alpha\gamma}^R(0) = \int v_{\alpha\gamma}^R(\tau)d\tau. \tag{7.198}$$

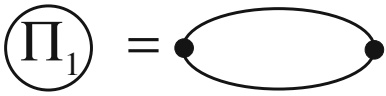

Fig. 7.2 Diagrammatic representation of the first-order polarization operator

Finally, the Fourier transforms are

$$\Sigma^{R(1)}_{\alpha\beta}(\epsilon) = \delta_{\alpha\beta}\sum_{\gamma}\tilde{v}^{R}_{\alpha\gamma}(0)n^{(0)}_{\gamma} + i\int\frac{d\epsilon'}{2\pi}\left[v^{R}_{\alpha\beta}(\epsilon')G^{R(0)}_{\alpha\beta}(\epsilon-\epsilon') + v^{<}_{\alpha\beta}(\epsilon')G^{R(0)}_{\alpha\beta}(\epsilon-\epsilon') + v^{R}_{\alpha\beta}(\epsilon')G^{<(0)}_{\alpha\beta}(\epsilon-\epsilon')\right], \tag{7.199}$$

$$\Sigma^{<(1)}_{\alpha\beta}(\epsilon) = i\int\frac{d\epsilon'}{2\pi}v^{<}_{\alpha\beta}(\epsilon')G^{<(0)}_{\alpha\beta}(\epsilon-\epsilon'). \tag{7.200}$$

The second important function is the polarization operator ("self-energy for interaction"), shown in Fig. 7.2. Following the diagrammatic rules, we find

$$\Pi_1(1,2) = -iG_0(1,2)G_0(2,1), \tag{7.201}$$

note the order of times in this expression.

Using the Langreth rules,

$$\Pi^{R}_1(1,2) = iG^{R}_0(1,2)G^{<}_0(2,1) + iG^{<}_0(1,2)G^{A}_0(2,1), \tag{7.202}$$

$$\Pi^{<}_1(1,2) = iG^{<}_0(1,2)G^{>}_0(2,1). \tag{7.203}$$

And in the stationary case, restoring the matrix indices

$$\Pi^{R(1)}_{\alpha\beta}(\tau) = -i\left[G^{R(0)}_{\alpha\beta}(\tau)G^{<(0)}_{\beta\alpha}(-\tau) + G^{<(0)}_{\alpha\beta}(\tau)G^{A(0)}_{\beta\alpha}(-\tau)\right], \tag{7.204}$$

$$\Pi^{<(1)}_{\alpha\beta}(\tau) = -iG^{<(0)}_{\alpha\beta}(\tau)G^{>(0)}_{\beta\alpha}(-\tau). \tag{7.205}$$

In the Fourier representation

$$\Pi^{R(1)}_{\alpha\beta}(\epsilon) = -i\int\frac{d\epsilon'}{2\pi}\left[G^{R(0)}_{\alpha\beta}(\epsilon')G^{<(0)}_{\beta\alpha}(\epsilon'-\epsilon) + G^{<(0)}_{\alpha\beta}(\epsilon')G^{A(0)}_{\beta\alpha}(\epsilon'-\epsilon)\right], \tag{7.206}$$

$$\Pi^{<(1)}_{\alpha\beta}(\epsilon) = -i\int\frac{d\epsilon'}{2\pi}G^{<(0)}_{\alpha\beta}(\epsilon')G^{>(0)}_{\beta\alpha}(\epsilon'-\epsilon). \tag{7.207}$$

These expressions are quite general and can be used for both electron-electron and electron-vibron interaction.

For Coulomb interaction the bare interaction is is $v(1,2) \equiv U_{\alpha\beta}\delta(\tau_1^+ - \tau_2)$, so that

$$v^R(1,2) \equiv U_{\alpha\beta}\delta(t_1^+ - t_2), \tag{7.208}$$

$$v^<(1,2) = 0. \tag{7.209}$$

7.5.4 *Self-consistent Equations*

Hedin's Equations at Keldysh Contour

The diagrams can be partially summed in all orders of perturbation theory. The resulting equations are known as Dyson equations for the dressed Green function $G(1,2)$ and the effective interaction $W(1,2)$ (Fig. 7.3). Analytically these equations are written as (in general nonequilibrium case the functions are contour functions and integration is over Keldysh contour)

$$G(1,2) = G_0(1,2) + \int\int G_0(1,3)\Sigma(3,4)G(4,2)d3d4, \tag{7.210}$$

$$W(1,2) = v(1,2) + \int\int v(1,3)\Pi(3,4)W(4,2)d3d4. \tag{7.211}$$

In the perturbative approach the first order (or higher order) expressions for the self-energy and the polarization operator are used. The other possibility is to summarize further the diagrams and obtain the self-consistent approximations (Figs. 7.4 and 7.5), which include, however, a new unknown function, called vertex function. We shall write these expressions analytically, including the Hartree-Fock part in the unperturbed Green function $G_0(1,2)$.

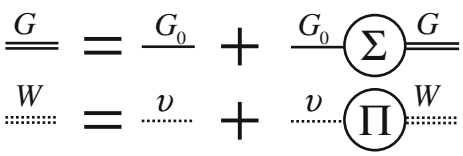

Fig. 7.3 Diagrammatic representation of the Dyson equations

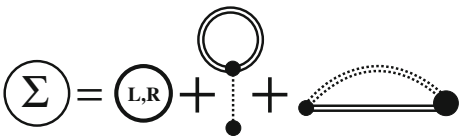

Fig. 7.4 Diagrammatic representation of the full self-energy

Fig. 7.5 Diagrammatic representation of the full polarization operator

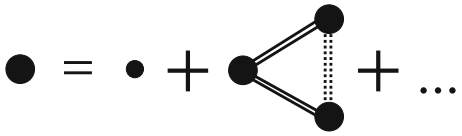

Fig. 7.6 Diagrammatic representation of the vertex function

$$\Sigma'(1,2) = i \iint W(1,3)G(1,4)\Gamma(3;4,2)d3d4, \tag{7.212}$$

$$\Pi(1,2) = -i \iint G(1,3)G(4,1)\Gamma(2;3,4)d3d4. \tag{7.213}$$

Here we introduce the vertex function $\Gamma(1;2,3)$ which depends on three coordinates and connects two electron lines and one interaction line. The equation for the vertex function can not be closed diagrammatically (Fig. 7.6). Nevertheless, it is possible to write a closed set of equations (*Hedin's equations* [2]), which are exact equations for full Green functions written through a functional derivative. Hedin's equations are (7.210)–(7.213) and the equation for the vertex function

$$\Gamma(1;2,3) = \delta(1,2)\delta(1,3) + \iiint G(4,6)G(7,5)\Gamma(1;6,7)\frac{\delta\Sigma(2,3)}{\delta G(4,5)}d4d5d6d7. \tag{7.214}$$

Real-Time Equations

There are several ways to get real-time equations from Hedin's equations for contour functions. One is to use the Langreth rules. The other, equivalent, method was suggested by Keldysh [3]. Retarded G^R, advanced G^A and Keldysh G^K (or lesser $G^<$) functions can be considered as the components of matrices

$$\check{G} = \begin{pmatrix} G^R & G^K(G^<) \\ 0 & G^A \end{pmatrix}, \quad \check{\Sigma} = \begin{pmatrix} \Sigma^R & \Sigma^K(\Sigma^<) \\ 0 & \Sigma^A \end{pmatrix}. \tag{7.215}$$

Below, the symbol $\check{...}$ denotes the matrix in Keldysh space, and the spin-matrix structure of Green functions $G^{(R,A,K)}$ and $\Sigma^{(R,A,K)}$ is assumed if necessary. In the spin-degenerate case $G^{(R,A,K)}_{\alpha\beta} = G^{(R,A,K)}\delta_{\alpha\beta}$, in general $\check{G}$ and $\check{\Sigma}$ are matrices in Keldysh and spin spaces. It was shown that diagrammatic expansions for the matrix functions $\check{G}$ and $\check{\Sigma}$ are similar to corresponding expansions for equilibrium Green functions (see [4] and references there). If $\check{\Sigma}$ is the known functional of $\check{G}$,

then the functions $G^{(R,A,K)}$ can be determined from the Dyson-Keldysh equation in differential form

$$\left[i\frac{\partial}{\partial t_1} - \breve{H}(t_1)\right]\breve{G} - \left\{\breve{\Sigma}\breve{G}\right\} = \breve{\delta}, \tag{7.216}$$

or in integral form

$$\breve{G} = \breve{G}_0 + \{\breve{G}_0\breve{\Sigma}\breve{G}\}, \tag{7.217}$$

where $\breve{\delta} = \breve{I}\delta_{\eta\eta'}\delta(t_1 - t_2)$, $\breve{I}$ is the unity matrix in Keldysh space,

$$\{AB\}_{\eta\eta'}(t_1, t_2) = \sum_{\gamma}\int dt_3 A_{\eta\gamma}(t_1, t_3)B_{\gamma\eta'}(t_3, t_2),$$

and $\breve{H}(t)$ is the single-particle Hamiltonian which determines the bare Green function $\breve{G}_0$. The self-energy $\breve{\Sigma}$ describes interactions. These equations are mathematically equivalent to the contour equation (7.210). Take now the components of this matrix equations.

The equations for the retarded (advanced) functions are:

$$\left[i\frac{\partial}{\partial t_1} - H\right]G^{R(A)} - \left\{\Sigma^{R(A)}G^{R(A)}\right\} = \delta(x_1 - x_2). \tag{7.218}$$

Or in integral form

$$G^{R(A)} = G_0^{R(A)} + \left\{G_0^{R(A)}\Sigma^{R(A)}G^{R(A)}\right\}. \tag{7.219}$$

And the equation for the Keldysh function is

$$\left[i\frac{\partial}{\partial t_1} - H\right]G^{K} - \left\{\Sigma^{R}G^{K} + \Sigma^{K}G^{A}\right\} = 0, \tag{7.220}$$

it is the same as the *Kadanoff-Baym equation* for the lesser function $G^{<}$. Or in integral form

$$G^{K} = \left\{G^{R}\Sigma^{K}G^{A}\right\}, \tag{7.221}$$

this equation is known as *Keldysh equation*. The time-independent equations are obtained then in usual way.

Self-consistent GW Approximation

One of the popular approximations is GW approximation, neglecting the vertex part. Here we present this equations already in explicit matrix notation.

For the self-energy shown in Fig. 7.4 we obtain

$$\Sigma^R_{\alpha\beta}(\epsilon) = i \int \frac{e^{i\eta\epsilon'} d\epsilon'}{2\pi} \Big[W^R_{\alpha\beta}(\epsilon') G^<_{\alpha\beta}(\epsilon - \epsilon') + W^<_{\alpha\beta}(\epsilon') G^R_{\alpha\beta}(\epsilon - \epsilon') + W^R_{\alpha\beta}(\epsilon') G^R_{\alpha\beta}(\epsilon - \epsilon') - \sum_\gamma v^R_{\alpha\gamma} G^<_{\gamma\gamma}(\epsilon') \delta_{\alpha\beta} \Big], \tag{7.222}$$

$$\Sigma^<_{\alpha\beta}(\epsilon) = i \int \frac{d\epsilon'}{2\pi} W^<_{\alpha\beta}(\epsilon') G^<_{\alpha\beta}(\epsilon - \epsilon'). \tag{7.223}$$

The usual self-consistent Hartree-Fock approximation is obtained from this self-energy if one neglects renormalization of the effective interaction $W_{\alpha\beta}$, and uses unperturbed values $v^R_{\alpha\beta}(\epsilon) = v^A_{\alpha\beta}(\epsilon) = U_{\alpha\beta}$, $v^<_{\alpha\beta}(\epsilon) = 0$.

For the polarization operator one gets

$$\Pi^R_{\alpha\beta}(\epsilon) = -i \int \frac{d\epsilon'}{2\pi} \left[G^<_{\alpha\beta}(\epsilon') G^A_{\beta\alpha}(\epsilon' - \epsilon) + G^R_{\alpha\beta}(\epsilon') G^<_{\beta\alpha}(\epsilon' - \epsilon) \right], \tag{7.224}$$

$$\Pi^<_{\alpha\beta}(\epsilon) = -i \int \frac{d\epsilon'}{2\pi} G^<_{\alpha\beta}(\epsilon') G^>_{\beta\alpha}(\epsilon' - \epsilon). \tag{7.225}$$

References

1. D. Langreth, in *Linear and Nonlinear Electron Transport in Solid*, ed. by J. Devreese, E. van Doren (Plenum, New York, 1976)
2. L. Hedin, Phys. Rev. **139**, A796 (1965)
3. L.V. Keldysh, Zh. Eksp. Teor. Fiz. **47**, 1515 (1964). [Sov. Phys. JETP **20**, 1018 (1965)]
4. J. Rammer, H. Smith, Rev. Mod. Phys. **58**, 323 (1986)

Chapter 8
NGF Method for Transport Through Nanosystems

In this chapter we start to describe quantum transport systematically using the technique of the nonequilibrium many-body theory. Our main focus is the Nonequilibrium Green Function (NGF) method, which is very convenient approach for transport in both noninteracting and interacting nanosystems.

In Sects. 8.1 and 8.2 we introduce a model used in the last part of the book, it includes the discrete-level basis noninteracting Hamiltonian, the tunneling coupling to the ideal electrodes, the electron-electron interaction in the form of the Hubbard Hamiltonian, linear vibrons and the linear electron-vibron interaction. Although this model is only one particular case of the many-body models, it is general enough to describe all main inelastic and interacting effects in quantum transport and we consider it as the "standard" model in this sense.

In Sect. 8.3 we present the Dyson-Keldysh equations for nanosystems in integral and differential forms. We start from time-dependent matrix formulation and get the system of coupled equations for retarded (advanced) and for lesser functions. These equations with corresponding self-energies give in principle a complete description of quantum transport through interacting systems.

Finally in Sect. 8.4 we obtain the Meir-Wingreen-Jauho current formula, which is the central expression of the theory for standard model with noninteracting electrodes. We consider time-dependent and stationary formulas and some limiting cases.

8.1 Standard Transport Model: A Nanosystem Between Ideal Electrodes

First of all, we formulate a discrete-level model to describe nanoscale quantum systems (quantum dots, systems of many quantum dots, molecules) with and without interactions, coupled to free conduction electrons in the electrodes (Fig. 8.1). Without the electron-electron and electron-vibron interactions this model is equivalent to the models considered in Chap. 3. From this point of view it is straightforward to extend

D.A. Ryndyk, *Theory of Quantum Transport at Nanoscale*,
Springer Series in Solid-State Sciences 184,
DOI 10.1007/978-3-319-24088-6_8

the matrix Green function method from noninteracting to interacting systems. The electrodes are assumed to be ideal in the same sense as in the Landauer approach: they are noninteracting and in equilibrium, the electrochemical potentials can be shifted by external voltage, all electrons, coming through the central system from one electrode to the other one, are thermalized in the electrodes.

We include the Coulomb interaction through the Hubbard Hamiltonian to be able to describe correlation effects, such as Coulomb blockade and Kondo effect, which dominate at low temperatures. At high temperatures or weak interaction the self-consistent mean-field effects are well reproduced by the same model. Furthermore, electrons are coupled to vibrational modes, below we use the electron-vibron model Hamiltonian. Different parts of this model were already discussed before in detail, we combine it here for convenience. We present the particular forms of the electron-electron and electron-vibron interactions, which are used in the examples below. Of course, there are many other types of interactions with corresponding Hamiltonians. We do not aim to give a comprehensive review of all possible many-body models. On the other hand, the model we take is quite general and describes resonant transport, interference, inelastic transport, inelastic electron-vibron effects, all main many-body strongly correlated phenomena, such as Coulomb Blockade, Kondo effects, polaron effects, and many other. Thus, our model can be considered as a good framework to model many-body quantum transport at nanoscale. For this reason we call it "standard transport model". Actually, full solution of this model will be a big step towards quantitative modeling of quantum transport at nanoscale. Unfortunately, even the computational modeling is still a challenge.

The full Hamiltonian is the sum of the noninteracting central system Hamiltonian $\hat{H}_C^{(0)}$, the inter-system electron-electron interaction Hamiltonian $\hat{H}_{ee}$, the vibron Hamiltonian $\hat{H}_V$ including the electron-vibron interaction and coupling of vibrations to the environment (dissipation of vibrons), the Hamiltonians of the leads $\hat{H}_{R(L)}$, and the tunneling Hamiltonian $\hat{H}_T$ describing the system-to-lead coupling:

$$\hat{H} = \hat{H}_C^{(0)} + \hat{H}_{ee} + \hat{H}_V + \hat{H}_L + \hat{H}_R + \hat{H}_T. \tag{8.1}$$

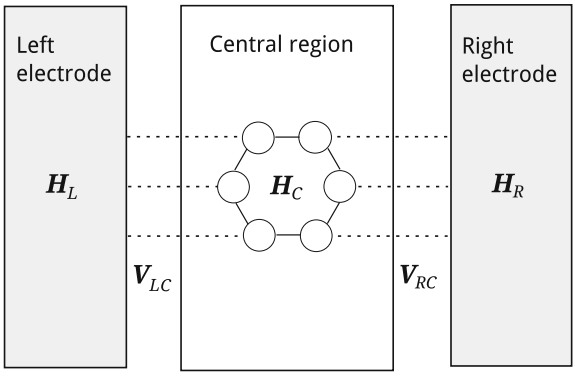

Fig. 8.1 A nanosystem between ideal leads: schematic representation of the standard transport model

An isolated noninteracting nanosystem is described as a set of discrete states $|\alpha\rangle$ with energies ε_α and inter-orbital overlap integrals $t_{\alpha\beta}$ by the following model Hamiltonian:

$$\hat{H}_C^{(0)} = \sum_{\alpha\beta} \tilde{\varepsilon}_{\alpha\beta} d_\alpha^\dagger d_\beta = \sum_\alpha \left(\varepsilon_\alpha + e\varphi_\alpha(t)\right) d_\alpha^\dagger d_\alpha + \sum_{\alpha\neq\beta} t_{\alpha\beta} d_\alpha^\dagger d_\beta, \tag{8.2}$$

where $d_\alpha^\dagger$,d_α are creation and annihilation operators in the states $|\alpha\rangle$, and $\varphi_\alpha(t)$ is the effective (self-consistent, can be time-dependent) electrical potential. The index α is used to mark single-electron states (e.g. atomic orbitals) including the spin degree of freedom. In the eigenstate (molecular orbital) representation the second term is absent and the Hamiltonian is diagonal.

For molecular transport the parameters of a model are to be determined by *ab initio* methods or considered as semi-empirical. This is a compromise, which allows us to consider complex molecules with a relatively simple model.

The electrical potential of the molecule φ_α plays an important role in transport at finite voltages. It describes the shift of the molecular level by the bias voltage, which is divided between the left lead (tip), the right lead (substrate), and the molecule as $\varphi_\alpha = \varphi_R + \eta_\alpha(\varphi_L - \varphi_R)$ [1]. We assume the simplest linear dependence of the molecular potential ($\eta_\alpha = const$), but its nonlinear dependence [2] can be easily included in our model.

The Hamiltonians of the right (R) and left (L) leads are

$$\hat{H}_{s=L(R)} = \sum_{k\sigma} (\varepsilon_{sk\sigma} + e\varphi_s(t)) c_{sk\sigma}^\dagger c_{sk\sigma}, \tag{8.3}$$

$\varphi_i(t)$ are the electrical potentials of the leads, the index k is the wave vector, but can be considered as representing an other conserved quantum number, σ is the spin index, but can be considered as a generalized channel number, describing e.g. different bands or subbands in semiconductors. Alternatively, the tight-binding model can be used also for the leads, then (8.3) should be considered as a result of the Fourier transformation. The leads are assumed to be noninteracting and in equilibrium.

The tunneling Hamiltonian

$$\hat{H}_T = \sum_{s=L,R} \sum_{k\sigma,\alpha} \left(V_{sk\sigma,\alpha} c_{sk\sigma}^\dagger d_\alpha + V_{sk\sigma,\alpha}^* d_\alpha^\dagger c_{sk\sigma} \right) \tag{8.4}$$

describes the hopping between the leads and the system. The direct hopping between two leads is neglected (relatively weak molecule-to-lead coupling case). Note, that the direct hoping between equilibrium leads can be easy taken into account as an additional independent current channel.

The Coulomb interaction inside a system is described by the Hubbard Hamiltonian (see discussion in Sect. 5.1.3):

$$\hat{H}_{ee} = \frac{1}{2}\sum_{\alpha\neq\beta} U_{\alpha\beta}\hat{n}_\alpha\hat{n}_\beta. \tag{8.5}$$

This Hamiltonian is used usually only for the short-range part of Coulomb interaction. The long-range interactions can be better introduced through the self-consistent electrical potential φ_α, which is determined by the Poison equation with the average electron density.

Vibrations and the electron-vibron coupling are described by the Hamiltonian (derived in Sect. 6.1.2):

$$\hat{H}_V = \sum_q \hbar\omega_q a_q^\dagger a_q + \sum_{\alpha\beta}\sum_q \lambda_{\alpha\beta}^q (a_q + a_q^\dagger) d_\alpha^\dagger d_\beta + \hat{H}_e. \tag{8.6}$$

Here vibrations are considered as localized phonons and q is the index labeling them, not the wave-vector. The first term describes free vibrons with the energy $\hbar\omega_q$. The second term represents the electron-vibron interaction. The third term describes the coupling to the environment and the dissipation of vibrons. We include both diagonal coupling, which originates from a change of the electrostatic energy with the distance between atoms, and the off-diagonal coupling, which can be obtained from the dependence of the matrix elements $t_{\alpha\beta}$ over the distance between atoms.

We will also use the Hamiltonian in the following matrix form:

$$\boldsymbol{H} = \begin{pmatrix} \boldsymbol{H}_L & \boldsymbol{V}_{LC} & 0 \\ \boldsymbol{V}_{CL} & \boldsymbol{H}_C & \boldsymbol{V}_{CR} \\ 0 & \boldsymbol{V}_{RC} & \boldsymbol{H}_R \end{pmatrix}, \tag{8.7}$$

where $\boldsymbol{H}_C$ includes all interactions, and $\boldsymbol{V}_{sp}$ represent coupling to the leads.

8.2 Nonequilibrium Current and Charge

To connect the microscopic description of a system with the macroscopic (electromagnetic) equations and calculate the observables, we need the expressions for the nonequilibrium electrical charge of the system and the current between the system and the leads.

The charge in a nonequilibrium state is given by (Q_0 is the background charge)

$$Q_C(t) = e\sum_\alpha \left\langle d_\alpha^\dagger d_\alpha \right\rangle - Q_0. \tag{8.8}$$

To calculate the current we find the time evolution of the particle number operator $\hat{N}_C = \sum_\alpha d_\alpha^\dagger d_\alpha$ due to tunneling from the left ($i = L$) or right ($i = R$) contact.

The current *from* the left ($i = L$) or right ($i = R$) contact *to* the nanosystem is determined by (note, that we consider e as the charge of the electron (negative) or

the hole (positive))

$$J_i(t) = -e\left\langle\left(\frac{dN_C}{dt}\right)_i\right\rangle = -\frac{ie}{\hbar}\left\langle[H_T^{(i)}, N_C]\right\rangle, \tag{8.9}$$

where

$$H_T^{(i)} = \sum_{k\sigma,\alpha}\left(V_{ik\sigma,\alpha}c_{ik\sigma}^{\dagger}d_\alpha + V_{ik\sigma,\alpha}^{*}d_\alpha^{\dagger}c_{ik\sigma}\right) \tag{8.10}$$

is the Hamiltonian of the coupling to the corresponding contact. The current is determined by only this part of the full Hamiltonian (8.1), because all other terms commute with $\hat{N}_C$.

Applying the commutation relation

$$\begin{aligned}\left[d_\alpha, d_\beta^{\dagger}d_\beta\right] &= d_\alpha d_\beta^{\dagger}d_\beta - d_\beta^{\dagger}d_\beta d_\alpha = d_\alpha d_\beta^{\dagger}d_\beta + d_\beta^{\dagger}d_\alpha d_\beta \\ &= (d_\alpha d_\beta^{\dagger} + \delta_{\alpha\beta} - d_\alpha d_\beta^{\dagger})d_\beta = \delta_{\alpha\beta}d_\alpha,\end{aligned} \tag{8.11}$$

one obtains finally

$$J_i(t) = \frac{ie}{\hbar}\sum_{k\sigma,\alpha}\left[V_{ik\sigma,\alpha}\left\langle c_{ik\sigma}^{\dagger}d_\alpha\right\rangle - V_{ik\sigma,\alpha}^{*}\left\langle d_\alpha^{\dagger}c_{ik\sigma}\right\rangle\right]. \tag{8.12}$$

The averages of the operators in (8.8) and (8.12) are the elements of the density matrix in the single-particle space

$$\rho_{\alpha\alpha}(t) = \left\langle d_\alpha^{\dagger}(t)d_\alpha(t)\right\rangle, \tag{8.13}$$

$$\rho_{\alpha,ik\sigma}(t) = \left\langle c_{ik\sigma}^{\dagger}(t)d_\alpha(t)\right\rangle. \tag{8.14}$$

It is possible, also, to express it as a two-time Green function at equal times

$$Q_C(t) = e\sum_\alpha \rho_{\alpha\alpha}(t) = -ie\sum_\alpha G_{\alpha\alpha}^{<}(t,t), \tag{8.15}$$

$$J_i(t) = \frac{2e}{\hbar}\mathrm{Im}\left(\sum_{k\sigma,\alpha}V_{ik\sigma,\alpha}\rho_{\alpha,ik\sigma}(t)\right) = \frac{2e}{\hbar}\mathrm{Re}\left(\sum_{k\sigma,\alpha}V_{ik\sigma,\alpha}G_{\alpha,ik\sigma}^{<}(t,t)\right), \tag{8.16}$$

where we define the system-to-lead lesser Green function

$$G_{\alpha,ik\sigma}^{<}(t_1,t_2) = i\left\langle c_{ik\sigma}^{\dagger}(t_2)d_\alpha(t_1)\right\rangle, \tag{8.17}$$

while the nonequilibrium charge distribution of the molecule is determined by the system lesser function

$$G^{<}_{\alpha\beta}(t_1, t_2) = i \left\langle d^{\dagger}_{\beta}(t_2) d_{\alpha}(t_1) \right\rangle . \tag{8.18}$$

The lesser Green function is a new type of Green function, which should be used in addition to the retarded Green function introduced in Chap. 3. The retarded Green function describes the spectral and scattering properties of the system, such as eigenstates of the isolated systems, transmission and reflection amplitudes, density of states, etc. The lesser function, as we will see, is the analog of the classical distribution function, and in nonequilibrium states it is independent from the retarded function. Actually, the formalism of nonequilibrium Green functions is a general formulation of the quantum kinetic theory.

One can ask: what is the advantage to use more complex two-time Green functions instead of density matrices? There are several reasons. First of all, NGFs give a description of both density of states and distribution of particles over this states. Then, the equations of motion including interactions and the influence of environment can be obtained with the help of a diagrammatic technique, and (very important) all diagrammatic results of *equilibrium* theory can be easily incorporated. In the noninteracting case the NFG method reproduces all results of the Green function theory considered in Chap. 3, and in many cases it is more compact. Retardation effects are conveniently taken into account by two-time Green functions. And, finally, one can always go back to the density matrix when necessary.

There is, however, an alternative approach based on the *exact many-body states* of the isolated systems and the Quantum Master Equations (QME) for the density matrix in the basis of this many-body states. This method extends the master equation for sequential tunneling considered in Sect. 4.2.4. This approach is used in the case of very weak system-to-lead coupling, while the NGF methods are more successful in the description of strong and intermediate coupling to the leads. The convenience of one or other method is determined essentially by the type of interaction. In the rest of this book we will consider the NGF method.

8.3 Dyson-Keldysh Equations

8.3.1 General Time-Dependent Equations

In the previous chapter we established a general form of the Dyson-Keldysh equations for contour and real-time Green functions. Now we apply this formalism to the standard model described above. We start from the two-time matrix Green function $\check{\boldsymbol{G}}_{sp}(t_1, t_2)$, in the compact matrix form:

$$\check{\boldsymbol{G}}_{sp}(t_1, t_2) = \begin{pmatrix} \boldsymbol{G}^{R}_{sp}(t_1, t_2) & \boldsymbol{G}^{K(<)}_{sp}(t_1, t_2) \\ 0 & \boldsymbol{G}^{A}_{sp}(t_1, t_2) \end{pmatrix}, \tag{8.19}$$

or, equivalently, in the explicit matrix form

$$\check{G}_{s\alpha,p\beta}(t_1,t_2)=\begin{pmatrix} G^R_{s\alpha,p\beta}(t_1,t_2) & G^{K(<)}_{s\alpha,p\beta}(t_1,t_2) \\ 0 & G^A_{s\alpha,p\beta}(t_1,t_2)\end{pmatrix}, \tag{8.20}$$

where $s,p=L,C,R$ are the indices of the system parts: left electrode, central region and right electrode. Matrix indices $\alpha\in\{\alpha_s\}$, $\beta\in\{\beta_p\}$ correspond to the central or electrode (usually $\boldsymbol{k}\sigma$) states, with the additional relations

$$\boldsymbol{A}=i\left(\boldsymbol{G}^R-\boldsymbol{G}^A\right), \tag{8.21}$$

$$\boldsymbol{G}^<=\frac{1}{2}\left(\boldsymbol{G}^K+i\boldsymbol{A}\right). \tag{8.22}$$

The Dyson-Keldysh equation (7.216) can be written as

$$i\frac{\partial}{\partial t_1}\check{\boldsymbol{G}}_{sp}(t_1,t_2)-\sum_q\check{\boldsymbol{H}}_{sq}\check{\boldsymbol{G}}_{qp}(t_1,t_2)-\sum_q\int dt_3\check{\boldsymbol{\Sigma}}_{sq}(t_1,t_3)\check{\boldsymbol{G}}_{qp}(t_3,t_2)=\delta_{sp}\check{\boldsymbol{I}}\delta(t_1-t_2), \tag{8.23}$$

in our case we use the Hamiltonian (8.7) and get the following main equation

$$\left(i\frac{\partial}{\partial t_1}-\boldsymbol{H}_s\right)\check{\boldsymbol{G}}_{sp}(t_1,t_2)-\sum_q\boldsymbol{V}_{sq}\check{\boldsymbol{G}}_{qp}(t_1,t_2)$$
$$-\int dt_3\check{\boldsymbol{\Sigma}}_C(t_1,t_3)\check{\boldsymbol{G}}_{Cp}(t_3,t_2)\delta_{sC}\delta_{pC}=\delta_{sp}\check{\boldsymbol{I}}\delta(t_1-t_2). \tag{8.24}$$

We include all interaction effects into the self-energy $\check{\boldsymbol{\Sigma}}_C$. The coupling matrix $\boldsymbol{V}$ is defined as

$$\boldsymbol{V}=\begin{pmatrix}0 & \boldsymbol{V}_{LC} & 0\\ \boldsymbol{V}_{CL} & 0 & \boldsymbol{V}_{CR}\\ 0 & \boldsymbol{V}_{RC} & 0\end{pmatrix}. \tag{8.25}$$

Up to now we did not make any approximations and the above expressions can be applied for systems with interactions and arbitrary coupling with electrodes. The equations can be significantly simplified in two important cases.

(i) In the general case (also for *interacting electrodes*) if we can treat *the coupling as a perturbation*, then the Dyson-Keldysh equation for the electrode-center Green function has the following general solution

$$\check{\boldsymbol{G}}_{sC}=\left\{\check{\boldsymbol{G}}_s\boldsymbol{V}_{sC}\check{\boldsymbol{G}}_C\right\}. \tag{8.26}$$

To demonstrate that, let us write (8.24) as

$$\check{\boldsymbol{G}}_s^{-1}\check{\boldsymbol{G}}_{sp}-\sum_q\boldsymbol{V}_{sq}\check{\boldsymbol{G}}_{qp}=\check{\delta}_{sp}. \tag{8.27}$$

Without coupling ($\boldsymbol{V}_{sq} = 0$) the solution of this equation is $\breve{\boldsymbol{G}}_{sp} = \breve{\boldsymbol{G}}_s \delta_{sp}$, where $\breve{\boldsymbol{G}}_s \equiv \breve{\boldsymbol{G}}_{sp}$ is the Green function of an isolated system including all interactions, time-dependence, etc. If we now include coupling as a perturbation, we obtain immediately (8.26) from ($s \neq p$):

$$\breve{\boldsymbol{G}}_s^{-1} \breve{\boldsymbol{G}}_{sp} - \boldsymbol{V}_{sp} \breve{\boldsymbol{G}}_{pp} = 0. \tag{8.28}$$

The basic equations can now be formulated for the central region Green function $\breve{\boldsymbol{G}}_C(t_1, t_2)$:

$$\left(i \frac{\partial}{\partial t_1} - \boldsymbol{H}_C(t_1) \right) \breve{\boldsymbol{G}}_C - \sum_{s=L,R} \left\{ \boldsymbol{V}_{sC}^* \breve{\boldsymbol{G}}_s \boldsymbol{V}_{sC} \breve{\boldsymbol{G}}_C \right\} - \left\{ \breve{\boldsymbol{\Sigma}}_C \breve{\boldsymbol{G}}_C \right\} = \breve{\boldsymbol{I}} \delta(t_1 - t_2). \tag{8.29}$$

Note that from this equation it follows that weak coupling between two nanostructures can be described by the *self-energy* ($V_{\alpha,ik\sigma} = V_{ik\sigma,\alpha}^*$)

$$\breve{\boldsymbol{\Sigma}}_{sp} = \left\{ \boldsymbol{V}_{sp} \breve{\boldsymbol{G}}_p \mathbf{V}_{ps} \right\} = \left\{ \boldsymbol{V}_{ps}^* \breve{\boldsymbol{G}}_p \mathbf{V}_{ps} \right\}. \tag{8.30}$$

(ii) For *noninteracting leads* this result for $\breve{\boldsymbol{G}}_{sC}$ and $\breve{\boldsymbol{\Sigma}}_{sp}$ is *exact* [3].

Here we use the slightly modified approach of Meir, Wingreen, and Jauho [3, 4].

Let us write the Dyson-Keldysh equation as

$$\breve{\boldsymbol{G}}_s^{-1} \breve{\boldsymbol{G}}_{sp} - \sum_q \boldsymbol{V}_{sq} \breve{\boldsymbol{G}}_{qp} = \breve{\delta}_{sp} \;:\; \begin{cases} \breve{\boldsymbol{G}}_L^{-1} \breve{\boldsymbol{G}}_{LC} - \boldsymbol{V}_{LC} \breve{\boldsymbol{G}}_{CC} = 0, \\ \breve{\boldsymbol{G}}_R^{-1} \breve{\boldsymbol{G}}_{RC} - \boldsymbol{V}_{RC} \breve{\boldsymbol{G}}_{CC} = 0, \\ \breve{\boldsymbol{G}}_C^{-1} \breve{\boldsymbol{G}}_{CC} - \boldsymbol{V}_{CC} \breve{\boldsymbol{G}}_{LC} - \boldsymbol{V}_{CR} \breve{\boldsymbol{G}}_{RC} = \breve{1}. \end{cases} \tag{8.31}$$

For zero coupling with electrodes ($\boldsymbol{V}_{CL} = \boldsymbol{V}_{CR} = 0$) the solutions of this equations are $\breve{\boldsymbol{G}}_{sp} = \breve{\boldsymbol{G}}_s' \delta_{sp}$, where $\breve{\boldsymbol{G}}_s' \equiv \breve{\boldsymbol{G}}_{ss}'$ includes all interactions, time-dependence, etc. For equilibrium noninteracting leads $\breve{\boldsymbol{G}}_{sC} = \breve{\boldsymbol{G}}_{sC}'$, and we can write exact solution for the electrode-center functions

$$\breve{\boldsymbol{G}}_{sC} = \breve{\boldsymbol{G}}_s \boldsymbol{V}_{sC} \breve{\boldsymbol{G}}_C, \quad \breve{\boldsymbol{G}}_{Cs} = \breve{\boldsymbol{G}}_C \boldsymbol{V}_{Cs} \breve{\boldsymbol{G}}_s, \tag{8.32}$$

or, going back to indices,

$$\breve{G}_{\alpha,ik\sigma} = \sum_\beta V_{\beta,ik\sigma} \left\{ \breve{G}_{\alpha\beta} \breve{G}_{ik\sigma} \right\}. \tag{8.33}$$

Matrix Green functions of noninteracting equilibrium leads are diagonal, e.g. $G^R_{Lk\sigma,k'\sigma'} = G^R_{Lk\sigma} \delta(k - k') \delta_{\sigma\sigma'}$, and the equations are significantly simplified. Note that this expression is valid also in general case (interacting and nonequilibrium leads) when coupling is so weak, that perturbation in tunneling can be used.

8.3.2 Time-Independent Equations

In the stationary case $\check{\boldsymbol{G}}(\varepsilon)$ is the matrix Green function, and also the matrix in the Keldysh space

$$\check{\boldsymbol{G}} = \begin{pmatrix} \boldsymbol{G}^R & \boldsymbol{G}^< \\ 0 & \boldsymbol{G}^A \end{pmatrix}. \tag{8.34}$$

It is calculated from the Dyson-Keldysh equation

$$(\varepsilon \boldsymbol{I} - \boldsymbol{H})\,\check{\boldsymbol{G}}(\varepsilon) - \check{\boldsymbol{\Sigma}}(\varepsilon)\check{\boldsymbol{G}}(\varepsilon) = \check{\boldsymbol{I}}. \tag{8.35}$$

In the integral form it can be written as

$$\check{\boldsymbol{G}}(\varepsilon) = \check{\boldsymbol{G}}_0(\varepsilon) + \check{\boldsymbol{G}}_0(\varepsilon)\check{\boldsymbol{\Sigma}}(\varepsilon)\check{\boldsymbol{G}}(\varepsilon). \tag{8.36}$$

Equations for the retarded and advanced functions follow from the diagonal (in Keldysh space) part of (8.35)

$$(\varepsilon \boldsymbol{I} - \boldsymbol{H})\,\boldsymbol{G}^{R(A)}(\varepsilon) - \boldsymbol{\Sigma}^{R(A)}(\varepsilon)\boldsymbol{G}^{R(A)}(\varepsilon) = \boldsymbol{I}, \tag{8.37}$$

or

$$(\varepsilon - \varepsilon_\alpha - e\varphi_\alpha)G^{R(A)}_{\alpha\beta} - \sum_\gamma t_{\alpha\gamma} G^{R(A)}_{\gamma\beta} - \sum_\gamma \Sigma^{R(A)}_{\alpha\gamma} G^{R(A)}_{\gamma\beta} = \delta_{\alpha\beta}, \tag{8.38}$$

and the equation for the lesser function (quantum kinetic equation) follows from the off-diagonal part of (8.35) combined with its conjugate

$$\check{\boldsymbol{G}}(\varepsilon)\,(\varepsilon \boldsymbol{I} - \boldsymbol{H}) - \check{\boldsymbol{G}}(\varepsilon)\check{\boldsymbol{\Sigma}}(\varepsilon) = \check{\boldsymbol{I}}. \tag{8.39}$$

Finally we get the equation

$$-\left[\boldsymbol{H}, \boldsymbol{G}^<(\varepsilon)\right]_- - \boldsymbol{\Sigma}^R(\varepsilon)\boldsymbol{G}^<(\varepsilon) - \boldsymbol{\Sigma}^<(\varepsilon)\boldsymbol{G}^A(\varepsilon) + \boldsymbol{G}^R(\varepsilon)\boldsymbol{\Sigma}^<(\varepsilon) + \boldsymbol{G}^<(\varepsilon)\boldsymbol{\Sigma}^A(\varepsilon) = 0, \tag{8.40}$$

or

$$\left(\varepsilon_\beta - \varepsilon_\alpha\right) G^<_{\alpha\beta} - \sum_\gamma \left(t_{\alpha\gamma} G^<_{\gamma\beta} - G^<_{\alpha\gamma} t_{\gamma\beta}\right) \tag{8.41}$$

$$- \sum_\gamma \left(\Sigma^R_{\alpha\gamma} G^<_{\gamma\beta} + \Sigma^<_{\alpha\gamma} G^A_{\gamma\beta} - G^R_{\alpha\gamma}\Sigma^<_{\gamma\beta} - G^<_{\alpha\gamma}\Sigma^A_{\gamma\beta}\right) = 0. \tag{8.42}$$

In the integral form the equations for retarded and lesser functions are

$$\boldsymbol{G}^R(\varepsilon) = \boldsymbol{G}^R_0(\varepsilon) + \boldsymbol{G}^R_0(\varepsilon)\boldsymbol{\Sigma}^R(\varepsilon)\boldsymbol{G}^R(\varepsilon), \tag{8.43}$$

$$\boldsymbol{G}^{<}(\varepsilon) = \boldsymbol{G}^{R}(\varepsilon)\boldsymbol{\Sigma}^{<}(\varepsilon)\boldsymbol{G}^{A}(\varepsilon). \tag{8.44}$$

The second of these equations is called *Keldysh equation*. We neglect the second term $(1 + G^R\Sigma^R)G_0^<(1 + \Sigma^A G^A)$ in the Keldysh equation, which is nonzero only for free particles.

8.4 Meir-Wingreen-Jauho Formula for Current

Now we consider the central point of the NGF transport theory through nanosystems—the Meir-Wingreen-Jauho current formula [3–5]. This important expression shows that the current can be calculated, if the spectral and kinetic Green functions of the central system are known, and it is exact in the case of noninteracting electrodes. The details of the derivation can be found in the above cited papers, so we only briefly outline it.

8.4.1 General Expression

Now we proceed with the current expression (8.16). Using perturbation theory (in coupling between dot and leads) we showed, that in the main approximation (or for noninteracting leads) the lead-dot Green functions are

$$\breve{G}_{\alpha,ik\sigma} = \sum_{\beta} V^*_{ik\sigma,\beta}\left\{\breve{G}_{\alpha\beta}\breve{G}_{ik\sigma}\right\}. \tag{8.45}$$

Thus we obtain

$$J_i(t) = \frac{2e}{\hbar}\mathrm{Re}\left[\sum_{k\sigma,\alpha\beta} V_{ik\sigma,\alpha}V^*_{ik\sigma,\beta}\left\{\breve{G}_{\alpha\beta}\breve{G}_{ik\sigma}\right\}^{<}(t,t)\right], \tag{8.46}$$

or

$$G^{<}_{\alpha,ik\sigma}(t_1,t_2) = \sum_{\beta}\int dt_3 V^*_{ik\sigma,\beta}\left[G^R_{\alpha\beta}(t_1,t_3)G^{<}_{ik\sigma}(t_3,t_2) + G^{<}_{\alpha\beta}(t_1,t_3)G^A_{ik\sigma}(t_3,t_2)\right], \tag{8.47}$$

and

$$J_i(t) = \frac{2e}{\hbar}\mathrm{Re}\left[\sum_{k\sigma,\alpha\beta}\int dt_3 V_{ik\sigma,\alpha}V^*_{ik\sigma,\beta}\left[G^R_{\alpha\beta}(t,t_3)G^{<}_{ik\sigma}(t_3,t) + G^{<}_{\alpha\beta}(t,t_3)G^A_{ik\sigma}(t_3,t)\right]\right]. \tag{8.48}$$

We do not consider here time-dependent matrix elements $V_{ik\sigma,\alpha}$, this extension can be found in the papers of Jauho et al. [3, 5].

Using the exact expressions for the time-dependent Green functions of the electrodes:

$$G^{<}_{k\sigma}(t_1,t_2) = if^0_\sigma(\varepsilon_{k\sigma})\exp\left[i\int_{t_1}^{t_2}(\varepsilon_{k\sigma}+e\varphi(t))dt\right], \tag{8.49}$$

$$G^{R}_{k\sigma}(t_1,t_2) = -i\theta(t_1-t_2)\exp\left[i\int_{t_1}^{t_2}(\varepsilon_{k\sigma}+e\varphi(t))dt\right], \tag{8.50}$$

$$G^{A}_{k\sigma}(t_1,t_2) = i\theta(t_2-t_1)\exp\left[i\int_{t_1}^{t_2}(\varepsilon_{k\sigma}+e\varphi(t))dt\right], \tag{8.51}$$

and substituting it into the current formula

$$J_i(t) = \frac{2e}{\hbar}\mathrm{Re}\left[\sum_{k\sigma,\alpha\beta}V_{ik\sigma,\alpha}V^*_{ik\sigma,\beta}\left\{G^R_{\alpha\beta}G^{<}_{ik\sigma}+G^{<}_{\alpha\beta}G^A_{ik\sigma}\right\}(t,t)\right]. \tag{8.52}$$

we get the following general expression for the time-dependent current from the i-th electrode to the central region:

$$J_i(t) = -\frac{2e}{\hbar}\mathrm{Im}\Bigg[\sum_{k\sigma,\alpha\beta}V_{ik\sigma,\alpha}V^*_{ik\sigma,\beta}\int_{-\infty}^{t}dt_3 e^{i\int_{t_3}^{t}(\varepsilon_{k\sigma}+e\varphi_i(t))dt} \left[G^R_{\alpha\beta}(t,t_3)f^0_{i\sigma}(\varepsilon_{k\sigma})+G^{<}_{\alpha\beta}(t,t_3)\right]\Bigg]. \tag{8.53}$$

Let us introduce the level-width functions (below without *spin polarization* of the leads)

$$\tilde{\boldsymbol{\Gamma}}_{i=L(R)}(\varepsilon)\equiv\tilde{\Gamma}_{i\alpha\beta}(\varepsilon)=2\pi\sum_{k\sigma}V_{ik\sigma,\beta}V^*_{ik\sigma,\alpha}\delta(\varepsilon-\varepsilon_{ik\sigma})=2\pi\sum_{\sigma}\rho_{i\sigma}(\varepsilon)V_{i\sigma,\beta}(\varepsilon)V^*_{i\sigma,\alpha}(\varepsilon). \tag{8.54}$$

The expression for the current is, finally,

$$J_i(t) = -\frac{2e}{\hbar}\int_{-\infty}^{t}dt_3\int\frac{d\varepsilon}{2\pi}\mathrm{Im}\mathrm{Tr}\left[e^{i\int_{t_3}^{t}(\varepsilon+e\varphi_i(t))dt}\tilde{\boldsymbol{\Gamma}}(\varepsilon)\left[\boldsymbol{G}^R(t,t_3)f^0_{i\sigma}(\varepsilon)+\boldsymbol{G}^{<}(t,t_3)\right]\right]. \tag{8.55}$$

We use notation $\tilde{\boldsymbol{\Gamma}}(\varepsilon)$ with tilde because in Chap. 3 we determined $\boldsymbol{\Gamma}(\varepsilon)$ without tilde as a function of the energy shifted by the external potential φ, and $\tilde{\boldsymbol{\Gamma}}(\varepsilon)$ is a

function of energy for the electrode with $\varphi = 0$. Here we use the same notations. Otherwise it is the same level-width function.

8.4.2 Stationary Time-Independent Current

In the stationary case

$$G^{<}_{\alpha,ik\sigma}(\varepsilon) = \sum_{\beta} V^{*}_{ik\sigma,\beta}\left[G^{R}_{\alpha\beta}(\varepsilon)G^{<}_{ik\sigma}(\varepsilon) + G^{<}_{\alpha\beta}(\varepsilon)G^{A}_{ik\sigma}(\varepsilon)\right], \tag{8.56}$$

and for the current

$$J_i(t) = \frac{2e}{\hbar}\int \frac{d\varepsilon}{2\pi}\mathrm{Re}\left[\sum_{k\sigma,\alpha\beta} V_{ik\sigma,\alpha}V^{*}_{ik\sigma,\beta}\left[G^{R}_{\alpha\beta}(\varepsilon)G^{<}_{ik\sigma}(\varepsilon) + G^{<}_{\alpha\beta}(\varepsilon)G^{A}_{ik\sigma}(\varepsilon)\right]\right]. \tag{8.57}$$

For equilibrium right or left lead Green functions we obtain directly

$$G^{<}_{k\sigma}(t_1 - t_2) = i\left\langle c^{\dagger}_{k\sigma}(t_2)c_{k\sigma}(t_1)\right\rangle = if^{0}_{\sigma}(\varepsilon_{k\sigma})e^{-i(\varepsilon_{k\sigma}+e\varphi)(t_1-t_2)}, \tag{8.58}$$

$$G^{R}_{k\sigma}(t_1 - t_2) = -i\theta(t_1 - t_2)\left\langle\left[c_{k\sigma}(t_1), c^{\dagger}_{k\sigma}(t_2)\right]_{+}\right\rangle = -i\theta(t_1 - t_2)e^{-i(\varepsilon_{k\sigma}+e\varphi)(t_1-t_2)}, \tag{8.59}$$

$$G^{A}_{k\sigma}(t_1 - t_2) = i\theta(t_2 - t_1)\left\langle\left[c_{k\sigma}(t_1), c^{\dagger}_{k\sigma}(t_2)\right]_{+}\right\rangle = i\theta(t_2 - t_1)e^{-i(\varepsilon_{k\sigma}+e\varphi)(t_1-t_2)}, \tag{8.60}$$

or after the Fourier transform

$$G^{<}_{k\sigma}(\varepsilon) = \int G^{<}_{k\sigma}(t_1 - t_2)e^{i\varepsilon(t_1-t_2)}d(t_1 - t_2) = 2\pi i f^{0}_{\sigma}(\varepsilon_{k\sigma})\delta(\varepsilon - \varepsilon_{k\sigma} - e\varphi), \tag{8.61}$$

$$G^{>}_{k\sigma}(\varepsilon) = -2\pi i[1 - f^{0}_{\sigma}(\varepsilon_{k\sigma})]\delta(\varepsilon - \varepsilon_{k\sigma} - e\varphi), \tag{8.62}$$

$$G^{R}_{k\sigma}(\varepsilon) = \frac{1}{\varepsilon - \varepsilon_{k\sigma} - e\varphi + i\eta}, \quad G^{A}_{k\sigma}(\varepsilon) = \frac{1}{\varepsilon - \varepsilon_{k\sigma} - e\varphi - i\eta}, \tag{8.63}$$

$$f^{0}_{\sigma}(\varepsilon) = \frac{1}{\exp\left(\frac{\varepsilon-\mu_{\sigma}}{T}\right)+1}. \tag{8.64}$$

We use now the level-width function (8.54) and change the momentum summation to the energy integration $\sum_{k} \Rightarrow \int \rho(\varepsilon_k)d\varepsilon_k$. Then for the current one obtains

$$J_{i=L,R} = \frac{ie}{\hbar}\int \frac{d\varepsilon}{2\pi}\mathrm{Tr}\left\{\tilde{\boldsymbol{\Gamma}}_i(\varepsilon - e\varphi_i)\left(\boldsymbol{G}^<(\varepsilon) + f_i^0(\varepsilon - e\varphi_i)\left[\boldsymbol{G}^R(\varepsilon) - \boldsymbol{G}^A(\varepsilon)\right]\right)\right\}, \tag{8.65}$$

where f_i^0 is the equilibrium Fermi distribution function with chemical potential μ_i. Thus, we obtain the well-known Meir-Wingreen formula. Note, that we use explicitly the electrical potential of the leads in this expression. It is important to mention, that at finite voltage the arguments of the left and right level-width functions are changed in a different way, which means, in particular, that the known condition of proportional coupling $\boldsymbol{\Gamma}_L = \lambda\boldsymbol{\Gamma}_R$ can be fulfilled only in the wide-band limit, when both functions are energy independent.

Different Forms of the Meir-Wingreen Formula

In the stationary state $J_R = -J_L = J$ and one can use the symmetric form

$$J = \frac{ie}{2\hbar}\int \frac{d\varepsilon}{2\pi}\mathrm{Tr}\Big\{\Big[\tilde{\boldsymbol{\Gamma}}_L(\varepsilon - e\varphi_L) - \tilde{\boldsymbol{\Gamma}}_R(\varepsilon - e\varphi_R)\Big]\boldsymbol{G}^<(\varepsilon)$$
$$+\Big[\tilde{\boldsymbol{\Gamma}}_L(\varepsilon - e\varphi_L)f_L^0(\varepsilon - e\varphi_L) - \tilde{\boldsymbol{\Gamma}}_R(\varepsilon - e\varphi_R)f_R^0(\varepsilon - e\varphi_R)\Big]\Big[\boldsymbol{G}^R(\varepsilon) - \boldsymbol{G}^A(\varepsilon)\Big]\Big\}. \tag{8.66}$$

For the proportional coupling $\boldsymbol{\Gamma}_L(\varepsilon) = \lambda\boldsymbol{\Gamma}_R(\varepsilon)$ in *linear response* (φ_i dependence of Γ_i is ignored)

$$J = \frac{2e}{\hbar}\int \frac{d\varepsilon}{4\pi}\left[f_L^0(\varepsilon - e\varphi_L) - f_R^0(\varepsilon - e\varphi_R)\right]\mathrm{Tr}\left(\frac{\boldsymbol{\Gamma}_L(\varepsilon)\boldsymbol{\Gamma}_R(\varepsilon)}{\boldsymbol{\Gamma}_L(\varepsilon) + \boldsymbol{\Gamma}_R(\varepsilon)}\boldsymbol{A}(\varepsilon)\right). \tag{8.67}$$

$\boldsymbol{A} = i(\boldsymbol{G}^R - \boldsymbol{G}^A)$ is the spectral function. This expression is valid for *nonlinear response* if the energy dependence of $\boldsymbol{\Gamma}$ can be neglected (wide band limit).

Noninteracting Case

Finally, in the noninteracting case it is possible to obtain the usual Landauer-Büttiker formula with the transmission function

$$T(\varepsilon) = \mathrm{Tr}\left[\tilde{\boldsymbol{\Gamma}}_L(\varepsilon - e\varphi_L)\boldsymbol{G}^R(\varepsilon)\tilde{\boldsymbol{\Gamma}}_R(\varepsilon - e\varphi_R)\boldsymbol{G}^A(\varepsilon)\right]. \tag{8.68}$$

This expression is equivalent to the one derived earlier by the single-particle Green function method.

We should stress once more that this formula is valid for finite voltage. Therefore, the voltage dependence of the level-width functions is important.

References

1. S. Datta, W. Tian, S. Hong, R. Reifenberger, J.I. Henderson, C.P. Kubiak, Phys. Rev. Lett. **79**, 2530 (1997)
2. T. Rakshit, G.C. Liang, A.W. Gosh, M.C. Hersam, S. Datta, Phys. Rev. B **72**, 125305 (2005)
3. A.P. Jauho, N.S. Wingreen, Y. Meir, Phys. Rev. B **50**, 5528 (1994)
4. Y. Meir, N.S. Wingreen, Phys. Rev. Lett. **68**, 2512 (1992)
5. H. Haug, A.P. Jauho, *Quantum Kinetics in Transport and Optics of Semiconductors, Springer Series in Solid-State Physics*, vol. 123 (Springer, Berlin, 1996)

Chapter 9
Some Nonequilibrium Problems

In the last chapter we give some examples of the NGF method for electron-electron and electron-vibron interactions.

In Sect. 9.1 the Dyson-Keldysh equations are used to calculate current through the system with electron-vibron interaction. We focus on weak to intermediate electron-vibron interaction, but arbitrary coupling to the leads. This parameter range is inaccessible for master equation, valid only in the weak coupling limit, and the NGF method is only one working approach. Besides, all advantages of the nonequilibrium self-consistent approach are demonstrated in the problem of nonequilibrium vibrons with weak enough electron-vibron interaction. The weakness of interaction allows us to use rather simple self-consistent approximation, but with both electron and vibron nonequilibrium distributions. So that one can describe not only the spectroscopic problems with equilibrium vibrons, but also the situations with vibronic instability and strongly nonequilibrium vibrons.

The other example, the equation-of-motion method applied to the Coulomb blockade problem is considered in Sect. 9.2. In the case of strong electron-electron interaction (when Coulomb blockade or Kondo effect are observed) there are no good approximations for the self-energies at present and the EOM method is a possible alternative. We consider how the equations for Green functions can be obtained starting from the Hubbard-Anderson Hamiltonian and the equations for Heisenberg time-dependent particle operators. This technique gives good results in some cases, although its perspectives are not very clear.

9.1 Vibronic Effects (Self-consistent Dyson-Keldysh Method)

We already considered some electron-vibron effects in Chap. 6. Now we come back to this topic with new possibilities of the NGF transport method. The master equation approach used in Chap. 6 is valid only for very weak coupling to electrodes,

D.A. Ryndyk, *Theory of Quantum Transport at Nanoscale*,
Springer Series in Solid-State Sciences 184,
DOI 10.1007/978-3-319-24088-6_9

but in some cases with very strong electron-vibron interaction. In this section we investigate the behavior of the electron-vibron systems with weak to intermediate electron-vibron interactions, but arbitrary couplings to the leads. To reach this aim, we will develop a nonequilibrium self-consistent theory which allows us to explore the nonperturbative regime via the nonequilibrium Green function formalism. We will see that the nonequilibrium resonant spectroscopy is able to determine the energies of molecular orbitals and the spectrum of molecular vibrations. This results are relevant to scanning tunneling spectroscopy experiments and demonstrate the importance of the systematic and self-consistent investigation of the effects of vibronic dynamics onto the transport through single molecules.

9.1.1 The Electron-Vibron Hamiltonian

We use the minimal transport model described in the previous sections. For convenience, we present the Hamiltonian here one more time. The full Hamiltonian is the sum of the central Hamiltonian $\hat{H}_C$, the Hamiltonians of the electrodes $\hat{H}_{R(L)}$, the tunneling Hamiltonian $\hat{H}_T$ describing the coupling to the electrodes, the vibron Hamiltonian $\hat{H}_V$ including electron-vibron interaction and coupling of vibrations to the environment (describing dissipation of vibrons)

$$\hat{H} = \hat{H}_C + \hat{H}_V + \hat{H}_L + \hat{H}_R + \hat{H}_T. \tag{9.1}$$

The central part is described by a set of localized states $|\alpha\rangle$ with energies ε_α and inter-orbital overlap integrals $t_{\alpha\beta}$ by the following model Hamiltonian:

$$\hat{H}_C^{(0)} = \sum_\alpha \left(\varepsilon_\alpha + e\varphi_\alpha(t)\right) d_\alpha^\dagger d_\alpha + \sum_{\alpha\neq\beta} t_{\alpha\beta} d_\alpha^\dagger d_\beta. \tag{9.2}$$

Vibrations and the electron-vibron coupling are described by the Hamiltonian ($\hbar = 1$)

$$\hat{H}_V = \sum_q \omega_q a_q^\dagger a_q + \sum_{\alpha\beta}\sum_q \lambda_{\alpha\beta}^q (a_q + a_q^\dagger) d_\alpha^\dagger d_\beta. \tag{9.3}$$

Here vibrations are considered as localized phonons and q is an index labeling them, not the wave-vector. The first term describes free vibrons with the energy ω_q. The second term represents the electron-vibron interaction. We include both diagonal coupling, which describes a change of the electrostatic energy with the distance between atoms, and the off-diagonal coupling, which describes the dependence of the matrix elements $t_{\alpha\beta}$ over the distance between atoms.

The Hamiltonians of the right (R) and left (L) electrodes read

$$\hat{H}_s = L(R) = \sum_{k\sigma} (\varepsilon_{sk\sigma} + e\varphi_s) c_{sk\sigma}^\dagger c_{sk\sigma}, \tag{9.4}$$

$\varphi_s(t)$ are the electrical potentials of the leads. Finally, the tunneling Hamiltonian

$$\hat{H}_T = \sum_{s=L,R} \sum_{k\sigma,\alpha} \left(V_{sk\sigma,\alpha} c^\dagger_{sk\sigma} d_\alpha + \text{h.c.} \right) \tag{9.5}$$

describes the hopping between the electrodes and the central system. A direct hopping between two electrodes is neglected.

9.1.2 Dyson-Keldysh Equations and Self-energies

We use the nonequilibrium Green function (NGF) method. The current from the left ($s = L$) or right ($s = R$) electrode to the molecule is described by the expression (8.65).

The lesser (retarded, advanced) Green function matrix $\boldsymbol{G}^{<(R,A)} \equiv G^{<(R,A)}_{\alpha\beta}$ can be found from the Dyson-Keldysh equations in the integral form

$$\boldsymbol{G}^R(\varepsilon) = \boldsymbol{G}^R_0(\varepsilon) + \boldsymbol{G}^R_0(\varepsilon)\boldsymbol{\Sigma}^R(\varepsilon)\boldsymbol{G}^R(\varepsilon), \tag{9.6}$$

$$\boldsymbol{G}^<(\varepsilon) = \boldsymbol{G}^R(\varepsilon)\boldsymbol{\Sigma}^<(\varepsilon)\boldsymbol{G}^A(\varepsilon), \tag{9.7}$$

or from the corresponding (8.38), (8.42) in the differential form.

Here

$$\boldsymbol{\Sigma}^{R,<} = \boldsymbol{\Sigma}^{R,<(T)}_L + \boldsymbol{\Sigma}^{R,<(T)}_R + \boldsymbol{\Sigma}^{R,<(V)} \tag{9.8}$$

is the total self-energy of the molecule composed of the tunneling (coupling to the left and right leads) self-energies

$$\boldsymbol{\Sigma}^{R,<(T)}_{s=L,R} \equiv \Sigma^{R,<(T)}_{s\alpha\beta} = \sum_{k\sigma} \left\{ V^*_{sk\sigma,\alpha} G^{R,<}_{sk\sigma} V_{sk\sigma,\beta} \right\}, \tag{9.9}$$

and the vibronic self-energy $\boldsymbol{\Sigma}^{R,<(V)} \equiv \Sigma^{R,<(V)}_{\alpha\beta}$.

For the retarded tunneling self-energy $\boldsymbol{\Sigma}^{R(T)}_s$ one obtains

$$\boldsymbol{\Sigma}^{R(T)}_s(\varepsilon) = \boldsymbol{\Lambda}_s(\varepsilon - e\varphi_s) - \frac{\mathrm{i}}{2}\tilde{\boldsymbol{\Gamma}}_s(\varepsilon - e\varphi_s), \tag{9.10}$$

where $\boldsymbol{\Lambda}_s$ is the real part of the self-energy, which usually can be included in the single-particle Hamiltonian $\hat{H}^{(0)}_C$, and $\tilde{\boldsymbol{\Gamma}}_s$ describes level broadening due to coupling to the leads. For the corresponding lesser function one finds

$$\boldsymbol{\Sigma}^{<(T)}_s(\varepsilon) = \mathrm{i}\tilde{\boldsymbol{\Gamma}}_s(\varepsilon - e\varphi_s) f^0_s(\varepsilon - e\varphi_s). \tag{9.11}$$

In the standard self-consistent Born approximation, using the Keldysh technique, one obtains for the vibronic self-energies [1–8]

$$\boldsymbol{\Sigma}^{R(V)}(\varepsilon) = \frac{i}{2}\sum_q \int \frac{d\omega}{2\pi}\left(\boldsymbol{M}^q \boldsymbol{G}^R_{\varepsilon-\omega}\boldsymbol{M}^q D^K_{q\omega} + \boldsymbol{M}^q \boldsymbol{G}^K_{\varepsilon-\omega}\boldsymbol{M}^q D^R_{q\omega} - 2D^R_{q\omega=0}\boldsymbol{M}^q \mathrm{Tr}\left[\boldsymbol{G}^<_\omega \boldsymbol{M}^q\right]\right), \tag{9.12}$$

$$\boldsymbol{\Sigma}^{<(V)}(\varepsilon) = i\sum_q \int \frac{d\omega}{2\pi}\boldsymbol{M}^q \boldsymbol{G}^<_{\varepsilon-\omega}\boldsymbol{M}^q D^<_{q\omega}, \tag{9.13}$$

where $\boldsymbol{G}^K = 2\boldsymbol{G}^< + \boldsymbol{G}^R - \boldsymbol{G}^A$ is the Keldysh Green function, and $\boldsymbol{M}^q \equiv \lambda^q_{\alpha\beta}$.

If vibrons are noninteracting, in equilibrium, and non-dissipative, then the vibronic Green functions write:

$$D^R_0(q,\omega) = D^{A*}_0(q,\omega) = \frac{1}{\omega-\omega_q+\mathrm{i}\eta} - \frac{1}{\omega+\omega_q+\mathrm{i}\eta}, \tag{9.14}$$

$$A_V(q,\omega) = i\left(D^R_0(q,\omega) - D^A_0(q,\omega)\right) = 2\pi\left(\delta(\omega-\omega_q) - \delta(\omega+\omega_q)\right), \tag{9.15}$$

$$D^<_0(q,\omega) = -2\pi\mathrm{i}\left[(f^0_B(\omega_q)+1)\delta(\omega+\omega_q) + f^0_B(\omega_q)\delta(\omega-\omega_q)\right], \tag{9.16}$$

where the equilibrium Bose distribution function is

$$f^0_B(\omega) = \frac{1}{\exp(\omega/T)-1}. \tag{9.17}$$

Note that $f^0_B(-\omega) = -(f^0_B(\omega)+1)$.

When some *external* dissipation of vibrons is taken into account, then the equilibrium Green functions are

$$D^R_0(q,\omega) = D^{A*}_0(q,\omega) = \frac{2\omega_q}{\omega^2-\omega_q^2+i\omega_q\gamma_q(\omega)\mathrm{sgn}(\omega)}, \tag{9.18}$$

$$A_V(q,\omega) = i\left(D^R_0(q,\omega) - D^A_0(q,\omega)\right), \tag{9.19}$$

$$D^<_0(q,\omega) = D^>_0(q,-\omega) = -iA_V(q,\omega)f^0_B(\omega) = \begin{cases} -iA_V(q,\omega)f^0_B(\omega), & \omega>0, \\ -iA_V(q,|\omega|)[f^0_B(|\omega|)+1], & \omega<0, \end{cases} \tag{9.20}$$

These expressions can be used if we assume that vibrations are in thermal equilibrium with the environment and dissipation of vibrations is determined by the environment. However, if the coupling of vibrations to the leads is weak, we should

consider the case when vibrations are excited by the current flowing through a molecule, and the dissipation of vibrations is also determined essentially by the coupling to electrons.

In our model vibron coherences, described by Green functions $D(q, q', \omega)$, are not excited and the diagonal in index space function $\check{D}(q, \omega)$ is the matrix in Keldysh space

$$\check{D} = \begin{pmatrix} D^R & D^< \\ 0 & D^A \end{pmatrix}. \tag{9.21}$$

It is calculated from the vibron Dyson-Keldysh equation

$$\check{D}(q, \omega) = \check{D}_0(q, \omega) + \check{D}_0(q, \omega)\check{\Pi}(q, \omega)\check{D}(q, \omega). \tag{9.22}$$

where $\check{\Pi}(q, \omega)$ is the polarization operator (vibron self-energy).

The retarded functions are calculated from the equation

$$D^R(q\omega) = D_0^R(q\omega) + D_0^R(q\omega)\Pi^R(q\omega)D^R(q\omega), \tag{9.23}$$

$$D^R(q, \omega) = \frac{2\omega_q}{\omega^2 - \omega_q^2 - 2\omega_q \Pi^R(q, \omega)}. \tag{9.24}$$

The equation for the lesser function (quantum kinetic equation in the integral form) is

$$(\Pi^R_{q\omega} - \Pi^A_{q\omega})D^<_{q\omega} - (D^R_{q\omega} - D^A_{q\omega})\Pi^<_{q\omega} = 0, \tag{9.25}$$

this equation in the stationary case considered here is algebraic in the frequency domain.

In the integral form one has the Keldysh equation for the lesser function

$$D^<(q, \omega) = D^R(q, \omega)\Pi^<(q, \omega)D^A(q, \omega). \tag{9.26}$$

The polarization operator is the sum of two parts, environmental and electronic: $\Pi^{R,<}_{q\omega} = \Pi^{R,<(\mathrm{env})}_{q\omega} + \Pi^{R,<(\mathrm{el})}_{q\omega}$.

The environmental equilibrium part of the polarization operator can be approximated by the simple expressions

$$\Pi^{R(\mathrm{env})}(q, \omega) = -\frac{i}{2}\gamma_q \mathrm{sign}(\omega), \tag{9.27}$$

$$\Pi^{<(\mathrm{env})}(q, \omega) = -i\gamma_q f_B^0(\omega)\mathrm{sign}(\omega), \tag{9.28}$$

where γ_g is the vibronic dissipation rate, and $f_B^0(\omega)$ is the equilibrium Bose-Einstein distribution function.

The electronic contribution to the polarization operator within the Self-Consistent Born Approximation (SCBA) is

$$\Pi^{R(\mathrm{el})}(q,\omega) = -i\int \frac{d\varepsilon}{2\pi}\mathrm{Tr}\left(\boldsymbol{M}^q \boldsymbol{G}^<_\varepsilon \boldsymbol{M}^q \boldsymbol{G}^A_{\varepsilon-\omega} + \boldsymbol{M}^q \boldsymbol{G}^R_\varepsilon \boldsymbol{M}^q \boldsymbol{G}^<_{\varepsilon-\omega}\right), \tag{9.29}$$

$$\Pi^{<(\mathrm{el})}(q,\omega) = -i\int \frac{d\varepsilon}{2\pi}\mathrm{Tr}\left(\boldsymbol{M}^q \boldsymbol{G}^<_\varepsilon \boldsymbol{M}^q \boldsymbol{G}^>_{\varepsilon-\omega}\right). \tag{9.30}$$

We obtained the full set of equations, which can be used for numerical calculations.

9.1.3 Single-Level Model: Spectroscopy of Vibrons

The isolated single-level electron-vibron model is described by the Hamiltonian

$$\hat{H}_{M+V} = (\varepsilon_0 + e\varphi_0)d^\dagger d + \omega_0 a^\dagger a + \lambda\left(a^\dagger + a\right)d^\dagger d, \tag{9.31}$$

where the first and the second terms describe the free electron state and the free vibron, and the third term is electron-vibron minimal coupling interaction (Fig. 9.1).

Here we assume, that the vibrons are in equilibrium and are not excited by the current, so that the SCBA is a good starting point. The vibron Green function are assumed to be in equilibrium with the broadening defined by the external thermal bath, see for details [3, 5–9].

For the single-level model all equations are significantly simplified.

Combining J_L and J_R the expression for the current can be written for energy independent $\Gamma_{L(R)}$ (wide-band limit) as

$$J = \frac{e}{h}\frac{\Gamma_L\Gamma_R}{\Gamma_R+\Gamma_L}\int d\varepsilon A(\varepsilon)\left[f^0(\varepsilon - e\varphi_L) - f^0(\varepsilon - e\varphi_R)\right]. \tag{9.32}$$

It looks as simple as the Landauer-Büttiker formula, but it is not trivial, because the spectral density $A(\varepsilon) = -2\mathrm{Im}G^R(\varepsilon)$ now depends on the distribution function of the electrons in the fluctuating molecule and hence the applied voltage, $\varphi_L = -\varphi_R = V/2$ [10]. Indeed, $G^R(\varepsilon)$ can be found from

$$G^R(\varepsilon) = \frac{1}{\varepsilon - \tilde{\varepsilon}_0 - \Sigma^{R(V)}(\varepsilon) + i(\Gamma_L+\Gamma_R)/2}, \tag{9.33}$$

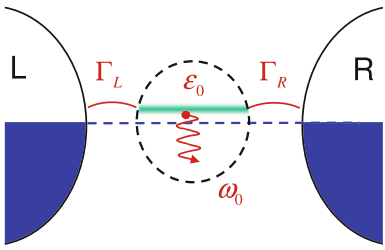

Fig. 9.1 Schematic picture of the considered electron-vibron single-level model, coupled to the *left* and *right* leads

where $\Sigma^{R(V)}(\varepsilon)$ is a functional of the electron distribution function inside a molecule. Actually, the lesser function $G^<(\varepsilon)$ is used in the quantum kinetic formalism as a distribution function. In the single-level case the usual distribution function can be introduced through the relation

$$G^<(\varepsilon) = iA(\varepsilon) f(\varepsilon). \tag{9.34}$$

Note the essential difference between symmetric ($\Gamma_L = \Gamma_R$) and asymmetric junctions. It is clear from the noninteracting solution of the transport problem. Neglecting for a moment the vibron self-energies, we obtain the noninteracting distribution function

$$f(\varepsilon) = \frac{\Gamma_L f_L^0(\varepsilon - e\varphi_L) + \Gamma_R f_R^0(\varepsilon - e\varphi_R)}{\Gamma_L + \Gamma_R}. \tag{9.35}$$

For strongly asymmetric junctions (e.g. $\Gamma_L \ll \Gamma_R$) the distribution function remains close to the equilibrium function in the right lead $f_R^0(\varepsilon - e\varphi_R)$, thus essentially simplifying the solution. While for symmetric junctions the distribution function has the double-step form and is very different from the equilibrium one.

A typical example of the spectral function at zero voltage is shown in Fig. 9.2. At finite voltage it should be calculated self-consistently. In the insert the spectral function of the symmetric junction at finite voltage is shown, it is changed essentially because the distribution function is changed.

Let us discuss a general picture of the vibronic transport in symmetric and asymmetric single-molecule junctions, provided in experiments with the molecular bridges and STM-to-molecule junctions, respectively. The differential conductance, calculated at different molecule-to-lead coupling, is shown in Fig. 9.3 (symmetric) and Fig. 9.4 (asymmetric). At weak coupling, the vibronic side-band peaks are observed, reproducing the corresponding peaks in the spectral function. At strong couplings the broadening of the electronic state hides the side-bands, and new features become visible. In the symmetric junction, a suppression of the conductance at $V \simeq \pm\hbar\omega_0$ takes place as a result of inelastic scattering of electrons from the left lead to the right lead. In the asymmetric junction (Fig. 9.4), the usual IETS increase of the conductance is observed at a negative voltage $V \simeq -\hbar\omega_0$, this feature is weak and can be observed only in the incoherent tail of the resonant conductance. We conclude, that the vibronic contribution to the conductance can be distinguished clearly in both coherent and tunneling limits.

In conclusion, at weak molecule-to-lead (tip, substrate) coupling the usual vibronic side-band peaks in the differential conductance are observed; at stronger coupling to the leads (broadening) these peaks are transformed into step-like features. A vibronic-induced decrease of the conductance with voltage is observed in high-conductance junctions. The usual IETS feature (increase of the conductance) can be observed only in the case of low off-resonant conductance. By changing independently the bias voltage and the tip position, it is possible to determine the energy of molecular orbitals and the spectrum of molecular vibrations. In the multi-level systems with strong electron-electron interaction further effects, such as Coulomb

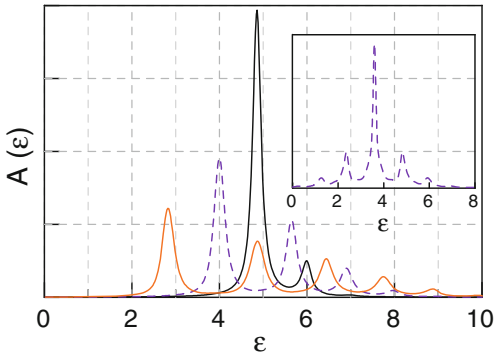

Fig. 9.2 Spectral function at different electron-vibron couplings: $\lambda/\omega_0 = 0.4$ (*black*), $\lambda/\omega_0 = 1.2$ (*blue*, *dashed*), and $\lambda/\omega_0 = 2$ (*red*); at $\varepsilon_0/\omega_0 = 5$, $\Gamma_L/\omega_0 = \Gamma_R/\omega_0 = 0.1$. In the insert the spectral function at $\lambda/\omega_0 = 1.2$ is shown at finite voltage, when the level is partially filled. Energies are in units of $\hbar\omega_0$.

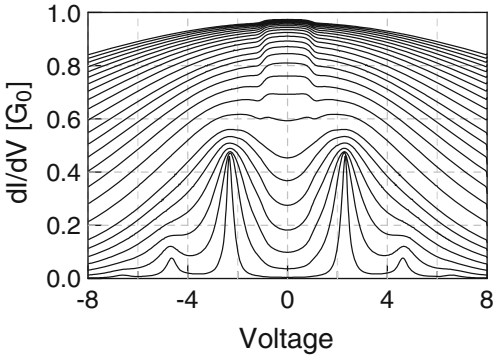

Fig. 9.3 Differential conductance of a symmetric junction: $\eta = 0.5$, $\Gamma_R = \Gamma_L$, at different molecule-to-lead couplings, from $\Gamma_L/\omega_0 = 0.1$ (*lower curve*) to $\Gamma_L/\omega_0 = 10$ (*upper curve*), $\lambda/\omega_0 = 1$, $\varepsilon_0/\omega_0 = 2$

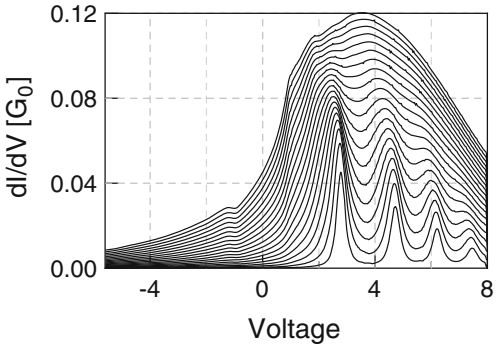

Fig. 9.4 Differential conductance of an asymmetric junction: η=0, Γ_R=20Γ_L, from $\Gamma_R/\omega_0 = 0.2$ (*lower curve*) to $\Gamma_R/\omega_0 = 4$ (*upper curve*), $\lambda/\omega_0 = 2$, $\varepsilon_0/\omega_0 = 5$. The voltage is in the units of $\hbar\omega_0/e$

blockade and Kondo effect, could dominate over the physics which we address here; these effects have to be included in a subsequent step.

9.1.4 Multi-level Model: Nonequilibrium Vibrons

If the mechanical degrees of freedom are coupled strongly to the environment (dissipative vibron), then the dissipation of molecular vibrations is determined by the environment. However, if the coupling of vibrations to the leads is weak, we should consider the case when the vibrations are excited by the current flowing through a molecule, and the dissipation of vibrations is also determined essentially by the coupling to the electrons. Here we show that the effects of vibron emission and vibronic instability are important especially in the case of electron-vibron resonance.

We simplify the equations and obtain some analytical results in the *vibronic quasiparticle approximation*, which assumes weak electron-vibron coupling limit and weak external dissipation of vibrons:

$$\gamma_q^* = \gamma_q - 2\mathrm{Im}\Pi^R(\omega_q) \ll \omega_q. \tag{9.36}$$

Thus the spectral function of vibrons can be approximated by the Dirac δ, and the lesser function reads

$$D^<(q,\omega) = -2\pi i\left[(N_q+1)\delta(\omega+\omega_q) + N_q\delta(\omega-\omega_q)\right], \tag{9.37}$$

where N_q is (nonequilibrium) number of vibrations in the q-th mode. So, in this approximation the spectrum modification of vibrons is not taken into account, but the possible excitation of vibrations is described by the nonequilibrium N_q. The dissipation of vibrons is neglected in the spectral function, but is taken into account later in the kinetic equation for N_q. A similar approach to the single-level problem was considered recently in [1, 5, 6, 11–14]. The more general case with broadened equilibrium vibron spectral function seems to be not very interesting, because in this case vibrons are not excited. Nevertheless, in the numerical calculation it can be easily taken into consideration.

From the general quantum kinetic equation for vibrons, we obtain in this limit

$$N_q = \frac{\gamma_q N_q^0 - \mathrm{Im}\Pi^<(\omega_q)}{\gamma_q - 2\mathrm{Im}\Pi^R(\omega_q)}. \tag{9.38}$$

This expression describes the number of vibrons N_q in a nonequilibrium state, and $N_q^0 = f_B^0(\omega_q)$ is the equilibrium number of vibrons. In the linear approximation the polarization operator is independent of N_q and $-2\mathrm{Im}\Pi^R(\omega_q)$ describes additional dissipation. Note that in equilibrium $N_q \equiv N_q^0$ because $\mathrm{Im}\Pi^<(\omega_q) =$

$2\mathrm{Im}\Pi^R(\omega_q) f_B^0(\omega_q)$. See also detailed discussion of vibron emission and absorption rates in [11–14].

For weak electron-vibron coupling the number of vibrons is close to equilibrium and is changed because of *vibron emission* by nonequilibrium electrons, N_q is roughly proportional to the number of such electrons, and the distribution function of nonequilibrium electrons is not changed essentially by the interaction with vibrons (perturbation theory can be used). The situation changes, however, if nonequilibrium dissipation $-2\mathrm{Im}\Pi^R(\omega_q)$ is *negative*. In this case the number of vibrons can be essentially larger than in the equilibrium case (*vibronic instability*), and the change of the electron distribution function should be taken into account self-consistently.

In the stationary state the *nonlinear* dissipation rate

$$\gamma_q^* = \gamma_q - 2\mathrm{Im}\Pi^R(\omega_q) \tag{9.39}$$

is positive, but the nonequilibrium contribution to dissipation $-2\mathrm{Im}\Pi^R(\omega_q)$ remains negative.

Additionally to the vibronic quasiparticle approximation, the *electronic quasiparticle approximation* can be used when the coupling to the leads is weak. In this case the lesser function can be parameterized through the number of electrons F_η *in the eigenstates of the noninteracting molecular Hamiltonian* $H_C^{(0)}$

$$G^<_{\alpha\beta} = i \sum_{\gamma\eta} A_{\alpha\gamma} S_{\gamma\eta} F_\eta S^{-1}_{\eta\beta}, \tag{9.40}$$

we introduce the unitary matrix $\boldsymbol{S}$, which transfers the Hamiltonian $\boldsymbol{H} \equiv H^{(0)}_{C\alpha\beta}$ into the diagonal form $\tilde{\boldsymbol{H}} = \boldsymbol{S}^{-1}\boldsymbol{H}\boldsymbol{S}$, so that the spectral function of this diagonal Hamiltonian is

$$\tilde{A}_{\delta\eta}(\varepsilon) = 2\pi\delta(\varepsilon - \tilde{\varepsilon}_\delta)\delta_{\delta\eta}, \tag{9.41}$$

where $\tilde{\varepsilon}_\delta$ are the eigenenergies.

Note that in the calculation of the self-energies and polarization operators we can not use the δ-approximation for the spectral function (this is too rough and results in the absence of interaction out of the exact electron-vibron resonance). So that in the calculation we use actually (9.40) with broadened equilibrium spectral function. This approximation can be systematically improved by including nonequilibrium corrections to the spectral function, which are important near the resonance. It is important to comment that for stronger electron-vibron coupling *vibronic side-bands* are observed in the spectral function and voltage-current curves at energies $\tilde{\varepsilon}_\delta \pm n\omega_q$, but we do not consider these effects in the rest of our book and concentrate on resonance effects.

After corresponding calculations we obtain finally

$$N_q = \frac{\gamma_q N_q^0 - \sum_{\eta\delta} \kappa_{\eta\delta}(\omega_q) F_\eta (F_\delta - 1)}{\gamma_q - \sum_{\eta\delta} \kappa_{\eta\delta}(\omega_q)(F_\eta - F_\delta)}, \tag{9.42}$$

where coefficients $\kappa_{\eta\delta}$ are determined by the spectral function and electron-vibron coupling in the diagonal representation

$$\kappa_{\eta\delta}(\omega_q) = \int \frac{d\varepsilon}{2\pi} \tilde{M}^q_{\eta\delta} \tilde{A}_{\delta\delta}(\varepsilon - \omega_q) \tilde{M}^q{}_{\delta\eta} \tilde{A}_{\eta\eta}(\varepsilon), \tag{9.43}$$

$$F_\eta = \frac{\tilde{\Gamma}_{L\eta\eta} f^0_{L\eta} + \tilde{\Gamma}_{R\eta\eta} f^0_{R\eta} + \sum_{q\eta} \left[\zeta^{-q}_{\eta\delta} F_\delta N_q + \zeta^{+q}_{\eta\delta} F_\delta (1 + N_q) \right]}{\tilde{\Gamma}_{L\eta\eta} + \tilde{\Gamma}_{R\eta\eta} + \sum_{q\eta} \left[\zeta^{-q}_{\eta\delta} (1 - F_\delta + N_q) + \zeta^{+q}_{\eta\delta} (F_\delta + N_q) \right]}, \tag{9.44}$$

$$\zeta^{\pm q}_{\eta\delta} = \tilde{M}^q{}_{\eta\delta} \tilde{A}_{\delta\delta}(\tilde{\varepsilon}_\eta \pm \omega_q) \tilde{M}^q{}_{\delta\eta}, \tag{9.45}$$

here $\tilde{\Gamma}_{i\eta\eta}$ and $f^0_{i\eta}$ are the level width matrix in the diagonal representation and Fermi function at energy $\tilde{\varepsilon}_\eta - e\varphi_i$.

These kinetic equations are similar to the usual golden rule equations, but are more general.

Now let us consider several examples of vibron emission and vibronic instability.

First we consider the most simple case, when the instability is not possible and only vibron emission takes place. This corresponds to a negative imaginary part of the electronic polarization operator: $\mathrm{Im}\Pi^R(\omega_q) < 0$. From (9.43) one can see that for any two levels with the energies $\tilde{\varepsilon}_\eta > \tilde{\varepsilon}_\delta$ the coefficient $\kappa_{\eta\delta}$ is larger than $\kappa_{\delta\eta}$, because the spectral function $\tilde{A}_{\delta\delta}(\varepsilon)$ has a maximum at $\varepsilon = \tilde{\varepsilon}_\delta$. The contribution of $\kappa_{\eta\delta}(\omega_q)(F_\eta - F_\delta)$ is negative if $F_\eta < F_\delta$. This takes place in equilibrium, and in nonequilibrium for transport through *symmetric* molecules, when higher energy levels are populated after lower levels. The example of such a system is shown in Fig. 9.5. Here we consider a simple three-level system ($\tilde{\varepsilon}_1 = 1$, $\tilde{\varepsilon}_2 = 2$, $\tilde{\varepsilon}_3 = 3$) coupled symmetrically to the leads ($\Gamma_{L\eta} = \Gamma_{R\eta} = 0.01$). The current-voltage curve is the same with and without vibrations in the case of symmetrical coupling to the leads and in the weak electron-vibron coupling limit (if we neglect change of the spectral function). The figure shows how vibrons are excited, as the number of vibrons N_V in the mode with frequency ω_0 is presented for two cases. In the off-resonant case (green triangles) N_V is very small compared to the resonant case ($\omega_0 = \tilde{\varepsilon}_2 - \tilde{\varepsilon}_1$, red crosses, the vertical scale is changed for the off-resonant points). In fact, if the number of vibrons is very large, the spectral function and voltage-current curve are changed.

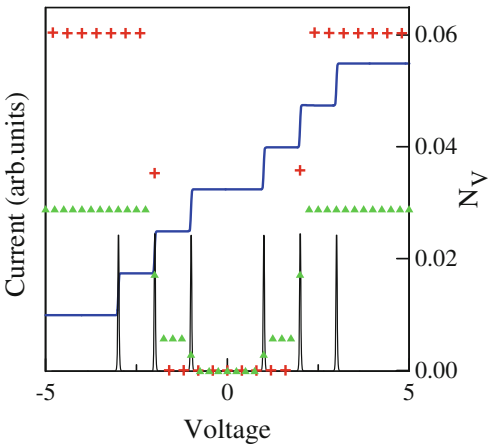

Fig. 9.5 Vibronic emission in the symmetric multilevel model: voltage-current curve, differential conductance, and the number of excited vibrons in the off-resonant (*triangles*) and resonant (*crosses*) cases. *Dashed line* show the voltage-current curve without vibrons

Vibronic Instability

Now let us consider the situation when the imaginary part of the electronic polarization operator can be positive: $\mathrm{Im}\Pi^R(\omega_q) > 0$. Above we considered the normal case when the population of higher energy levels is smaller than lower levels. The opposite case $F_2 > F_1$ is known as inversion in laser physics. Such a state is unstable if the total dissipation γ_q^* (9.39) is negative, which is possible only in the nonstationary case. As a result of the instability, a large number of vibrons is excited, and in the stationary state γ_q^* is positive. This effect can be observed for transport through *asymmetric* molecules, when higher energy levels are populated *before* lower levels. The example of a such system is shown in Fig. 9.6. It is the same three-level system as before, but the first and second levels are coupled not symmetrically to the leads

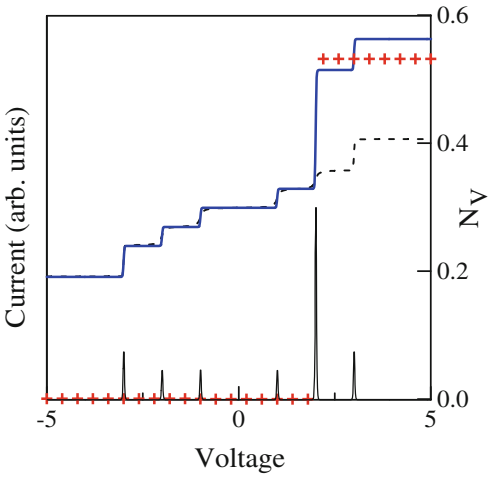

Fig. 9.6 Vibronic emission in the asymmetric multilevel model: voltage-current curve, differential conductance, and the number of excited vibrons in the off-resonant (*triangles*) and resonant (*crosses*) cases. *Dashed line* show the voltage-current curve without vibrons

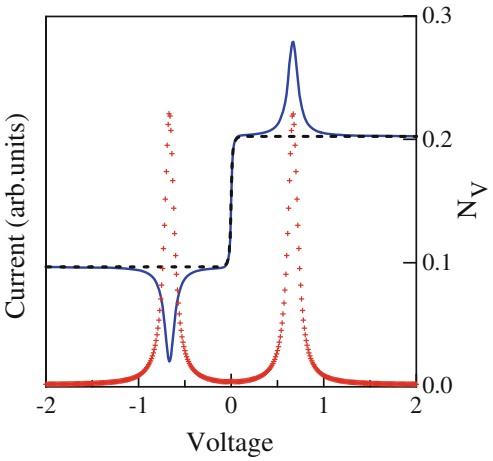

Fig. 9.7 Floating level resonance: voltage-current curve and the number of excited vibrons (*crosses*) *Dashed line* show the voltage-current curve without vibrons (details see in the text)

($\Gamma_{L1} = 0.001$, $\Gamma_{R1} = 0.1$, $\Gamma_{L2} = 0.1$, $\Gamma_{R2} = 0.001$). The vibron couples resonantly these levels ($\omega_q = \tilde{\varepsilon}_2 - \tilde{\varepsilon}_1$). The result is qualitatively different from the symmetrical case. The voltage-current curve is now asymmetric, a large *step* corresponds to the resonant level with inverted population.

Note the importance of the off-diagonal electron-vibron coupling for the resonant effects. If the matrix $\tilde{\boldsymbol{M}}$ in the eigen-state representation is diagonal, there is no resonant coupling between different electronic states.

Finally, let us consider the important case, when initially symmetric molecule becomes asymmetric when the external voltage is applied. The reason for such asymmetry is simply that in the external electric field left and right atoms feel different electrical potentials and the position of the levels $\varepsilon_\alpha = \varepsilon_\alpha^{(0)} + e\varphi_\alpha$ is changed (float) with the external voltage. The example of a such system is shown in Fig. 9.7. Here we consider a two-level system, one level is coupled electrostatically to the left lead $\tilde{\varepsilon}_1 \propto \varphi_L$, the other level to the right lead $\tilde{\varepsilon}_2 \propto \varphi_R$, the tunneling coupling to the leads also is not symmetrical ($\Gamma_{L1} = 0.1$, $\Gamma_{R1} = 0.001$, $\Gamma_{L2} = 0.001$, $\Gamma_{R2} = 0.1$). The frequency of the vibration, coupling these two states, is $\omega_0 = 1$. When we sweep the voltage, a *peak* in the voltage-current curve is observed when the energy difference $\tilde{\varepsilon}_1 - \tilde{\varepsilon}_2 \propto eV$ is going through the resonance $\tilde{\varepsilon}_1 - \tilde{\varepsilon}_2 \approx \omega_0$.

9.2 Coulomb Blockade (EOM Method)

Coulomb blockade phenomena mediated by electron-electron interactions on a quantum dot can be dealt with in a straightforward way by using master equation (ME) approaches, which are based on Fermi Golden Rule [15–22]. However, due to its intrinsic perturbative character in the lead-dot coupling, ME techniques cannot cover the whole interaction range from weak-coupling (Coulomb blockade), intermediate

coupling (Kondo physics), up to strong coupling (Fabry-Pérot physics). It is thus of methodological and practical interest to develop schemes which allow, in a systematic way, to describe the three mentioned regimes also in out-of-equilibrium situations. As stated in the introduction, we believe that Green function techniques are such a tool; in this section we will show how a non-equilibrium treatment of the Hubbard-Anderson model together with appropriate approximations allow us to reproduce the well-known Coulomb blockade stability diagrams obtained with the master equation approach. For the sake of simplicity we will deal with the problem of single and double-site dots in the CB regime, although the method can be straightforwardly extended to multi-level systems. Our purpose is to study the problem of a two site donor/acceptor molecule in the CB regime within the NGF as a first step to deal with the phenomenology of a rigid multilevel island. The nuclear dynamics (vibrations) always present in molecular junctions could be then modularly included in this theory. Our method can be calibrated on the well-studied double quantum dot problem [21, 23] and could be possibly integrated in the density functional theory based approaches to molecular conductance. The Kondo regime would require a separate treatment involving more complex decoupling schemes and will be thus left out of this review, for some new results see [24] (EOM method) and [25–27] (the self-consistent GW approximation).

The *linear conductance* properties of a single site junction (SSJ) with Coulomb interactions (Anderson impurity model), have been extensively studied by means of the EOM approach in the cases related to CB [28, 29] and the Kondo effect [30]. Later the same method was applied to some two-site models [31–34]. Multi-level systems were started to be considered only recently [35, 36]. For out-of-equilibrium situations (finite applied bias), there are some methodological unclarified issues for calculating correlation functions using EOM techniques [24, 34, 37]. We have developed an EOM-based method which allows to deal with the finite-bias case in a self-consistent way [38].

9.2.1 The Hubbard-Anderson Hamiltonian

We consider the following model Hamiltonian (which can be also called the multilevel Anderson impurity model, the Hubbard model, or the quantum cluster model)

$$\hat{H} = \sum_{\alpha\beta} \tilde{\varepsilon}_{\alpha\beta} d_\alpha^\dagger d_\beta + \frac{1}{2} \sum_{\alpha\beta} U_{\alpha\beta} \hat{n}_\alpha \hat{n}_\beta + \sum_{ik\sigma} \tilde{\varepsilon}_{ik\sigma} c_{ik\sigma}^\dagger c_{ik\sigma} + \sum_{ik\sigma,\alpha} \left(V_{ik\sigma,\alpha} c_{ik\sigma}^\dagger d_\alpha + h.c. \right), \tag{9.46}$$

electrical potentials are included into the energies $\{\tilde{\varepsilon}_{ik\sigma} = \varepsilon_{ik\sigma} + e\varphi_i(t)$ and $\tilde{\varepsilon}_{\alpha\alpha} = \varepsilon_{\alpha\alpha} + e\varphi_\alpha(t)$.

This model is quite universal, describing a variety of correlated electron systems coupled to the leads: the Anderson impurity model, the multilevel quantum dot with diagonal noninteracting Hamiltonian $\tilde{\varepsilon}_{\alpha\beta}$, a system (cluster) of several quantum dots,

when the off-diagonal matrix elements of $\tilde{\varepsilon}_{\alpha\beta}$ describe hopping between individual dots, and, finally, the 1D and 2D quantum point contacts.

9.2.2 Nonequilibrium EOM Formalism

EOM for Heisenberg Operators

Using the Hamiltonian (9.46) one derives

$$i\frac{\partial c_{ik\sigma}}{\partial t} = \left[c_{ik\sigma}, \hat{H}\right]_- = \tilde{\varepsilon}_{ik\sigma}c_{ik\sigma} + \sum_{\alpha} V_{ik\sigma,\alpha}d_{\alpha}, \tag{9.47}$$

$$i\frac{\partial c^{\dagger}_{ik\sigma}}{\partial t} = -\tilde{\varepsilon}_{ik\sigma}c^{\dagger}_{ik\sigma} - \sum_{\alpha} V^{*}_{ik\sigma,\alpha}d^{\dagger}_{\alpha}, \tag{9.48}$$

$$i\frac{\partial d_{\alpha}}{\partial t} = \sum_{\beta}\tilde{\varepsilon}_{\alpha\beta}d_{\beta} + \sum_{\beta\neq\alpha} U_{\alpha\beta}\hat{n}_{\beta}d_{\alpha} + \sum_{ik\sigma} V^{*}_{ik\sigma,\alpha}c_{ik\sigma}, \tag{9.49}$$

$$i\frac{\partial d^{\dagger}_{\alpha}}{\partial t} = -\sum_{\beta}\tilde{\varepsilon}_{\alpha\beta}d^{\dagger}_{\beta} - \sum_{\beta\neq\alpha} U_{\alpha\beta}\hat{n}_{\beta}d^{\dagger}_{\alpha} - \sum_{ik\sigma} V_{ik\sigma,\alpha}c^{\dagger}_{ik\sigma}, \tag{9.50}$$

$$\begin{aligned} i\frac{\partial \hat{n}_{\gamma}}{\partial t} = &\sum_{ik\sigma}\left[-V_{ik\sigma,\gamma}c^{\dagger}_{ik\sigma}d_{\gamma} + V^{*}_{ik\sigma,\gamma}d^{\dagger}_{\gamma}c_{ik\sigma}\right] \\ &+ \sum_{\beta}\tilde{\varepsilon}_{\gamma\beta}d^{\dagger}_{\gamma}d_{\beta} - \sum_{\alpha}\tilde{\varepsilon}_{\alpha\gamma}d^{\dagger}_{\alpha}d_{\gamma}. \end{aligned} \tag{9.51}$$

These equations look like a set of ordinary differential equations, but are, in fact, much more complex. The first reason is, that there are the equations for *operators*, and special algebra should be used to solve it. Secondly, the number of $c_{ik\sigma}$ operators is infinite! Because of that, the above equations are not all sufficient, but are widely used to obtain the equations for Green functions.

Spectral (Retarded and Advanced) Functions

Now we follow the general NEOM method described in Sect. 7.4. Using (9.49), we get the equation for $G^{R}_{\alpha\beta} = -i\left\langle\left[d_{\alpha}, d^{\dagger}_{\beta}\right]_{+}\right\rangle_{\varepsilon}$

$$(\varepsilon + i\eta)G^{R}_{\alpha\beta} - \sum_{\gamma}\tilde{\varepsilon}_{\alpha\gamma}G^{R}_{\gamma\beta} = \delta_{\alpha\beta} + \sum_{\gamma\neq\alpha} U_{\alpha\gamma}G^{(2)R}_{\alpha\gamma,\beta} + \sum_{ik\sigma} V^{*}_{ik\sigma,\alpha}G^{R}_{ik\sigma,\beta} \tag{9.52}$$

which includes two new functions: $G^{(2)R}_{\alpha\gamma,\beta}$ and $G^{R}_{ik\sigma,\beta}$.

The equation for $G^R_{ik\sigma,\beta}$ is closed (includes only the function $G^R_{\alpha\beta}$ introduced before)

$$(\varepsilon + i\eta - \tilde{\varepsilon}_{ik\sigma})G^R_{ik\sigma,\beta} = \sum_\delta V_{ik\sigma,\delta} G^R_{\delta\beta}. \tag{9.53}$$

The equation for

$$G^{(2)R}_{\alpha\gamma,\beta}(t_1 - t_2) = -i\theta(t_1 - t_2)\left\langle \left[d_\alpha(t_1)\hat{n}_{\gamma(t_1)}, d^\dagger_\beta(t_2)\right]_+ \right\rangle \tag{9.54}$$

is more complicated

$$\begin{aligned}
&(\varepsilon + i\eta)G^{(2)R}_{\alpha\gamma,\beta} - \sum_\delta \tilde{\varepsilon}_{\alpha\delta} G^{(2)R}_{\delta\gamma,\beta} = n_\gamma \delta_{\alpha\beta} + (\delta_{\alpha\beta} - \rho_{\alpha\beta})\delta_{\beta\gamma} \\
&+ \sum_\delta U_{\alpha\delta} \left\langle\left\langle \hat{n}_\delta d_\alpha \hat{n}_\gamma ; d^\dagger_\beta \right\rangle\right\rangle^R + \sum_{ik\sigma} V^*_{ik\sigma,\alpha} \left\langle\left\langle c_{ik\sigma} n_\gamma ; d^\dagger_\beta \right\rangle\right\rangle^R \\
&+ \sum_{ik\sigma} V^*_{ik\sigma,\gamma} \left\langle\left\langle d_\alpha d^\dagger_\gamma c_{ik\sigma} ; d^\dagger_\beta \right\rangle\right\rangle^R - \sum_{ik\sigma} V_{ik\sigma,\gamma} \left\langle\left\langle d_\alpha c^\dagger_{ik\sigma} d_\gamma ; d^\dagger_\beta \right\rangle\right\rangle^R \\
&+ \sum_\delta \tilde{\varepsilon}_{\gamma\delta} \left\langle\left\langle d_\alpha d^\dagger_\gamma d_\delta ; d^\dagger_\beta \right\rangle\right\rangle^R - \sum_\delta \tilde{\varepsilon}_{\delta\gamma} \left\langle\left\langle d_\alpha d^\dagger_\delta d_\gamma ; d^\dagger_\beta \right\rangle\right\rangle^R .
\end{aligned} \tag{9.55}$$

The equation (9.55) is not closed again and produces new Green functions of higher order. And so on. We present here one of the next order equations, for the function $\left\langle\left\langle c_{ik\sigma} n_\gamma ; d^\dagger_\beta \right\rangle\right\rangle^R$

$$\begin{aligned}
&(\varepsilon + i\eta - \tilde{\varepsilon}_{ik\sigma}) \left\langle\left\langle c_{ik\sigma} n_\gamma ; d^\dagger_\beta \right\rangle\right\rangle^R = i \int \frac{d\varepsilon}{2\pi} G^<_{ik\sigma,\beta}\delta_{\beta\gamma} + \sum_\alpha V_{ik\sigma,\alpha} G^{(2)R}_{\alpha\gamma,\beta} \\
&+ \sum_{ik'\sigma'} V^*_{ik'\sigma',\gamma} \left\langle\left\langle c_{ik\sigma} d^\dagger_\gamma c_{ik'\sigma'} ; d^\dagger_\beta \right\rangle\right\rangle^R - \sum_{ik'\sigma'} V_{ik'\sigma',\gamma} \left\langle\left\langle c_{ik\sigma} c^\dagger_{ik'\sigma'} d_\gamma ; d^\dagger_\beta \right\rangle\right\rangle^R .
\end{aligned} \tag{9.56}$$

This sequence of equations can not be given in a closed form in the general case and should be truncated at some point. Below we consider some possible approximations. The other important point is, that average populations and lesser Green functions should be calculated self-consistently. In equilibrium (linear response) these functions are easily related to the spectral functions. But at finite voltage it should be calculated independently.

Kinetic (Lesser) Function

Following the same way, as for the retarded functions (using only the definitions of NGF and Heisenberg equations of motion) one derives instead of (9.52)–(9.55)

$$\varepsilon G^<_{\alpha\beta} - \sum_\gamma \tilde{\varepsilon}_{\alpha\gamma} G^<_{\gamma\beta} = \sum_{\gamma\neq\alpha} U_{\alpha\gamma} G^{(2)<}_{\alpha\gamma,\beta} + \sum_{ik\sigma} V^*_{ik\sigma,\alpha} G^<_{ik\sigma,\beta}, \tag{9.57}$$

$$(\varepsilon - \tilde{\varepsilon}_{ik\sigma}) G^{<}_{ik\sigma,\beta} = \sum_{\delta} V_{ik\sigma,\delta} G^{<}_{\delta\beta}, \tag{9.58}$$

$$\begin{aligned}
\varepsilon G^{(2)<}_{\alpha\gamma,\beta} - \sum_{\delta} \tilde{\varepsilon_{\alpha\delta}} G^{(2)<}_{\delta\gamma,\beta} = \sum_{\delta\neq\alpha} U_{\alpha\delta} \left\langle\left\langle \hat{n}_\delta d_\alpha \hat{n}_\gamma; d^\dagger_\beta \right\rangle\right\rangle^{<} \\
+ \sum_{ik\sigma} V^*_{ik\sigma,\alpha} \left\langle\left\langle c_{ik\sigma} n_\gamma; d^\dagger_\beta \right\rangle\right\rangle^{<} + \sum_{ik\sigma} V^*_{ik\sigma,\gamma} \left\langle\left\langle d_\alpha d^\dagger_\gamma c_{ik\sigma}; d^\dagger_\beta \right\rangle\right\rangle^{<} - \sum_{ik\sigma} V_{ik\sigma,\gamma} \left\langle\left\langle d_\alpha c^\dagger_{ik\sigma} d_\gamma; d^\dagger_\beta \right\rangle\right\rangle^{<} \\
+ \sum_{\delta} \tilde{\varepsilon_{\gamma\delta}} \left\langle\left\langle d_\alpha d^\dagger_\gamma d_\delta; d^\dagger_\beta \right\rangle\right\rangle^{<} - \sum_{\delta} \tilde{\varepsilon_{\delta\gamma}} \left\langle\left\langle d_\alpha d^\dagger_\delta d_\gamma; d^\dagger_\beta \right\rangle\right\rangle^{<}.
\end{aligned} \tag{9.59}$$

$$\begin{aligned}
(\varepsilon - \tilde{\varepsilon}_{ik\sigma}) \left\langle\left\langle c_{ik\sigma} n_\gamma; d^\dagger_\beta \right\rangle\right\rangle^{<} = \sum_{\alpha} V_{ik\sigma,\alpha} G^{(2)<}_{\alpha\gamma,\beta} \\
+ \sum_{ik'\sigma'} V^*_{ik'\sigma',\gamma} \left\langle\left\langle c_{ik\sigma} d^\dagger_\gamma c_{ik'\sigma'}; d^\dagger_\beta \right\rangle\right\rangle^{<} - \sum_{ik'\sigma'} V_{ik'\sigma',\gamma} \left\langle\left\langle c_{ik\sigma} c^\dagger_{ik'\sigma'} d_\gamma; d^\dagger_\beta \right\rangle\right\rangle^{<}.
\end{aligned} \tag{9.60}$$

To find $G^{<}_{ik\sigma,\beta}$ we should divide the right parts by $(\varepsilon - \tilde{\varepsilon}_{ik\sigma})$, which is not well defined at $\varepsilon = \tilde{\varepsilon}_{ik\sigma}$. In Sect. 7.4 we considered the general prescription to avoid this problem, we use (7.168), and instead of (9.58) and (9.60) we obtain

$$G^{<}_{ik\sigma,\beta} = g^{R}_{ik\sigma} \sum_{\delta} V_{ik\sigma,\delta} G^{<}_{\delta\beta} + g^{<}_{ik\sigma} \sum_{\delta} V_{ik\sigma,\delta} G^{A}_{\delta\beta}. \tag{9.61}$$

$$\begin{aligned}
\left\langle\left\langle c_{ik\sigma} n_\gamma; d^\dagger_\beta \right\rangle\right\rangle^{<} = g^{R}_{ik\sigma} \sum_{\alpha} V_{ik\sigma,\alpha} G^{(2)<}_{\alpha\gamma,\beta} + g^{<}_{ik\sigma} \sum_{\alpha} V_{ik\sigma,\alpha} G^{(2)A}_{\alpha\gamma,\beta} \\
+ g^{R}_{ik\sigma} \sum_{ik'\sigma'} V^*_{ik'\sigma',\gamma} \left\langle\left\langle c_{ik\sigma} d^\dagger_\gamma c_{ik'\sigma'}; d^\dagger_\beta \right\rangle\right\rangle^{<} - g^{R}_{ik\sigma} \sum_{ik'\sigma'} V_{ik'\sigma',\gamma} \left\langle\left\langle c_{ik\sigma} c^\dagger_{ik'\sigma'} d_\gamma; d^\dagger_\beta \right\rangle\right\rangle^{<} \\
+ g^{<}_{ik\sigma} \sum_{ik'\sigma'} V^*_{ik'\sigma',\gamma} \left\langle\left\langle c_{ik\sigma} d^\dagger_\gamma c_{ik'\sigma'}; d^\dagger_\beta \right\rangle\right\rangle^{A} - g^{<}_{ik\sigma} \sum_{ik'\sigma'} V_{ik'\sigma',\gamma} \left\langle\left\langle c_{ik\sigma} c^\dagger_{ik'\sigma'} d_\gamma; d^\dagger_\beta \right\rangle\right\rangle^{A}.
\end{aligned} \tag{9.62}$$

The equation (9.57) and (9.59) can be used without modifications because they include the imaginary parts (dissipation) from the lead terms.

Now we consider some approximations which can be used to truncate the system of equations.

Hubbard I Approximation

In this approximation we use exact relations $\hat{n}^2_\gamma = \hat{n}_\gamma$, so that ($\gamma \neq \alpha$ here and below)

$$\left\langle\left\langle \hat{n}_\gamma \hat{d}_\alpha \hat{n}_\gamma; d^\dagger_\beta \right\rangle\right\rangle = \left\langle\left\langle \hat{d}_\alpha n_\gamma; d^\dagger_\beta \right\rangle\right\rangle = G^{(2)R}_{\alpha\gamma,\beta}, \tag{9.63}$$

opposite-spin correlations in the leads are neglected

$$\left\langle\left\langle d_\alpha d_\gamma^\dagger c_{ik\sigma}; d_\beta^\dagger\right\rangle\right\rangle = \left\langle\left\langle d_\alpha c_{ik\sigma}^\dagger d_\gamma; d_\beta^\dagger\right\rangle\right\rangle = 0, \tag{9.64}$$

and all other high-order Green functions in (9.55) are approximated on the Hartree-Fock level

$$\left\langle\left\langle \hat{n}_\delta d_\alpha \hat{n}_\gamma; d_\beta^\dagger\right\rangle\right\rangle \simeq \langle\hat{n}_\delta\rangle\langle\hat{n}_\gamma\rangle\left\langle\left\langle d_\alpha d_\beta^\dagger\right\rangle\right\rangle = \langle\hat{n}_\delta\rangle\langle\hat{n}_\gamma\rangle G_{\alpha\beta}^R, \tag{9.65}$$

$$\left\langle\left\langle c_{ik\sigma} n_\gamma; d_\beta^\dagger\right\rangle\right\rangle \simeq \langle\hat{n}_\gamma\rangle\left\langle\left\langle c_{ik\sigma} d_\beta^\dagger\right\rangle\right\rangle = \langle\hat{n}_\gamma\rangle G_{ik\sigma,\beta}^R. \tag{9.66}$$

Finally, in this approximation we obtain a closed equation for $G_{\delta\gamma,\beta}^{(2)R}$ $(\gamma \neq \alpha)$

$$(\varepsilon + i\eta - U_{\alpha\gamma})G_{\alpha\gamma,\beta}^{(2)R} - \sum_\delta \tilde{\varepsilon}_{\alpha\delta} G_{\delta\gamma,\beta}^{(2)R} = \langle\hat{n}_\gamma\rangle\delta_{\alpha\beta} + i\int \frac{d\varepsilon}{2\pi} G_{\alpha\beta}^< \delta_{\beta\gamma} + \sum_{\delta\neq\alpha,\gamma} U_{\alpha\delta}\langle\hat{n}_\delta\rangle\langle\hat{n}_\gamma\rangle G_{\alpha\beta}^R + \sum_{ik\sigma} V_{ik\sigma,\alpha}^* \langle\hat{n}_\gamma\rangle G_{ik\sigma,\beta}^R. \tag{9.67}$$

Improved Hubbard Approximation

The main difference from the Hubbard I approximation is that the function $\left\langle\left\langle c_{ik\sigma} n_\gamma; d_\beta^\dagger\right\rangle\right\rangle$ is not truncated as in (9.66), but one step further using (9.56) and (9.62).

We obtain the following set of equations for **the retarded functions**

$$(\varepsilon + i\eta)G_{\alpha\beta}^R - \sum_\gamma \tilde{\varepsilon}_{\alpha\gamma} G_{\gamma\beta}^R = \delta_{\alpha\beta} + \sum_{\gamma\neq\alpha} U_{\alpha\gamma} G_{\alpha\gamma,\beta}^{(2)R} + \sum_{ik\sigma} V_{ik\sigma,\alpha}^* G_{ik\sigma,\beta}^R, \tag{9.68}$$

$$(\varepsilon + i\eta - \tilde{\varepsilon}_{ik\sigma})G_{ik\sigma,\beta}^R = \sum_\delta V_{ik\sigma,\delta} G_{\delta\beta}^R, \tag{9.69}$$

$$(\varepsilon + i\eta - U_{\alpha\gamma})G_{\alpha\gamma,\beta}^{(2)R} - \sum_\delta \tilde{\varepsilon}_{\alpha\delta} G_{\delta\gamma,\beta}^{(2)R} = \langle\hat{n}_\gamma\rangle\delta_{\alpha\beta} + i\int \frac{d\varepsilon'}{2\pi} G_{\alpha\beta}^<(\varepsilon')\delta_{\beta\gamma} + \sum_{\delta\neq\alpha,\gamma} U_{\alpha\delta}\langle\hat{n}_\delta\rangle\langle\hat{n}_\gamma\rangle G_{\alpha\beta}^R + \sum_{ik\sigma} V_{ik\sigma,\alpha}^* \left\langle\left\langle c_{ik\sigma} n_\gamma; d_\beta^\dagger\right\rangle\right\rangle, \tag{9.70}$$

$$(\varepsilon + i\eta - \tilde{\varepsilon}_{ik\sigma})\left\langle\left\langle c_{ik\sigma} n_\gamma; d_\beta^\dagger\right\rangle\right\rangle = i\int \frac{d\varepsilon'}{2\pi} G_{ik\sigma,\beta}^<(\varepsilon')\delta_{\beta\gamma} + \sum_\delta V_{ik\sigma,\delta} G_{\alpha\gamma,\beta}^{(2)R}. \tag{9.71}$$

These equations are not enough for the Kondo effect, but describe quite successfully the Coulomb blockade.

Now we have from (9.69)

$$G^R_{ik\sigma,\beta} = \sum_\delta V_{ik\sigma,\delta} G^R_{\delta\beta} \frac{1}{\varepsilon + i\eta - \tilde{\varepsilon}_{ik\sigma}}, \tag{9.72}$$

and from (9.71)

$$\left\langle\left\langle c_{ik\sigma} n_\gamma; d^\dagger_\beta \right\rangle\right\rangle = \left[i \int \frac{d\varepsilon'}{2\pi} G^<_{ik\sigma,\beta}(\varepsilon') \delta_{\beta\gamma} + \sum_\delta V_{ik\sigma,\delta} G^{(2)R}_{\alpha\gamma,\beta} \right] \frac{1}{\varepsilon + i\eta - \tilde{\varepsilon}_{ik\sigma}}. \tag{9.73}$$

Substituting these expressions into (9.68) and (9.70) we obtain finally

$$(\varepsilon + i\eta) G^R_{\alpha\beta} - \sum_\gamma \tilde{\varepsilon}_{\alpha\gamma} G^R_{\gamma\beta} = \delta_{\alpha\beta} + \sum_{\gamma\neq\alpha} U_{\alpha\gamma} G^{(2)R}_{\alpha\gamma,\beta} + \sum_{i\delta} \Sigma^{R(T)}_{i\alpha\delta} G^R_{\delta\beta}, \tag{9.74}$$

$$(\varepsilon + i\eta - U_{\alpha\gamma}) G^{(2)R}_{\alpha\gamma,\beta} - \sum_\delta \tilde{\varepsilon}_{\alpha\delta} G^{(2)R}_{\delta\gamma,\beta} = \langle \hat{n}_\gamma \rangle \delta_{\alpha\beta} + i \int \frac{d\varepsilon'}{2\pi} G^<_{\alpha\beta}(\varepsilon') \delta_{\beta\gamma} + \sum_{\delta\neq\alpha,\gamma} U_{\alpha\delta} \langle \hat{n}_\delta \rangle \langle \hat{n}_\gamma \rangle G^R_{\alpha\beta} + \sum_{i\delta} \Sigma^{R(T)}_{i\alpha\delta} G^{(2)R}_{\delta\gamma,\beta}, \tag{9.75}$$

where

$$\Sigma^{R(T)}_{i\alpha\delta} = \sum_{ik\sigma} \frac{V^*_{ik\sigma,\alpha} V_{ik\sigma,\delta}}{\varepsilon + i\eta - \tilde{\varepsilon}_{ik\sigma}} \tag{9.76}$$

is the usual tunneling self-energy for the right and left leads ($i = L, R$).

The equations for **the lesser functions** are

$$\varepsilon G^<_{\alpha\beta} - \sum_\gamma \tilde{\varepsilon}_{\alpha\gamma} G^<_{\gamma\beta} = \sum_{\gamma\neq\alpha} U_{\alpha\gamma} G^{(2)<}_{\alpha\gamma,\beta} + \sum_{ik\sigma} V^*_{ik\sigma,\alpha} G^<_{ik\sigma,\beta}, \tag{9.77}$$

$$G^<_{ik\sigma,\beta} = g^R_{ik\sigma} \sum_\delta V_{ik\sigma,\delta} G^<_{\delta\beta} + g^<_{ik\sigma} \sum_\delta V_{ik\sigma,\delta} G^A_{\delta\beta}, \tag{9.78}$$

$$(\varepsilon - U_{\alpha\gamma}) G^{(2)<}_{\alpha\gamma,\beta} - \sum_\delta \tilde{\varepsilon}_{\alpha\delta} G^{(2)<}_{\delta\gamma,\beta} = \sum_{\delta\neq\alpha,\gamma} U_{\alpha\delta} \langle \hat{n}_\delta \rangle \langle \hat{n}_\gamma \rangle G^<_{\alpha\beta} + \sum_{ik\sigma} V^*_{ik\sigma,\alpha} \left\langle\left\langle c_{ik\sigma} n_\gamma; d^\dagger_\beta \right\rangle\right\rangle^<, \tag{9.79}$$

$$\left\langle\left\langle c_{ik\sigma} n_\gamma; d^\dagger_\beta \right\rangle\right\rangle^< = g^R_{ik\sigma} \sum_\alpha V_{ik\sigma,\alpha} G^{(2)<}_{\alpha\gamma,\beta} + g^<_{ik\sigma} \sum_\alpha V_{ik\sigma,\alpha} G^{(2)A}_{\alpha\gamma,\beta}, \tag{9.80}$$

$$g^R_{ik\sigma} = \frac{1}{\varepsilon + i\eta - \tilde{\varepsilon}_{ik\sigma}}, \quad g^<_{ik\sigma} = 2\pi f_0(\varepsilon)\delta(\varepsilon - \tilde{\varepsilon}_{ik\sigma}), \tag{9.81}$$

and finally

$$\varepsilon G^<_{\alpha\beta} - \sum_\gamma \tilde{\varepsilon}_{\alpha\gamma} G^<_{\gamma\beta} = \sum_{\gamma\neq\alpha} U_{\alpha\gamma} G^{(2)<}_{\alpha\gamma,\beta} + \sum_{i\delta} \Sigma^{R(T)}_{i\alpha\delta} G^<_{\delta\beta} + i \sum_{i\delta} \tilde{\Gamma}_{i\alpha\delta}(\varepsilon) f_i(\varepsilon) G^A_{\delta\beta}, \tag{9.82}$$

$$(\varepsilon - U_{\alpha\gamma}) G^{(2)<}_{\alpha\gamma,\beta} - \sum_\delta \tilde{\varepsilon}_{\alpha\delta} G^{(2)<}_{\delta\gamma,\beta} = \sum_{\delta\neq\alpha,\gamma} U_{\alpha\delta} \langle \hat{n}_\delta \rangle \langle \hat{n}_\gamma \rangle G^<_{\alpha\beta} + \sum_{i\delta} \Sigma^{R(T)}_{i\alpha\delta} G^{(2)<}_{\delta\gamma,\beta} + i \sum_{i\delta} \tilde{\Gamma}_{i\alpha\delta}(\varepsilon) f_i(\varepsilon) G^{(2)A}_{\delta\gamma,\beta}, \tag{9.83}$$

where

$$\tilde{\Gamma}_{i\alpha\beta}(\varepsilon) = 2\pi \sum_{k\sigma} V^*_{ik\sigma,\alpha} V_{ik\sigma,\beta} \delta(\varepsilon - \tilde{\varepsilon}_{ik\sigma}), \tag{9.84}$$

$$\sum_i \tilde{\Gamma}_{i\alpha\delta}(\varepsilon) f_i(\varepsilon) = \Gamma_{L\alpha\delta}(\varepsilon - e\varphi_\alpha) f^0_L(\varepsilon - e\varphi_L) + \Gamma_{R\alpha\delta}(\varepsilon - e\varphi_\alpha) f^0_R(\varepsilon - e\varphi_R), \tag{9.85}$$

$$\Gamma_{i\alpha\beta}(\varepsilon) = \tilde{\Gamma}_{i\alpha\beta}(\varepsilon + e\varphi_i) = 2\pi \sum_{k\sigma} V^*_{ik\sigma,\alpha} V_{ik\sigma,\beta} \delta(\varepsilon - \varepsilon_{ik\sigma}). \tag{9.86}$$

We derived the full set of equations for both retarded and lesser functions, which can be applied to describe transport through multi-level quantum dots with Coulomb blockade at finite voltage (nonequilibrium case).

9.2.3 Anderson Impurity Model

As a simple limiting case we consider the two-level Anderson impurity model (AIM),

$$\hat{H} = \sum_{\sigma=\uparrow\downarrow} \tilde{\varepsilon}_\sigma d^\dagger_\sigma d_\sigma + U \hat{n}_\uparrow \hat{n}_\downarrow + \sum_{ik\sigma} \tilde{\varepsilon}_{ik\sigma} c^\dagger_{ik\sigma} c_{ik\sigma} + \sum_{ik\sigma} \left(V_{ik\sigma} c^\dagger_{ik\sigma} d_\sigma + h.c. \right), \tag{9.87}$$

this model corresponds to a single-level quantum dot with spin in an external magnetic field.

In the limit of a two-level system our approach reproduce the Meir-Wingreen-Lee approximation for the retarded functions. Indeed, the equations are

$$(\varepsilon + i\eta - \tilde{\varepsilon}_\sigma) G^R_\sigma = 1 + U G^{(2)R}_\sigma + \sum_{ik} V^*_{ik\sigma} G^R_{ik\sigma,\sigma}, \tag{9.88}$$

$$(\varepsilon + i\eta - \tilde{\varepsilon}_{ik\sigma}) G^R_{ik\sigma,\sigma} = V_{ik\sigma} G^R_\sigma, \tag{9.89}$$

$$(\varepsilon + i\eta - \tilde{\varepsilon}_\sigma) G^{(2)R}_\sigma = \langle n_{\bar{\sigma}} \rangle + U G^{(2)R}_\sigma + \sum_{ik} V^*_{ik\sigma} \left\langle \left\langle c_{ik\sigma} n_{\bar{\sigma}}; d^\dagger_\sigma \right\rangle \right\rangle, \tag{9.90}$$

$$(\varepsilon + i\eta - \tilde{\varepsilon}_{ik\sigma}) \left\langle \left\langle c_{ik\sigma} n_{\bar{\sigma}}; d^\dagger_\sigma \right\rangle \right\rangle = V_{ik\sigma} G^{(2)R}_\sigma. \tag{9.91}$$

From these equations one has

$$(\varepsilon - \tilde{\varepsilon}_\sigma - \Sigma_{\sigma 0}) G^R_\sigma = 1 + U G^{(2)R}_\sigma, \tag{9.92}$$

$$G^{(2)R}_\sigma = \frac{\langle n_{\bar{\sigma}} \rangle}{\varepsilon - \tilde{\varepsilon}_\sigma - U - \Sigma_{\sigma 0}}, \tag{9.93}$$

with $\Sigma_{\sigma 0} = \Sigma^{R(T)}_{L\sigma} + \Sigma^{R(T)}_{R\sigma}$ and

$$G^R_\sigma(\varepsilon) = \frac{1 - \langle n_{\bar{\sigma}} \rangle}{\varepsilon - \tilde{\varepsilon}_\sigma - \Sigma_{\sigma 0}} + \frac{\langle n_{\bar{\sigma}} \rangle}{\varepsilon - \tilde{\varepsilon}_\sigma - U - \Sigma_{\sigma 0}}. \tag{9.94}$$

For the lesser functions we have

$$(\varepsilon - \tilde{\varepsilon}_\sigma - \Sigma_{\sigma 0}) G^<_\sigma = U G^{(2)<}_\sigma + i(\Gamma_{L\sigma} f^0_L + \Gamma_{R\sigma} f^0_R) G^A_\sigma, \tag{9.95}$$

$$(\varepsilon - \tilde{\varepsilon}_\sigma - U - \Sigma_{\sigma 0}) G^{(2)<}_\sigma = i(\Gamma_{L\sigma} f^0_L + \Gamma_{R\sigma} f^0_R) G^{(2)A}_\sigma. \tag{9.96}$$

For $G^{(2)<}_\sigma$ we obtain

$$G^{(2)<}_\sigma = \frac{i(\Gamma_{L\sigma} f^0_L + \Gamma_{R\sigma} f^0_R) G^{(2)A}_\sigma}{\varepsilon - \tilde{\varepsilon}_\sigma - U - \Sigma_{\sigma 0}} = \frac{i(\Gamma_{L\sigma} f^0_L + \Gamma_{R\sigma} f^0_R) G^{(2)R}_\sigma G^{(2)A}_\sigma}{\langle n_{\bar{\sigma}} \rangle}, \tag{9.97}$$

and

$$G^<_\sigma = \frac{i(\Gamma_{L\sigma} f^0_L + \Gamma_{R\sigma} f^0_R)}{\varepsilon - \tilde{\varepsilon}_\sigma - \Sigma_{\sigma 0}} \left[\frac{U G^{(2)R}_\sigma G^{(2)A}_\sigma}{\langle n_{\bar{\sigma}} \rangle} + G^A_\sigma \right]. \tag{9.98}$$

These equations give rather good description of Coulomb blockade [29]. For more details of this approach we recommend Sect. 2.7 of the book of Haug and Jauho [39].

It is instructive to compare the Green function (9.94) with the Green function of the Hartree approximation

$$G^R_\sigma(\varepsilon) = \frac{1}{\varepsilon - \tilde{\varepsilon}_\sigma - U \langle n_{\bar{\sigma}} \rangle - \Sigma_{\sigma 0}}. \tag{9.99}$$

This expression is obtained if instead of solving (9.90) for the function $G^{(2)R}_\sigma$ we simply approximate it by the mean-field expression:

$$G_{\sigma}^{(2)R} \equiv G_{\sigma\bar{\sigma},\sigma}^{(2)R} = \left\langle\left\langle \left[d_{\sigma}\hat{n}_{\bar{\sigma}}, d_{\sigma}^{\dagger}\right]_{+}\right\rangle\right\rangle \simeq \langle n_{\bar{\sigma}}\rangle \left[d_{\sigma}, d_{\sigma}^{\dagger}\right]_{+} = \langle n_{\bar{\sigma}}\rangle . \tag{9.100}$$

In the Hartree approximation the spectral function for spin σ has only one maximum at the energy $\varepsilon = \tilde{\varepsilon}_{\sigma} + U\langle n_{\bar{\sigma}}\rangle$. The physical sense is very transparent: the energy of this level is shifted by the Coulomb repulsion from the other level with the average number of electrons $\langle n_{\bar{\sigma}}\rangle$. At low temperature and weak coupling to the electrode one state is fully occupied $\langle n_{\sigma}\rangle = 1$ and the other state is empty $\langle n_{\bar{\sigma}}\rangle = 0$. It means that the state is *magnetic*. Actually this solution can not be exact because two spin sates are equivalent and should form a superposition with the same contribution of both. In other words, quantum fluctuations between two spin orientations will destroy the magnetic state. Spin polarization is an artifact of the mean-field Hartree approximation.

In the approximation (9.94) the spectral function for any spin has *two* maxima, corresponding to the quantum superposition of states with energies $\varepsilon = \tilde{\varepsilon}_{\sigma}$ and $\varepsilon = \tilde{\varepsilon}_{\sigma} + U\langle n_{\bar{\sigma}}\rangle$. Instead of the spin-polarized state in the Hartree approximation, we get the solution with $\langle n_{\sigma}\rangle = \langle n_{\bar{\sigma}}\rangle$. This state is not magnetic, but the solution shows that the system "spends time" in one of the Hartree states, because the spectral functions have maxima near the energies of these states.

References

1. A. Mitra, I. Aleiner, A.J. Millis, Phys. Rev. B **69**, 245302 (2004)
2. T. Frederiksen, M. Brandbyge, N. Lorente, A.P. Jauho, Phys. Rev. Lett. **93**, 256601 (2004)
3. T. Frederiksen, Inelastic electron transport in nanosystems. Master's thesis, Technical University of Denmark (2004)
4. M. Hartung, Vibrational effects in transport through molecular junctions. Master's thesis, University of Regensburg (2004)
5. M. Galperin, M.A. Ratner, A. Nitzan, Nano Lett. **4**, 1605 (2004)
6. M. Galperin, M.A. Ratner, A. Nitzan, J. Chem. Phys. **121**(23), 11965 (2004)
7. M. Galperin, M.A. Ratner, A. Nitzan, J. Phys. Condens. Matter **19**, 103201 (2007)
8. D.A. Ryndyk, M. Hartung, G. Cuniberti, Phys. Rev. B **73**, 045420 (2006)
9. D.A. Ryndyk, G. Cuniberti, Phys. Rev. B **76**, 155430 (2007)
10. D.A. Ryndyk, J. Keller, Phys. Rev. B **71**, 073305 (2005)
11. S. Tikhodeev, M. Natario, K. Makoshi, T. Mii, H. Ueba, Surf. Sci. **493**, 63 (2001)
12. T. Mii, S. Tikhodeev, H. Ueba, Surf. Sci. **502**, 26 (2002)
13. T. Mii, S. Tikhodeev, H. Ueba, Phys. Rev. B **68**, 205406 (2003)
14. S. Tikhodeev, H. Ueba, Phys. Rev. B **70**, 125414 (2004)
15. C.W.J. Beenakker, Phys. Rev. B **44**, 1646 (1991)
16. D.V. Averin, A.N. Korotkov, K.K. Likharev, Phys. Rev. B **44**, 6199 (1991)
17. H. van Houten, C.W.J. Beenakker, A.A.M. Staring, in *Single Charge Tunneling*, vol. 294, NATO ASI Series B, ed. by H. Grabert, M.H. Devoret (Plenum, New York, 1992), p. 167
18. J. von Delft, D.C. Ralph, Phys. Rep. **345**, 61 (2001)
19. E. Bonet, M.M. Deshmukh, D.C. Ralph, Phys. Rev. B **65**, 045317 (2002)
20. M.H. Hettler, W. Wenzel, M.R. Wegewijs, H. Schoeller, Phys. Rev. Lett. **90**, 076805 (2003)
21. W.G. van der Wiel, S. De Franceschi, J.M. Elzerman, T. Fujisawa, S. Tarucha, L.P. Kouwenhoven, Rev. Mod. Phys. **75**, 1 (2002)
22. B. Muralidharan, A.W. Ghosh, S. Datta, Phys. Rev. B **73**, 155410 (2006)

23. J.N. Pedersen, B. Lassen, A. Wacker, M.H. Hettler, Phys. Rev. B **75**, 235314 (2007)
24. R. Swirkowicz, J. Barnas, M. Wilczynski, Phys. Rev. B **68**, 195318 (2003)
25. K.S. Thygesen, A. Rubio, J. Chem. Phys. **126**, 091101 (2007)
26. K.S. Thygesen, Phys. Rev. Lett. **100**, 166804 (2008)
27. K.S. Thygesen, A. Rubio, Phys. Rev. B **77**, 115333 (2008)
28. C. Lacroix, J. Phys. F Met. Phys. **11**, 2389 (1981)
29. Y. Meir, N.S. Wingreen, P.A. Lee, Phys. Rev. Lett. **66**, 3048 (1991)
30. Y. Meir, N.S. Wingreen, P.A. Lee, Phys. Rev. Lett. **70**, 2601 (1993)
31. C. Niu, L.J. Liu, T.H. Lin, Phys. Rev. B **51**, 5130 (1995)
32. P. Pals, A. MacKinnon, J. Phys. Condens. Matter **8**, 5401 (1996)
33. S. Lamba, S.K. Joshi, Phys. Rev. B **62**, 1580 (2000)
34. B.R. Bulka, T. Kostyrko, Phys. Rev. B **70**, 205333 (2004)
35. J.J. Palacios, L. Liu, D. Yoshioka, Phys. Rev. B **55**, 15735 (1997)
36. L. Yi, J.S. Wang, Phys. Rev. B **66**, 085105 (2002)
37. C. Niu, D.L. Lin, T.H. Lin, J. Phys. Condens. Matter **11**, 1511 (1999)
38. B. Song, D.A. Ryndyk, G. Cuniberti, Phys. Rev. B **76**, 045408 (2007)
39. H. Haug, A.P. Jauho, *Quantum Kinetics in Transport and Optics of Semiconductors, Springer Series in Solid-State Physics*, vol. 123 (Springer, Berlin, 1996)

Index

B
Breit-Wigner formula, 30

C
Conductance quantization, 37
Cotunneling, 144
Coulomb blockade, 7, 123
  Anderson impurity model, 240
  CB oscillations, 135
  charging energy, 123
  constant-interaction model, 126
  cotunneling, 144
  Coulomb staircase, 136
  electron-electron interaction in nanosystems, 123
  equation of motion method, 233
  Hubbard-Anderson model, 126
  in quantum dots, 139
  single-electron box, 128
  single-electron transistor, 132

D
Dyson equation, 77
Dyson-Keldysh equations, 212

F
Fisher-Lee relation, 65

G
Green functions, 55
  coordinate representation, 59
  definitions, 56
  eigenstate expansion, 59
  electrode self-energies, 72
  Fisher-Lee relation, 65
  matrix, 67
  recursive method, 77
  retarded and advanced, 56
  semi-infinite electrodes, 83
  surface Green function, 83

L
Landauer-Büttiker method, 5, 17
  adiabatic junction, 21
  conductance quantization, 37
  contact resistance, 39
  Landauer formula, 31
  linear response theory, 47
  multi-channel scattering, 41
  multi-terminal systems, 49
  normalization of wave functions, 27
  quantum junctions, 18
  quantum point contact, 38
  reflection and transmission, 23
  scattering matrix, 26
  Sharvin conductance, 39
  transfer matrix, 26
  transport channels, 19
Landauer formula
  3-terminal, 52
  4-terminal, 53
  heuristic derivation, 33
  multi-channel, 41
  multi-terminal, 49
  single-channel, 31
Lippmann-Schwinger equation, 62

D.A. Ryndyk, *Theory of Quantum Transport at Nanoscale*,
Springer Series in Solid-State Sciences 184,
DOI 10.1007/978-3-319-24088-6

M
Master equation, 119
for polarons, 167
for quantum dots, 139
for single electron transistor, 134
quantum master equation, 6
Matrix Green functions, 67
Mesoscopic systems, 1

N
Nanojunction, 4
Nanoscale systems, 1
NGF method for transport through nanosystems, 207
Dyson-Keldysh equations, 212
Meir-Wingreen-Jauho formula, 216
standard transport model, 207
Nonequilibrium equation of motion method, 193
Nonequilibrium Green functions, 6, 173
contour Green function, 191
definition and properties, 174
equilibrium case, 179
for vibrons, 183
free fermions, 180
Hedin's equations, 202
interaction representation, 186
Kadanoff-Baym-Keldysh method, 196
Langreth rules, 198
lesser and greater, 177
nonequilibrium equation of motion method, 193
retarded and advanced, 174
Schwinger-Keldysh time contour, 189
self-consistent equations, 202

Q
Quantum master equation, 6

R
Recursive method, 77
Resonant transport, 89
interference, 93
single-level model, 90
two-level model, 93

S
Scattering matrix, 26
Self-energy
1D analytical solution, 85
electrode, 72
iterative method, 87
semi-infinite electrodes, 83
Sequential tunneling, 116
Surface Green function, 83

T
Tight-binding model, 68
Tunneling, 99
Bardeen's matrix elements, 108
Breit-Wigner formula, 30
master equation, 119
planar barrier, 100
resonant, 89
sequential, 116
tunneling current, 110
Tunneling Hamiltonian, 102

V
Vibrons and polarons, 8, 149, 221
Dyson-Keldysh method, 221
electron-vibron interaction in nanosystems, 150
Franck-Condon blockade, 168
inelastic electron tunneling spectroscopy (IETS), 154
Lang-Firsov transformation, 159
local polaron, 159
multi-level model, 229
nonequilibrium vibrons, 229
single-level model, 226
single-particle approximation, 164
spectroscopy of vibrons, 226